

University of Pretoria
Faculty of Health Sciences
School of Medicine

Isolation and characterization of human adipose derived mesenchymal stem cells and production of GFP-labeled primary cells for *in vivo* tracking following transplantation

Masters Degree in Immunology

Fiona Anastasia van Vollenstee

21104370

Department of Immunology and Institute for Cellular and Molecular Medicine

Supervisor: Prof MS Pepper
Michael.pepper@up.co.za

Co-Supervisor: Dr M Potgieter
marnipotgieter@yahoo.com

Author Contact details

Physical: 1211 Dr Keyser str
Queenswood X1

Postal: PO Box 13570
Sinoville
0129

Email: fionavanvollenstee@gmail.com

Mobile: 082 859 4239



Abstract to dissertation

Hell is empty and all devils are here!

Shakespeare W, *The Tempest* (1610-1611), Act I, Scene 2, line 215.

Introduction

It is well known that resident adipose stem/stromal cells (ASCs) are a heterogeneous population of multipotent cells characterized by (a) their ability to adhere to plastic; (b) immunophenotypic expression of certain cell surface markers, while lacking others; and (c) the capacity to differentiate into cells of mesodermal origin including osteocytes, chondrocytes and adipocytes. Adipose derived stromal cells offer great therapeutic potential in multiple medical fields, including, orthopedics, cardiology, oncology and degenerative diseases, to name a few. Combining different disciplines of medicine and engineering, organ and tissue repair can be achieved through tissue engineering and regenerative medicine. Adipose derived stromal cells (ASCs) can be utilized as biological vehicles for vector-based gene delivery systems, since they home to sites of inflammation and infection *in vivo*. In order to reach the long-term aim of clinical translation of cell-based therapy, preclinical safety and efficacy need to be shown in animal models. This has motivated the development of standardized isolation, characterization and differentiation operating procedures as well as

an *in vivo* tracking system for ASCs and lentiviral vector transduction for a vector-based gene delivery system.

Methodology

Human ASCs were isolated from lipoaspirate, expanded in culture, immunophenotyped using flow cytometry and induced to differentiate into adipogenic, osteogenic and chondrogenic lineages. Tri-lineage differentiation was confirmed by microscopy. The ASCs were then transduced with green fluorescent protein (GFP)-expressing lentiviral vectors *in vitro*. The effect of the GFP lentiviral vector on ASCs was investigated by studying ASC immunophenotypic expression of surface markers as well as their capacity to differentiate into osteocytes, chondrocytes and adipocytes.

Results

The isolated and expanded cell population, from harvested lipoaspirate adhered to recommended ASC identity criteria. The heterogeneity of ASCs was confirmed by the presence of sub-populations. Transduction efficiency in ASC cultures of approximately 80% was observed after introducing a total of 300 μ l of concentrated lentiviral vector suspension per 4.8×10^4 cells. No immunophenotypic differences were observed between GFP positive and GFP negative cultures. Flow cytometric analysis revealed a progressive increase in GFP expression following *in vitro* expansion of transduced ASCs. Both non-transduced and transduced cultures successfully differentiated into osteocytes, chondrocytes and adipocytes.

Conclusion

The isolated and expanded cell population conformed to the recommended characterization criteria. Heterogeneity was demonstrated with the identification of immunophenotypic sub-populations and semi-quantification of adipogenesis was performed. ASCs were efficiently transduced using the GFP lentiviral vectors produced in our facility. In addition, transduced ASCs maintained adherence to plastic, ASC immunophenotype and were able to differentiate successfully into cells of the three lineages of mesodermal origin. This optimized GFP-ASC transduction technique offers a feasible tracking system as well as a vector-based gene delivery system for future preclinical studies.

Key words: mesenchymal stem cells, adipose derived stromal cells (ASCs), isolation, expansion, characterization, ASC immunophenotype, differentiation, green fluorescent protein (GFP), lipoaspirate



Extending my appreciation to mentors and colleagues giving me the opportunity, guidance and assistance to complete this study.

This was the noblest Roman of them all

Shakespeare W, *Julius Caesar* (1599), Act V, Scene 5, line 68.

- Prof Michael Sean Pepper (Supervisor)
- Prof Riana Cockeran (Head of Immunology Department) and the Department of Immunology
- Dr Marnie Potgieter (Co-supervisor)
- Dr Danie Hoffmann (Collaborator, Plastic and Reconstruction Surgeon)
- Miss Karlien Kallmeyer (Colleague)
- Mr Carlo Jackson (Colleague)
- Dr Chrisna Durant (Colleague)
- Dr Eddie Silberbouer (Assistance with graphics)
- Dr AW Dreyer (Husband: Manuscript editing as well as all his love and support)
- Lucia van Vollenstee (Mommy: For motherly wisdom and support)

Dear Lord thank you for using me as your tool to reveal knowledge to mankind. Humbly I know that I could not achieve anything if You do not will it so. I thank You.

Amen



A list containing all the abbreviations used throughout this dissertation.

Where words are scarce, they are seldom spent in vain,

Shakespeare W, *King Richard II* (1592), Act 2, Scene 1, line 7.

%	percent/percentage
°C	degrees Celsius
°C/min	degrees Celsius per minute
<	less than
>	more than
≤	less than and equal to
µg/ml	micrograms per millilitre
10x	ten times magnification
293T cells	human embryonic kidney 293 cell/ HEK 293 cells
ADAS	adipose derived adult stem

AD-SVF	adipose derived stromal vascular fraction
ANOVA	analysis of variance
ASAPS	American Society for Aesthetic Plastic Surgery
ASCs	adipose derived stem cells/adipose derived stromal cells
AT-CFU-F	adipose derived fibroblastic like colonies
BM	bone marrow
BMI	body mass index
BMSC	bone marrow stromal cell
BSA	bovine serum albumin
BSC-II	type II biosafety cabinet
Ca ²⁺	Calcium ions
CaCl ₂	calcium chloride
CAL	calibration factor
Cat#	catalogue number
cc	cubic centimetre
CCR5	C-C chemokine receptor type 5
CD105	cluster of differentiation 105
CD34	cluster of differentiation 34
CD4	cluster of differentiation 4
CD45	cluster of differentiation 45
CD73	cluster of differentiation 73
CD90	cluster of differentiation 90
cDNA	complementary deoxyribonucleic acid
cells/cm ²	cells per square centimetre/density
cells/ml	cell per millilitres
CFU-F	fibroblastic like colonies
CFU-Fs	colony-forming unit fibroblasts

GMP	current good manufacturing practices
cm	centimetre
cm ²	centimetre squared
CO ₂	carbon dioxide
CP	cryopreserved cultures
CXCR4	C-X-C chemokine receptor type 4
DAPI	4',6-Diamidino-2-phenylindole
ddH ₂ O	doubled distilled water
dH ₂ O	distilled water
DH5α	cloning strain of E. Coli bacteria
DMEM	Dulbecco's Modified Eagle Medium
DMSO	dimethyl sulfoxide
DNA	Deoxyribonucleic acid
<i>e.g.</i>	example
ECD	electron coupled dye
EDTA	ethylene diamine tetraacetic acid
<i>et al.</i>	and others
EU	European Union
FBS	fetal bovine serum
FDA	United States Food and Drug Administration
FFA	free fatty acids
FGF-2	fibroblast growth factor 2
FITC	fluorescein isothiocyanate
FS lin	forward scatter linear
F-value	random variable with an <i>f</i> distribution
g	gram
<i>g</i>	gravitational force/ centrifugal force

G ₀	quiescent state
G _{1b}	committed to advance to S phase within the cell cycle
GFP-	green fluorescent protein negative (lacking expression)
GFP	green fluorescent protein
GFP+	green fluorescent protein positive (expression)
Gp120	envelope glycoprotein
GVHD	graft versus host disease
HBS	HANKS Ca ²⁺ Mg ²⁺ solution
HBV	hepatitis B virus
HCl	hydrochloric acid
HCV	hepatitis C virus
HIV	human immunodeficiency virus
HIV-1	human immunodeficiency virus type 1
HIV-2	human immunodeficiency virus type 2
HLA	human leukocyte antigen
HLA-DR	class II human leukocyte antigen
hrs	hours
HSCs	haematopoietic stem cells
hUCMSCs	human umbilical cord blood mesenchymal stem cells
<i>i.e.</i>	in other words
IA	intra-arterial
IC	intra-cardiac
ICAM-1	intercellular adhesion molecule-1
IDO	indoleamine 2, 3-dioxygenase
IFATS	International Fat Applied Technology Society
IFN-β- hUCMSCs	interferon-beta transduced gene human umbilical cord blood mesenchymal stem cells

IFN- β	interferon-beta
IFN- γ	interferon-gamma
<i>in vitro</i>	in glass/not within the living
<i>in vivo</i>	within the living
IP	intra-peritoneal
ISCT	International Society for Cellular Therapy
ISO	International Organization for Standardization
IV	intravenous
JNK	c-jun N-terminal kinase
L	liter
LV	lentiviral stock solution
mg	milligram
Mg ²⁺	Magnesium ions
MgCl ₂	magnesium chloride
MHC	major histocompatibility complex
min	minutes
ml	millilitres
mM	millimolar
mm	millimetre
mm/Hg	millimetres mercury
MSCs	mesenchymal stem cell/ mesenchymal stromal cells
NaCl	sodium chloride
NaCO ₃	sodium carbonate
NC	non-cryopreserved cultures
nm	nanometer
O ₂	Oxygen
PAS	Periodic Acid Schiff

PBS	phosphate buffer solution
PC5	phycoerythrin-cyanine 5.1
PC7	phycoerythrin-cyanine 7
PE	phycoerythrin
pen/strep	penicillin and streptomycin
pH	potential of hydrogen
PLA	processed lipoaspirate
PPAR- γ	peroxisome proliferator-activated receptor gamma
P-value	probability of testing a statistical significance
RCF	relative centrifugal force
RCRs	replication competent recombinants
RNA	ribonucleic acid
ROS	reactive oxygen species
rpm	revolutions per minute
s	seconds
SCID	severe combined immunodeficiency
SS lin	side scatter linear
STD Dev	standard deviation
Students T-test	statistical hypothesis test
SVF	stromal vascular fraction
T-cells	T-lymphocytes
TEM	transmission electron microscope
TGF- β 3	transforming growth factor beta-3
TZDs	thiazolidinediones
UCB	umbilical cord blood
USA	United States of America
VCAM-1	vascular adhesion molecule-1

vs.	versus
VSV-G	G glycoprotein of the vesicular stomatis virus
Wj-MSCs	Wharton's jelly derived MSCs
α	alpha
α -MEM	alpha-Modified Eagle Medium
β	beta
γ	gamma
μ l	microlitre
μ m	micrometer



Tables of contents.

Yea, from the table of my memory

I'll wipe away all trivial fond records

Shakespeare W, *Hamlet* (1600), Act 1, Scene 5, line 99-100.

List of figures of dissertation.	xv
List of tables of dissertation.	xxiv
Introduction to dissertation.	1
A historical overview of the nomenclature of mesenchymal stem cells and their properties.	4
Introduction	4
History and nomenclature of mesenchymal stem cells.....	5
Development of isolation processes.....	8
Properties of MSC's.....	9
Homing of MSCs.....	9
Immunosuppression	11
Cancer Inhibiting Properties	12
Antibacterial properties.....	12

ASC associated Clinical trials	13
Medicolegal aspects.....	18
Conclusion.....	19
References	21
Isolation and expansion of peripheral abdominal adipose tissue derived stromal cells and comparison of cell viability before and after cryopreservation	27
Introduction	27
Characteristics of different adipose tissue types.....	28
Stem cells resident in adipose tissue	29
Adipose tissue harvesting techniques	32
Background on liposuction	33
ASC isolation techniques.....	35
Cryopreservation of ASCs.....	38
Aims and objectives	40
Materials and Methods.....	40
Collection of human adipose samples	41
Transportation of the lipoaspirate	46
Sample codification.....	46
Isolation of ASCs.....	47
Cell counting techniques.....	52
Trypan Blue (40%) dye exclusion assay.....	53
Cell count determined by flow cytometric analysis.....	54
Seeding.....	55
<i>In vitro</i> nourishment maintenance of MSC cultures during culture expansion.....	56
<i>In vitro</i> passaging of MSC cultures	57
Growth kinetics	58
Long term Expansion.....	58
Cryo-preserving and thawing of cryo-preserved MSCs samples	58
Results.....	59
Adipose tissue harvesting and transportation to the laboratory	59
Isolation of ASCs.....	60
Growth kinetics	61
Expansion of ASCs	64
Cryopreservation.....	64
Discussion.....	65
Lipoaspirate harvesting and ASC isolation.....	65

Growth kinetics	66
ASC Expansion	67
Cryopreservation.....	68
Conclusion.....	69
References	70
Immunophenotype characterisation and tri-lineage differentiation of peripheral abdominal adipose resident stromal cells	76
Introduction	76
<i>In vitro</i> Characterisation.....	76
<i>In vivo</i> Characterisation	78
Differentiation.....	78
Materials and Methods.....	79
Immunophenotypic characterisation.....	79
Analysis of flow-cytometry characterisation data	81
Sub-population analysis by flow cytometric analysis	83
Tri-lineage Differentiation.....	83
Assessment of differentiation capacity.....	88
Validation of homogeneity and estimation of the required number of visual fields per well necessary for semi-quantification.....	89
Adipocyte induced assessment.....	91
Osteocyte induced assessment.....	92
Chondrocyte induced assessment	92
Quantification of differentiation.....	93
Results.....	94
Immunophenotypic characterisation.....	94
ASC Phenotype expression Profile	100
Tri-lineage Differentiation.....	106
Quantification of differentiation.....	111
Discussion.....	113
Immunophenotypic characterization	113
Sub-population analysis	115
Differentiation.....	116
Limitations.....	117
Conclusion.....	117
References	118

Immunophenotypic characterisation and differentiation capacity of human adipose derived mesenchymal stromal cells transduced with lentiviral vectors expressing GFP.....	122
Introduction	122
HIV-1 based lentiviral vectors	123
A three plasmid expression system of HIV-1 based lentiviral vectors.....	123
Material and Methods	125
Co-transfection of plasmids in 293T cells for the production of GFP lentiviruses.....	125
Optimization of ASC transduction by the GFP lentivirus vector	127
Immunophenotype characterization of transduced ASCs	130
Tri lineage differentiation	131
Quantification and assessment of differentiation	131
Statistical analysis	132
Results.....	132
Immunophenotypic characterisation.....	134
Sub-population analysis from cryopreserved cultures	141
Tri-lineage Differentiation.....	144
Quantification of differentiation.....	149
Statistical analysis of quantification.....	152
Discussion.....	153
Conclusion.....	155
References	156
Conclusion to dissertation.....	157
Appendix 2.1. Clinical trials search using Adipose derived stem cells	159
Appendix 3.1.	172
All Ethics approval letters and documentation.....	172
Appendix 4.1.	187
Appendix 4.2.	189



List of figures of dissertation.

For when my outward action doth demonstrate

The native act and figure of my heart

Shakespeare W, *Othello* (1604), Act 1, Scene 1, line 61-62.

- Figure 2.1.** A world map indicating a total of 104 clinical trials found using search terms ‘adipose derived stem cells’ cited at www.clinicaltrials.gov **13**
- Figure 2.2.** Clinical trials listed on www.clinicaltrials.gov using search term ‘adipose derived stem cells’ that are registered globally. Trials registered within more than one country or not associated to any country are displayed within the multi countries group. **14**
- Figure 2.3.** A total 103 clinical trial registrations listed on www.clinicaltrials.gov under search term ‘adipose derived stem cells’ was received globally since 2005. The figure illustrates the number of trial registrations received per year. **15**
- Figure 2.4.** The recruitment status of clinical trials listed on www.clinicaltrials.gov under the search term ‘adipose derived stem cells’ **15**
- Figure 2.5.** The number of trials listed (under search terms ‘adipose derived stem cells’ on website www.clinicaltrials.gov) within a specific condition category. The summary of each trial is available within Appendix 2.1..... **16**

Figure 2.6. Different routes of ASC administration within the listed clinical trials on www.clinicaltrials.gov under search term ‘adipose derived stem cells’ 17

Figure 2.7. Specified ASC sources used as intervention for different conditions within the listed clinical trials on www.clinicaltrials.gov under search term ‘adipose derived stem cells’ 18

Figure 3.1. Sterile instrument table and bowl containing antiseptic cleaning solution. The blue cloth indicates a sterile field. 42

Figure 3.2. Harvesting cannula with a blunt tip in the shape of a bucket handle..... 42

Figure 3.3. The proximal end of the harvesting cannula is shaped to fit securely into a 10cc luer lock syringe..... 42

Figure 3.4. A puncture wound made with a no. 15 scalpel blade in the aseptically cleaned donor area..... 42

Figure 3.5. The harvesting cannula is inserted through the puncture wound in the donor area. 43

Figure 3.6. The harvesting cannula is advanced within the adipose layer of the donor area and the plunger is withdrawn 1 to 3 ml at a time to create a low negative pressure within the barrel of the syringe..... 43

Figure 3.7. The negative pressure decreases within the suction system as the barrel of the syringe fills with adipose tissue. The plunger is then redrawn to create a vacuum to allow more adipose tissue to be suctioned through the harvesting cannula into the barrel of the syringe..... 43

Figure 3.8. The surgeon grips the donor area with the non-dominant hand, while easily manipulating the 10 cc luer lock syringe to maintain a low negative pressure during harvesting. The surgeon advances and retracts the harvesting cannula quickly and forcefully trough the adipose layer. 43

Figure 3.9 The harvesting cannula is advanced in a lateral direction (A) and retracted. This movement was repeated in a more inferior direction than the last until the cannula was advanced in an inferior (B) direction. This fan formation technique (C) of harvesting decreases the risk of harvesting blood contaminants with the subcutaneous adipose tissue..... 44

Figure 3.10. Lipoaspirate fills the syringe during the harvesting process due to the negative suction pressure..... 44

Figure 3.11. The plunger is withdrawn completely from the syringe barrel and the lipoaspirate is decanted into a sterile bottle containing PBS..... 44

Figure 3.12. Lipoaspirate harvesting using the suction assisted tumescent liposuction technique. The donor site was infiltrated with a wetting solution using a 50 cc syringe and needle. The aspirator (suction machine), created a negative pressure of approximately 500 mmHg. Silicone tubes were used to connect the harvesting cannula, the collection test tube and the aspirator creating a closed vacuum system. The harvesting cannula was randomly advanced and retracted through the donor area. When the collecting test tube was filled (80%), the silicone tubes were detached and the plunger removed from the proximal end. The lipoaspirate was decanted into an autoclaved sterile bottle containing PBS and 5% pen/strep. 46

Figure 3.13. During transportation the lipoaspirate started to segregate into layers consisting of (a) oil supernatant, (b) lipoaspirate and (c) PBS, supplemented with 5% pen/strep, containing blood contaminants. The gentle shaking of the collection bottle during transportation will allow more blood contaminants to move out of the adipose tissue into the liquid portion of the segregated sample.....**47**

Figure 3.14. The codification given to samples collected from adipose tissue to ensure patient anonymity.....**47**

Figure 3.15. Adipose sample transferred into 50 ml Falcon tubes and centrifuged to obtain the various supernatant layers. From the top, (a) the floating oil layer, (b) compact adipose tissue layer, (c) PBS supplemented with 5% pen/strep and blood, (d) blood cells (mostly red blood cells).....**49**

Figure 3.16. The oil supernatant layer was aspirated with a suction-assisted glass pipette.....**49**

Figure 3.17. The supernatant consisted of four different layers displayed after the three washing procedures of sample presented by picture 1, 2 and 3 respectively. (a) A decrease in the blood cell contaminants in the PBS supplemented with 5% pen/strep was observed with increased washing. (b) A decrease in the oil supernatant layer was also observed with increased washing.**49**

Figure 3.18. Centrifuged compacted adipose tissue indicated by (a). Volume of (a) was noted to determine the volume of 0.1% Collagenase Type I solution needed during the collagen digestion procedure.....**50**

Figure 3.19. The compacted adipose tissue was transferred into sterile 50 ml tubes to be weighed.**50**

Figure 3.20. The adipose tissue was decanted from the 50 ml Falcon tubes onto sterile tissue culture plates. The 0.1% Collagenase Type 1 solution was added to the adipose tissue.**50**

Figure 3.21. The adipose tissue and 0.1% collagenase Type 1 solution was incubated for 45 min at 37°C and 5% CO₂ for the process of collagen digestion to take place.....**50**

Figure 3.22. The adipose tissue with 0.1% collagenase Type 1 solution was taken out of the incubator and aspirated with a Pasteur pipette.**51**

Figure 3.23. Centrifuged collagen digested adipose tissue displaying four layers: (a) a small floating supernatant oil layer; (b) compact adipose tissue; (c) a light pink layer containing 0.1% collagenase Type 1 solution and red blood cells; and (d) the red blood cell pellet.**51**

Figure 3.24. The centrifuged sample vigorously shaken to disrupt the digested adipose tissue and pellet within the tube.**51**

Figure 3.25. When using the centrifuge, the rotator was balanced in order to obtain the same weight on the opposite side. A balance or a sample with equal volume was inserted to counter balance the respective sample.**52**

Figure 3.26. After centrifuging for 5 min at 1200 rpm the pooled cell suspension formed a pellet. (a) The pellet contains adipocytes, ASCs, as well as cells from the hematopoietic lineage and (b) stromal medium.....**52**

- Figure 3.27.** The pellet of ASCs and red blood cells was re-suspended in Versalyse™ and incubated for 10 min at room temperature to lyse the red blood cells.52
- Figure 3.28.** A) A cell counter clicker to assist with cell counting; B) Neubauer counting chamber (haemocytometer) with two chambers on each side. Each chamber contains a grid displaying four counting quadrants ; C) a glass cover slip, that is placed on top of the haemocytometer after 10 µl of the Trypan Blue stain solution is loaded; D) The 40% Trypan Blue stain solution containing, 80 µl Trypan Blue stain, 100 µl PBS and 20 µl of cell suspension.....54
- Figure 3.29.** Calculations used to determine the number of cells within a cell suspension. (A) Calculation performed when using the Trypan Blue (40%) dye exclusion assay. (B) Calculation performed when using flow cytometric analysis.54
- Figure 3.30.** A side scatter linear and forward scatter linear dot plot displaying the events measured by the flow cytometer. The flow beads (pink) and a gate were used to encircle the cell population that was counted until the CAL factor was reached. The gate labelled cell population displayed the cell population count that was expressed as the number of cells per µl cell suspension.....55
- Figure 3.31.** A histogram, displaying the flow beads with a gating placed over the peak of the flow beads labelled as CAL. The specific calibration factor for CAL was 986. The dot plot (Figure 3.27.) was gated on gate D within the histogram in order to display only the flow beads.....55
- Figure 3.32.** Considering the quantification, the number of events within the gated population was represented by the cell population gated in Figure 3.28 (9 187 events). The fluorescent bead region is represented by CAL in Figure 3.29 (3 657 events) times by the respective cell suspension volume (µl).....56
- Figure 3.33.** The flow cytometric analysis program Kaluza, does not display the result as the number of events per µl of a respective gated region. The Flow cytometer expresses this measurement, which was an easier way to calculate the cell density within the respective cell suspension.....56
- Figure 3.34.** Calculation to determine the volume of cell suspension needed to seed cells at an initial seeding density of 5×10^5 cells/cm². The volume of cell suspension was then added to the respective tissue flask containing fresh α-MEM supplemented with 10% FBS and 1% pen/strep.56
- Figure 3.35.** Calculation to determine the volume of cell suspension needed to seed cells for expansion purposes during passaging procedures at a density of 5×10^3 cells/cm². The volume of cell suspension was then added to the respective tissue flask containing stromal medium..56
- Figure 3.36.** The growth kinetics of 5 cultures over a period of 9 days. The SVF cells were seeded in a six well plate and the non-adherent cells washed off after 24 hours. A well was trypsinized on day 1, 3, 5, 7 and 9 respectively. The cell counts of the viable cells were performed using a 40% Trypan Blue Exclusion Assay, at 24 hours (day 1), 72 hours (day 3), 120 hours (day 5), 168 hours (day 7) and 216 hours (day 9) in respective culture plates, after an initial seeding density of 5×10^5 cells per cm².62
- Figure 3.37.** The kinetics of 4 cultures over a period of 9 days. Cell counts of the non-viable cells were performed using a Trypan Blue (40%) dye exclusion assay, at 24 hours (day 1), 72 hours

(day 3), 120 hours (day 5), 168 hours (day 7) and 216 hours (day 9) in respective culture plates, after an initial seeding density of 5×10^5 cells per cm^2 **63**

Figure 3.38. The growth kinetics of 10 cultures over a period of 9 days. Cell counts of the viable and non-viable cells were performed using flow cytometry, at 24 hours (day 1), 72 hours (day 3), 120 hours (day 5), 168 hours (day 7) and 216 hours (day 9) in respective culture plates, after an initial seeding density of 5×10^5 cells per cm^2 **64**

Figure 3.39. Average ASC yield per cm^2 for every passage (up to passage 16) of 11 different cultures. Cell counts, determined by flow cytometry (pink line) and manual using a Trypan Blue 40% dye exclusion assay (Blue line) was used to calculate the cell yield that was passaged from a surface area. **65**

Figure 3.40. The percentage of viable ASCs determined across 14 cultures using the Trypan Blue (40%) dye exclusion assay before cryopreservation (indicated in blue) and after thawing procedures (indicated in pink). The difference between the blue and pink values indicates the percentage of cells lost due to the freezing-thawing process. **66**

Figure 3.41. Expanded MSCs stained with a nuclear stain DAPI. The red in-circled nucleus bundles indicate that the nuclei are in very close proximity and on top of one another. It is also evident that within these bundles that some nuclei are slightly more in focus than the other background nuclei (circled in yellow), suggesting that the nuclei are on top of one another. This is evidence that ASCs are not contact inhibited during culturing procedures. **69**

Figure 4.1. An unstained flow cytometric sample. The voltages were set to indicate a negative reading within the X-Y- quadrant of a 2-parameter plot (indicated in A) as well as in the first decade of a 1-parameter plot (indicated in B). All plots were gated on [A], which was the population of cells studied on a forward and side scatter plot. **82**

Figure 4.2. An explanation of the tree plot analysis. The forward and side scatter plot indicates the relevant cell population. Gating on this region, the 2-parameter plot in B indicates CD45- and CD34- population. Gating Figure C on the CD45- and CD34- parameter region in figure B, we are only considering the cells gated within the CD45- and CD34- parameter. Figure C demonstrates that the cell population in the CD73+ and CD90+ gating region are also CD34- and CD45- populations within the parameter from figure B. Gating figure D on the CD73+ and CD90+ only cells with CD34-, CD45-, CD73+ and CD90+ marker expression are considered. Figure D displays then a cell population with the characteristic ASCs phenotype (CD34-, CD45-, CD73+, CD90+ and CD105+)..... **83**

Figure 4.3. Summary of the tri-lineage differentiation characterisation of immunophenotyped ASCs. The tri-lineage cultures include induced as well as non-induced cultures for adipocyte and osteocyte differentiation, where the non-induced ASCs served as an internal control for the classical staining that was performed. Fluorescent nuclear staining using DAPI was performed for the semi-quantification of induced as well as non-induced cells within the adipocyte and osteocyte lineages. The chondrogenic induced and non-induced cultures were sectioned and stained with 1% Toluidine Blue, due to the nature of the spherical culture. **85**

Figure 4.4. Representative 6 well plate indicating induced cultures and non-induced controls. Adipocyte and osteocyte differentiation were performed in duplicate (indicated as A and B) with

two non-induced wells serving as an internal control for classical staining (one for each lineage).
.....88

Figure 4.5. Cartilage cultures. (A) After the cells were removed enzymatically from the T25 flask, the trypsin and α -MEM were aspirated after centrifugation. The pellet was re-suspended in 1 ml cartilage induction medium. (B) The cell suspension was centrifuged to form a pellet in the 15 ml tube and incubated under standard conditions for 21 days. The induction medium was replaced every 2 days. (C) Within 24 hours of incubation the cells appear to contract into a sphere.89

Figure 4.6. The grid formation covering a 6 well plate. Every small round dot indicates a photograph (vision field) microscopically analyzed, with a total of 25 vision fields per well. The DAPI stained nuclei of the two non-induced controls, two adipocyte induced and two osteocyte induced wells were quantified using Image J software cell counter.91

Figure 4.7. Representation of the eight different counting strategies. Every individual well was photographed and cells manually counted using Image J software cell counter, means were calculated and statistically compared: (A) All 25 vision fields; (B) 5 around outside of the grid with 1 center field; (C) 5 fields within 1 quadrant; (D) 5 random fields; (E) 5 random fields around the outside of grid; (F) 8 random fields; (G) 10 random fields; and (H) 15 random fields.91

Figure 4.8. Example of all the possible 2-parameter plots, displayed in density plot formation to indicate the rounded cell populations. The 2-parameter plots were used to optimize colour compensation during the analysis process.97

Figure 4.9. The unstained and antibody labelled 1-parameter plots as well as overlaying plots for every respective antibody expression measured. (A) CD 34; (B) CD 45; (C) CD 73; (D) CD 90; and (E) CD 105 respectively.99

Figure 4.10. Examples of two tree plots (A) the unstained from the turquoise protocol group (see appendix 4.1) and (B) and antibody labelled sample (A270611-01 P8). The tree plot groups the cells within a specific combination phenotype expressed and displays the results as a percentage from the respective cell population gated in the forward and side scatter plot.100

Figure 4.11. All possible combinations of positive and negative markers that were analyzed. The yellow highlighted combination represents the ASC phenotype used to characterize the respective population. The combinations phenotypes highlighted violet are the respective sub-populations (N=8) identified.101

Figure 4.12. ASC phenotype of all the cultures across 15 passages. The blue dotted line indicates the threshold of the 95%, demonstrating >95% expression of CD73, CD90, CD105 and >95% lacking expression of CD34 and CD45. The Green dotted line indicates the adjusted threshold of >90%. The red gridline indicates the separation between respective passages.103

Figure 4.13. The percentage cultures adhering to the respective standard >95% expression (Blue) criteria threshold (CD 34-, CD 45-, CD 73+, CD 90+ CD 105+ set out by Domenici *et al.*, 2006 and the adjusted cut off criteria threshold >90% expression (Green). (See Figure 4.12.)103

Figure 4.14. The mean ASC phenotype (CD34-, CD45 -, CD73+, CD90+ and CD105+) expression of cultures phenotyped within a respective passage. The trend line indicates a steady linear increase in the ASC phenotype expression across all passage.103

Figure 4.15. Percentage gated cells expressing respective sub-population phenotype combinations across passages in a single patient culture (A270611-02).104

Figure 4.16. Percentage gated cells expressing respective sub-population phenotype combinations across passages in patient A220611-01. **105**

Figure 4.17. The ASCs sub-population phenotypes in the heterogeneous ASC population across 15 passages. The frequencies of significant expression across all cultures within a respective passage are demonstrated as a percentage within the passage. **106**

Figure 4.18. Adipogenic lineage microscopy analysis. **109**

Figure 4.19. Osteogenic microscopy analysis. **110**

Figure 4.20. Chondrogenic microscopy analysis. **112**

Figure 4.21. The mean cell counts of vision fields from respective DAPI stained non-induced control (blue), adipogenic (pink) and osteogenic (green) induced cultures for all cultures.... **113**

Figure 4.22. The mean cell counts from 5 vision fields of the Oil Red O stained adipogenic induced cultures. The preadipocytes (blue), more mature preadipocytes (pink) and adipocytes (green). The adipogenic induced cells were quantified according to set out parameters (See Figure 4.18.). **114**

Figure 5.1. Representative 6 well plate indicating transduced (green) and non-transduced (blue) cultures within the three individual ASC cultures (A270611-01; A270611-02; A100511-01). The transduced cultures received 300 µl lentiviral stock solution (LV) and the non-transduced cultures received 300 µl PBS acting as the control group. The transduced cultures code was GFPA270611-01 and the non-transduced culture code was CA270611-01..... **130**

Figure 5.2. Codifications used within study. Transduced cultures received a prefix of ‘GFP’ and the corresponding control cultures a ‘C’..... **131**

Figure 5.3. Percentage of ASCs transduced with different lentiviral vector titrations, indicated by GFP positive expression, measured over ten passages using flow cytometry. A transition phase is visible between passages 1 and 5 with a slight decrease in percentage GFP positive cells. After passage 5, the percentage positive cells steadily increased. **134**

Figure 5.4. Percentage cells expressing GFP within transduced cultures (GFPA100511-01; GFPA270611-01; GFPA270611-02) across 12 passages represented by ‘T’ (passage after transduction was performed). **135**

Figure 5.5. Three individual cell population expression histograms (A) unstained non-transduced control sample, indicated a true negative expression for both CD73 and GFP; (B) a CD73 FITC stained, non-transduced sample indicating a positive CD73 expression; (C) a CD 73 stained transduced sample indicating two different cell populations, GFP+ and CD73+, as well as GFP- and CD73+. In the overlaying plot (D) all histograms (A-C) were superimposed to show that the left sided population of the transduced cultures (green) shows positive CD73 expression in the same region as the CD73+ cell population of the non-transduced culture (blue). It could therefore be concluded that the right sided population of the transduced cultures are the GFP+ and CD73+ population respectively..... **136**

Figure 5.6. Comparing the phenotype (CD34-, CD45-, CD+90 and CD105+) of GFP positive and negative cells within transduced (green) and non-transduced (blue) cultures. Three different cultures and three different post-transduction passages..... **137**

- Figure 5.7.** Three different sub-populations were identified using antibody panel 1. A combinational antibody threshold was >1% expression displayed in >1 culture. Comparing the percentage gated cells expressing the respective sub-populations were (A) CD34-, CD45-, CD90- and CD105-; (B) CD34+, CD45+, CD90+ and CD105+; and (C) CD34+, CD45-, CD90+ and CD105+, within the transduced and non-transduced. 139
- Figure 5.8.** The percentage of GFP expressing cells within the gated cell population on the forward and side scatter plot of the transduced cultures after freezing and thawing. 140
- Figure 5.9.** The ASC recommended criteria (turquoise: CD34-, CD45-, CD73+, CD90+ and CD105+) as well as new adopted criteria (pink: CD34+, CD45-, CD73+, CD90+ and CD105+) within the non-transduced cultures, the GFP+ and GFP- cell populations within the transduced cultures. The cells expressing relative ASC profiles were displayed as a percentage of respective gated cell populations. 141
- Figure 5.10.** The mean percentage of cells expressing the ASC recommended immunophenotypic profile (CD34-, CD45-, CD73+, CD90+ and CD105+) across 4 passages within the respective gated cell populations in three individual cultures. Non-transduced (blue), GFP+ (green) and GFP- (purple) cell populations within the transduced culture. 142
- Figure 5.11.** The immunophenotypic expression profile of the individual culture A100511-01. Only significant populations were considered with threshold expression of >1%, present more than once across four passages. The comparison was drawn between the non-transduced, GFP positive and GFP negative cell populations within transduced cultures. 143
- Figure 5.12.** The immunophenotypic expression profile of the individual culture A270611-01. Only significant populations were considered with threshold expression >1% being present more than once across four passages. The comparison was drawn between the non-transduced, GFP positive and GFP negative cell populations within transduced cultures. 144
- Figure 5.13.** The immunophenotypic expression profile of the individual cultures A270611-02. Only significant populations were considered with threshold expression >1%, present more than once across four passages. The comparison was drawn between the non-transduced, GFP positive and GFP negative cells populations within transduced cultures. 145
- Figure 5.14.** Microscopy analyses of the DAPI stained non-, adipogenic- and osteogenic induced, non-transduced (A, E and I) and the transduced (B, F and J) cultures. The transduced cultures demonstrated GFP fluorescence expression within the non-induced (B, C and D), adipogenic induced (F, G and H) and osteogenic induced (J, K and L). These images are only representative of induction timepoint week 3 (day 21). 148
- Figure 5.15.** Microscopic analysis of the adipogenic and osteogenic induced cultures accompanied by their respective non-induced controls. Oil Red O stained oil droplets confirms adipogenic differentiation in the non-transduced (B) and transduced (C) cultures and Alizerin Red S stained calcium within the mineral deposition confirms osteogenic differentiation within the non-transduced (G) and transduced (H) cultures. These images are only representative of induction timepoint week 3 (day 21). 149
- Figure 5.16.** Microscopic analysis of chondrogenic induced pellet cultures stained with toluidine Blue O. 150

Figure 5.17. The mean number of DAPI stained cells in five images across the induction period of day 7, 14 and 21. Comparing the differences of the non-induced, adipogenic induced and osteogenic induced cultures within both the non-transduced and transduced cultures..... **151**

Figure 5.18. Comparing the mean cell counts for the five DAPI stained vision fields between the non-induced, adipogenic and osteogenic induced cultures, within both transduced and non-transduced cultures over 3 different post-transduction passages. **152**



List of tables of dissertation.

I do beseech you, sir, trouble yourself no further.

Shakespeare W, *Othello* (1597), Act 4, Scene 3, line1.

Table 2.1 Different sources from which MSCs have been isolated.....	8
Table 3.1. Tissue culture flasks with respective tissue culture surface areas and volumes of stromal medium additions and changes during expansion of cultures.....	57
Table 3.2. Sample collections recorded and standardized as cells isolated per unit.....	61
Table 4.1. Summary of the different antibody panels that were used in specific fluorescent channels. Monoclonal mouse anti-human antibodies were used as available within the laboratory.....	81
Table 4.2. The different lineage induction media and the exact concentrations of chemicals added to DMEM and volume or mass of chemicals used to produce a final 100 ml solution of the respective induction media. All induction media were stored at 4°C.....	86
Table 4.3. The passage number at which the cultures were induced to be differentiated....	87
Table 4.4. The mean cell counts of the respective counting strategies.	92
Table 4. 5. The frequency of significant sub-population expressions for all passages of every culture phenotypically analyzed according to respective threshold parameters. The percentage frequency expressions across all passages for the respective culture were calculated to indicate inter patient variability.....	105

Table 4.6. Sub-population profiles found among isolated and expanded ASCs.....	107
Table 5.1. Adding substances together in a specific chronological order in 1 ml Eppendorfs.	127
Table 5.2. Volume of vector stock added to a 9.6 cm ² ASC culture. The ASCs were seeded at 5x10 ³ cells/cm ² 12 hrs prior to transduction.....	128
Table 5.3. The two different antibody panels as well as the fluorescence channels used for detection on the flow cytometer used throughout the study.....	132
Table 5.4. Comparing the non-induced, adipogenic and osteogenic induced cultures over 3 weeks between the transduced and non-transduced cultures.....	153
Table 5.5. Comparing the P values for non-induced, adipogenic induced and osteogenic induced between respective post-transduction passages.....	153



Introduction to dissertation.

Friends, Romans, countrymen, lend me your ears!

Shakespeare W, *Julius Caesar* (1599), Act III, Scene 2, line 74.

Introduction

The fields of tissue engineering and regenerative medicine are regarded as interdisciplinary and are evolving in parallel with biotechnological advances, applying both the principles of biology and engineering to advance applications in medicine. The combination of using stem cells together with growth factors and selective biomaterials can already be used to repair failing organs. The discovery of adult stem cells in adipose tissue however, has *imparted great impetus* to the field of tissue regeneration not only as a potential source of stem cells but also due to the relative abundance and potential ease of harvesting from the donor.

Over the last decade there has been a clear shift away from using embryonic stem cells due to ethical considerations to adult stem cells (post neonate) and more specifically non-hematopoietic stem cells. Limited information is however, available on the therapeutic potential and clinical efficiency of these cells and the mechanisms of tissue repair. We thus need to know more about the *in vivo* location and behaviour as well as methods to accurately identify these cells. There are no single or specific sets of markers to accurately identify and characterize these cells immunophenotypically, and considering

the properties and the potential use in regenerative medicine this field needs to be scientifically and ethically explored in great depth.

Mesenchymal stem cell (MSC) research relating to clinical translation is still in its infancy. Research groups around the world are working on the concept of using MSCs for clinical applications in the medical field. The aims of various groups are to optimize and resolve issues pertaining to the use of these cells to address different tissue traumas and illnesses and hereby to advance the field into what is likely initially to be costly individualized medicine. The MSC domain lacks standardization with regard to isolation, expansion, identification of cells, tissue lineage induction, engraftment as well as the best route of administration. There is a definite need for consensus and standardization within this domain not just within South Africa, but internationally as well.

The concept of translational research has become a great priority within the medical field. The considerable time and cost spent in research attempts often lead to the development of applications that do not always answer the patient's needs. A new way of thinking, "from bedside to bench" is very applicable to research in the stem cell field. Taking into account the specific needs of the patients *e.g.* burn wounds and applying autologous use of stem cells to treat this specific need is the way forward in individualized medicine. However, implementing this concept poses significant challenges, especially with regard to applying first world medicine within a third world heavy disease burden setting. Before exploring the various clinical applications of stem cells we must go "back to basics". Understanding the basic biology of cell based therapies which lead to stem cell therapy will contribute to the success of bringing biological treatments to South African patients.

Extensive basic research on cell based therapy has to precede pre-clinical animal studies as well as human clinical trials. A broad basic research base needs to be established to ensure that all processes, from collection of material to possible administration of stem cells are optimized. This includes collection of stem cells from a defined source (*e.g.* lipoaspirate), isolation of the respective stem cells, expansion, characterization, manipulation, safety and efficacy as well as administration and engraftment of these stem cells.

The long term objective of this project is to establish a facility for cell-based therapy using human MSCs isolated from autologous and allogeneic sources. The administration and application of these cells could offer correction of dysfunction to patients suffering from degenerative diseases and tissue defects due to trauma and/or disease where cellular integrity is compromised.

One of the great potential characteristics of transplanted MSCs, derived from a healthy donor, is the ability to overcome the immune response of the host as MSCs are known to be immune privileged. It is to our knowledge still undetermined what the relative potential is of MSCs derived from different adult tissues with regard to their application

in cell-based therapy. In order to generate a cell-based therapy appropriate for clinical translation, it is essential to identify the most suitable source, preferably obtainable by minimal invasive procedures. Sufficient numbers of cells must be harvested from the identified source to be further expanded in culture in order to reach numbers that can be applied therapeutically with success. It is therefore important to study adipose tissue derived MSCs to determine their different respective characteristics and growth abilities.

Collaborative efforts are also necessary early in research attempts especially when considering harvesting from healthy donors. Protocols for correct harvesting techniques need to be established in order to standardize findings. Similarly, a routine protocol for the isolation, expansion and characterization and differentiation of MSCs needs to be developed, before applications of these cells can be considered for therapeutic purposes in South Africa. Stem cell therapy is in its early stages in South Africa and considerable investigation has to be done before application of these cells can be justified in clinical settings.

The aim of this project is to establish a fundamental basis to cell based therapy, by obtaining a population of adipose-derived stromal cells (ASCs) that is well defined and whose behaviour is understood. This will be done by assessing firstly the plastic adherence capacity of the cells, secondly their immunophenotype using a set of cell surface markers (CD34, CD45, C73, CD90 CD105) by flow cytometry and thirdly, differentiation into adipogenic, osteogenic and chondrogenic will be examined.

The second aim is to transduce ASCs with green fluorescent protein positive lentiviruses and to confirm that the population of ASCs adhere to the characterization criteria listed above. This procedure will be useful for future *in vivo* studies, to study the homing properties as well as growth, proliferation and differentiation capacities of ASCs.

The objective of this study is to explore optimal adipose tissue harvesting techniques, to establish standard operating procedures for ASC isolation, expansion and immunophenotypical characterizing, tri-lineage differentiation (adipocytes, osteocytes and chondrocytes) and confirmation using lineage specific classical stains for differentiation. In preparation for future pre-clinical studies, a viable tracking system is needed to study ASCs *in vivo*. The second objective of this study is to determine if transduced ASCs adhere to ASC characterization criteria and if differentiated cells still express GFP.

The findings of this project will establish a strong foundation for future research. We aim to address and discuss basic cell biology findings keeping in mind the important concept of using translational research from bedside to bench.



A historical overview of the nomenclature of mesenchymal stem cells and their properties.

What's in a name? That which we call a rose

By any other name would smell as sweet. '

Shakespeare W. *Romeo and Juliet*, (1594). Act II, scene II, line

Introduction

A stem cell is defined by its ability to self-renew and its ability to differentiate along multiple lineage pathways. These unspecialized cells have the potential to develop into many different cell types in the body during their lifespan, serving as an internal repair system. Even after long periods in quiescence, stem cells retain the ability to divide and the two daughter cells have the potential to either remain a stem cell within the stem cell niche or to develop into a more specialized cell with specific cell functions.

Stem cells should meet the following criteria for regenerative medical applications: (1) found in abundant quantities; (2) require minimally invasive harvesting procedures; (3)

differentiate along multiple cell lineage pathways in a regulatable and reproducible manner; (4) be safe and effective in transplantations to either an autologous or allogeneic host; (5) should be manufactureable in accordance with current Good Manufacturing Practise guidelines (Gimble *et al.*, 2007).

History and nomenclature of mesenchymal stem cells

About 40 years ago Friedenstein and co-workers (1968) isolated stem cells from bone marrow (BM). With low-density culturing of BM the non-adherent haematopoietic stem cells (HSCs) were discarded and fibroblast-like plastic-adherent cells with the capacity to differentiate into bone were identified. These fibroblastic precursors derived from an entity with unknown anatomical location within BM were later described as colony-forming unit fibroblasts (CFU-Fs) when Friedenstein and colleagues demonstrated colony formation initiated by single cells after seeding BM cell suspensions at clonal density. In addition, these colonies demonstrated a linear dependence of colony formation on the number of cells explanted (Friedenstein *et al.*, 1968; Friedenstein *et al.*, 1970).

Friedenstein together with Owen experimentally generated skeletal tissues *in vivo* from the progeny of a single BM stromal cell (BMSC) and called this cell an ‘osteogenic stem cell’ or a ‘stromal stem cell’ (Friedenstein *et al.*, 1987; Owen, 1988; Owen and Friedenstein, 1988).

Supported by published experimental results, the concept of a non-hematopoietic stem cell in BM was proposed as a sub-population. This second type of stem cell, present in the hematopoiesis-supporting stroma of BM, was introduced as mesenchymal stem cells (MSCs), mesenchymal stromal cells, or bone marrow stromal stem cells (Owen and Friedenstein, 1988). Although experimental evidence was published and widely reproduced, the concept of a non-hematopoietic stem cell in BM only echoed worldwide until a commercial entity, Osiris Therapeutics Inc, published similar findings in 1999 (Pittenger *et al.*, 1999). Although the term ‘mesenchymal stem cell’ was introduced during the 1980s, it was Caplan (1991) who popularised this term for the non-hematopoietic stem cells found *ex vivo* (Abdi *et al.*, 2008; Caplan, 1991).

Culture expanded cells become more uniform, because clones of cells which divide rapidly have the greatest capacity for proliferation and a competitive advantage. *In vitro* expansion therefore produces selective cell populations that have been ascribed various names, including bone marrow stromal cells, mesenchymal stem cells and adult multipotent progenitor cells. These terms are not synonymous with regard to their precise definitions and biological capabilities (Muschler *et al.*, 2004). By the year 2005, the acronym ‘MSC’ for plastic-adherent cells isolated from various tissues with multipotent differentiation capacity *in vitro*, was firmly engrained in the vernacular of stem cell biologists and clinical cell therapists. After concerns were raised over the use of the term ‘mesenchymal stem cells’, calls for a consensus on the standardization and

clarity of nomenclature and terminology was launched to reduce confusion and avoid misrepresentation in the field (Horwitz *et al.*, 2005; Diminici *et al.*, 2006; Wagner *et al.*, 2005).

Horwitz believed maintaining the acronym MSC is vital as it has been used in the literature for at least two decades and it indicates a general cell type, but suggested that the term mesenchymal stem cell be replaced with multipotent mesenchymal stromal cell. Furthermore it was suggested that the term mesenchymal stem cells be used for a sub-population within the heterogeneous population of cells that can generate fibroblastic like colonies (CFU-F) since the data was insufficient to characterize unfractionated plastic adherent marrow stem cells (Horwitz *et al.*, 2005).

Bianco and colleagues reviewed MSC history, concepts and assays and found that the term MSC is questionable. They claimed that assumptions revolving around two defining characteristic properties of stem cells, multipotency and self-renewal, were neither included in the original concept of non-hematopoietic stem cells in the BM nor were they supported by direct experimental evidence relevant to both properties as well as additional criteria such as clonogenicity. In addition, the original notion of MSCs specifically referred to stem cells within the bone marrow, but has now been extended to include cells from virtually all postnatal tissue sources (Bianco *et al.*, 2008).

Bianco and co-workers suggested that multiple dimensions, such as function, assays or surface phenotype and anatomy be used to develop terminology for these cells. Relating HSC bioassay principles to MSCs: (1) probing stemness through *in vivo* transplantation experiments; (2) only investigating multipotency abilities at a single cell level; and (3) self-renewal would refer to the reconstitution of a stem cell population, identical in phenotype and function to the original explanted cell (Bianco *et al.*, 2008).

When using the functional dimension, a postnatal stem cell would usually be defined by the types of cells it generates (Bianco *et al.*, 2008). Without direct evidence demonstrating that a single BM-MSc can generate tissue types beyond skeletal tissue *in vivo*, it was proposed to refer to these cells as 'skeletal stem cell'. On another note, with the nomenclature extending across most post-natal tissues, they further suggested that 'CFU-F' to be used to describe a cell that is assayed as clonogenic in culture (indicating the experimental dimension, reflecting the origin of the population in question) and that isolation from a specific tissue can be specified with a prefix (AT-CFU-F for adipose derived cells) (Bianco *et al.*, 2008).

Taking only MSCs resident in adipose tissue into consideration the following nomenclature appears to be acceptable: adipose-derived stem cells, adipose-derived stromal cells (ASCs), adipose derived adult stem (ADAS) cells, adipose-derived adult stromal cells, adipose stromal cell blasts, preadipocyte and processed lipoaspirate cells, are all different names found in the literature, that hold the same merit (Gimble *et al.*, 2007). After an incubation process at 37°C/5% CO₂ in non-inductive control medium the SVF of adipose tissue takes on different terminology.

Zuk and co-workers (2001) uses different terminology at different stages of isolation and culturing. After an incubation process at 37°C/5% CO₂ in non-inductive control medium, the adipose derived stromal vascular fraction (SVF) is then termed processed lipoaspirate (PLA) (Zuk *et al.*, 2001) and clonal isolates from adipose tissue are termed adipose derived stem cells (ADSCs) (Zuk *et al.*, 2002).

Careful consideration should be taken regarding pericytes. Considering Bianco and co-workers' approach with regard to functionality and phenotype, a pericyte candidate emerges as a potential MSC population (Bianco *et al.*, 2008). According to this theory pericytes should be classified as MSCs, but where do we draw the line?

A pericyte by definition is an elongated, contractile cell that is wrapped around a precapillary arteriole outside the basement membrane of the vascular endothelial cells (Saunders, 2000). Since pericytes were first described about 120 years ago, they have been isolated from various tissues. Their function is a little mysterious, though through their contractile activity, it is hypothesized that they contribute to the regulation of microvascular bloodflow. Morphological similarities shown between pericytes and smooth muscle cells, as well as cytoplasmic proteins of smooth muscle cells present in pericytes (cyclic GMP-dependent protein kinase, smooth muscle-specific isoforms of myosin and tropomyosin), support this hypothesis (Tilton *et al.*, 1979; Joyce *et al.*, 1985a; Joyce *et al.*, 1985b; Joyce *et al.*, 1984). Using immunoelectron microscopy, Skalli and co-workers (1989) found that pericytes from several organs in humans and rat contain α -smooth muscle actin. This actin isoform is usually found in smooth muscle cells and vascular smooth muscle cells, where the α -smooth muscle actin is localized only in microfilaments, used during contraction.

In vitro expansion produces selective cell populations that have been ascribed various names, including bone marrow stromal cells, mesenchymal stem cells and adult multipotent progenitor cells. These terms are not synonymous with regard to their precise definitions and biological capabilities (Muschler *et al.*, 2004). The International Society for Cellular Therapy (ISCT) stated that the term multipotent mesenchymal stromal cells (MSCs) will be used for cells obtained from BM and other tissues that adhere to plastic (Horwitz *et al.*, 2005).

Gimble and colleagues (2007) reported on the consensus reached by the International Fat Applied Technology Society (IFATS) to adopt the term 'adipose-derived stem cells' (ASCs) to identify the isolated, plastic-adherent, fibroblastic like, multipotent cell population derived from adipose tissue. With the validity of the term 'stem cell' to be questioned, the Society proposes that the acronym 'adipose-derived stromal cells' would also be accepted (Gimble *et al.*, 2007).

In 2013, the ISCT reviewed the nomenclature and characterising guidelines for ASCs. The International Federation for Adipose Therapeutics and Science and the ISCT deemed it important to distinguish between AD-SVF and culture expanded adipose tissue-derived stromal/stem cells (ASCs). After the neutralisation of the digestion procedure, the

released elements defined as the SVF will be separated from the mature adipocytes by centrifugation. The SVF, consisting of a heterogeneous mesenchymal population of cells, is seeded into culture selecting for an adherent cell population less heterogeneous than the SVF. This adherent heterogeneous sub-population is then termed the adipose tissue-derived stromal cells. Since ASCs are derived from the SVF, the authorities have restricted the description of the heterogeneous SVF cell populations to stromal cells (Bourin *et al.*, 2013).

Development of isolation processes

The isolation of MSCs from most postnatal organs and tissue has been well described in the literature (Table 2.1). Dominici and colleagues raised the following question in 2006: ‘If these different tissue sources and methodologies are used for the preparation of MSCs, are these MSCs sufficiently similar to allow for direct comparison of reported biological properties and experimental outcomes, especially in the context of cell based therapy?’

Table 2.1 Different sources from which MSCs have been isolated.

Tissue type	MSC abbreviation	Author and Year Reference
Bone marrow	BM-MSCs/ MSCs	Friedenstein <i>et al.</i> , 1968
Mandibular bone marrow	MBMSC	Jo <i>et al.</i> , 2007
Umbilical cord blood	UCB-MSCs/ hUCMSCs	Bieback <i>et al.</i> , 2004; Kern <i>et al.</i> , 2006; Matsuzuka <i>et al.</i> , 2010; Wang <i>et al.</i> , 2004
Adipose tissue	ASCs	Zuk <i>et al.</i> , 2001
Skeletal Muscle	Satellite Cells	Lee <i>et al.</i> , 2000; Charge and Rudnicki, 2004
Menstrual blood/ Endometrial blood	Endometrial Regenerative Cells (ERC)	Meng <i>et al.</i> , 2007
Umbilical cord (Wharton’s jelly)	hUC-MSCs	Pereira <i>et al.</i> , 2008
Brain-Neural stem cells	NSCs	Doetsch <i>et al.</i> , 1999; Morshead <i>et al.</i> , 1994; Xu <i>et al.</i> , 2008
Deciduous teeth (dental pulp)	SHED	Miura <i>et al.</i> , 2003
Wisdom teeth (dental pulp)	DPSCs	Gronthos <i>et al.</i> , 2000
Permanent teeth (dental pulp)	DPSCs	Suchánek <i>et al.</i> , 2007
Apical papilla	SCAP	Govindasamy <i>et al.</i> , 2010
Periodontal ligament	PDLSC	Park <i>et al.</i> , 2011 Shi <i>et al.</i> , 2005
Periapicalfollicular	PAFSC	Jo <i>et al.</i> , 2007
Skin (skin –derived precursor cells)	SKPs	Toma <i>et al.</i> , 2001
Blood vessel associated stem cells	Mesoangioblasts	Sampaolesi <i>et al.</i> , 2003
Epithelium tissue, epidermis and intestinal crypts	Epithelium tissues have different structural units of stem cells	Slack, 2000

Hair follicle dermis	HFD-MSCs	Hoogduijn <i>et al.</i> , 2006; Yu <i>et al.</i> , 2006
Pancreas	PMSCs	Hu <i>et al.</i> , 2003
Prostate epithelium	Prostate colony-forming cell (Pr-CFC)/ prostate stem cells	Collins <i>et al.</i> , 2001
Kidney	Renal stem cells/ MRPC	Gupta <i>et al.</i> , 2006
Periosteum	PDPCs	Nakahara <i>et al.</i> , 1991; De Bari <i>et al.</i> , 2001, 2006
Synovial membrane	SMSCs	De Bari <i>et al.</i> , 2001, 2003
Liver	HLSCs	Herrera <i>et al.</i> , 2006
Central nervous system	CNS stem cells/ Neural stem cells	McKay, 1997 ; Morshead <i>et al.</i> , 1994; Reynolds and Weiss, 1992; Gage, 2000
Peripheral nervous system	PNS stem cells	McKay, 1997

Although these MSC isolates from different sources ostensibly share similar properties (Dominici *et al.*, 2006; Sarugaser *et al.*, 2009; Si *et al.*, 2010), isolating protocols as well as generated data between different scientific groups differ. Various laboratories have developed in-house methods to isolate, expand and differentiate MSCs, some of which differ quite significantly while others are quite similar. These differences result in controversies regarding terminology used as well as data comparisons between different research groups.

Properties of MSC's

The advantages of using ASCs rather than embryonic stem cells or other sources of adult stem cells are underscored by: i) the ease in obtaining MSC containing tissue, via minimal invasive procedures; ii) the lack of ethical controversies; iii) the immunosuppressive effects that MSCs display *in vivo*; iv) their ability to home to the site of injury; v) their ability to attenuate tumour formation and vi) their antibacterial properties. The mechanisms by which some of these events occur are not yet fully understood.

Homing of MSCs

Trafficking and homing of MSCs to sites of inflammation is a property of particular interest for clinical applications. It has been demonstrated that MSCs express a variety of chemokines and chemokine receptors and home to inflammatory sites by migrating towards inflammatory chemokines and cytokines (Sordi *et al.*, 2005). Mesenchymal stem cell homing is defined as the arrest of MSCs within the vasculature of a tissue followed by transmigration across the endothelium. This definition is non-mechanistic because of the current absence of a definite MSC homing mechanism (Karp and Teo, 2009).

The site, route and manner of administration play an important role in the fate of the transplanted cells and the success of engraftment. Systemic administration is the least invasive, but would require the cells to home to the site of injury. These procedures include intravenous (IV) injection or infusion, intra-peritoneal (IP) injection, intra-arterial (IA) injection or infusion and intra-cardiac (IC) injection (Chamberlain *et al.*, 2007).

Various studies have reported complications of entrapment of donor cells in the lung when MSCs are delivered intravenously. This complication could be caused by the culture expanded MSCs that are relatively high in number, with enlarged cells that are activated and express adhesion molecules. It was further suggested that co-administration of MSCs with a vasodilator (sodium nitroprusside) would decrease the number of entrapped cells (Chamberlain *et al.*, 2007). The collective term for access to substrate molecules (oxygen, glucose and amino acids) and the clearance of metabolic products (CO₂, lactate and urea) is *mass transport*. Because of the diffusion limitations of these molecules, the transplanted cells are at high risk of dying before significantly contributing to the healing response (Muschler *et al.*, 2004).

Wu and colleagues (2003) delivered rat MSCs intravenously to treat heart allograft rejection. They found that infused MSCs vigorously migrated to the site of immune rejection, where they mainly differentiated into fibroblasts and a small number of myocytes (Wu *et al.*, 2003). Another study by Ortiz and co-workers showed that intravenously administered MSCs home to the site of injury in the lungs, where they differentiate into epithelial-like cells and reduce inflammation (Ortiz *et al.*, 2003). Karp and Teo reviewed in 2009 that significant evidence indicates that in settings of inflammation or injury, infused MSCs have higher engraftment efficiency (Karp and Teo, 2009). A possible mechanism is that MSCs actively home to tissues using leukocyte-like cell-adhesion and transmigration mechanisms. Investigators suggested that specific MSC-endothelial interactions regulate transmigration, although further studies are required to study this phenomenon in an induced inflammatory condition (Karp and Teo, 2009). Ruster and colleagues used intravital microscopy in 2006 to observe intravenously administered human MSCs which rolled along the walls of blood vessels in the ear veins of mice. This phenomenon was significantly decreased in P-selectin deficient mice, suggesting that P-selectin and a counter-ligand are involved in the extravasation of MSCs. Since neither P-selectin glycoprotein ligand-1 nor the alternative ligand CD24 are present on human MSCs, it was proposed by Ruster and co-workers that a novel MSC expressed carbohydrate ligand was the counter ligand for endothelially expressed P-selectin. Although E- and L-selectin have been reported absent, similarities can be drawn between the transmigration mechanism of leukocytes and MSCs, for example the rolling effect upon and adhesion to endothelium (Ruster *et al.*, 2006).

Immunosuppression

Transplanted MSCs derived from a healthy donor are expected to overcome the immune response of the host as MSCs are known to be immune privileged. With genetic disorders, theoretically two therapeutic options with regard to stem cells are considered. One, autologous genetically engineered stem cells to ‘repair’ the defect and two, allogeneic stem cells in combination with life-long immunosuppressive treatment in order to avoid graft versus host disease (GVHD). Both of these options expose the patient to significant risk. A third option is made possible through the capacity of MSCs to ‘evade’ the host immune system by suppressing the function of T-lymphocytes (T-cells). The immune phenotype of MSCs is regarded as non-immunogenic and, therefore, transplantation into an allogeneic host may not require immunosuppression.

Major histocompatibility complex class I (MHC) may activate T-cells but, in the absence of co-stimulatory molecules, a second signal cannot engage, leaving the T-cell anergic. Many reports have described MSCs to modulate many T-cell functions including cell activation. This form of suppression is independent of MHC matching between recipient T-cells and donor MSCs. MSCs have also been shown to have immune modulatory properties by impairing maturation and function of dendritic cells and B-cell proliferation, differentiation and chemotaxis (Chamberlain *et al.*, 2007).

Mesenchymal stem cell-mediated immune regulation is the result of the cumulative action of several molecules. Interferon- γ (IFN- γ) mediates this unique property by acting through soluble secretory molecules (cytokines and chemokines). These molecules are induced or up-regulated following cross-talk with target cells (Ghannam *et al.*, 2010). Mesenchymal stem cells do not constitutively express indoleamine 2, 3-dioxygenase (IDO), but can be induced by IFN- γ to catalyse a tryptophan to kynurenine conversion, thereby depleting tryptophan and inhibiting T-cell proliferation (Munn *et al.*, 1998). In the absence of IFN- γ , MSC immune suppressive activity is augmented by Toll-like cell surface receptors through an autocrine interferon- β (IFN- β) signalling loop (Opitz *et al.*, 2009). Immune suppressive mechanisms also differ between species. For example, nitric oxide plays a vital role in the immune regulation of murine MSCs, while human MSCs employ the effector molecule IDO to catalyse the rate-limiting step in the degradation of tryptophan (Ren *et al.*, 2009).

Recent data from Ghannam and co-workers (2010) suggests that MSCs exert their action at two levels. First, action occurs locally with the secretion of mediators to inhibit the proliferation of immune cells in the vicinity of MSCs and second, action involves the induction of a systemic response, either an anti-inflammatory Th2 immune profile or the generation of T-regulatory cells (Ghannam *et al.*, 2010).

Cancer Inhibiting Properties

It is well known that IFN- β has the ability to strongly inhibit tumor cell growth and induce apoptosis *in vivo* (Wong *et al.*, 1989; Zhang *et al.*, 1999; Chawla-sarkar *et al.*, 2001). The anticancer potential of Wharton's jelly-derived stem cells was evaluated by the co-culturing these MSCs and MDA 231 human breast carcinoma line. Colony growth and DNA synthesis of the latter was significantly reduced. It was also shown by Ayuzawa and co-workers that the MSC-conditioned media attenuated growth of the MDA 231 cell line and increased the G2 (cell cycle point) population (Ayuzawa *et al.*, 2009).

Interferon- β has a short half-life and the maximum tolerated dose is lower than the effective dose *in vivo*, which renders administration of INF- β unsuccessful. Several studies demonstrate effective administration of IFN- β by incorporating the IFN- β gene into adenoviral vectors. However, the effectiveness of adenoviral vector-based gene delivery to tumour tissues is still unclear and vector-based gene delivery is not cancer specific (Matsuzuka *et al.*, 2010). To address this quandary, human MSCs have been utilized as biological vehicles for IFN- β gene delivery. Systemic administration of MSC-based IFN- β gene therapy shows effective attenuation of metastasis of breast cancer, melanoma (Studený *et al.*, 2002) and glioma (Nakamizo *et al.*, 2005; Studený *et al.*, 2004).

It has previously been demonstrated that human umbilical cord blood mesenchymal stem cells (hUCMSCs) do not form teratomas when injected into severe combined immunodeficiency (SCID) mice and furthermore that systemic IFN- β gene transduced hUCMSCs (IFN- β -hUCMSCs) successfully home to tumour sites and attenuate growth of lung-metastasized breast tumor (Matsuzuka *et al.*, 2010; Rachakatla *et al.*, 2007). Recently the same group evaluated this novel therapy in more difficult cancers and reported that IFN- β -hUCMSCs are capable of decreasing tumour formation by human bronchioloalveolar carcinoma cells through producing IFN- β and inducing cell death via both intrinsic and extrinsic apoptotic pathways (Matsuzuka *et al.*, 2010).

Antibacterial properties

Among the key effector molecules responsible for bacterial killing are antimicrobial proteins and peptides. One of the main antibacterial peptide families present in mammals, the cathelicidin family, is represented in humans by hCAP-18 or LL-37 which are either constitutively produced or induced upon stimulation. Although these peptides are known to be produced mainly by phagocytic leukocytes and epithelial cells, it was suggested that MSCs also express LL-37 which exerts anti-microbicidal activity by disrupting bacterial membrane integrity (Coffelt *et al.*, 2009; Zanetti *et al.*, 2005). Nijnikand and Hancock (2009) indicated that LL-37 has a wide range of biological activities that includes direct killing of organisms, chemotaxis and chemokine induction, regulation of inflammatory responses, wound healing, angiogenesis, anti-apoptosis and aids in horizontal DNA intracellular transfer (Nijnik and Hancock, 2009).

Krasnodembskaya and colleagues (2010) demonstrated that the expression of LL-37 peptide by MSCs is inducible by *E coli* exposure at both the mRNA and protein levels. They further demonstrated that MSCs produce and secrete substantial quantities of this antimicrobial soluble peptide that inhibits bacterial (Gram positive and Gram negative) growth *in vitro* and *in vivo*. These results demonstrate that MSCs participate in the host defence system through the secretion of an antimicrobial peptide, which is one of the essential parts of the innate immune system (Krasnodembskaya *et al.*, 2010).

ASC associated Clinical trials

There are currently 397 clinical trials registered on the United States Food and Drug Administration (FDA) website using the search term ‘mesenchymal stem cells’. These trials include application of MSCs derived from different sources. The search term ‘adipose derived stem cells’ on the same website produced 104 studies worldwide (Figure 2.1.), applying adipose derived stem cells to different diseases or injuries such as: spinal cord injury, liver cirrhosis, Crohn’s disease and chronic fistulae, muscular skeletal injuries, neurodegenerative diseases, cardiomyopathy as well as GVHD and autoimmune diseases. Different diseases, injuries and defects all have different conditions and complications and although ASCs serve as a common intervention denominator, large differences exist with the application, dose, as well as the specified source of ASCs (see Appendix 2.1)(<http://clinicaltrials.gov>).

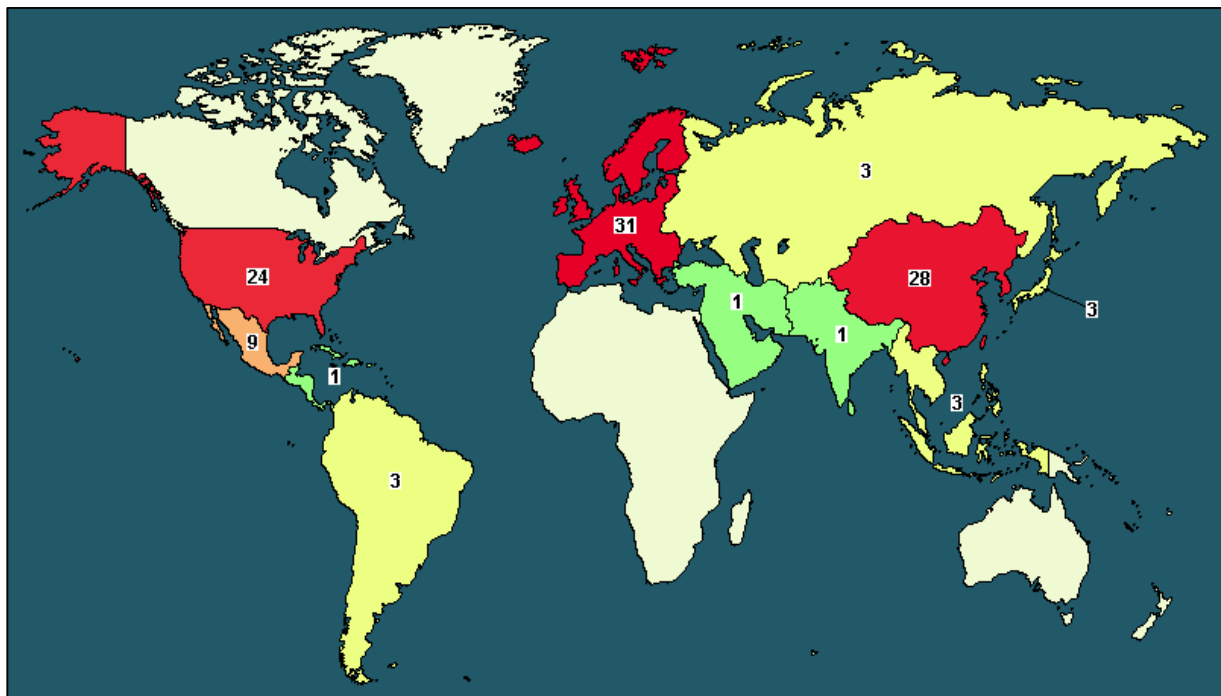


Figure 2.1. A world map indicating a total of 104 clinical trials found using search terms ‘adipose derived stem cells’ cited at www.clinicaltrials.gov

According to the search, the front runners in this field are North America, Europe and Asia, while Africa and Australia takes a back seat with no registered ASC associated clinical trial to date (<http://clinicaltrials.gov>). Interestingly, only four countries within

the above mentioned continents are the major role players: for North America, the United States and Mexico; in Europe it is Spain; and in Asia it is the Republic of Korea (Figure 2.2.).

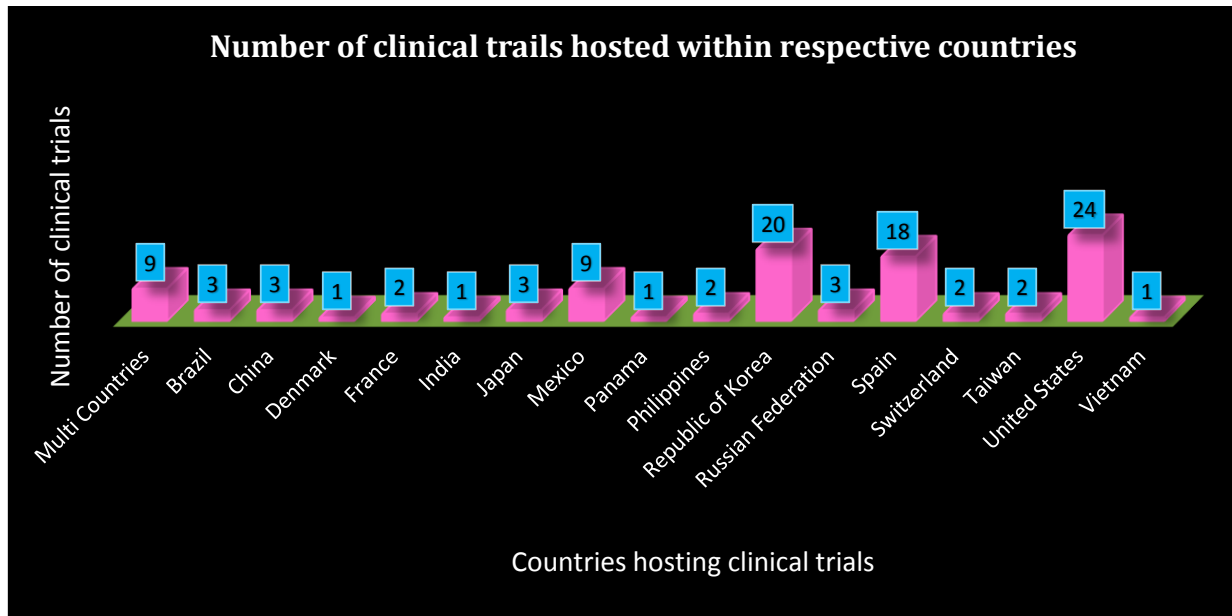


Figure 2.2. Clinical trials listed on www.clinicaltrials.gov using search term ‘adipose derived stem cells’ that are registered globally. Trials registered within more than one country or not associated to any country are displayed within the multi countries group.

The first ASC associated clinical trial registration was received on 22 June 2005, with identity number NCT00115466 (See Appendix 2.1). The safety and efficacy of interlesional injections with autologous expanded (cultured) ASCs loaded into a fibrin glue graft were analysed in patients with Crohn’s associated anal fistulae. A steady incline in new trial registrations was observed from 2005 till 2010. Since 2011 this promising field received a growth spurt of interest with new registrations despite the shortage of research funds with the world economic recession in the background (Figure2.3.).

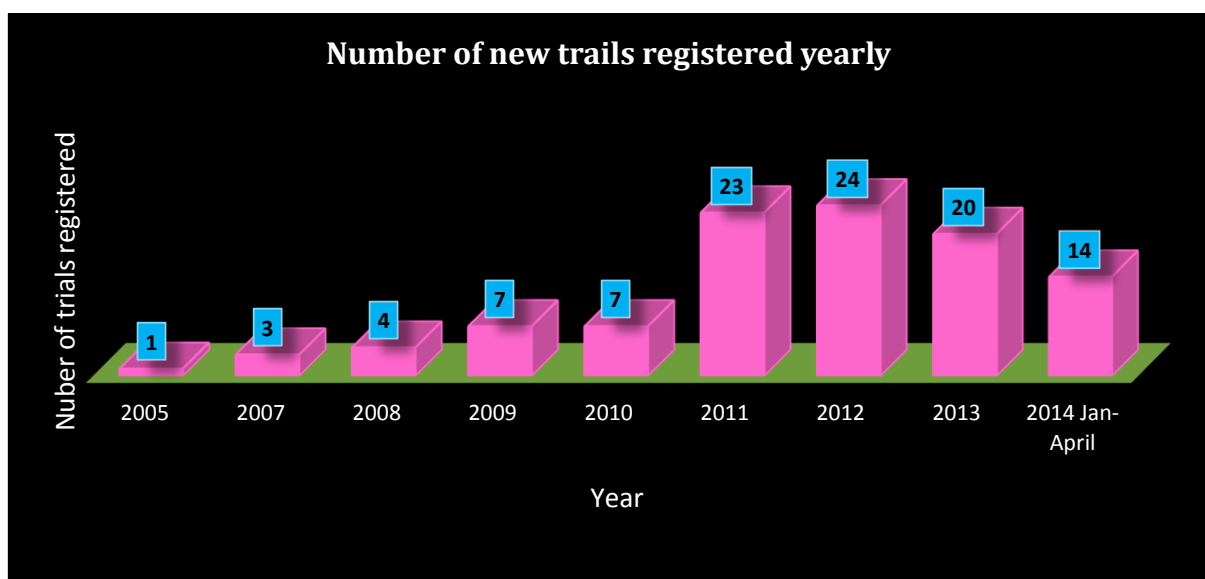


Figure 2.3. A total 103 clinical trial registrations listed on www.clinicaltrials.gov under search term 'adipose derived stem cells' was received globally since 2005. The figure illustrates the amount of trial registrations received per year.

With increasing interest in the stem cell field, clinical trials are showing high activity in terms of recruitment (> 50% currently recruiting and 20% completed). For rare conditions patients are recruited by invitation, where the newly registered studies are not yet recruiting patients and studies that have not updated their progress reports or their recruiting status, are active but not recruiting at the moment. For unknown reasons three studies were terminated (Figure 2.4.).

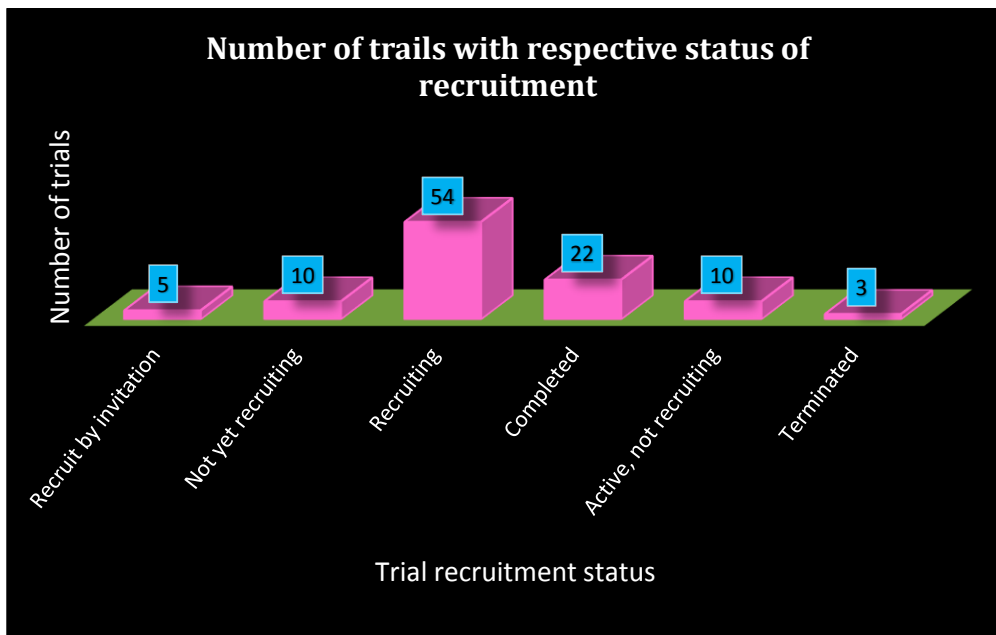


Figure2.4. The recruitment status of clinical trials listed on www.clinicaltrials.gov under the search term 'adipose derived stem cells'.

A wide variety of conditions are studied within the listed trials (Figure 2.5.). The high interest in Cohn's disease or complex fistula is a clear demonstration of bio-entrepreneurs taking direct advantage of the immunosuppressive property and anti-inflammatory quality of ASCs. The most obvious application of ASCs or AD-SVF would be fat grafts with ASC assisted lipotransfer in breast reconstruction, but most breast reconstruction trials listed were only recently registered between 2012 and 2014. Observed within the trials (see Appendix 2.1) and reviewed by Zuk in 2013 certain conditions *e.g.* rheumatoid arthritis, other autoimmune diseases and multiple sclerosis have been using culture expanded ASCs and reported favourable functional outcomes to date (www.clinicaltrials.gov; Zuk, 2013).

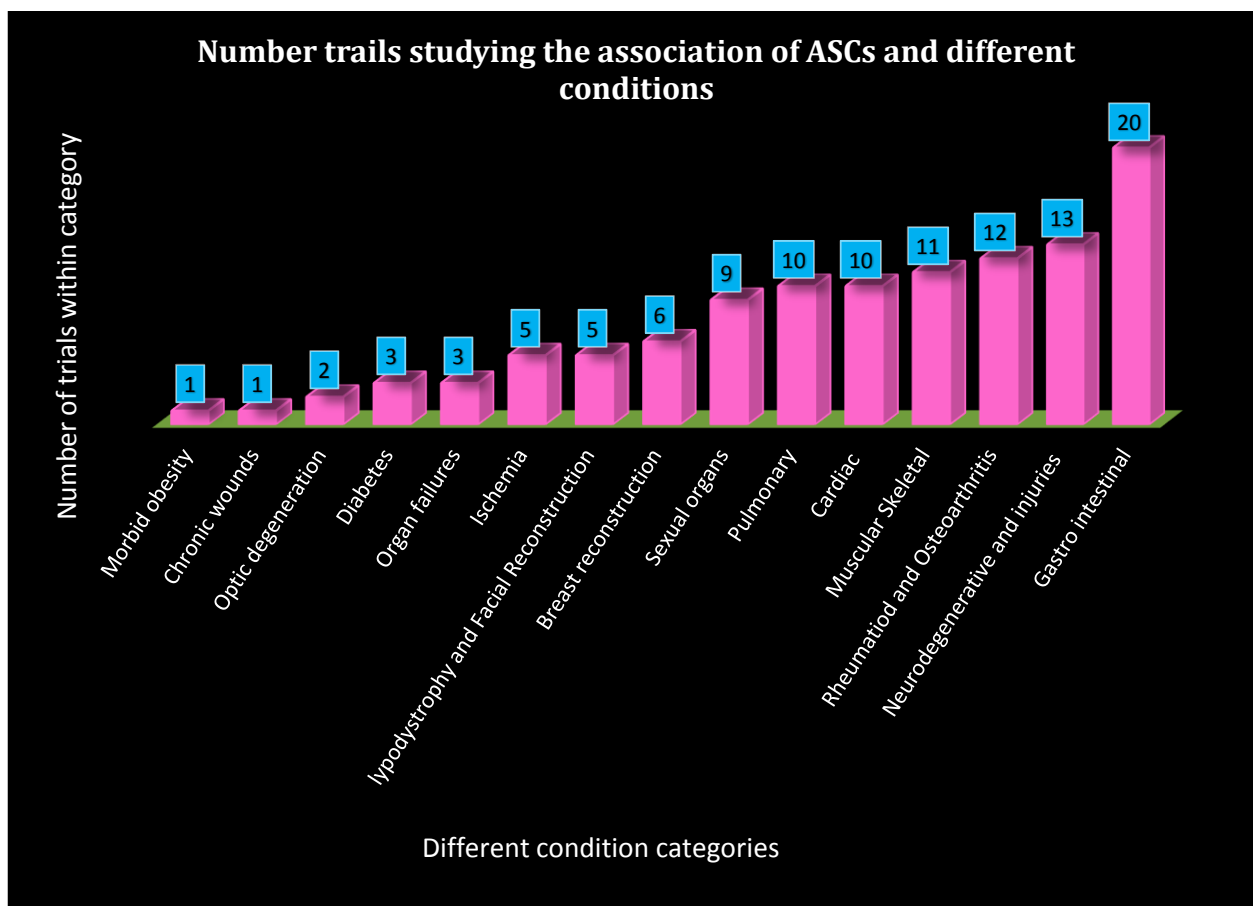


Figure 2.5. The number of trials listed (under search terms ‘adipose derived stem cells’ on website www.clinicaltrials.gov) within a specific condition category. The summary of for each trial is available within Appendix 2.1.

There is controversy about the *in vivo* localization and persistence of ASCs after administration and the route of administration plays a direct role. The route of administration within the listed trials definitely favours local or site specific injections (65%) rather than intravenous infusions or intra-arterial injections (Figure 2.6.). Eggenhofer and colleagues (2012) however stated that intravenous ASCs infusion has proven to be safe and large amounts can be administered at one time (Eggenhofer *et al.*, 2012).

Tracking studies have indicated that most intravenously infused ASCs are short-lived and retained in the lungs due to size constrictions, but tend to migrate to other tissues and sites of injury within hours (Assis *et al.*, 2010; Barbash *et al.*, 2003; Eggenhofer *et al.*, 2012; Kraitchman *et al.*, 2005; Fisher *et al.*, 2009; Yukawa *et al.*, 2012). Cultured ASCs are more than 20 μm in diameter which is much larger than circulating immune cells as well as micro-capillaries within the lungs (Crop *et al.*, 2010).

Care should be taken with alternative routes of ASC administration, as ASCs can be localized within alternative filtering organs. Shi and colleagues found that ASCs administered via the portal vein were found in the liver (Shi *et al.*, 2010; Yukawa *et al.*, 2012). Various studies found that following site specific administration of ASCs *e.g.* intra-

muscular, intra-theacal and intra-articular, the cells remained present locally for up to several weeks following the procedure (Boulland *et al.*, 2012; Hu *et al.*, 2012).

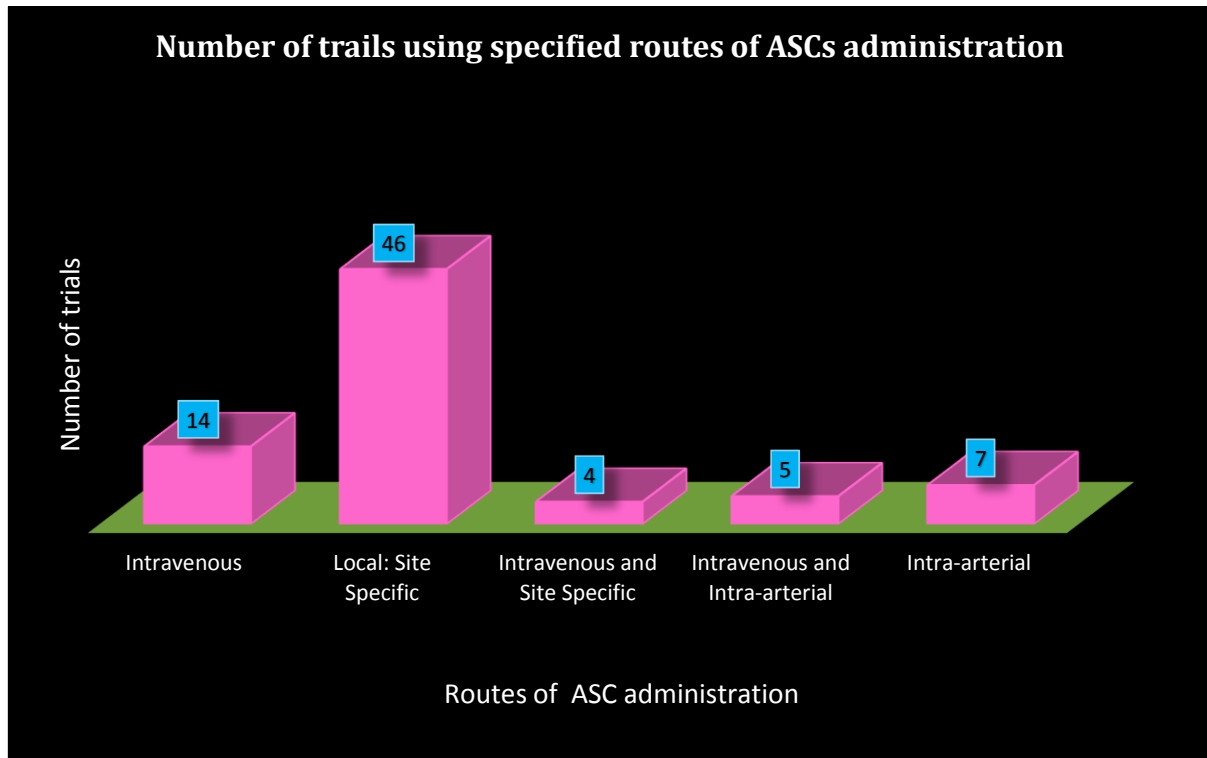


Figure 2.6. Different routes of ASC administration within the listed clinical trials on www.clinicaltrials.gov under search term 'adipose derived stem cells'.

Great variability is observed between the different sources of ASCs used in clinical trials, although autologous ASCs are definitely favoured above allogeneic ASCs as a source (Figure 2.7.). The field of immune suppression and immune modulation by ASCs are not yet well defined and understood. Researchers, bio-entrepreneurs and clinical trials could therefore favour autologous vs. allogeneic transplantation because of the decreased risk of GVHD, rejection of transplanted cells and/or graft, as well as contracting infectious diseases. Little difference is seen between the number of autologous SVF and the autologous cultured ASCs (Figure 2. 7.), even though strict rules and regulations are associated with the transplantation, implantation, infusion or transfer of expanded stem cells.

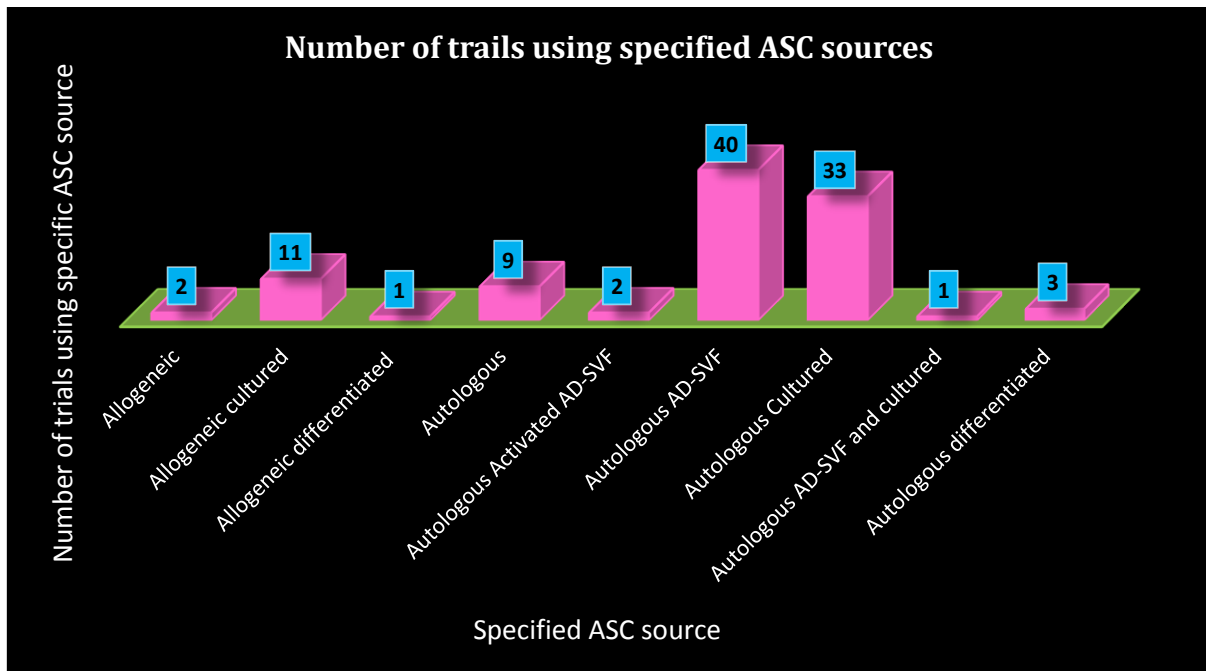


Figure 2.7. Specified ASC sources used as intervention for different conditions within the listed clinical trials on www.clinicaltrials.gov under search term 'adipose derived stem cells'.

Medicolegal aspects

The concept of “stem cell tourism” has been used for facilities *e.g.* stem cell clinics, that offer various stem cell based interventions for a range of conditions to desperate patients for a hefty fee. These interventions are often in early research phases with some of them having improbable outcomes. The absence of regulatory bodies promotes this ongoing activity especially in countries like China, Mexico and the Bahamas.

Despite the lack of legislation in South Africa with regard to stem cell banking and treatment, globalization of stem cell regulations or international agreements are highly recommended and desired to promote ethical application of cell therapy and tissue engineering to patients. In general, responses to the ethical, cultural and legal issues on human cellular and tissue-based technologies for clinical applications are multiple and differ among nations. Regulations tend to be unified at least within the European Union (EU), which considers the International Organization for Standardization (ISO) system as the standard, but the USA and major Asian countries have their own regulations, although they do respect the ISO and FDA regulatory systems (Lysaght and Campbell, 2011).

In the United States of America (USA), any tissues used for medical purposes are categorized either as devices (as in the case of allograft heart valves and dura mater), as biologics (as in the case of blood components and products) or as a drug. Biologics that meet all the criteria according to section 1271.10 of the Code of Federal Regulations for Food and Drugs are exempted from premarket approval. Human cells and tissue-based products must be: (1) minimally manipulated; (2) intended only for autologous use only;

(3) not combined with another article, except for water, sterilizing, preservation or storage agents; (4) have no systemic or metabolic effect, or (5) for autologous use, allogeneic use for first and second degree blood relatives, or reproductive use (Lysaght and Campbell, 2011).

Engineered tissue products would be classified according to certain characteristics: (1) the relationship between the donor and recipient of the biological material used to produce the tissue product; (2) the degree of *ex vivo* manipulation of the cells comprising the tissue products; (3) whether the tissue product is intended for autologous use, for metabolic or structural purposes, or to be combined with a device, drug, or biologic. The FDA classifies allogeneic living engineered skin tissue as a medical device and autologous cultured chondrocytes as a biologic device. The regulation pertaining to the clinical use of autologous cells differs among nations (Ikada, 2006).

Currently the Regenerative Sciences Inc vs. FDA lawsuit is questioning the authority of the FDA to determine if cultured expanded autologous ASCs fall in the medical procedure or drug manufacturing regulation category. In the Federal Registration rules, the definition of ‘minimal manipulation’ is ‘processing that does not alter the relevant biological characteristics of cells or tissue’ (66 Fed. Reg. 5467), although it further states that ‘we do not agree that the expansion of mesenchymal stem cells in culture or the use of growth factors to expand umbilical cord blood stem cells are minimal manipulation’ (66 Fed. Reg. 5457). One of the arguments within this lawsuit counters the FDA on procedural grounds, failing to explain how culture expansion alters the relevant biological characteristics of stem cells as well as failing to use legislative rulemaking procedures (Lysaght and Campbell, 2011). The court upheld the FDA’s status quo and defined the Regenexx™ cell product as a ‘drug’, the reasons being 1) it is to affect the structure or function of the body and 2) it acts as a biologic product with application to prevention, treatment or cure of a disease, injury or condition in humans.

Medical innovators agree that stem cell therapies should be regulated, but argue that the context of autologous adult stem cells regulations should be recalibrated to consider a risk-benefit balance. A plea to the current regulations with regard to human cell, tissue and tissue based products, that they are ill-suited to many kinds of cellular therapies and must be redesigned to fit the parties and products being regulated (Chirba-Martin and Noble, 2013; Lysaght and Campbell, 2011).

Conclusion

With the fast emerging field of stem cell biology, no set guidelines exist with regard to tissue harvesting techniques, isolation and characterization processes as well as general concepts and assays. Laboratories around the world are only in their infancy with regard

to understanding the basic science of this heterogeneous population of cells, evident by the lack of standardization of terminology and processing procedures.

Despite the desperate need for further research, bio-entrepreneurs are jumping to opportunistic clinical and commercial settings to offer treatments to desperate patients and registering open ended patents. With the clinical stem cell field bursting its banks in co-operation with other disciplines such as engineering to formulate new fields like regenerative medicine and tissue engineering, it is *conditio sine qua non* that major loop holes, controversies and misunderstandings are found within the ethical and legal aspects within these fields. It goes without saying that more research and litigation by governmental bodies needs to be undertaken and reviewed within the fields and the bridge between the fields needs to be crossed.

References

- Abdi R, Fiorina P, Adra CN, Atkinson M and Sayegh MH. Immunomodulation by mesenchymal stem cells: a potential therapeutic strategy for type 1 diabetes. *Diabetes*. 2008;Jul;57;7:1759-1767.
- Alhadlaq A and Mao JJ. Mesenchymal stem cells: Isolation and Therapeutics. *Stem cells and Development*. 2004;13:436-448.
- Assis AC, Carvalho JL, Jacoby BA, Ferreira RL, Castanheira P, Diniz SO, *et al.* Time-dependent migration of systemically delivered bone marrow mesenchymal stem cells to the infarcted heart. *Cell Transplant*. 2010;19:219-230.
- Ayuzawa R, Chiyo D, Rachakatla RS, Pyle MM, Maurya DK, Troyer D, *et al.* Naive human umbilical cord matrix derived stem cells significantly attenuate growth of human breast cancer cells *in vitro* and *in vivo*. *Cancer Letters*. 2009;280;1:31-37.
- Barbash IM, Chouraqui P, Baron J, Feinberg MS, Etzion S, Tessone A, *et al.* Systemic delivery of bone marrow derived mesenchymal stem cells to the infarcted myocardium: feasibility, cell migration and body distribution. *Circulation*. 2003;108:863-868.
- Bianco P, Robey PG and Simmons PJ. Mesenchymal stem cells: revisiting history, concepts and assays. *Cell Stem Cell*. 2008;2;4:313-319.
- Bieback K, Kern S, Klüter H and Eichler H. Critical parameters for the isolation of mesenchymal stem cells from umbilical cord blood. *Stem Cells*. 2004;22:625-634.
- Boulland JL, Leung DS, Thuen M, Vik-Mo E, Joel M, Perreault MC, *et al.* Evaluation of intracellular labelling with micron-sized particles of iron oxide (MPIOs) as a general tool for *in vitro* and *in vivo* tracking of human stem and progenitor cells. *Cell Transplantation*. 2012;21;8:1743-1759.
- Bourin P, Bunnell BA, Casteilla L, Dominici M, Katz AJ, March KL, *et al.* Stromal cells from the adipose tissue-derived stromal vascular fraction and culture expanded adipose tissue-derived stromal/stem cell: a joint statement of the International Federation for Adipose Therapeutics and Science (IFATS) and the International Society for Cellular Therapy (ISCT). *Cytotherapy*. 2013;15:641-648.
- Caplan AI. Mesenchymal Stem Cells. *Journal of Orthopaedic Research*. 1991;9:641-650.
- Chamberlain G, Fox J, Ashton B and Middleton J. Concise Review: Mesenchymal stem cells: Their phenotype, differentiation capacity, immunological features and potential for homing. *Stem Cells*. 2007;25:2739-2749.
- Chargé SBP and Rudnicki MA. Cellular and molecular regulation of muscle regeneration. *Physiological Reviews*. 2004;84:209-238.
- Chawla-Sarkar M, Leaman DW and Borden EC. Preferential induction of apoptosis by interferon (IFN)-beta compared with IFN-alpha2: correlation with TRAIL/Apo2L induction in melanoma cell lines. *Clinical cancer research: an official journal of the American Association for Cancer Research*. 2001;7:1821-1831.
- Chirba-Martin MA and Noble A. Our Bodies, our cells: FDA regulation of autologous adult stem cell therapies. *Bill of Health*. 2013
- ClinicalTrials.gov. Rockville Pike, Bethesda: U.S. National Library of Medicine [updated daily; cited 2014 May 10]. Available from: <http://clinicaltrials.gov>
- Coffelt SB, Marini FC, Watson K, Zwezdaryk KJ, Dembinski JL, LaMarca HL, *et al.* The pro-inflammatory peptide Il-37 promotes ovarian tumor progression through recruitment of multipotent mesenchymal stromal cells. *Proceedings of National Academy of Science of the United States of America*. 2009;106(10);106:3806-3811.
- Collins AT, Habib FK, Maitland NJ and Neal DE. Identification and isolation of human prostate epithelial stem cells based on $\alpha\beta_1$ -integrin expression. *Journal of Cell Science*. 2001;114:3865-3872.
- Crop MJ, Baan CC, Korevaar SS, Ijzermans JN, Pescatori M, Stubbs AP, *et al.* Inflammatory conditions affect gene expression and function of human adipose tissue-derived mesenchymal stem cell. *Clinical and Experimental Immunology*. 2011;20:1547-1559.

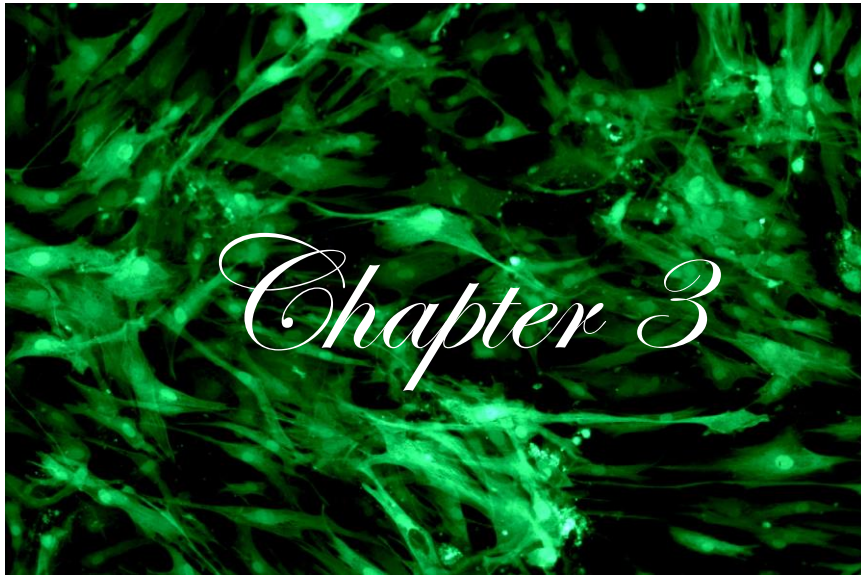
- Cui CH, Uyama T, Miyado K, Terai M, Kyo S, Kiyono T, *et al.* Menstrual blood-derived cells confur human dystrophin expression in the murine model of Duchenne muscular dystrophy via cell fusion and myogenic transdifferentiation. *Molecular Biology of the Cell.* 2007;18:1586-1594.
- De Bari C, Dell'Accio F and Luyten FP. Human periosteum-derived cells maintain phenotypic stability and chondrogenic potential throughout expansion regardless of donor age. *Arthritis and Rheumatism.* 2001;44:85-95.
- De Bari C, Dell'Accio F, Vandenabeelde F, Vermeesch JR, Raymackers JM and Luyten FP. Skeletal muscle repair by adult human mesenchymal stem cells from synovial membrane. *The Journal of Cell Biology.* 2003;160:909-918.
- De Bari C, Dell'Accio F, Vanlauwe J, Eyckmans J, Khan IM, Archer CW, *et al.* Mesenchymal multipotency of adult human periosteal cells demonstrated by single-cell lineage analysis. *Arthritis and Rheumatism.* 2006;54:1209-1221.
- Doetsch F, Ca illé I, Lim DA, García-Verdugo JM and Alvarez-Buylla A. Subventricular zone astrocytes are neural stem cells in the adult mammalian brain. *Cell.* 1999;97:703-716.
- Dominici M, Le Blanc K, Mueller I, Slaper-Cortenbach I, Marini FC, Krause DS, *et al.* Minimal criteria for defining multipotent mesenchymal stromal cells. The International Society for Cellular Therapy position statement. *Cytotherapy* 2006;8;4:315-317.
- Eggenhofer E, Benseler V, Kroemer A, Popp FC, Geissier EK, Schlitt HJ, *et al.* Mesenchymal stem cells are short-live and do not migrate beyond the lungs after intravenous infusion. *Frontiers in Immunology.* 2012;September;3;297:1-7.
- Federal Register Online via GPA Access [wais.access.gpo.gov]: January 19 (2001) vol 66 no 13 pg 5447-5469 [DOCID:fr19ja01-4]
- Fischer UM, Harting MT, Jimenez F, Monzon-Posadas WO, Xue H, Savitz SI, *et al.* Pulmonary passage is a major obstacle for intravenous stem cell delivery: the pulmonary first-pass effect. *Stem Cells and Development.* 2009;18:683-692.
- Friedenstein AJ, Chajlakjan RK, Gorskaya UF. Bone marrow osteogenic stem cells: *in vitro* cultivation and transplantation in diffusion chambers. *Cell and Tissue Kinetics.* 1987;20:263-272.
- Friedenstein AJ, Chajlakjan RK and Lalykina KS. The development of fibroblast colonies in monolayer cultures of guinea-pig bone marrow and spleen cells. *Cell and Tissue Kinetics.* 1970;4:393-403.
- Friedenstein AJ, Petrakova KV, Kurolesova AI and Frolova GP. Heterotopic of bone marrow: analysis of precursor cells for Osteogenic and hematopoietic tissues. *Transplantation.* 1968;6:230-247.
- Gage FH. Mammalian neural stem cells. *Science.* 2000;287:1433-1438.
- Ghannam S, Bouffi C, Djouad F, Forgensen C, Noël D. Immunosuppression by mesenchymal stem cells: mechanisms and clinical application. *Stem Cell Research and Therapy.* 2010;1:2-8.
- Gimble JM, Adam JK and Bruce AB. Adipose-derived stem cells for regenerative medicine. *Circulation Research: Journal of American Heart Association.* 2007;100:1249-1260.
- Govindasamy V, Abdullah AN, Ronald VS, Musa S, Aziz ZACA, Zain RB, *et al.* Inherent differential Propensity of dental pulp stem cells derived from human deciduous and permanent teeth. *Journal of Endodontics.* 2010;36;9:1504-1515.
- Gronthos A, Mankani M, Brahimi J, Robey G and Shi S. Postnatal human dental pulp stem cells (DPSCs) *in vitro* and *in vivo.* *Proceedings of the National Academy of Sciences of the United States of America.* 2000;97;5:13625-13630.
- Gupta S, Verfaillie C, Chmielewski D, Kren S, Eidman K, Connaire J, *et al.* Isolation and characterisation of kidney-derived stem cells. *Journal of the American Society of Nephrology.* 2006;17;11:3028-3040.

- Herrera MB, Bruno S, Buttiglieri S, Tetta C, Gatti S, Deregibus MC, *et al.* Isolation and characterisation of a stem cell population from adult human liver. *Stem Cells*. 2006;24:2840-2850.
- Hoogduijn MJ, Gorjup E and Genever PG. Comparative characterisation of hair follicle dermal stem cells and bone marrow mesenchymal stem cells. *Stem Cells and Development*. 2006;15:49-60.
- Horwitz E, Le BK, Dominici M, Mueller I, Slaper-Cortenbach I, Marini FC, *et al.* Clarification of the nomenclature for MSC: the International Society for Cellular Therapy position statement. *Cytotherapy*. 2005;7:393-395.
- Hu SL, Lu PG, Zhang LJ, Li F, Chen Z, Wu N, *et al.* *In vivo* magnetic resonance imaging tracking of SPIO-labeled human umbilical cord mesenchymal stem cells. *Journal of Cellular Biochemistry*. 2012;113:1005-1012.
- Hu Y, Liao L, Wang Q, Ma L, Ma G, Jiang X, *et al.* Isolation and identification of mesenchymal stem cells from human fetal pancreas. *Journal of Laboratory and Clinical Medicine*. 2003;141;5:342-349.
- Ikada Y. *Tissue Engineering: Fundamentals and Applications*. Elsevier. Oxford 2006: 459-460.
- JO YY, Lee HJ, Kook SY, Choung HW, Park JY, Chung JH, *et al.* Isolation and characterisation of postnatal stem cells from human dental tissues. *Tissue Engineering*. 2007;13;4:767-773.
- Joyce NC, De-Camilli P, Boyles J. Pericytes, like vascular smooth muscle cells, are immunocytochemically positive for cyclic GMP-dependent protein kinase. *Microvascular Research*. 1984;28:206.
- Joyce NC, Haire MF and Palade GE. Contractile proteins in pericytes. I. Immunoperoxidase localization of tropomyosin. *Journal of Cell Biology*. 1985a;100:1379.
- Joyce NC, Haire MF, Palade GE. Contractile proteins in pericytes. II. Immunocytochemical evidence for the presence of two isomyosins in graded concentrations. *Journal of Cell Biology*. 1985a;100:138.
- Karp JM and Teo GSL. Mesenchymal stem cell homing: The devil is in the details. *CellStem Cell*. 2009;4:206-216.
- Kern S, Eichler H, Stoeve J, Klüter H and Bieback K. Comparative analysis of mesenchymal stem cells from bone marrow, umbilical cord blood, or adipose tissue. *Stem Cells*. 2006;24:1294-1301.
- Kingham PJ, Kalbermatten DF, Mahay D, Armstrong SJ, Wiberg M and Terenghi G. Adipose-derived stem cells differentiate into a Schwann cell phenotype and promote neurite outgrowth *in vitro*. *Experimental Neurology*. 2007;207:267-274.
- Kraitchman DL, Tatsumi M, Gilson WD, Ishimori T, Kedziorek D, Walczak P, *et al.* Dynamic imaging of allogeneic mesenchymal stem cells trafficking to myocardial infarction. *Circulation*. 2005;112:1451-1461.
- Krasnodembskaya A, Yuanlin S, Fang X, Gupta N, Serikov V, Lee JW, *et al.* Antibacterial effect of human mesenchymal stem cells is mediated in part from the secretion of the antimicrobial peptide LL-37. *Stem Cells*. 2010;28:2229-2238.
- Lee JY, Qu- Petersen Z, Cao B, Kimura S, Jankowski R, Cummins J, *et al.* Clonal isolation of muscle-derived cells capable of enhancing muscle regeneration and bone healing. *Journal of Cell Biology*. 2000;150;5:1085-1100.
- Lysaght T and Campbell AV. Regulating autologous adult stem cells: The FDA Steps up. *Cell Stem Cell*. 2011;November;9:393-396.
- Matsuzuka T, Rachkatla RS, Doi C, Maurya DK, Ohta N, Kawabata A, *et al.* Human umbilical cord matrix-delivered stem cells expressing interferon- β gene significantly attenuate bronchioloalveolar carcinoma xenografts in SCID mice. *Lung Cancer*. 2010;70:28-36.
- McKay R. Stem Cells in the Central Nervous System. *Science*. 1997;276:66-71.
- Meng X, Ichim TE, Zhong J, Rogers A, Yin Z, Jackson J, *et al.* Endometrial regenerative cell: A novel stem cell population. *Journal of Translational Medicine*. 2007;5:57-67.

- Miura M, Gronthos S, Zhao M, Lu B, Fisher LW, Robey PG and Shi S. SHED: Stem cells from human exfoliated deciduous teeth. *Proceedings of the National Academy of Sciences of the United States of America*. 2003;100;10:5807-5812.
- Morshead CM, Reynolds BA, Craig CG, McBurney MW, Staines WA, Morassutti D, *et al*. Neural stem cells in the adult mammalian forebrain: a relatively quiescent sub-population of subependymal cells. *Neuron*. 1994;13;5:1071-1082.
- Munn DH, Zhou M, Attwood JT, Bondarev I, Conway SJ, Marshall B, *et al*. Prevention of allogeneic fetal rejection by tryptophan catabolism. *Science*. 1998;281:1191-1193.
- Muschler GF, Nakamoto C and Griffith LG. Engineering principles of clinical cell-based tissue engineering. *The Journal of Bone and Joint Surgery. American Volume*. 2004;86-A:1541-1558.
- Nakahara H, Dennis JE, Bruder SP, Haynesworth SE, Lennon DP and Caplan AI. In vitro differentiation of bone and hypertrophic cartilage from periosteal-derived cells. *Experimental Cell Research*. 1991;195:492-503.
- Nakamizo A, Marini F, Amano T, Khan A, Studeny M, Gumin J, *et al*. Human bone-marrow-derived mesenchymal stem cells in the treatment of gliomas. *Cancer Research*. 2005;65:3307-3318.
- Nijnik A and Hancock REW. The roles of Cathelicidin LL-37 in immune defences and novel clinical applications. *Current Opinion in Hematology*. 2009;16:41-47.
- Opitz CA, Litzenburger UM, Lutz C, Lanz TV, Tritschler I, Koppel A, *et al*. Toll-like receptor engagement enhances the immunosuppressive properties of human bone marrow-derived mesenchymal stem cells by inducing indoleamine-2.3-dioxygenase-1 via interferon- β and protein kinase R. *Stem Cells*. 2009;27:909-919.
- Ortiz LA, Gambelli F, McBride C, Gaupp D, Baddoo M, Kaminski N, *et al*. Mesenchymal stem cell engraftment in lung is enhanced in response to bleomycin exposure and ameliorates its fibrotic effects. *Proceedings of the National Academy of Sciences of the United States of America*. 2003;100;14:8407-8411.
- Owen M and Friedenstein AJ. Stromal stem cells: marrow-derived osteogenic precursors. *Ciba Foundation Symposium*. 1988;136:42-60.
- Owen M. Marrow stromal cells. *Journal of Cell Science Supplement*. 1988;10:63-76.
- Park JC, Kim JM, Jung IH, Kim JC, Choi SH, Cho KS, *et al*. Isolation and characterization of human periodontal ligament (PDL) stem cells (PDLSCs) from the inflamed PDL tissue: *in vitro* and *in vivo* evaluations. *Journal of Clinical Periodontology*. 2011;38:721-731.
- Pereira WC, Khushnooma I, Madkaikar M and Ghosh K. Reproducible methodology for the isolation of mesenchymal stem cells from human umbilical cord and its potential for cardiomyocyte generation. *Journal of Tissue Engineering and Regenerative Medicine*. 2008;2:394-399.
- Pittenger MF, Mackay AM, Beck SC, Jaiswal RK, Douglas R, Mosca JD, *et al*. Multilineage potential of adult human mesenchymal stem cells. *Science*. 1999;284;5411:143-147.
- Rachakatla RS, Marini F, Weis ML, Tamura M and Troyer D. Development of human umbilical cord matrix stem cell-based gene therapy for experimental lung tumors. *Cancer Gene Therapy*. 2007;14:828-835.
- Ren G, Su J, Zhang L, Zhao L, Ling W, L'huillie A, *et al*. Species variation in the mechanisms of mesenchymal stem cell-mediated immunosuppression. *Stem Cells*. 2009;27:1954-1962.
- Reynolds BA and Weiss S. Generation of neurons and astrocytes from isolated cells of the adult mammalian central nervous system. *Science*. 1992;255;5052:1707-1710..
- Ruster B, Gottig S, Ludwig RJ, Bistrrian R, Müller S, Seifried E, *et al*. Mesenchymal stem cells display coordinated rolling and adhesion behaviour on endothelial cells. *Blood*. 2006;108;12:3938-3944.
- Safford KM, Safford SD, Gimble JM, Shetty AK and Rice HE. Characterization of neuronal/glial differentiation of murine adipose-derived stromal cells. *Experimental Neurology* 2004;187:319-328.

- Sampaolesi M, Torrente Y, Innocenzi A, Tonlorenzi R, D'Antona G, Pelegriano MA, *et al.* Cell therapy of α -Sarcoglycan Null dystrophic Mice Through Intra-arterial delivery of mesoangioblasts. *Science*. 2003;301;5632:487-492.
- Sarugaser R, Hanoun L, Keating A, Stanford WL and Davies JE. Human mesenchymal stem cells self-renew and differentiate According to a Deterministic Hierarchy. *PLoS ONE* 2009;4;8:e6498.
- Saunders WB. Dorland's illustrated medical dictionary. 30th ed. *Philadelphia*. (2000). *Elsevier Imprint*. Pericyte: 1401.
- Seo MJ, Suh SY, Bae YC and Jung JS. Differentiation of human adipose stromal cells into hepatic lineage *in vitro* and *in vivo*. *Biochemical and Biophysical Research Communications*. 2005;328:258-264.
- Shi S, Bartold PM, Miura M, Seo BM, Robey PG and Gronthos S. The efficacy of mesenchymal stem cells to regenerate and repair dental structures. *Orthodontics & Craniofacial Research*. 2005;8;3:191-199.
- Shi XL, Gu JY, Han B, Xu HY, Fang L and Ding YT. Magnetically labelled mesenchymal stem cells after autologous transplantation into acutely injured liver. *World Journal of Gastroenterology*. 2010;16:3674-3679.
- Si Y-L, Zhao Y-L, Hao H-J, Fu X-B and Han W-D. MSCs: Biological characteristics, clinical applications and their outstanding concerns. *Ageing Research Reviews*. 2010;10;1:93-103.
- Skalli O, Pelte MF, Peclat MC, Gabbiani G, Gugliotta P, Bussolati G, *et al.* Alpha-smooth muscle actin, a differentiation marker of smooth muscle cells, is present in microfilamentous bundles of pericytes. *Journal of Histochemistry and Cytochemistry*. 1989;37;3:315-321.
- Slack JM. Stem Cells in epithelial tissues. *Science*. 2000;287:1431-1433.
- Sordi V, Malosio ML, Marchesi F, Mercalli A, Melzi R, Giordano T, *et al.* Bone Marrow mesenchymal stem cells express a restricted set of functionally active chemokine receptors capable of promoting migration to pancreatic islets. *Blood*. 2005;106:419-427.
- Studeny M, Marini FC, Champlin RE, Zompetta C, Fidler IJ and Andreeff M. Bone marrow-derived mesenchymal stem cells as vehicles for interferon-beta delivery into tumors. *Cancer Research*. 2002;62:3603-3608.
- Studeny M, Marini FC, Dembinski JL, Zompetta C, Cabreira-Hansen M, Bekele BN, *et al.* Mesenchymal stem cells: potential precursors for tumorstroma and targeted-delivery vehicles for anticancer agents. *Journal of the National Cancer Institute*. 2004;96:1593-1603.
- Suchánek J, Soukup T, Ivančáková R, Karbanová J, Hubková V, Pytlík R, *et al.* Human dental pulp stem cells-Isolation and long term cultivation. *Acta Medica*. 2007;50;3:195-201.
- Takahashi K, Igura K, Zhang X, Mitsuru A, Takahashi TA. Effects of osteogenic induction on mesenchymal cells from fetal and maternal parts of human placenta. *Cell Transplantation*. 2004;13;4:337-341.
- Tilton RG, Kilo C and Williamson JR. Pericyte-endothelial relationships in cardiac and skeletal muscle capillaries. *Microvascular Research*. 1979;18;3:325-335.
- Timper K, Seboek D, Eberhart M, Linscheid P, Christ-Crain M, Keller U, *et al.* Human adipose tissue-derived mesenchymal stem cells differentiate into insulin, somatostatin, and glucagon expressing cells. *Biochemical and Biophysical Research Communications*. 2006;341:1135-1140.
- Toma JG, Akhayan KJ, Fernandes KJL, Barnabé-Heider F, Sadikot A, Kaplan DR, *et al.* Isolation of multipotent adult stem cells from the dermis of mammalian skin. *Nature Cell Biology*. 2001;3:778-784.
- Trottier V, Marceau-Fortier G, Germain L, Vincent C and Fradette J. IFATS collection: using human adipose-derived stem/stromal cells for the production of new skin substitutes. *Stem Cells*. 2008;26:2713-2723.
- Wagner W, Wein F, Seckinger A, Frankhauser M, Wirkner U, Krause U and *et al.* Comparative Characteristics of Mesenchymal Stem Cells from human bone marrow, adipose tissue and umbilical cord blood. *Experimental Hematology*. 2005;33:1402-1416.
- Wang HS, Hung SC and Peng ST. Mesenchymal stem cells in the Wharton's jelly of the human umbilical cord. *Stem Cells*. 2004;22;7:1330-1337.

- Wong VL, Rieman DJ, Aronson L, Dalton BJ, Greig R and Anzano MA. Growth-inhibitory activity of interferon-beta against human colorectal carcinoma cell lines. *International journal of cancer*. 1989;43:526-530.
- Wu GD, Nolte JA, Jin YS, Barr ML, Hong Y, Stranes VA, *et al.* Migration of mesenchymal stem cells to heart allografts during chronic rejection. *Transplantation*. 2003;75;5:679-685.
- Xu Y, Liu L, Li Y, Zhou C, Xiong F, Liu Z, *et al.* Myelin forming ability of Schwann cell-like cells induced from rat adipose-derived stem-cells *in vitro*. *Brain Research* 2008;1239:49-55.
- Yu H, Fang D, Kumar SM, Li L, Nguyen TK, Acs G, *et al.* Isolation of a novel population of multipotent adult stem cells from human hair follicles. *The American Journal of Pathology*. 2006;168;6:1879-1888.
- Yukawa H, Watanabe M, Kaji N, Okamoto Y, Tokeshi M, Miyamoto Y, *et al.* Monitoring transplanted adipose tissue-derived stem cells combined with heparin in the liver by fluorescence imaging using quantum dots. *Biomaterials*. 2012;33:2177-2186.
- Zanetti M. The role of cathelicidins in the innate host defences of mammals. *Current Issues in Molecular Biology*. 2005;7:179-196.
- Zhang H, Koty PP, Mayotte J and Levitt ML. Induction of multiple programmed cell death pathways by IFN-beta in human non-small-cell lung cancer cell lines. *Experimental cell Research*. 1999;247:133-141.
- Zuk P (2013). The ASC: Critical Participants in Paracrine-Mediated Tissue Health and Function, *Regenerative Medicine and Tissue Engineering*, Prof. Jose A. Andrades (Ed.), ISBN: 978-953-51-1108-5, InTech, DOI: 10.5772/55545. Available from: <http://www.intechopen.com/books/regenerative-medicine-and-tissue-engineering/the-asc-critical-participants-in-paracrine-mediated-tissue-health-and-function>
- Zuk PA, Zhu MIN, Ashjian P, De Ugarte DA, Huang JI, Mizuno H, *et al.* Human Adipose Tissue Is a Source of Multipotent Stem Cells. *Molecular Biology of the Cell*. 2002;13;Dec:4279-4295.
- Zuk PA, Zhu MIN, Mizuno H, Huang J, Futrell JW, Katz AJ, *et al.* Multilineage Cells from Human Adipose Tissue: Implications for cell based Therapies. *Tissue Engineering*. 2001;7;2:211-228.



Isolation and expansion of peripheral abdominal adipose tissue derived stromal cells and comparison of cell viability before and after cryopreservation

*We fat all creatures else to fat us,
and we fat ourselves for maggots*

Shakespeare W, Hamlet (1600), Act IV, Scene 3, line 23-24.

Introduction

The process of manufacturing good quality mesenchymal stem cells (MSCs) for clinical application poses significant challenges. Adherence to current good manufacturing practices (GMP) is an absolute requirement. It is clear from the literature that MSCs can be maintained and proliferated in culture for long periods of time without losing their differentiation capacity or genetic compliment. This makes MSCs very attractive for research and clinical applications due to their ability to generate large numbers of cells.

Extensive research is however required to eliminate xenogeneic components as well as cryo-protectants during cellular processing and also to optimize freezing and thawing techniques in order to store and deliver a final product to the end user that will be GMP compliant (Kocaoemer *et al.*, 2007). There is also confusion about the Food and Drug Administration (FDA) regulations with regard to storage, expansion and treatment of stem cells. There is a critical need for consensus among manufacturers of cell products with respect to processing and storage of cells for clinical applications (Lindroos *et al.*, 2010; Thirumala *et al.*, 2009).

All stem cell facilities, especially stem cell banks, have to ensure that the principles of GMP are applied during the entire process from collection to freezing and storage of MSCs. To provide stored cells are intended for clinical transplantation or transfusion, a reliable source of cells that is safe, free from contamination and of high quality will need to be produced.

Characteristics of different adipose tissue types

There are five types of adipose tissue: (1) bone marrow, (2) brown, (3) mammary, (4) mechanical and (5) white. These macroscopically-distinct tissues all serve well-defined biological functions within the human body. Bone marrow adipose tissue passively occupies space no longer required for hematopoiesis and actively serves as an energy reservoir and cytokine source for osteogenic and hematopoietic events. Brown adipose tissue, anatomically located around the major organs in a neonate and known to dissipate with age, contains large numbers of intracellular mitochondria that release heat via oxidation of fatty acids and therefore provide a thermogenic function. During lactation, energy and some nutrients are provided by mammary adipose tissue, regulated in part by pregnancy associated hormones (Gimble *et al.*, 2007). It was suggested by Hamosh and colleagues that lipoprotein lipase activity from mammary adipose tissue diverts dietary lipid from storage in adipose tissue to mammary gland for milk formation (Hamosh *et al.*, 1970). Mechanical adipose tissue offers support to critical structures in the body such as the retro-orbital fat pads, which provide support to the eye. White adipose tissue stores energy and provides insulation to the human body (Gimble *et al.*, 2007).

Over the past decade it has become clear that adipose tissue must be regarded as a complex organ with metabolic functions that extend beyond the classical role of thermoregulation and storage of free fatty acids (FFA) after food intake, as well as the release of FFA during periods of fasting to ensure a sufficient and constant source of energy (Hajer *et al.*, 2008; Harwood, 2012). Recent studies have described adipose tissue as a metabolic and endocrine organ secreting various substances including adipocyte derived hormones such as leptin and adiponectin; bioactive peptides known as adipokines such as adiponectin, visfatin, omentin, resistin, cortisol, to name a few; as well as various sex- and steroid hormones. These secreted substances act both locally

(paracrine/autocrine) and systemically (endocrine), exerting various physiological effects (Gimble *et al.*, 2007; Harwood, 2012; Kershaw and Flier, 2004).

It is well established that adipose tissue plays a critical role in the maintenance of energy homeostasis through secretion of a large number of adipokines that interact with peripheral and central organs such as the brain, vasculature, liver, pancreas and skeletal muscle to control diverse processes. These processes include feeding behaviour, blood coagulation, carbohydrate metabolism, lipid metabolism, inflammation and energy expenditure (Chu *et al.*, 2001; Ran *et al.*, 2006; Yamauchi *et al.*, 2001). It has also been demonstrated in humans that the anatomical location of adipose tissue has an impact on metabolic function. Visceral adipocytes have been shown to be more resistant to the antilipolytic effects of insulin and are more sensitive to the stimulation of lipolysis by catecholamines when compared to subcutaneous adipocytes (Bjorntorp, 2000).

Marked differences have been observed between genders in both the metabolism and endocrine function of adipose tissue. Women are known to have a higher percentage of body fat and mainly store adipose tissue in the gluteal-femoral region. Adiposity in this region is associated with larger fat cell size with increased stimulated lipolysis and triglyceride synthesis. Adipose tissue storage in men is primarily in the visceral and abdominal regions. Obesity in men is associated with increased lipoprotein lipase activity with decreased stimulated lipolysis and triglycerides synthesis (Blaak, 2001; Edens *et al.*, 1993; Fried *et al.*, 1993). Several studies have shown that the differences in visceral adipocyte metabolism between genders disappears with menopause. It was further suggested that the female sex hormones may play a role in this gender-specific adipose deposition for example weight gain in the abdominal region of post-menopausal women, as well as associated metabolic (Rebuffe-Scrive *et al.*, 1989; Trujillo and Scherer 2006).

Stem cells resident in adipose tissue

Adipose tissue, like bone marrow, is also derived from the embryonic mesodermal layer and contains a heterogeneous population of cells (Zuk *et al.*, 2001). Adult MSCs, present in many tissues in small numbers, are required to restore normal tissue function via repair and regeneration mechanisms (Jones *et al.*, 2002). Mesenchymal stem cells have been successfully isolated from nearly all postnatal organs and tissues namely bone marrow (Friedenstein *et al.*, 1968), placenta (Takahashi *et al.*, 2004), umbilical cord blood (Kern *et al.*, 2006), dermis, dental pulp (deciduous teeth, wisdom teeth or permanent teeth) (Gronthos *et al.*, 2000), hair follicles, pericytes, trabecular bone, infrapatellar fat pad, articular cartilage, Wharton's jelly within umbilical cord (Fong *et al.*, 2007) and fetal liver (Fukuchi *et al.*, 2004) and also from adipose tissue (Zuk *et al.*, 2001). The cells derived from these sources share similar properties (Dominici *et al.*, 2006; Sarugaser *et al.*, 2009; Si *et al.*, 2010). However, despite these various isolation reports, controversy still exists with regard to isolation protocols from these tissues and in particular from adipose tissue itself.

Prunet-Marcassus and co-workers (2006) demonstrated the complex nature of adipose tissue by showing different antigenic features and differentiation potentials among subcutaneous- and internal white and brown adipose tissue in a murine model and also different heterogeneous MSC subsets depending on the anatomical location of the fat pads. Brown adipose tissue displayed a reduced plasticity and fewer MSC numbers when compared to white adipose tissue. Furthermore, the subcutaneous- and internal white adipose tissue demonstrated discrete differences in the phenotype of their cell populations (Prunet-Marcassus *et al.*, 2006). This raises the question as to whether the anatomical location of white adipose tissue could affect the functional capabilities of ASCs.

Loss of function studies have indicated that peroxisome proliferator-activated receptor gamma (PPAR- γ) is required for both *in vivo* and *in vitro* adipogenesis. Thiazolidinediones (TZDs) act by binding to PPAR- γ , thereby activating the protein cascade that affects metabolism as well as differentiation capacity. The latter occurs by increasing adipogenesis and lipid accumulation (Kelly *et al.*, 1999; Schipper *et al.*, 2008). It was further demonstrated by Tchkonja and colleagues (2002) that preadipocytes isolated from subcutaneous adipose tissue had the highest PPAR- γ activity, displayed the greatest effects of TZDs on differentiation and the lowest amount of apoptosis. These results suggested that ASCs isolated from subcutaneous adipose tissue may be more suited to differentiate into mature adipocytes than visceral adipose tissue (Tchkonja *et al.*, 2002).

Schipper and co-workers (2008) compared the functional variability between different anatomically located subcutaneous adipose tissue deposits. Apoptosis susceptibility was lowest in abdominal deposits while arm deposits showed consistent expression of PPAR- γ -2 without the addition of ciglitazone (TZD). Although the addition of TZDs can cause more extensive differentiation and lipid accumulation in subcutaneous compared to visceral adipose depositions, the expression of PPAR- γ was not found to be different between the different sites (Schipper *et al.*, 2008).

The yield and growth characteristics of isolated ASCs from different donor sites were evaluated by Oedayrajsingh-Varma (2006). No significant difference in terms of the yield or viability of ASCs obtained from the abdomen, hip or thigh donor areas was observed (Oedayrajsingh-Varma *et al.*, 2006). In contrast, Jurgens and co-workers (2008) found that the yield of ASCs from the stromal vascular fraction (SVF) is dependent on the specific tissue-harvesting site. The abdominal area yielded significantly more ASCs when compared to the hip and thigh regions, although no difference was found in the total number of nucleated cells per volume or the ASC proliferation and differentiation capacity. When cultured, ASCs from both regions displayed homogeneous cell populations with similar growth kinetics and phenotype (Jurgens *et al.*, 2008). Hauner and Entenmann (1991) also observed differences in the adipogenic differentiation

potential between SVF cells harvested from abdominal and femoral adipose tissue (Hauner and Entenmann, 1991). These findings highlight the importance of the specific anatomical location as a source of ASCs.

Age and gender are also important factors to consider when isolating MSCs from adipose tissue. In the publication by Schipper and colleagues (2008), the authors further stratified their study into different ages and compared the characteristics of ASCs isolated from the following age groups; 25-30, 40-45 and 55-60 years. The younger patients demonstrated significantly faster cell proliferation rates and higher lipolysis activity, with increased PPAR- γ expression in all of the subcutaneous deposits compared to the other two groups. Interestingly, with the addition of TZDs during *in vitro* adipogenic induction, the 40-45 year group showed statistically increased adipogenesis when compared to the other groups. When considering the site of isolation, only the upper arm deposits maintained a high lipolytic activity, regardless of the patient's age, when compared to the other sites (medial thigh, trochanteric and both superficial and deep abdominal adipose depots) (Schipper *et al.*, 2008). There is still controversy with regard to what causes ageing of MSCs, whether it is intrinsic or extrinsic factors, but in all likelihood, both? It was suggested by Zhou *et al.* (2008) that intrinsic factors such as senescence-associated β -galactosidase together with increased expression of p53 and its pathway genes (p21 and BAX) may be responsible for mediating reduced proliferation in MSCs from older patients by inducing senescence (Zhou *et al.*, 2008). In contrast, extrinsic factors such as a reduced synthesis of proteoglycans and glycoasminoglycans in the microenvironment reduce cell proliferation and viability *in vivo*. In addition, the accumulation of advanced glycosylated end products inhibits proliferation of MSCs by activating apoptosis and reactive oxygen species (ROS) production (Bi *et al.*, 2005; Kume *et al.*, 2005). This clearly illustrates the variability of ASCs isolated from patients from different age groups.

In contrast, no age-related or gender significant differences in cell surface marker expression (CD34, CD44, CD54, Cd73, CD80, CD90, CD105, CD106, CD166 and STRO-1) from MSCs isolated from synovial fat pads was observed (Fosset *et al.*, 2012). Also, the general trends observed with age-related decline in population doublings at low seeding densities and age-related incline in population doublings at higher seeding densities was not statistically significant. The older patients however, had a smaller regression coefficient than younger patients, demonstrating less change in population doublings with increasing seeding densities (Fossett *et al.*, 2012).

Fosset *et al.* (2012) further demonstrated that synovial fat pad derived MSCs plated at a density of 50 cells/cm² showed a 980-fold increase in ASC proliferation for females and 367-fold increase for male patients over a period of 21 days. In addition, the investigated cell surface markers indicated little significant difference between genders except for the STRO-1 marker, expressing significantly higher in female relative to male patients. Based on the fact that estrogens up-regulate receptor expression on embryonic stem cells and the previously suggested notion that androgens have inhibitory effects and estrogens an

excitatory effect on MSCs, the possibility was suggested that gender may account for the variability observed (Fossett *et al.*, 2012; Ray *et al.*, 2008).

Adipose tissue harvesting techniques

The ideal source of stem cells used for regenerative medical applications should (1) be easily obtainable, with minimal discomfort to the patient or by a minimal invasive procedure; (2) yield sufficient numbers of cells for extensive cell culturing; (3) be able to differentiate along multilineage pathways in a controlled and reproducible manner; (4) be transplantable to either autologous or allogeneic hosts safely and effectively; and (5) be able to be manufactured in accordance with GMP guidelines (Mizuno, 2009). Adipose tissue could be considered to fulfill all these criteria. With regard to harvesting, raw lipoaspirate can easily be obtained by suction-assisted lipectomy also known as liposuction, lipoplasty, lipolysis or simply fat suctioning. This method in comparison to other tissue harvesting techniques also has minimal ethical considerations, limited pain and discomfort to the patient and demonstrates an increased cellular yield and viability (Dominici *et al.*, 2006).

Oedayrajsingh-Varma *et al.*, (2006) also evaluated the yield and growth characteristics of isolated ASCs using different harvesting techniques. Their findings demonstrated that adipose tissue harvested by resection and tumescent liposuction provided high yields of rapidly growing ASCs, whereas adipose tissue obtained by ultra-sound assisted liposuction provided a low yield of ASCs exhibiting low proliferative capacity. In addition, more than 80% of the cells exhibited an ASC phenotype, irrespective of the operative procedure performed (Oedayrajsingh-Varma *et al.*, 2006).

A comparative study evaluating the viability of ASCs from excised *versus* aspirated adipose tissue showed a significant loss in viability of ASCs within the excised cultures, both isolated at 1 hour and at 24 hours. In addition, these results clearly demonstrated that adipose tissue extraction by suction does not damage the SVF. The group went further and suggested that liposuction is the better method for harvesting ASCs (von Heimburg *et al.*, 2004).

The procedure of performing liposuction has become a common practice amongst plastic and reconstructive surgeons. A 2010 survey indicated that 2 174 803 liposuctions are performed annually by approximately 33 000 plastic surgeons worldwide (International survey on Aesthetic/Cosmetic Procedures Performed). Liposuction was also scored at 23% of the total surgical procedures performed by plastic surgeons, clearly indicating that this is the most common surgical procedure in this field (<http://www.isaps.org>). The current trends in liposuction and other fat removal techniques in America were also surveyed by the American Society for Aesthetic Plastic Surgery (ASAPS). The number of liposuctions performed in America from 2010 to 2011 have increased by 12.6% and liposuction currently holds the position of the most popular cosmetic surgical procedure of 2011 with a total of 325 332 procedures (<http://www.surgery.org>). Multiple factors

such as genetic, epigenetic and behavioral factors contribute to the increasing global obesity epidemic. This epidemic favors adipose tissue as a stem cell source for regenerative medicine, as subcutaneous adipose tissue is abundant and readily accessible (Katz *et al.*, 1999).

Adipose tissue is the richest source of stem cells in the human body, containing 100 to 1000-fold more multipotent cells per volume unit compared to bone marrow. It was demonstrated that about $3,5 \times 10^4$ preadipocytes can be isolated from 1g of adipose tissue (Ersek and Salisbury, 1996; Fournier and Otteni, 1983; Strem *et al.*, 2005; von Heimburg *et al.*, 2004). Fraser and colleagues (2006) also demonstrated that 1 g of adipose tissue yields a 500-fold greater number of ASCs compared to 1 g of bone marrow yielding MSCs. Liposuction can yield anywhere from 100 ml to > 3 L of lipoaspirate, which is then routinely discarded. This data highlights the one ideal characteristic of a stem cell source, namely that it is easily obtainable in abundant numbers (Fraser *et al.*, 2006).

Background on liposuction

The surgical technique of removing fat through a small incision using suction was developed by Dr. Giorgio Fischer, a gynecologist from Rome, Italy in 1974. His instrument, the planatome, contained an electric curette that would cut the fat before suctioning the tissue. Liposuction burst on the scene with a lipoplasty technique demonstration by the French surgeon, Dr Yves-Gerard Illouz, at the 1982 annual meeting of the American Society of Plastic and Reconstructive Surgeons. The Illouz method involved suction-assisted lipolysis after infusing fluid into tissues using blunt cannulas and high-vacuum suction generated by a mechanical pump system (Illouz, 1983).

Classical liposuction consists of two types of techniques as described in the literature, namely the wet or tumescent and the dry technique. Both techniques are currently being used in clinical practice. The super wet technique was developed to reduce excessive bleeding to <1% compared to 30% as observed in the dry technique and was introduced by Klein in 1978 (Agostini *et al.*, 2012). Also known as the tumescent technique, this type of liposuction involves infusion of a saline solution containing a local anaesthetic agent and/or epinephrine (adrenaline) into the subcutaneous tissue that allows for regional anaesthesia and vasoconstriction before removing both the liquid and tissue using suction. The initial dry technique only involves suction or assisted suction (by mechanical pump) of adipose tissue without prior infusion of the tumescent or Klein solution and is therefore known to harvest virgin lipo-aspirate (Gimble *et al.*, 2007; Herold *et al.*, 2011; Klein, 1987; Coleman, 2001; Tommaso *et al.*, 2012). Finely minced tissue fragments are produced by both techniques, where the size of the fragments is dependent on the dimensions of the cannula used (Gimble *et al.*, 2007).

Over the past three decades, modern robust liposuction techniques have evolved to more refined techniques and improved patient safety. The emergence of new technologies however demands critical evaluation of basic science and clinical outcomes of these

modalities and these include: the super wet technique, ultrasound-assisted liposuction, power-assisted liposuction, laser-assisted liposuction and water-assisted liposuction (Ahmad *et al.*, 2011). Most ASAPS members currently in practice, with experience in different types of liposuction techniques, prefer suction-assisted liposuction to ultrasound-assisted liposuction and power-assisted liposuction (Ahmed *et al.*, 2011).

The introduction of a syringe instead of a machine to aspirate the fat was introduced by Fournier and later optimized by Coleman for the purpose of fat grafting in clinical practice (Colman, 2002, 2004; Fisher, 1975, 1976, 1977; Fournier, 1988a, 1988b, 1991). The Coleman technique tolerates local, regional, epidural, or general anaesthesia depending on the patient's preference and the anaesthetic risk. With local anaesthesia, lidocaine and epinephrine are used and during an epidural and general anaesthesia a solution of epinephrine and Ringer's lactate helps to maintain homeostasis. After a small puncture incision, a blunt lamis infiltration cannula is used to introduce and infiltrate the respective wetting solution into the donor area with an estimated ratio of 1cc solution per cm³ fat to be harvested. Through the same puncture incision, a blunt tip harvesting cannula with two distal openings in a shape reminiscent of a bucket handle is inserted. The cannula is connected to a 10cc luer-lock syringe, which creates minimal negative pressure, as the plunger is drawn out, while the cannula is advanced and retracted through the harvest site (Coleman, 2002).

A lipofilling study by Witort and co-workers (2007) evaluated the effects of different harvesting techniques on adipocytes. The results indicated that the gentle Coleman technique was less traumatic than the mechanical aspirator (680 mmHg vacuum) using power assisted aspiration (Witort *et al.*, 2007). These results were supported by Herold and co-workers (2012) who compared the fat graft viability of adipocytes using the Coleman technique and the Shippert technique. The Coleman technique involved manual aspiration using a syringe and centrifugation, while the Shippert technique used automatic liposuction (suction assistance from a mechanical pump system) and no centrifugation of adipose tissue. It was demonstrated using a WST-8 test (cell proliferation assay) and annexin V/IP FACS analysis (apoptotic assay) that the Coleman technique was superior with significantly increased fat graft viability (Herold *et al.*, 2012). An important observation however was that ASCs within the harvested adipose tissue were more resistant to handling and ischemia than mature adipocytes, which are more fragile cells with a shorter lifespan once harvested (Tommaso *et al.*, 2012).

It was observed by Amos *et al.* (2008) that harvesting techniques not only affect the viability of ASCs but also their level of adhesiveness to key adhesion proteins. Recent studies have indicated that ASCs are responsive to hypoxia, promoting the secretion of the proangiogenic growth factor VEGF. Some studies are in contrast to others, suggesting that hypoxia reduces ASC proliferation and attenuates adipogenic, chondrogenic and osteogenic differentiation (Lee *et al.*, 2006). Amos and colleagues showed that prolonged (>48 hrs) exposure to hypoxic conditions enhances the secretory, differentiation and

proliferative capacity of ASCs, in addition their ability to firmly adhere, making this a viable approach for cell activation prior to therapeutic delivery. In addition, they demonstrated that the extraction technique of ASCs (liposuction versus lipectomy) impacts the adhesion potential of these cells to proteins in the extra cellular matrix and the expressed proteins by activated vascular endothelium, as well as their response to hypoxic culture. ASCs were able to firmly adhere to type I collagen, fibronectin, vascular adhesion molecule-1 (VCAM-1) and intercellular adhesion molecule-1 (ICAM-1) substrates but not to any of the selectins (P-selectin, E-selectin, L-selectin). With hypoxia pretreatment, ASCs extracted by liposuction showed an increased ability to adhere to VCAM-1 and ICAM-1, whereas ASCs extracted by lipectomy did not show similar results (Amos *et al.*, 2008). In clinical practice the harvesting techniques of adipose tissue could have an effect on the homing mechanisms of ASCs, by aiding in the mobilization and trafficking of both tissue-resident and therapeutically delivered cells in a setting where interaction with inflamed or injured tissue is necessary.

Using a wetting solution reduces the risk of excessive bleeding during liposuction procedures and the patient will have less post-procedural bruising, although if liposuction is performed for the purpose of harvesting ASCs it is questioned if the anesthetics used in the wetting solution could have an effect on the respective ASCs. Tommaso and colleagues (2012) demonstrated through histological evidence and cell viability assessments that there was no substantial difference on cell phenotype using wet and dry liposuction techniques (Tommaso *et al.*, 2012). Keck and colleagues (2010) however noted that local anesthetics have a marked influence on the quantity and quality of viable preadipocytes and ASCs. After the SVF was cultured for 24 to 48 hours and non-adherent cells washed off, the ASCs were trypsinized and exposed for 30 min with different anesthetics before being analyzed by flow cytometry. It was demonstrated that articaine/epinephrine and lidocaine strongly impaired the viability of the ASCs, while bupivacaine had no effect. These exposed cells were then induced to differentiate into adipocytes for 12 days and the expression of adiponectin was measured using quantitative real-time polymerase chain reaction. All the anesthetics bupivacaine, mepivacaine, ropivacaine, articaine/Epinephrine and lidocaine induced a significant decrease in adiponectin expression and adipogenic differentiation capacity, compared to the saline control. Interestingly all anesthetic exposed ASC cultures except those exposed to articaine/epinephrine showed a similar phenotypic appearance to that of control cultures during and after the adipogenic induction period. The ASCs from the articaine/epinephrine exposed cultures appeared smaller in size while a similar percentage of cells demonstrated lipid droplet formation (Keck *et al.*, 2010).

ASC isolation techniques

The initial method for isolating MSCs from adipose tissue was pioneered in the 1960s. Minced rat fat pads were extensively washed to remove contaminating haematopoietic cells (HSCs), incubated with collagenase and centrifuged to obtain a pellet of SVF

containing a heterogeneous population of cells. The selection for plastic adherent fibroblastic like cells from the SVF concluded this isolation process (Rodbell, 1966b; Rodbell, 1966d; Rodell and Jones, 1966c). Mesenchymal stem cells resident in human adipose tissue were first described by Zuk and co-workers in 2001. The initial procedure of mincing human adipose tissue by hand was simplified by the development of liposuction surgery. Many stem cell laboratories have developed methods to isolate and expand MSCs from various tissue sources including adipose tissue. Although most of these methods share similarities, there are some that differ significantly which leads to the following very important unanswered question within the stem cell research community. If these different tissue sources and methodologies are used for the preparation of MSCs, are these MSCs sufficiently similar to allow for direct comparison of reported biological properties and experimental outcomes, especially in the context of cell based therapy (Dominici *et al.*, 2006)?

Dominici *et al.*, in 2006 suggested that the standard isolation protocol developed by Zuk and co-workers (2001; 2002) should be accepted as an established methodology to obtain the SVF from raw lipoaspirate (Dominici *et al.*, 2006). Most research groups however make adaptations to this methodology and this complicates comparison of results between groups. Previous studies suggest that ASCs exhibit an average population doubling time of 60 hours or generally 2 to 4 days, depending on the donor's age, the type (white or brown) and location (subcutaneous or visceral) of the adipose tissue, the type of surgical procedure, culture conditions, growth factors, plating or seeding densities, passage number and media formulations (Fossett *et al.*, 2012; Gimble *et al.*, 2007; Mizuno, 2009). This highlights the many factors to consider when developing isolation protocols.

Different fat processing techniques have also been evaluated. A prospective cross-sectional study evaluated three widely used fat processing techniques in plastic surgery for viability and number of adipocytes and ASCs isolated from collected lipoaspirate. All samples were collected using the established Coleman technique under regional anesthesia. The aspirate was processed using three different techniques namely (1) decantation, (2) washing and (3) centrifugation. The three basic layers, the superior oily liquid supernatant, the firmer white-yellow tissue and the inferior layer consisting mostly of blood contaminants including the infiltration and washing liquids was identified with all three techniques. A fourth layer, the pellet, was identified with centrifugation only. Histological quantification of nuclei using haematoxylin and Periodic Acid Schiff (PAS) staining was used to identify adipocytes and flow cytometric analysis was used for quantification of ASCs. Significant differences were observed with regard to viable intact adipocytes in the middle firm tissue layer between various processing techniques ($p=0.0075$). Decantation maintained the integrity and number of adipocytes, while washing significantly reduced the number of intact nucleated cells and centrifugation destroyed the majority of viable adipocytes. Flow cytometric analysis indicated various quantification differences of ASCs, hematopoietic cells (blood contaminants) and endothelial cells, comparing the middle firm tissue layers, of all three different processing

techniques and the pellet of the centrifuged samples. The firm tissue layer of the decantation process contained large amounts of blood contaminants and very few ASCs and endothelial cells. The firm tissue layer of the washed process contained little blood contaminants and more endothelial and ASCs, compared to the decantation process. The firm tissue layer of the centrifuged samples contained the least amount of ASCs, blood contaminants and endothelial cells, whereas the pellet of the centrifuged samples contained the greatest amount of ASCs, blood contaminants and endothelial cells. In addition, the firm tissue layer from the centrifuged samples did not expand and proliferate *in vitro*, while the pellet of the centrifuged samples demonstrated extensive proliferation and expansion (Condé- Green *et al.*, 2010). The results of this study also confirmed the proposition made by Tommaso *et al.* (2012), that ASCs are sturdier cells than adipocytes and can withstand centrifugal forces up to 3 000 rpm (Condé- Green *et al.*, 2010). The oil floating material layer (Figure 3.11.) seen in centrifuged samples was previously analyzed by Novaes and co-workers (1998). They used gas chromatography to examine the nature of this floating oil material and identified the substances as lauric acid, stearic acid, palmitic acid and araquidic acid, where the highest volume was occupied by palmitic acid (Novaes *et al.*, 1998) indicating contamination, which supports the practice of removal.

Various aspects surrounding the centrifugation process during the isolation procedure can influence the isolation yield. Baschert and co-workers suggested that centrifugation forces greater than 100 *g* are not appropriate for autologous fat transplantation as they observed an increased quantity of oil possibly due to adipocyte destruction (Baschert *et al.*, 2002). On the contrary, Kurita and colleagues found that more than a 100 *g* centrifugal force could be used for autologous fat grafting, since the increased oil portion does not necessarily mean an increase in adipocyte destruction, but rather an increase in the separation of oil from the adipose portion (Kurita *et al.*, 2008). Centrifugation of adipose tissue separates fat cells from lipid, blood cells, water and water-soluble ingredients such as proteases and lipases, but does not shift ASCs between the adipose and fluid portions, possibly due to the strong adherence to adipose tissue or since they are resident within the adipose tissue. It was also shown that increased centrifugal forces compacted the adipose portion more and therefore concentrated the red blood cells within the adipose portion rather than shifting the red blood cells into the fluid portion. In contrast to mature adipocytes, it was indicated that the yield of ASCs in culture for 1 week was consistent up to 3000 *g* but decreased with centrifugal forces of more than 3000 *g* (Kurita *et al.*, 2008). Dickens and co-workers demonstrated that gentle centrifugation produced the highest cell viability whereas long periods of centrifugation resulted in the selection of the most proliferative ASC sub-population (Dickens *et al.*, 2009).

Another factor to consider in the isolation process is the effect of seeding density on cell proliferation. Fossett and colleagues (2012) showed that low seeding densities increase the proliferation capacity *in vitro*. The effect of seeding density on cell MSC proliferation was demonstrated with BM-MSCs that were seeded at 100 cells/cm² and reached their

target of 200×10^6 cells 4.1 days faster than cells seeded at $5\,000$ cells/cm² (Both *et al.*, 2007). Similar results were observed by Lode and co-workers in 2008 using synovial fat pad MSCs seeded on three dimensional scaffolds (Lode *et al.*, 2008).

The proliferation of ASCs can be stimulated by several exogenous supplements including fibroblast growth factor 2 (FGF-2) via the FGF-2 receptor, sphingosylphosphorylcholine via activation of c-jun N-terminal kinase (JNK), platelet derived growth factors via the activation of JNK and oncostatin M via the activation of the microtubule-associated protein kinase or extracellular regulated kinase and the JAK3 or STAT1 pathway (Chiou *et al.*, 2006; Jeon *et al.*, 2006; Kang *et al.*, 2005; Mizuno, 2009; Song *et al.*, 2005). On the contrary, it was suggested by Zhang *et al.* (2010), that low-intensity and intermittent negative pressure treatment e.g. creating a vacuum environment within the processing cabinet, could inhibit MSC proliferation, promote cellular apoptosis and enhance induced osteogenic activity. Inhibition of proliferation could be attributed to temporal hypoxia, caused by negative pressure, which could cause HIF-1 up regulation. The HIF-1 heterodimer is composed of HIF-1 α , which is acutely regulated in response to hypoxia and HIF- β , which is insensitive to fluctuations in O₂ availability and allows for cellular adaptation to hypoxia (Zhang *et al.*, 2010).

Cryopreservation of ASCs

The two major constituents of cryopreservation media used in the cryopreservation of ASCs are serum, as a source of nutrients and cryoprotective agents. The addition of cryoprotective agents reduces the freezing induced damage to the cells by stabilizing the cell membrane bilayer gel phase rather than the interdigitated gel phase, even at low concentrations (Thirumala *et al.*, 2010). A large range of cryoprotective agents are used, from low molecular weight solutes, which are permeating, like dimethyl sulfoxide (DMSO) and glycerol, to sugars like sucrose and trehalose and also high molecular weight polymers which are non-permeable, like polyvinylpyrrolidone and hydroxyl-ethyl-starch (Fuller, 2004).

Most clinical stem cell banks use DMSO in their cryopreservation process. Although generally regarded as relatively non-toxic, the potential toxicity complicates the direct use of frozen-thawed cells in patients. During the freezing and thawing processes the addition and removal of DMSO is cytotoxic to ASCs due to the detrimental associated osmotic shock to the cells (Woods *et al.*, 2007). Furthermore, it has been reported that with the addition of DMSO into the cell culture medium, ASCs are induced to differentiate into cardiac and neural like cells (Woodbury *et al.*, 2000; Young *et al.*, 2004). The process of removing DMSO from frozen-thawed cells is also costly and time consuming with cell loss and clumping (Fleming and Hubel, 2006). Cryopreservation media commonly contain 10% DMSO. Recently the group of Thirumala observed no significant differences in ASC viability and apoptosis with DMSO concentrations ranging between 2-10% in cryopreservation media, although concentrations below 2% demonstrated detrimental

effects. The authors suggested that 2% DMSO could be the ‘minimal’ threshold concentration needed in cryopreservation media (Thirumala *et al.*, 2010). Another group demonstrated that 10% DMSO as a cryopreservation agent did not affect the phenotype, proliferation, or osteogenic differentiation of ASCs (Liu *et al.*, 2008). Optimal cryopreservation results were also reported using 10% DMSO as evaluated by membrane integrity and colony forming unit analysis (Goh *et al.*, 2007). The ongoing debate on whether to use DMSO and at what concentration will clearly remain a debate for now.

Animal serum is routinely added to cryopreservation media as a source of nutrients and other undefined factors. On the background of increasing availability of serum-free alternatives this practice poses many disadvantages including high costs, presence of xenogenic antigens and the risk of transmitting animal viral, prion and zoonotic contaminants. On the contrary, autologous serum eliminates the risk of infectious diseases although it remains costly and requires a preoperative blood donation by the patient. Human serum albumin or human allogeneic serum as an alternative does not eliminate the risk of transmitting infectious diseases (Thirumala *et al.*, 2009). A multitude of studies demonstrated no significant differences between autologous- and animal serum pertaining to isolation, expansion and differentiation (Matsuo *et al.*, 2008; Yamamoto *et al.*, 2003).

Various studies have demonstrated that other factors also contribute to the viability of ASCs during the cryopreservation process. It was found by Goh and colleagues that the post-thaw viability of ASCs is a function of the storage cell concentration and that optimal viability of cells was observed when a concentration of 500 000 cells/ml was used in the cryopreservation procedure (Goh *et al.*, 2007). Fuller and Devireddy compared two different cooling conditions and found that the post-thaw viability of frozen cells obtained from the controlled rate freezing technique was superior compared to the directional freezing technique (Fuller and Devireddy, 2008). Literature suggests that the freezing and thawing process induces extensive early apoptosis stress activation pathways, which could lead to a time-dependent decline in the viability and function of cell cultures.

The effect of various thermal parameters on the immediate post-thaw membrane integrity of ASCs was studied by Thirumala and associates using a two-level four-parameter (2⁴) experimental design. The membrane integrity of any cell depends on the thermal history of four parameters: (1) cooling rate, (2) storage temperature, (3) hold time or time spent at the storage temperature and (4) thawing rate (Thirumala *et al.*, 2005). A ‘fast’ cooling rate results in the permeation of intracellular water across the cell membrane to join the extracellular ice phase. On the contrary, a ‘slow’ cooling rate causes intracellular water to freeze and results in intracellular ice formation, rendering the cell osmotically inactive (lysed) due to the loss of membrane integrity.

The effects of lowering the storage temperature and increasing the holding time was studied on various cell types. The most significant parameters identified were the cooling

rate and the storage temperature while the holding time was the least significant. The study also revealed that increased thawing rate or 'rapid thawing' (40°C/min) decreases intracellular and extracellular re-crystallization injury and hence increases post-thaw membrane integrity (Thirumala *et al.*, 2005).

A recent study evaluated the use of an ethanol-jacketed closed container containing a sample of ASCs which were being cryopreserved with 80% FCS and 10% DMSO and that was placed in a -80°C freezer. Results showed satisfactory post/thaw membrane integrity. Interestingly, the cells within the ethanol-jacketed closed container were subjected to different cooling rates at different time points within the -80°C freezer. The cooling rate for the first ~ 50 min was ~ 0.7°C/min until ice nucleation was observed at -5°C and subsequently, a cooling rate of ~ 1.1 °C/min was imposed up to a temperature of -40°C. The cells experienced decreasing cooling rates of ~ 0.3°C/min and ~ 0.1°C/min respectively before reaching -80°C. The samples were then removed from the container and rapidly placed in liquid nitrogen (<-160°C) ensuring the total solidification and long-term stability of the frozen sample (Thirumala *et al.*, 2010). These cooling rates are slow enough to avoid intracellular ice formation during freezing and fast enough to avoid long term exposure to the concentrated extracellular salt solution.

Aims and objectives

The aims of this study discussed in this chapter were:

1. to isolate and expand MSCs from peripheral adipose collected tissue; and
2. to assess the viability of the cells before and after cryopreservation.

Materials and Methods

Collaborations were established between Prof Pepper's research group and Dr Danie Hoffmann (plastic and reconstructive surgeon in the private practice) as well as Prof Piet Coetzee (Department of Plastic Surgery, University of Pretoria, Steve Biko Academic Hospital).

There were no pre-selection criteria for patients used in the study. These patients included volunteers undergoing liposuction, breast augmentation and abdominoplasty procedures. No patient was placed under unnecessary aesthetic or other risk during the collection procedure for the purpose of this study. Every patient underwent the process of informed consent for the harvesting procedure to be done as well as for the research group to obtain their adipose tissue. The participants have no legal remedy nor do they

share in any financial gain that might be derived from this study. The study was approved by the Research Ethics Committee of the Faculty of Health Sciences, University of Pretoria (218/2010 and 179/2011) (Appendix 3.1).

Collection of human adipose samples

Lipoaspirate harvesting using the Coleman technique

The Coleman technique was used by Dr Hoffmann to collect all patient samples obtained from private hospital operating theatres. Verbal consent was given by the patient, Dr Hoffmann as well as the theatre sister, for all photographs taken.

The Coleman technique as described above is a dry needle aspiration procedure and was followed to obtain virgin adipose tissue. No additional pharmacological substances e.g. saline and/or lignocaine (wetting solution) were injected within the donor area before the procedure. The goal was to induce minimal trauma to the adipocytes and preadipocytes during collection, implying that fat harvesting techniques using high negative pressure were precluded from this study. All adipose tissue collections were restricted to using a 10cc syringe to create a low negative pressure system. The negative pressure created by a 10cc syringe was previously measured with an aneroid vacuum meter and shown to be 510 mm/Hg when the plunger was withdrawn to maximum and indicated a gradual decrease as the syringe filled with harvested lipoaspirate (Novaes *et al.*, 1998).

General anaesthesia was administered for the respective cosmetic surgery and antiseptic cleaning of the donor area with chlorhexidine was performed by the theatre nurse prior to the initiation of surgery (Figure 3.1). All areas above the blue sheets are considered sterile and a scientist scrubbed and dressed in the correct theater attire should not move above or around these areas. A small puncture wound (~10 mm) was made with a no. 15 scalpel blade through the epidermis in the donor areas *i.e.* in the infra umbilical and/or flank areas (supra-lateral pelvic area) (Figure 3.4). A Coleman blunt tip harvesting cannula with two distal openings, which give the tip a shape reminiscent of a bucket handle (Figure 3.2) attached to a 10cc luer-lock syringe (syringe) was used to allow for the collection of elegant strands of adipose tissue (Figure 3.3). Dry needle aspiration was performed with a harvesting cannula with dimensions of 150 mm in length, an outer diameter of 4 mm and inner diameter of 2.5 mm (Johnson & Johnson, Biron 02-331).



Figure 3.1. Sterile instrument table and bowl containing antiseptic cleaning solution. The blue cloth indicates a sterile field.



Figure 3.2. Harvesting cannula with a blunt tip in the shape of a bucket handle.



Figure 3.3. The proximal end of the harvesting cannula is shaped to fit securely into a 10cc luer lock syringe.



Figure 3.4. A puncture wound made with a no. 15 scalpel blade in the aseptically cleaned donor area.

The harvesting cannula was inserted through the puncture wound into the subcutaneous adipose layer of the abdominal donor site (Figures 3.5. and 3.6.). The plunger of the syringe was withdrawn 1-3 ml at a time to create the low negative pressure vacuum within the barrel of the harvesting cannula and syringe. The surgeon held the harvesting cannula attached to the syringe in his dominant hand while gently grasping the skin of the abdominal area with his non-dominant hand in order to lift the subcutis from the underlying structures (Figures 3.7. and 3.8.). The fat was aspirated with a meticulous, atraumatic technique by smoothly advancing and retracting the harvesting cannula through the subcutaneous adipose layer. This movement was done very quickly and forcefully through the donor area, in order to avoid blood contamination of the collected adipose tissue sample. The harvesting cannula was repeatedly advanced in a transverse direction while slowly progressed in a circular pattern until the needle pointed in an inferior direction from the puncture wound. This directional movement in the liposuction technique is called the fan formation (Figure 3.9). The harvesting fan formation was repeated on the opposite side. This fan formation of fat aspiration was used to avoid blood contamination of the sample during the harvesting process.



Figure 3.5. The harvesting cannula is inserted through the puncture wound in the donor area.



Figure 3.6. The harvesting cannula is advanced within the adipose layer of the donor area and the plunger is withdrawn 1 to 3 ml at a time to create a low negative pressure within the barrel of the syringe.



Figure 3.7. The negative pressure decreases within the suction system as the barrel of the syringe fills with adipose tissue. The plunger is then redrawn to create a vacuum to allow more adipose tissue to be suctioned through the harvesting cannula into the barrel of the syringe.



Figure 3.8. The surgeon grips the donor area with the non-dominant hand, while easily manipulating the 10 cc luer lock syringe to maintain a low negative pressure during harvesting. The surgeon advances and retracts the harvesting cannula quickly and forcefully through the adipose layer.

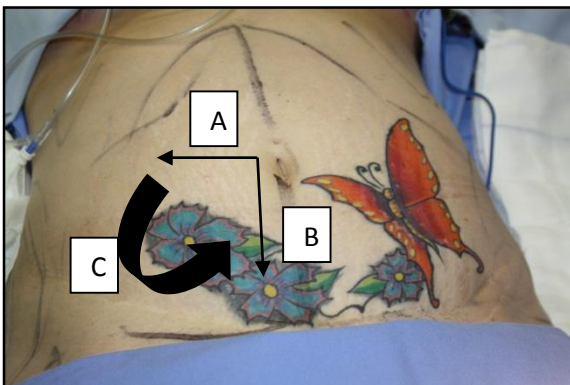


Figure 3.9 The harvesting cannula is advanced in a lateral direction (A) and retracted. This movement was repeated in a more inferior direction than the last until the cannula was advanced in an inferior (B) direction. This fan formation technique (C) of

harvesting decreases the risk of harvesting blood contaminants with the subcutaneous adipose tissue.

As the syringe filled with lipoaspirate, the negative pressure decreased until suction vacuum was not enough to allow further harvesting of adipose tissue (Figure 3.10.). The harvesting cannula was then extracted from the puncture wound and removed from the patient. The plunger was withdrawn from the syringe and the aspirate was decanted into a sterile bottle (Figure 3.11). The sterile bottle contained phosphate buffer solution pH of 7.4 (PBS) (Gibco, Cat# 10010-015) as well as 5% penicillin and streptomycin (pen/strep) (Gibco, Cat# 15140-122). The harvesting process was repeated until a reasonable amount of virgin fat was collected. The process was ceased when excessive blood contaminants appeared within the syringe.



Figure 3.10. Lipoaspirate fills the syringe during the harvesting process due to the negative suction pressure.



Figure 3.11. The plunger is withdrawn completely from the syringe barrel and the lipoaspirate is decanted into a sterile bottle containing PBS.

Lipoaspirate harvesting using the suction assisted tumescent technique

Two adipose tissue samples were harvested by the registrars in the Department of Plastic and Reconstructive Surgery at Steve Biko Academic Hospital. The donor areas for both patients were skin flaps retrieved from the thigh area and placed in the distal limb areas (foot and hand). These previous reconstructive surgeries had been successful, however, due to the weight gain experienced by the patients, the adipose layer in the skin flap expanded which rendered the flaps disfiguring.

After the patients had been placed under general anaesthesia, the surgeon used the super wet technique with machine-assisted suction, to obtain the lipoaspirate. A puncture wound was made with a scalpel blade and 50 – 150 ml wetting solution, containing adrenaline and saline, was injected into the donor area. A blunt tip harvesting cannula

was adapted to a long silicone tube, which was connected to a pump (aspirator). The adipose tissue along with the wetting solution was aspirated from the donor area and collected in the test tube. When the test tube filled up, the harvest process was paused and the sealing plunger was removed from the test tube to decant the lipoaspirate into a sterile bottle containing PBS supplemented with 5% pen/strep (Figure 3.12). The plunger was then used to reseat the negative pressure system and more lipoaspirate was collected. The collection ceased as soon as a reasonable amount of tissue was collected regardless of the amount of blood contamination. From here on all lipoaspirate was treated under the same conditions as previously described.

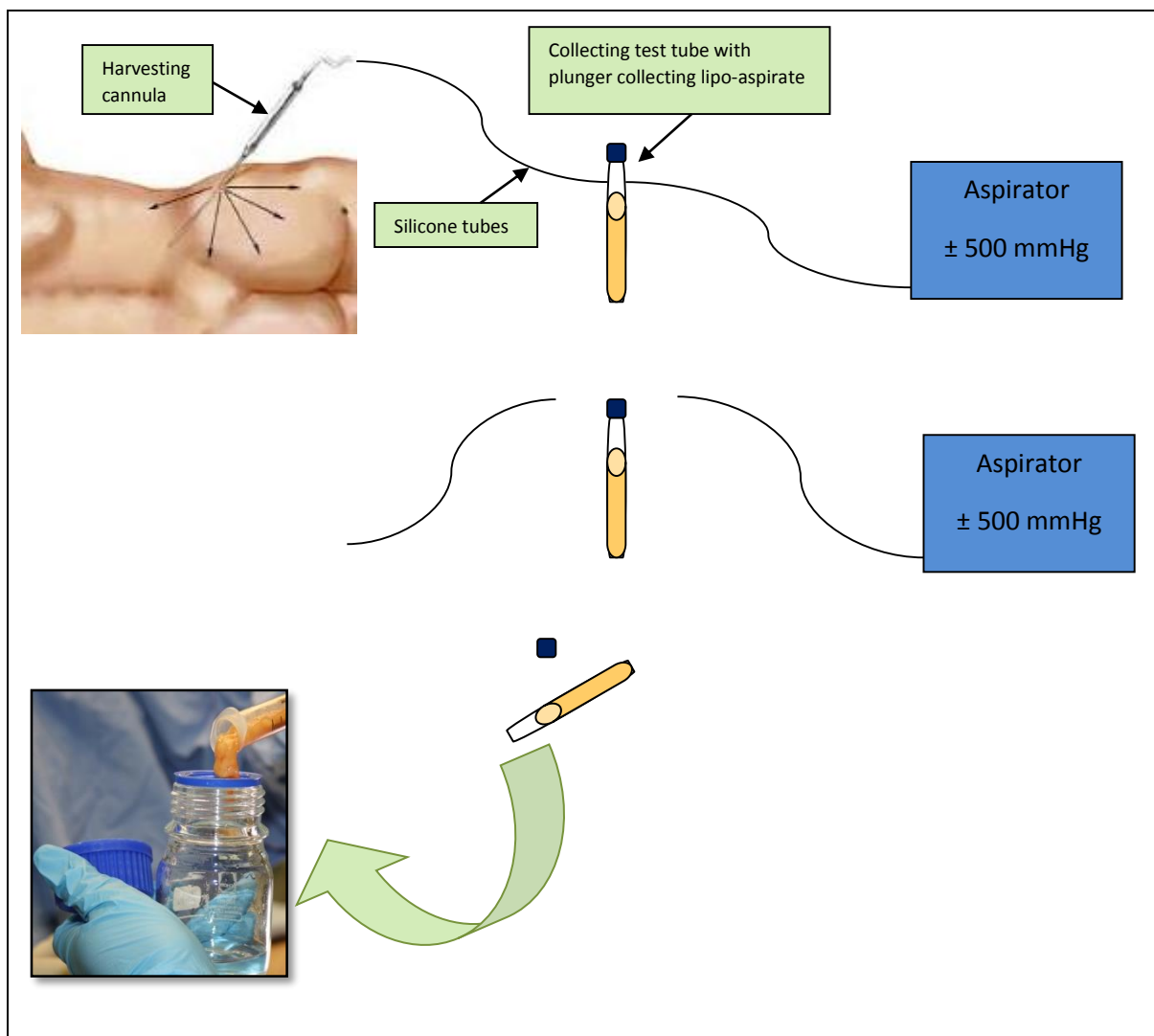


Figure 3.12. Lipoaspirate harvesting using the suction assisted tumescent liposuction technique. The donor site was infiltrated with a wetting solution using a 50 cc syringe and needle. The aspirator (suction machine), created a negative pressure of approximately 500 mmHg. Silicone tubes were used to connect the harvesting cannula, the collection test tube and the aspirator creating a closed vacuum system. The harvesting cannula was randomly advanced and retracted through the donor area. When the collecting test tube was filled (80%), the silicone tubes were detached and the plunger removed from the proximal end. The lipoaspirate was decanted into an autoclaved sterile bottle containing PBS and 5% pen/strep.

Transportation of the lipoaspirate

All the collection bottles containing the lipoaspirate and PBS supplemented with 5% pen/strep were transported at room temperature at (20-25 °C) to the cell culture laboratory within 2 hours of collection. During transportation the sample started to segregate into different layers of oil containing mostly lipids from damaged adipocytes and extracellular fluids; the adipose tissue layer containing adipose resident cells and structures; and PBS supplemented with 5% pen/strep containing blood contaminants. The collection bottle was also exposed to gentle shaking movements during travelling, which allowed the blood contaminants to move out of the segregated floating adipose tissue layer into the liquid layer beneath (Figure 3.13.).



Figure 3.13. During transportation the lipoaspirate started to segregate into layers consisting of (a) oil supernatant, (b) lipoaspirate and (c) PBS, supplemented with 5% pen/strep, containing blood contaminants. The gentle shaking of the collection bottle during transportation will allow more blood contaminants to move out of the adipose tissue into the liquid portion of the segregated sample.

Sample codification

The samples were codified to ensure patient anonymity. The first capital letter represents the source of tissue from which the stem cells are isolated from, 'A' for adipose tissue. The next six numbers represent the date of tissue collection, which is the same date the patient signed the informed consent, the isolation procedure was conducted and the isolates were placed in culture for expansion labeled as passage zero. The backslash separates the date code and the specified patient number, following numerical order in order of collection on the specific date (Figure 3.14). A lowercase 'b' indicates a different harvesting technique performed (Table 3. 1).

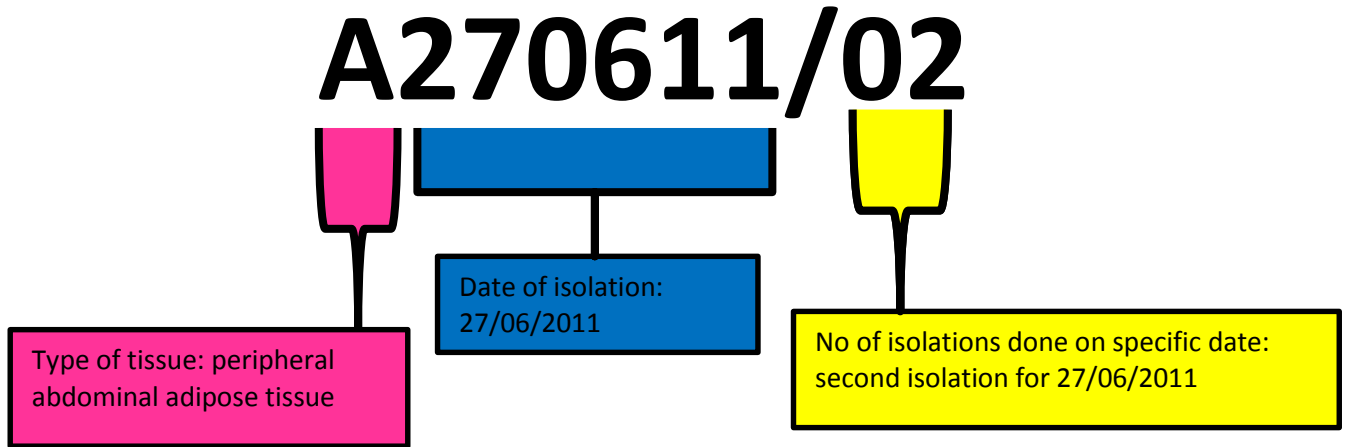


Figure 3.14. The codification given to samples collected from adipose tissue to ensure patient anonymity.

Isolation of ASCs

The isolation protocol followed was adapted from the described procedures of Zuk *et al.* (2001) and Bunnell *et al.* (2008).

The processing of adipose tissue for the isolation of ASCs was performed in a sterile environment. All aspects of the tissue processing, isolation and expansion were performed in a type II biosafety cabinet (BSC-II). The cabinet was sterilized with ultra violet light (UV light) for 15 min and also wiped down with 70% alcohol prior to use. All freshly prepared solutions were filtered prior to use with a 50 ml syringe connected to a 22 μ m filter (Corning, Cat# 431097N). All consumables and reagents used during the isolation and expansion processes were sterile, meeting standard cell culturing requirements. All solutions and equipment that was in contact with living cells were sterile and proper aseptic techniques were used. All culture incubations were performed in a humidified, 37°C, 5% CO₂ incubator unless otherwise specified. Good laboratory practice and laboratory safety principles were applied to all activities performed during the isolation process *e.g.* during centrifugation the instrument was counterbalanced by using the same volume of sample centrifuged or by balancing with distilled water (dH₂O) on the opposite side of the centrifuge loading circle (Figure 3.25.); laboratory attire was worn at all times including lab coats and gloves. All waste materials were placed into specified waste removal containers and a licensed medical and laboratory waste removal company was contracted to remove waste from the premises.

The speed of the centrifuge is described in revolutions per minute (rpm), although the rpm is dependent on the rotational radius of the centrifuge. Conversely, relative centrifugal force (RCF) commonly referred to as “g-force” is an acceleration constant

between different sizes, brands and types of centrifuges (<http://www.ehow.com>). Our centrifuge is a swinging bucket centrifuge (Thermo Fisher Scientific TX-200 Swing-out Rotor), therefore the length from the rotor axis to the centre of one of the buckets was measured to determine the rotational radius (11.45 cm) (Figure 3.25) and the RCF was determined using the formula: **RCF=0.0001118 x rotational radius x rpm²**. It was determined that 1200 rpm and 2000 rpm was the equivalent of 184 *g* and 512 *g* respectively.

The collected lipoaspirate was transferred in equal amounts from the collection bottle into four 50 ml tubes (Falcon) with the aid of a 25 ml serological pipette connected to a suction-assisted pipette aid. These samples were washed three times by transferring the centrifuged compacted lipoaspirate into sterile 50 ml Falcon tubes before introducing PBS containing 5% pen/strep to the sample followed by centrifugation at 3 000 rpm for 3 min. Thereafter, the oil supernatant was aspirated with a suction-assisted glass pipette system as shown in Figures 3.16 and 3.17. This system consisted of a glass pipette fitted to a silicon tube, connected to a waste collection bottle and a filter (22µm), which was fitted to a pump system, which generated the negative suction pressure. All waste was collected with this system and collected in a waste collection bottle. Once the waste collection bottle was filled, the bottle as well as the filter was replaced and all waste was discarded as described above.

After completion of the washing procedure, the volume of the centrifuged compacted adipose tissue was noted before the compacted adipose tissue layer (Figure 3.18) was transferred into sterile 50ml Falcon tubes to be weighed (Figure 3.19.). The recorded weight and volume of the compacted adipose tissue layer was used to calculate the amount of nucleated cells isolated per gram and milliliters relative to adipose tissue harvested.



Figure 3.15. Adipose sample transferred into 50 ml Falcon tubes and centrifuged to obtain the various supernatant layers. From the top, (a) the floating oil layer, (b) compact adipose tissue layer, (c) PBS supplemented with 5% pen/strep and blood, (d) blood cells (mostly red blood cells).



Figure 3.16. The oil supernatant layer was aspirated with a suction-assisted glass pipette.

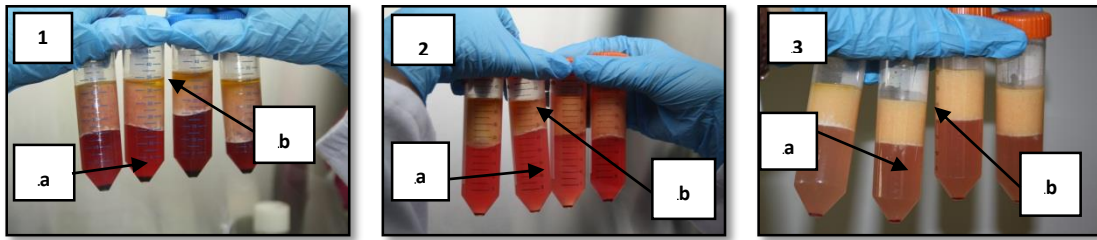


Figure 3.17. The supernatant consisted of four different layers displayed after the three washing procedures of sample presented by picture 1, 2 and 3 respectively. (a) A decrease in the blood cell contaminants in the PBS supplemented with 5% pen/strep was observed with increased washing. (b) A decrease in the oil supernatant layer was also observed with increased washing.

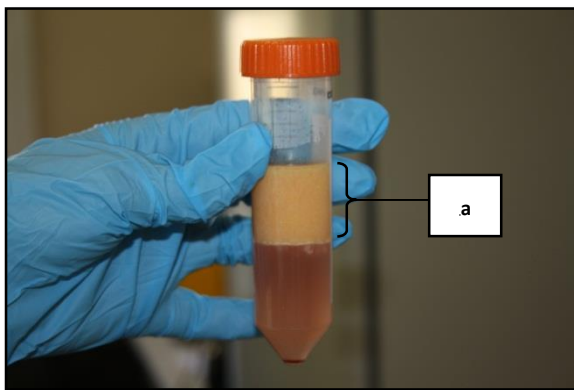


Figure 3.18. Centrifuged compacted adipose tissue indicated by (a). Volume of (a) was noted to determine the volume of 0.1% Collagenase Type I solution needed during the collagen digestion procedure.



Figure 3.19. The compacted adipose tissue was transferred into sterile 50 ml tubes to be weighed.

The adipose tissue was decanted from the tubes onto sterile culture plates. The number of plates filled was dependent on the volume of sample harvested and subjected to collagenase digestion (Figure 3.20.) to allow for the ASCs resident in the adipose tissue to be released from the fibrous network. A 0.1 % Collagenase Type I (Sigma, Cat# C9407-25 mg) solution using PBS, supplemented with 2% pen/strep (collagen digesting solution), was prepared for digestion and filtered to produce a sterile solution, as previously described. The volume of collagen digesting solution used was subject to the volume of centrifuged compacted adipose tissue previously recorded. The final volume of collagen digesting solution added to the adipose tissue in the culture plates was half that of the washed and centrifuged compacted adipose tissue volume. A sterile plastic Pasteur pipette was used to mix the adipose tissue well before incubation. The sample was incubated at 37°C in a 5% CO₂ incubator for 45 min (Figure 3.21.). The samples were agitated every 15 min during the incubation period with a plastic Pasteur pipette to aid the mechanical breakdown of the tissue in order to obtain single cell suspensions (Figure 3.22.).

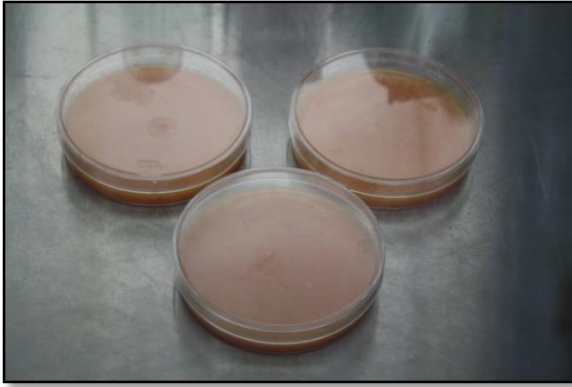


Figure 3.20. The adipose tissue was decanted from the 50 ml Falcon tubes onto sterile tissue culture plates. The 0.1% Collagenase Type 1 solution was added to the adipose tissue.

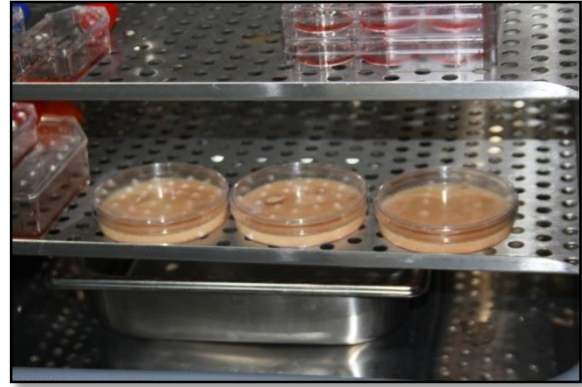


Figure 3.21. The adipose tissue and 0.1% collagenase Type 1 solution was incubated for 45 min at 37°C and 5% CO₂ for the process of collagen digestion to take place.

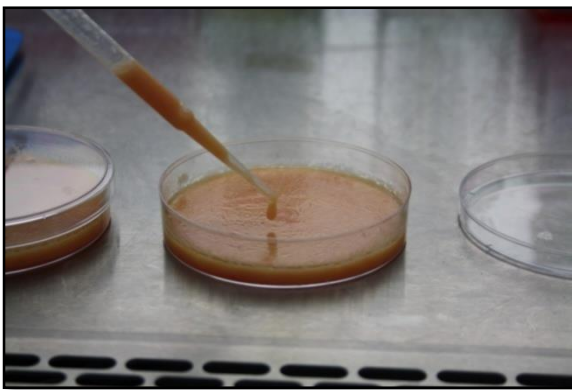


Figure 3.22. The adipose tissue with 0.1% collagenase Type 1 solution was taken out of the incubator and aspirated with a Pasteur pipette.

The next step was to transfer the collagen digested samples into sterile 50 ml tubes to be centrifuged at 2000 rpm for 5 min (Figure 3.23.). The tubes were then vigorously shaken in order to thoroughly disrupt the pellet and to mix the cells (Figure 3.24.). The samples were centrifuged again at 2000rpm for 5 min and the compact adipose tissue as well as the collagen solution was aspirated. The collagenase activity of the excess collagen solution on and within the pellet was neutralized by adding 2 ml of stromal medium. Stromal medium consisted of: alpha-Modified Eagle Medium (α -MEM GLutaMax™, no Nucleotides) (Gibco, Cat# 32561-029), supplemented with 10% fetal bovine serum (FBS), 1% L-Glutamine and 1% pen/strep).

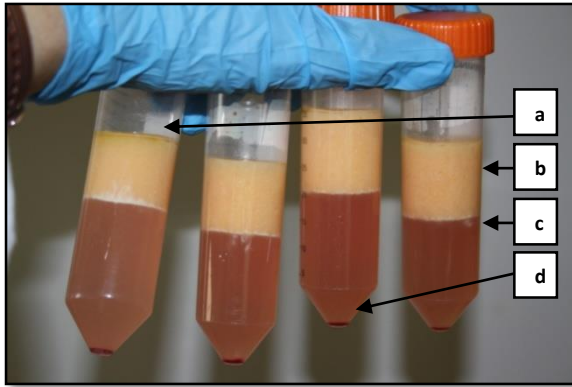


Figure 3.23. Centrifuged collagen digested adipose tissue displaying four layers: (a) a small floating supernatant oil layer; (b) compact adipose tissue; (c) a light pink layer containing 0.1% collagenase Type 1 solution and red blood cells; and (d) the red blood cell pellet.

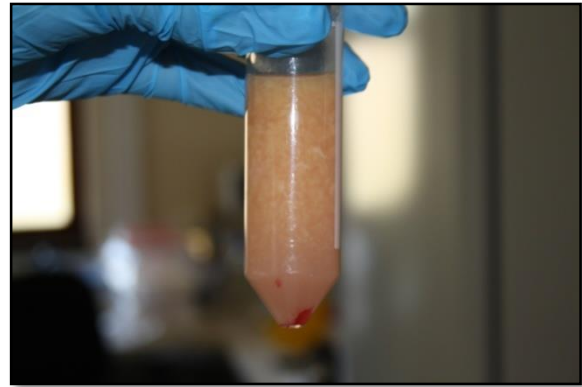


Figure 3.24. The centrifuged sample vigorously shaken to disrupt the digested adipose tissue and pellet within the tube.

The pellets were pooled together in a 15 ml tube and pipetted to mechanically disintegrate any aggregates of adipose tissue. The 15 ml tube was centrifuged at 1200 rpm for 5 min and the supernatant medium above the pellet was aspirated without disrupting the pellet (Figures 3.25. and 3.26.). The pellet was re-suspended in 1 ml Versalyse™ (Beckman Coulter, Cat#41116-015) and incubated for 10 min under standard culturing conditions in order to lyse the contaminating red blood cells (Figure 3.27.).

The lysing reaction was stopped with the addition of 8 ml PBS supplemented with 2% pen/strep. The sample was then centrifuged again at 1200 rpm for 5 min and the supernatant was aspirated. The pellet was washed again with 2 ml PBS containing 2% pen/strep and centrifuged at 1200 rpm for 5 min. The supernatant was aspirated and the cell pellet was re-suspended in 2 ml of stromal medium.



Figure 3.25. When using the centrifuge, the rotator was balanced in order to obtain the same weight on the opposite side. A balance or a sample with equal volume was inserted to counter balance the respective sample.

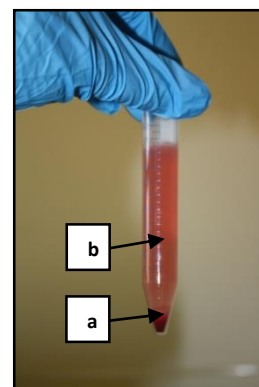


Figure 3.26. After centrifuging for 5 min at 1200 rpm the pooled cell suspension formed a pellet. (a) The pellet contains adipocytes, ASCs, as well as cells from the hematopoietic lineage and (b) stromal medium.



Figure 3.27. The pellet of ASCs and red blood cells was re-suspended in Versalyse™ and incubated for 10 min at room temperature to lyse the red blood cells.

The cell suspension was then filtered through a 70 μm Falcon cell strainer (BD Biosciences, Bedford, MA, USA) by using a Pasteur pipette. An extra 2 ml stromal medium was used to wash the cell strainer in order to collect additional cells. A cell count was performed using a Trypan Blue (40%) dye exclusion assay as described below. The number of viable cells within the cell suspension was determined from the cell count and from that the volume of cell suspension was determined to seed the cells at the initial required seeding density into tissue culture flasks (NUNC T80). The initial seeding density was 5×10^5 cells per cm^2 (Figure 3.34.). The calculated volume of cell suspension was pipetted into the tissue culture flasks containing a respective volume of stromal medium dependent on the total tissue culturing surface area available for the cells to adhere to.

The culture was subsequently placed into the incubator and maintained under standard cell culture conditions (humidity, 5% CO_2 and 37°C). After 24 hours the medium was aspirated from the cultures and the cultures were washed twice with PBS supplemented with 2% pen/strep, removing most of the non-adherent cells from the culture. Fresh stromal medium was placed in the culture flasks and the culture was further incubated under standard culture conditions.

Cell counting techniques

Two different cell counting techniques were compared and used during the course of the isolation and expansion procedures. These included the manual counting method of viable and non-viable cells using a Trypan blue dye exclusion assay, as well as counting cells and particles using flow cytometric analysis. Respective volumes for the two techniques were taken from the same cell suspension for each technique.

The Trypan Blue (40%) stain was used to perform cell counts of viable and non-viable cells. The total cell count determined from the assay was used to determine the volume

of cell suspension needed for the initial seeding of the cells after the isolation process from the SVF and for the re-seeding of cells during passage procedures, as well as after the thawing process of a cryo-preserved sample.

Flow cytometry was used to determine the cell density of cell suspensions (Figure 3.29.B). The cell density was used to determine the volume of cell suspension needed to re-seed cells during the process of passage (Figure 3.30.).

Trypan Blue (40%) dye exclusion assay

Trypan Blue is a nuclear stain that is used to assess the viability of cells as it does not cross the plasma membrane. Staining therefore occurs only in non-viable cells with a loss of plasma membrane integrity. A 0.5 ml Eppendorf tube was autoclaved. The 40% Trypan Blue stain solution was prepared by combining 80 μ l Trypan Blue stain (Sigma, Cat# T8154), 100 μ l PBS and 20 μ l of the respective cell suspension. The solution was mixed with an air displacement pipette and 10 μ l of the solution was loaded onto both sides of the Neubauer counting chamber (haemocytometer) (Figure 3.28.). A glass cover slip was placed in a slanting position on top of the haemocytometer to avoid any air bubbles. The haemocytometer with loaded sample and glass cover slip was placed under the microscope with the 10x objective lens to obtain one quadrant of grid within the vision field. With the aid of a cell counter clicker, the cells with illuminated cytoplasm were counted as viable cells and the dark blue cells were counted as non-viable cells (Figures 3.28. and 3.29.).

The number of viable and non-viable cells counted from eight quadrants was recorded. A calculation was performed to determine the respective viable and non-viable cells within the cell suspension. The total amount of viable cells was divided by the number of quadrants counted to obtain the number of cells per μ l. The amount of cells per μ l was then multiplied by the volume of the cell suspension to obtain the number of cells within the respective cell suspension known as the cell suspension cell density. The same calculation format was performed to determine the number of non-viable cells within the cell suspension (Figure 3.29.A).

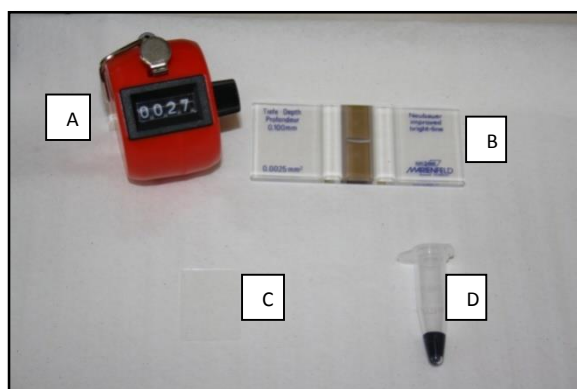


Figure 3.28. A) A cell counter clicker to assist with cell counting; B) Neubauer counting chamber

A	<u>Trypan Blue Assay calculation</u>
	[Total number of cells counted from quadrants \div Number of quadrants counted] X 100 000 (dilution factor) X volume of cell suspension in μ l
B	<u>Flow Cytometry cell count calculation</u>
	[Number of cells per μ l gated on the forward scatter linear and side scatter linear dot plot] X 1 000 (dilution factor) X the volume of the cell suspension in μ l

Figure 3.29. Calculations used to determine the number of cells within a cell suspension.

(haemocytometer) with two chambers on each side. Each chamber contains a grid displaying four counting quadrants; C) a glass cover slip, that is placed on top of the haemocytometer after 10 μ l of the Trypan Blue stain solution is loaded; D) The 40% Trypan Blue stain solution containing, 80 μ l Trypan Blue stain, 100 μ l PBS and 20 μ l of cell suspension.

(A) Calculation performed when using the Trypan Blue (40%) dye exclusion assay. (B) Calculation performed when using flow cytometric analysis.

Cell count determined by flow cytometric analysis

Polypropylene tubes (flow tube, Beckman Coulter, Cat# 2523749) were used for all experiments to minimize adherence of cells and fluorescent beads (Flow-Count™, Beckman Coulter, Cat# 7547053). A flow tube was prepared to determine the cell density of each cell suspension. The flow tube included the cell suspension and the fluorescent beads at a 1:1 ratio in 1000 μ l PBS. Both the cell suspension and fluorescent beads were well mixed before 100 μ l of each was transferred with a pipette to the flow tube.

The fluorescent beads are a suspension of fluorospheres used to determine absolute counts on the flow cytometer. Each fluorosphere contains a dye, which has a fluorescent emission range of 525nm to 700nm when excited at 488nm. They have uniform size and fluorescence intensity and an assayed concentration (calibration factor), which allows a direct determination of absolute event counts (package insert: <https://www.beckmancoulter.com>).

Standard operating procedures were followed for initializing the flow cytometer (Beckman Coulter, FC 500 and Gallios). In short, it was ensured that the levels of Cleanse and IsoFlow™ Sheath fluid (flow cytometersupport reagents, Beckman Coulter) were sufficient and the waste container level low. The laser was allowed enough time to warm up followed by performing a flow check. Flow-Check™ (Beckman Coulter, Cat# 6605359) in a flow tube was used with a Flow-Check standard protocol to ensure that the laser was lined up across all fluorochrome channels.

The prepared flow tube was placed in the carousel of the flow cytometer and the sample identity as well as the respective calibration factor of the Flow-Count fluorescent beads was inserted into the protocol panel under CAL. The cell counting protocol consisted of a side scatter linear (SS lin) and a forward scatter linear (FS lin) plot with a gate placed around the cell population and excluding the flow beads and debris (Figure 3.30.). A single channel histogram (FL1 or FL4) with a gate labeled as CAL was placed over the flow beads peak (Figure 3.31.). The cell population gated in the SS lin and FS lin plot (Figure 3.30.) was counted until the calibration factor was reached, determined by the beads counted within the CAL gate in the single channel histogram. The cell population count ceased when the number of beads counted per μ l was equal to the calibration factor.

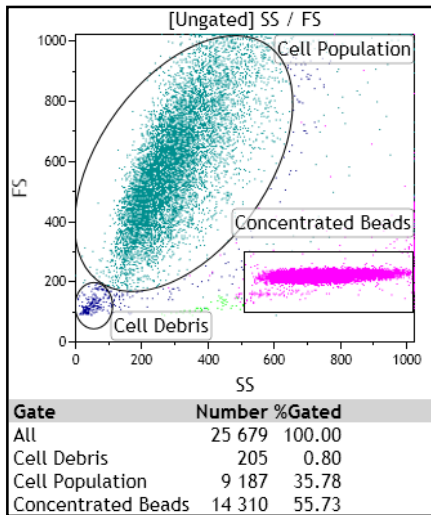


Figure 3.30. A side scatter linear and forward scatter linear dot plot displaying the events measured by the flow cytometer. The flow beads (pink) and a gate were used to encircle the cell population that was counted until the CAL factor was reached. The gate labelled cell population displayed the cell population count that was expressed as the number of cells per μl cell suspension.

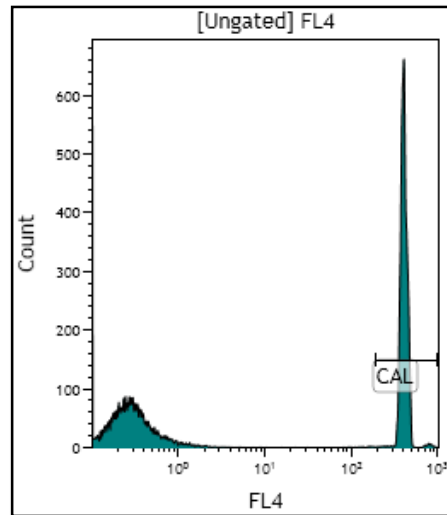


Figure 3.31. A histogram, displaying the flow beads with a gating placed over the peak of the flow beads labelled as CAL. The specific calibration factor for CAL was 986. The dot plot (Figure 3.27.) was gated on gate D within the histogram in order to display only the flow beads.

The gated cell population was displayed as the number of events within the gated population and with conversion calculations the total number of cells per $1 \mu\text{l}$ cell suspension can be calculated (Figure 3.29.B). With that the total number of cells present within the respective cell suspension as well as the volume of cell suspension are required to determine the density of the cell suspension.

Flow Cytometric quantification

(Number of events within gated population on the forward - and side light scatter linear plot \div the fluorescent bead region labelled CAL \times calibration factor of fluorescent bead suspension used

Figure 3.32. Considering the quantification, the number of events within the gated population was represented by the cell population gated in Figure 3.28 (9 187 events). The fluorescent bead region is represented by CAL in Figure 3.29 (3 657 events) times by the respective cell suspension volume (μl).

Flow Cytometry cell count calculation

Number of cells per μl gated on the forward scatter linear and side scatter linear dot plot \times 1 000 (dilution factor) \times the volume of the cell suspension in μl

Figure 3.33. The flow cytometric analysis program Kaluza, does not display the result as the number of events per μl of a respective gated region. The Flow cytometer expresses this measurement, which was an easier way to calculate the cell density within the respective cell suspension.

Seeding

Seeding refers to the cells being placed within a culturing flask to be expanded and seeding density refers to the number of cells that are placed on a specific size surface area. The initial seeding density was only performed at passage zero, which was the first seeding of the SVF after the isolation procedure and the re-seeding density of the expanded ASCs was then used during every consecutive passage.

The volume of cell suspension had to be determined, in order to seed the cultures at the required densities. Two different seeding densities were used, the initial seeding density of 5×10^5 cells per cm^2 for SVF (Figure 3.34.) and the re-seeding density of 5×10^3 cells per cm^2 for ASCs (Figure 3.35.).

Volume of cell suspension determined for initial seeding of cells

Total number of viable cells in cell suspension \div (initial seeding density X seeding surface area of tissue culture flask or well)

Initial seeding density: 5×10^5 cells/ cm^2

Figure 3.34. Calculation to determine the volume of cell suspension needed to seed cells at an initial seeding density of 5×10^5 cells/ cm^2 . The volume of cell suspension was then added to the respective tissue flask containing fresh α -MEM supplemented with 10% FBS and 1% pen/strep.

Volume of cell suspension determined for re-seeding of cells with passaging and thawed out samples

Total number of viable cells in cell suspension \div (re-seeding density X re-seeding surface area of tissue culture flask or well)

Re-seeding density: 5×10^3 cells/ cm^2

Figure 3.35. Calculation to determine the volume of cell suspension needed to seed cells for expansion purposes during passaging procedures at a density of 5×10^3 cells/ cm^2 . The volume of cell suspension was then added to the respective tissue flask containing stromal medium.

***In vitro* nourishment maintenance of MSC cultures during culture expansion**

All isolated cells were maintained under standard cell culture conditions and allowed to expand in the tissue culture flasks with either addition or replacement of fresh stromal medium at 48 hour intervals. Fresh stromal medium was added to the cultures 48 hours after the cells were seeded, at respective stromal medium addition volumes (Table 3.1). The entire conditioned medium was aspirated at 96 hours after seeding and replaced with fresh stromal medium, at respective stromal medium replacement volumes (Table 3.1.). The stromal medium replacement volumes were the same stromal medium volumes used during seeding procedures.

Table 3.1. Tissue culture flasks with respective tissue culture surface areas and volumes of stromal medium additions and changes during expansion of cultures.

Tissue culture flask or tissue culture plate	Tissue culture surface area (cm^2)	Stromal medium addition volume (ml)	Stromal medium replacement volume (ml)	0.25% Trypsin volume used (ml)
T80	80	3	7	4
T75	75	3	7	4
T25	25	1	4	3
6 well plate	(57.6 per plate)	6 per plate	12	6

1 well of a 6 well plate	9.6	1	2	1
--------------------------	-----	---	---	---

The cultures were maintained under standard culture conditions until sub-confluence (about 80 to 90% confluent) was reached. A culture was viewed under a microscope and if about 80 to 90% of the tissue culture flask's surface area was covered with cells, it was considered to be sub-confluent. When a culture was identified as sub-confluent it was passaged on the same day.

***In vitro* passaging of MSC cultures**

Passaging is a process in which cells are enzymatically detached from the tissue culture flask or plate and reseeded in a sterile tissue culture flask or plate. The conditioned medium was aspirated with a suction-assisted glass pipette and warm PBS supplemented with 2% pen/strep was placed in the flasks to wash excess conditioned medium off the cell culture. The PBS was aspirated using a suction-assisted glass pipette before pipetting preheated (37°C) 0.25% Trypsin/EDTA (Gibco, Cat# 25200072) into the culture flasks. The volume of Trypsin-EDTA used was dependent on the cell culture surface area that was targeted (Table 3.1.). The cultures were incubated under standard culture conditions (37°C) for 20 min or until approximately 99% of the cells had detached from the bottom of the flask. The progress of detachment was monitored under an inverted microscope.

The Trypsin-EDTA digestion was ceased by the addition of stromal medium at a 1:1 volume ratio to the Trypsin-EDTA solution. The culture flask was tilted and with 10 ml pipette the cell suspension was pipetted over the culture area to mechanically remove cells from the surface and to separate trypsin digested cells from each other. The cell suspension was then transferred into a 15 ml tube.

The culture flasks were washed with PBS, supplemented with 2% pen/strep. The PBS was then transferred with a 10 ml pipette to the 15 ml tube containing the trypsin and stromal medium cell suspension. After counter-balancing the centrifuge with either a balance or another tube containing another culture's cell suspension with the same volume, the samples were centrifuged for 5 min at 1200 rpm at a temperature of 21°C (Figure 3.25). The supernatant was aspirated with a suction-assisted glass pipette and the pellet was re-suspended in PBS supplemented with 2% pen/strep.

The density of cells within the cell suspension was determined by performing a Trypan Blue (40%) dye exclusion assay and flow cytometry. The total number of cells in the cell suspension was determined using the respective cell count technique calculations (Figures 3.29.A and 3.29.B). The total number of cells determined by flow cytometry was used to calculate the volume of cell suspension needed to re-seed the cells, at a density of 5×10^3 cells per cm^2 (Figure 3.35.). The respective volume of stromal medium dependent

of the surface area of the flask was spread over the cell culture surface area, using a tilting technique. The respective PBS-cell suspension volume calculated according to the cell culture surface area was pipetted into the stromal media in the tissue culture flask (Table 3.1.). The cultures were then shifted left to right and forward and back on the work counter, not allowing the flask to tilt. The cultures were placed very carefully in the incubator, where they were maintained under standard culture conditions.

Growth kinetics

After the SVF isolation, five separate culture plates were seeded at an initial seeding density of 5×10^5 cells per cm^2 (Figure 3.34.). After 24 hours, the cultures were washed twice with PBS containing 2% pen/strep in order to remove most of the non-adherent cells from the culture. All the cells were removed for quantification from one respective culture plate at 24 hours (day 1), 72 hours (day 3), 120 hours (day 5), 168 hours (day 7) and 216 hours (day 9). As described above, the cells were removed from the culture plates using trypsin-EDTA (0.25%) and quantified using the Trypan Blue (40%) dye exclusion assay as well as flow cytometry, after which the samples were discarded. The quantification of the cells was used to create a growth kinetic curve over 9 days and included cell counts performed by flow cytometry (both viable and non-viable cells) as well as viable and non-viable cells as counted by the haemocytometer.

Long term Expansion

Both quantification methods, Trypan Blue (40%) dye exclusion assay and flow cytometry (see above) of cell suspensions during passaging, were recorded, as was the time between passages (dates) and the total surface area that was passaged was noted. The collection of the lipoaspirate from the patient was considered as passage zero and for all purposes, the first trypsinization procedure was considered as passage 1 and so forth.

Cryo-preserving and thawing of cryo-preserved MSCs samples

After the different cell counting techniques had been performed, the re-seeded cultures were placed in the incubator, concluding the passaging process and the excess cells available within the left over cell suspension were cryo-preserved. Cultures were also cryo-preserved when the expansion of that culture was ceased. The cell suspensions were centrifuged for 5 min at 1200 rpm and 21°C , after which the supernatant was aspirated with a suction-assisted glass pipette. The pellet was re-suspended in Dulbecco's Modified Eagle Medium + GlutaMax +4.5g/L D-glucose+ Pyruvate (DMEM) (Gibco, Cat# 31966-021) containing 10%DMSO (Sigma, Cat# D2650) and 20% FBS. The cell suspension was then transferred into labelled cryo-preservation vials and placed on ice for 5 min. The vials were then transferred into a plastic container (Mr Frosty, by Nalgene) that floats on top of iso-propanol (alcohol-based freezing container). The sealed alcohol freezing containers were stored overnight in the -80°C freezer. The alcohol freezing

containers cooled the vials slowly, at approximately 1°C every minute until the vials reached a temperature of -80°C. The frozen cryo-preservation vials were then transferred into the storage tank, containing liquid nitrogen for long term storage at -150°C. The meticulous labeling on the sample (see figure 3.14.), which included the culture code and passage number as well as the date the culture was cryo-preserved, was also recorded in the inventory file under the position in which the sample was stored.

For thawing, the cryo-preserved samples were removed from the liquid nitrogen storage tank and immediately placed on ice to thaw slowly. The thawed cell suspensions in a volume of 1 to 2 ml were transferred into a 15 ml tube containing 4 ml of stromal medium. The samples were centrifuged at a temperature of 21°C for 5 min at 1200 rpm and the supernatant was aspirated with a suction-assisted glass pipette. The pellet was re-suspended in 2 ml stromal medium and the density of the cell suspension was determined using a Trypan Blue (40%) dye exclusion assay as described above. The viable and non-viable cell density were recorded, although only the viable cell density was used to determine the volume of cell suspension needed to seed the cells at a density of 5×10^3 cells per cm^2 . The cultures were maintained under standard culture conditions and nourished according to nourishment maintenance requirements of cultures during *in vitro* expansion, as described above.

The viability of MSCs before and after cryo-preservation was determined by comparing the non-viable and viable cell counts expressed as a percentage. Furthermore, the viable cell counts before and after cryo-preservation was compared to determine the number of viable cells lost during the cryo-preservation and thawing processes.

Results

Adipose tissue harvesting and transportation to the laboratory

The following general observations were made during the harvesting process. The two different harvesting techniques used both yielded sufficient amounts of adipose tissue in weight and visually contained the same amount of blood contaminants. The harvesting cannula appeared to advance and retract more smoothly through obese patients (BMI >30) vs. overweight patients (BMI 25 – 29). Lipoaspirate samples appeared brighter yellow in colour, containing visibly more oil and blood contaminants. The surgeon found the process of advancing the harvesting cannula through a skin flap more difficult and these samples also appeared more whitish in colour and 'stringy' in texture.

During transportation, the lipoaspirate started separating into layers within the collection bottles consisting of an oil supernatant, lipoaspirate and PBS containing blood contaminant (Figure 3.13).

Isolation of ASCs

Results of the adipose tissue harvested are presented in Table 3.2. This includes patient age, the actual volume of adipose tissue harvested and the number of cells isolated as determined using the haemocytometer as well as the number of cells per ml and gram of tissue. The mean age of the patients was 42 years with a median of 34 (18 – 82). The mean amount of adipose tissue harvested was 36 ml and the mean number of cells isolated per ml of tissue was 822 039. The least number of cells harvested per ml was from an 18 year old followed by a 39 year old, whereas a 41 year old yielded more than a million cells per ml and a 25 and a 68 year old yielded more than 2 million cells per ml. The average amounts of viable cells isolated per ml of lipoaspirate within age groups 0-25, 26-40, 41-50 and 51-82 was 862 330, 300 295, 907 346 and 1 378 666 respectively.

Table 3.2. Sample collections recorded and standardized as cells isolated per unit.

Culture Code	Age of Patient	Volume of adipose tissue sample collected (ml)	Weight of adipose collected (g)	Number of cells isolated (haemocytometer count)	Number cells isolated per lipoaspirate volume (ml)	Number cells isolated per weight (g)
A090311/01•	34	33	-	9 400 000	284 848	-
A040411/01 ^ψ	18	32	-	2 625 000	82 031	-
A130411/01	68	30	41.9	85 800 000	2 860 000	2 047 733
A130411/02	82	30	18.3	26 880 000	896 000	1 468 852
A130411/02b [†]	82	30	18.9	11 400 000	380 000	603 175
A200411/01	25	50	46.9	133 000 000	2 660 000	2 835 821
A050511/01	19	40	36.8	14 625 000	365 625	397 418
A100511/01	34	65.5	62.6	27 051 500	413 000	432 133
A220611/01	33	50	52.3	18 750 000	375 000	358 509
A270611/01	20	22.5	25.1	7 687 500	341 667	306 275
A270611/02	41	30	33.7	42 375 000	1 412 500	1 257 418
A050711/01	50	15	14.3	7 312 500	487 500	511 364
A180811/01*	39	45	55.6	5 775 000	128 333	103 867
Mean	42	36	37	30 206 269	822 039	938 415
Standard deviation	22.43	13.38	16.44	38 052 310.76	927 202.63	865 446.83

[†] The Coleman liposuction technique was followed, although a 20 cc syringe instead of a 10 cc syringe was used to harvest the adipose tissue at a higher negative pressure.

*Patient's sample collected from Steve Biko Academic Hospital and adipose sample was collected from an expanded skin flap (from hip area) on hand, using the 'super wet' liposuction technique and pump suction assistance.

‡Patient's sample collected from Steve Biko Academic Hospital and adipose sample was collected from an expanded skin flap (from thigh area) on foot, using the 'super wet' liposuction technique and pump suction assistance. The compacted adipose tissue was not weighed before digestion.
 • The Coleman liposuction technique was performed to harvest adipose tissue, although the compacted adipose tissue was not weighed before digestion.

Growth kinetics

The ability of the cells to expand over 9 days is illustrated in the various figures. Growth curves of selected cultures were drawn based on available cell count data. Figure 3.36 shows the growth kinetics as observed using the Trypan Blue (40%) dye exclusion assay and depicts viable cells. Variation among the viable cells between cultures at day one was observed possibly due to varying degree of blood contamination during the harvesting procedure. Point of reference was established by using Day 1 passages as these are considered to have proliferated minimally with the non-adherent cells being washed off and the adherent cells trypsinized and counted. A slight increase in growth was observed across all cell lines between days three and five with a steep increase in growth between days 5 and 7 except for culture A270611-02, which peaked at day 7. Between days 7 and 9, cultures seemed to decrease slightly with a plateau phase, but culture A270611-02 showed a steep increase towards day 9.

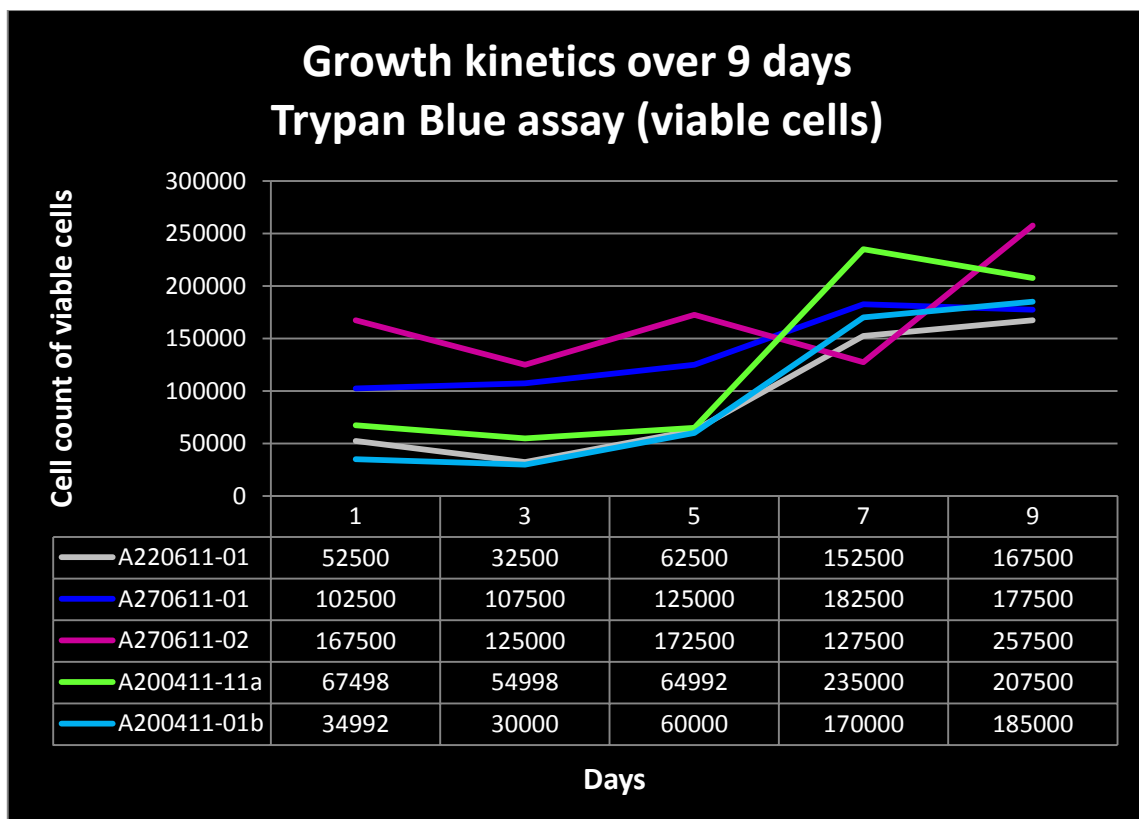


Figure 3.36. The growth kinetics of 5 cultures over a period of 9 days. The SVF cells were seeded in a six well plate and the non-adherent cells washed off after 24 hours. A well was trypsinized on day 1, 3, 5, 7 and 9 respectively. The cell counts of the viable cells were performed using a 40% Trypan Blue Exclusion Assay, at

24 hours (day 1), 72 hours (day 3), 120 hours (day 5), 168 hours (day 7) and 216 hours (day 9) in respective culture plates, after an initial seeding density of 5×10^5 cells per cm^2 .

Cell viability didn't decrease over the 9 days and remained below 10 000 non-viable cells, except for culture A100511-01 (Figure 3.36.).

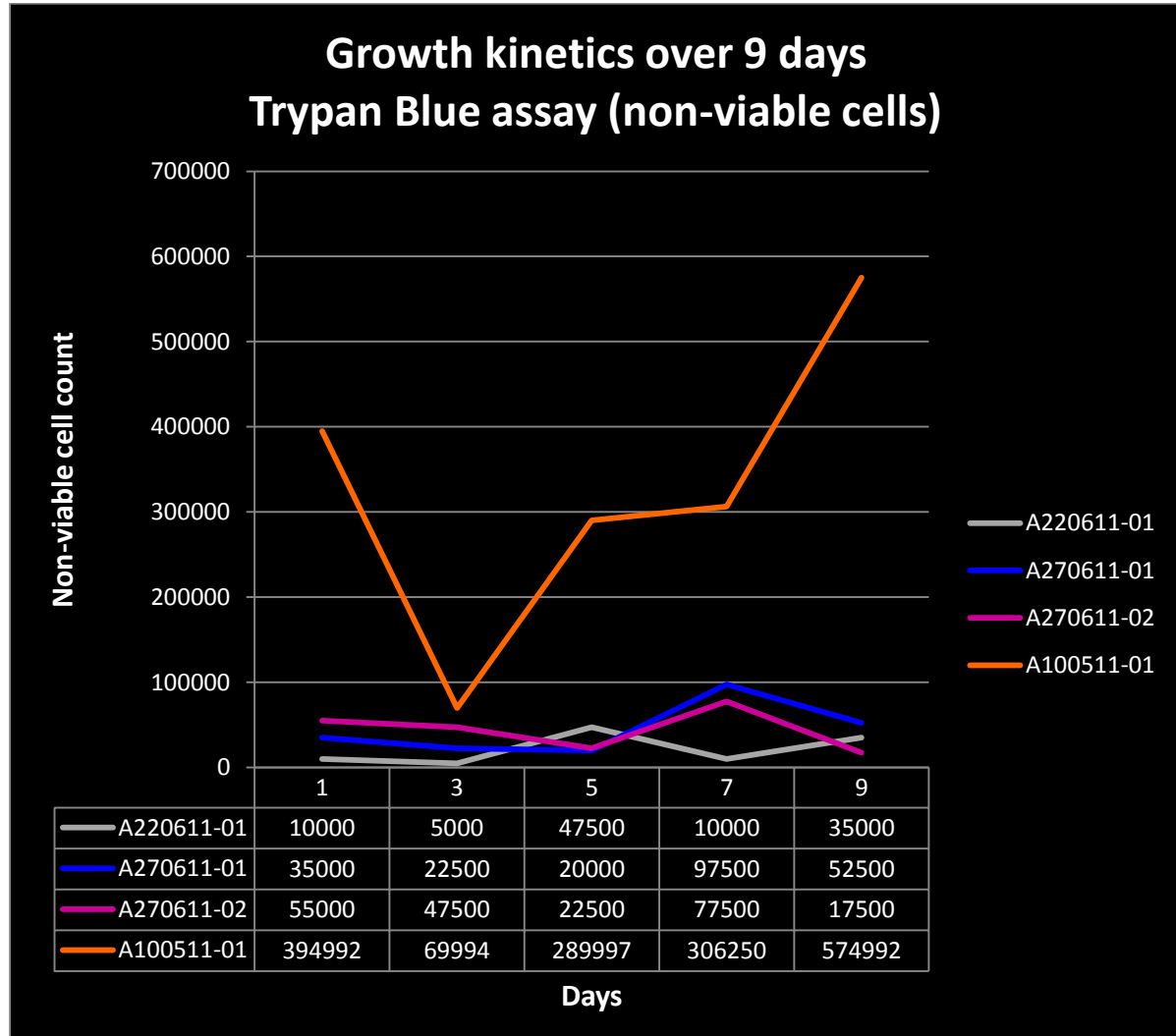


Figure 3.37. The kinetics of 4 cultures over a period of 9 days. Cell counts of the non-viable cells were performed using a Trypan Blue (40%) dye exclusion assay, at 24 hours (day 1), 72 hours (day 3), 120 hours (day 5), 168 hours (day 7) and 216 hours (day 9) in respective culture plates, after an initial seeding density of 5×10^5 cells per cm^2 .

The flow cytometric analysis also showed an increase in growth between day three and day seven with all the cultures reaching their peak at day 7. Culture A100511-01 showed a high growth rate. The growth rate increased within cells between different days and increased for all the cultures excluding A100511-01 between day 3 and 7. The difference between day 3 and 5 vs. day 5 and 7 is shown in and Figure 3.38.

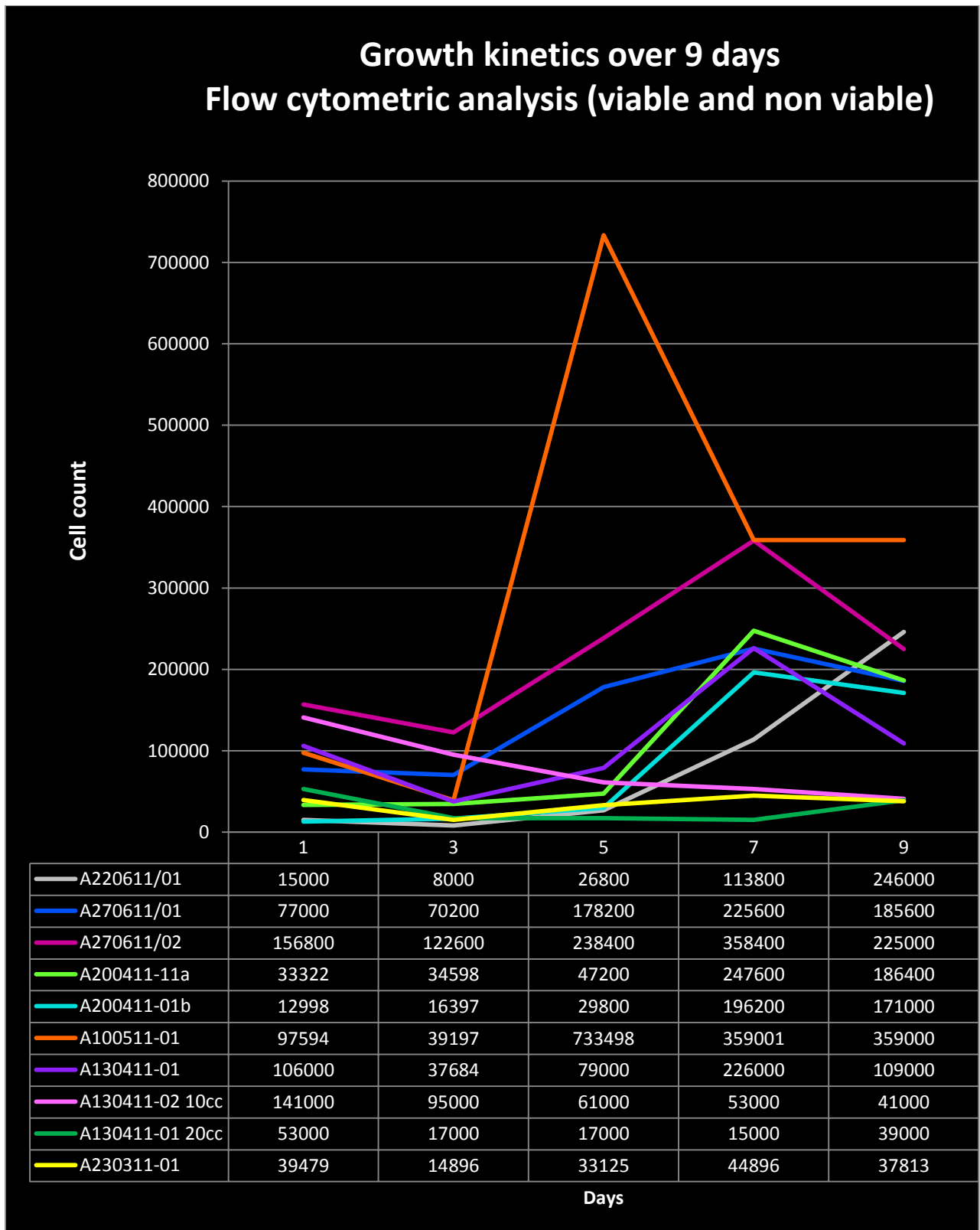


Figure 3.38. The growth kinetics of 10 cultures over a period of 9 days. Cell counts of the viable and non-viable cells were performed using flow cytometry, at 24 hours (day 1), 72 hours (day 3), 120 hours (day 5), 168 hours (day 7) and 216 hours (day 9) in respective culture plates, after an initial seeding density of 5×10^5 cells per cm^2 .

Expansion of ASCs

Most of the cultures were expanded beyond passage 10. The cell count determined using both methods, flow cytometry (Figure 3.30.) as well as a Trypan blue 40% dye exclusion assay (Figure 3.28. and 3.29.), was used to calculate the density of ASCs that was passaged from a surface area. Across 11 different cultures the average ASCs yielded up to passage 16 was more than 9 000 ASCs per cm² of plastic culture flask. Both ASC counting techniques correlate by following a similar trend line (Figure 3.39).

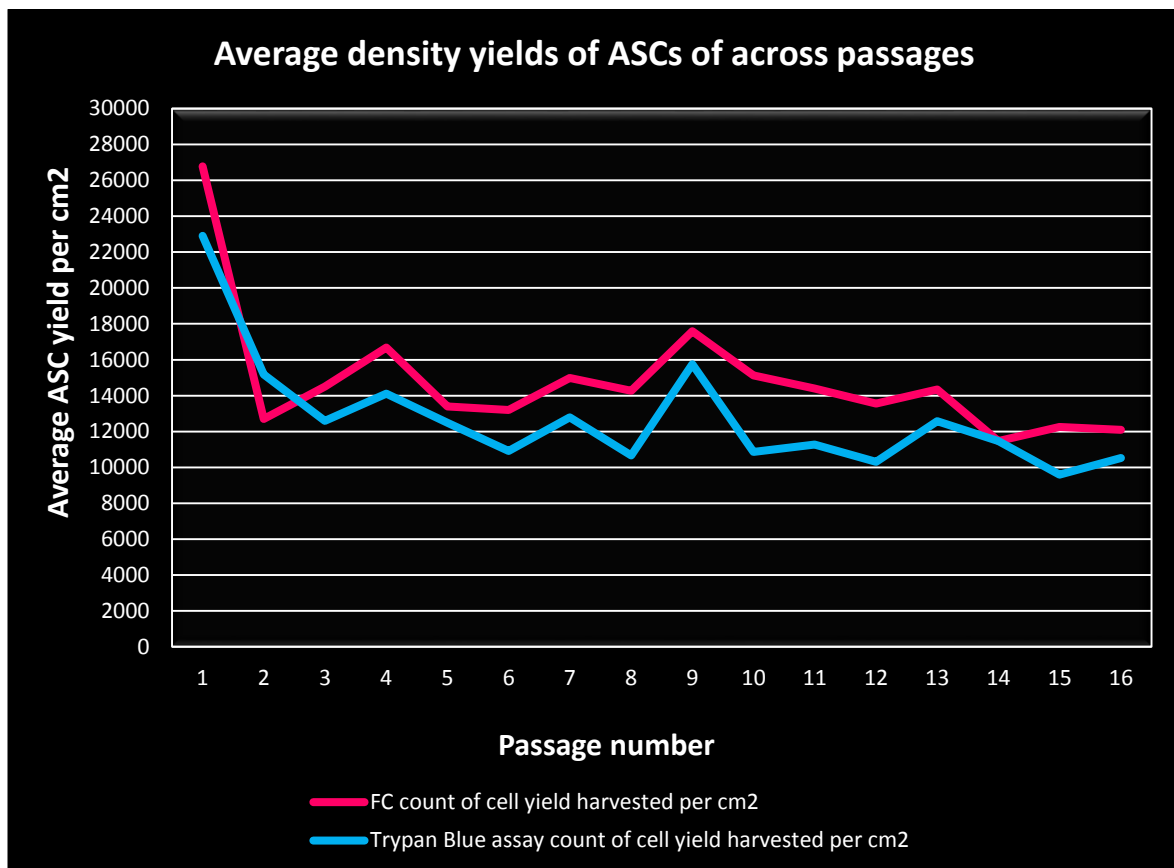


Figure 3.39. Average ASC yield per cm² for every passage (up to passage 16) of 11 different cultures. Cell counts, determined by flow cytometry (pink line) and manual using a Trypan Blue 40% dye exclusion assay (Blue line) was used to calculate the cell yield that was passaged from a surface area.

Cryopreservation

The percentage of viable cells prior to freezing and after thawing is displayed in Figure 3.40. The mean percentage viable cells prior to freezing was 86% (SD 6.0; 95% CI) while the mean percentage of viable cells after thawing was calculated at 64% (SD 9.5; 95% CI). A loss of 22% of cells was thus observed after the thawing process.

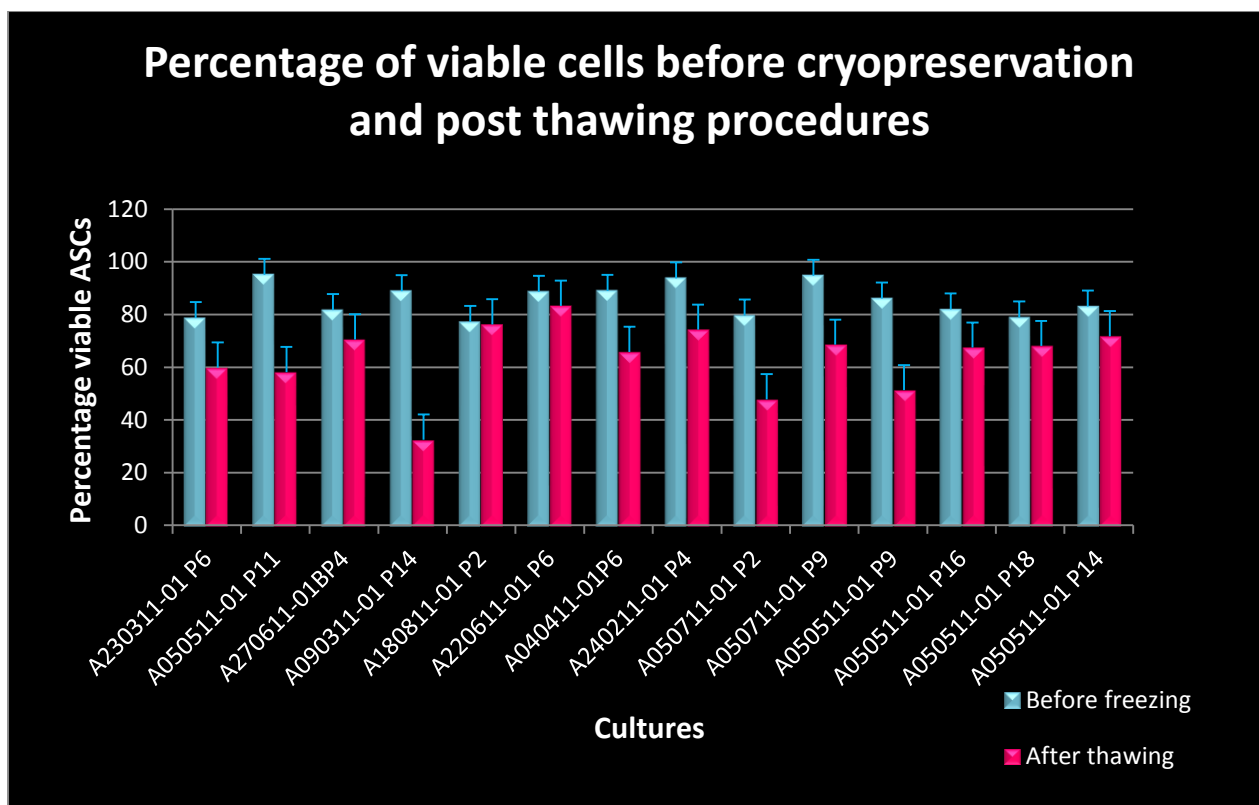


Figure 3.40. The percentage of viable ASCs determined across 14 cultures using the Trypan Blue (40%) dye exclusion assay before cryopreservation (indicated in blue) and after thawing procedures (indicated in pink). The difference between the blue and pink values indicates the percentage of cells lost due to the freezing-thawing process.

Discussion

Lipoaspirate harvesting and ASC isolation

The study included patients' samples from a wide age range (18 to 82). Age did not appear to influence the volume of adipose tissue harvested or the amount of cells isolated from the tissue, however this could not be assessed for statistical significance due to the small number of patients. Differences between genders could not be compared due to the small sample size used. Healthy lipoaspirate was only obtained from one male patient with age of 82 years. As discussed in the introduction, the effect of age and gender may play a very important role during the isolation process but due to the nature of this work and the study design no firm conclusions could be made. The author suggests a large randomized controlled trial to assess this phenomenon. It however remains very interesting and also useful to mention that more than 2 million cells per ml were isolated from both the 25 year old and the 68 year old. Furthermore the mean number of cells isolated as calculated per ml of tissue was 822 039 cells per ml. Although there may be variation among harvested tissue with regard to blood contaminants, this information is

critical in the development of an algorithm to assist the manufacturing process of cells for clinical application.

The Coleman technique was used to harvest all but two of the adipose samples. Of these, one sample was harvested with a 20 cc syringe vs. the conventional 10 cc syringe and showed an initial yield of cells much lower than the mean. This could be explained by increased cell damage created by the larger vacuum within the 20 cc syringe. Two other samples were obtained using the “super wet” liposuction technique. Interestingly, these two samples yielded the lowest number of cells per ml. The Coleman technique was used during routine liposuction procedures and the site was the abdominal region compared to the other two samples that included skin flaps from donor hip to hand and donor thigh to foot. The Coleman technique appears to be superior to the “super wet” technique due to the success rate in isolation cell yield and proliferation. This aspect has been well described and confirmed in the literature, the site of harvesting can influence the results.

Another interesting observation was that the harvesting cannula appeared to get stuck when advanced through a skin flap donor site. This could be because of the scar tissue that formed due to previous injury and healing since scar tissue mostly consists of fibrotic tissue. These specimens also appeared more stringy and whitish in colour. From these observations and results the author suggests that for the harvesting of adipose tissue for isolation of MSCs, the Coleman technique must be used together with a strong predilection for the sub-umbilical abdominal site. Sampling from skin flaps should be avoided due to the risk of fibrosis and lower yield of cells.

The motion during the transportation allowed the lipoaspirate within the collection bottles to gently mix with the PBS. This resulted in the formation of layers with the blood contaminants at the bottom and the adipose tissue floating on the top. This phenomenon could potentially add value to the isolation process by decreasing the amount of blood contamination from the initial isolation volume and may result in quicker expansion.

Growth kinetics

The growth kinetics assay is a useful tool to assess the growth rate of the cells whilst in culture and to assess at what stage it would be ideal to perform a subculture. It is clear from this study that the cells expand in a logarithmic fashion from D3 onward, with an exponential increase in growth rate towards day 7, followed by a plateau phase and finally a decrease in cell number. We can therefore deduct that within the first 10 days, the highest growth rate is achieved between days 5–7. When trying to analyze the growth rate further and to establish which period (day 3-5 or day 5-7) showed the highest growth rate, we were unsuccessful, as great variability occurred between the individual cultures as shown in Figure 3.39. This phenomenon could represent an inherent tendency of cells in the individual cultures to reach their exponential growth spurt earlier or later, however still within the first 5 – 7 days. Due to the lack of performing the assay over a

longer period of time, it remains uncertain as to whether the rate will increase further at a later stage *e.g.* 14 days. One culture did peak at a later stage.

With the growth kinetics assay we also compared the utility of using the Trypan Blue dye exclusion assay as well as the flow cytometer to perform cell counts. Our results indicate again a similar trend between the growth rates as determined by the number of viable cells *vs.* the total amount of cells counted by the flow cytometer. The reason for this similar trend is explained by the constant relationship of viable to non-viable cells as observed in Figure 3.37. These cells interestingly remained constant across all cultures and days and never exceeded 100 000 cells per ml. The only culture showing variability was A100511-01 and this could be due to the increased amount of dead cells and also the abnormal trend observed with the flow cytometry count. Despite the relation between the viable to non-viable cells during the expansion process and the ability to distinguish between viable and non-viable cells using both techniques, Trypan Blue (40%) dye exclusion assay and flow cytometry, are successful and correlates. The author recommends the use of flow cytometry to perform counting due to the ease of use as well as standardization to minimize human error.

ASC Expansion

Most ASC cultures were expanded well beyond passage 10, producing a considerable yield of cells at every passage (Figure 3.39.). It was evident that ASCs are not contact inhibited, since nuclei were microscopically situated on top of one another (Figure 3.41.).

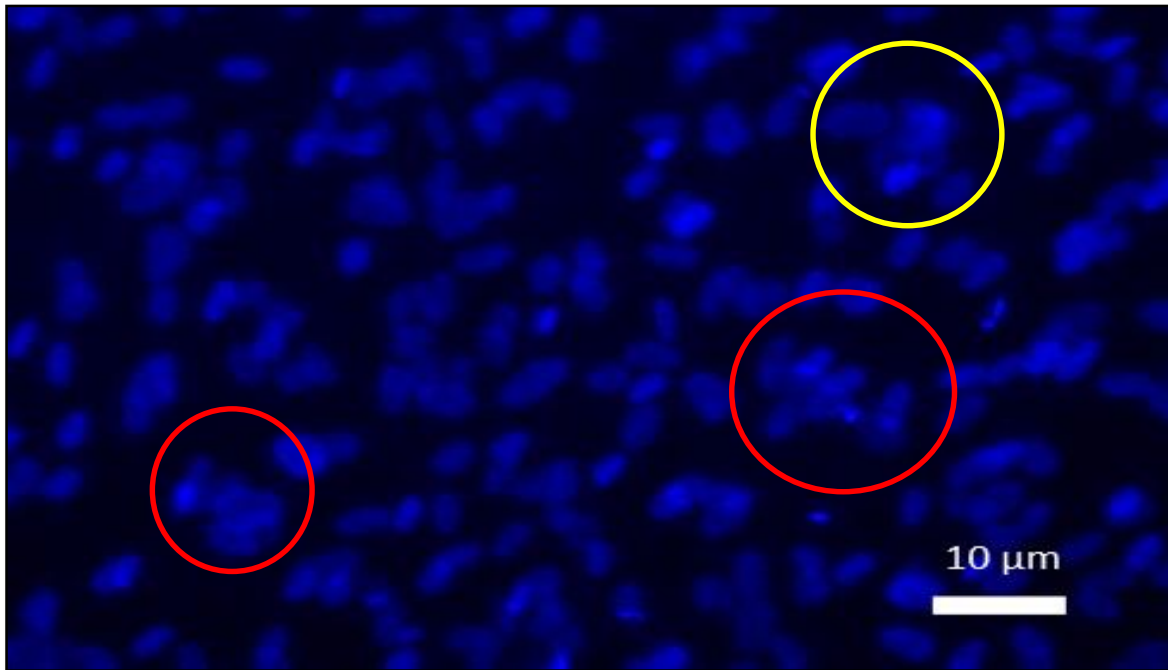


Figure 3.41. Expanded MSCs stained with a nuclear stain DAPI. The red in-circled nucleus bundles indicate that the nuclei are in very close proximity and on top of one another. It is also evident that within these bundles that some nuclei are slightly more in focus than the other background nuclei (circled in yellow), suggesting that the nuclei are on top of one another. This is evidence that ASCs are not contact inhibited during culturing procedures.

Cryopreservation

Our results confirm what has previously been shown in the literature, namely that the process of freezing and thawing induce stress to the ASCs, which results in activation of apoptosis pathways with associated loss of membrane integrity, ultimately leading to cell death. The stress experienced by ASCs on a genetic or molecular level was not considered in this study. However, it was recently demonstrated by Miyamoto and co-workers (2012) that repetitive freezing and thawing of ASCs could decrease their osteogenic differentiation potential. They went further to suggest that one should use serum-free cryopreservation medium containing 10% DMSO, sericin (silk protein) and oligosaccharides (as cryoprotectants) to control the decrease in multilineage potential (Miyamoto *et al.*, 2012).

Our results, like Wilson and co-workers, showed that fresh ASC cultures (non-frozen) have a higher viable cell yield before cryopreservation than post-thaw processing (Wilson *et al.*, 2010). The percentage of ASCs lost through cryopreservation is dismissible and since prior to cryopreservation the average ASC viability was 87% and post thawing an average across all cultures indicated a 68% viability. Therefore, on average 20% of viable ASCs are lost through the processes of cryopreservation and thawing.

This field remains an important avenue for future research for example many stem cell storage facilities use practices highlighted in this study, which may not be beneficial to

clinical application. Also, the effect of expansion prior to freezing is currently not performed due to the FDA regulation regarding the expanded cells as a drug or biologic and the various implications for clinical application. However, freezing the cells in a proliferative state for example, from day 5 onwards as was shown in the growth kinetics section, may have beneficial effects once thawed and further expanded for treatment.

Conclusion

Adipose tissue is known to be a rich source of stem cells and is potentially one of the most useful and easily accessible sources for clinical application. With this study we have shown successful harvesting of virgin lipoaspirate using the Coleman technique. A standard manual isolation, characterization and cryopreservation protocol for ASCs was developed.

Stem cell research and therapy are only in the developing stages in South Africa and considerable investigation has to be done before these cells can be applied in clinical settings. A routine xeno-free protocol for the isolation and culture of ASCs needs to be developed, before use of these cells can be considered in a clinical trial setting.

References

- Agostini T, Davide L, Alessandro P, Gaetano M, Alessandro QL, Daniele B, *et al.* Wet and Dry techniques for structural fat graft harvesting: Histomorphometric and cell viability assessments of lipoaspirated samples. *Plastic and Reconstructive Surgery*. 2012;130;2:331-339.
- Ahmad J, Eaves III FF, Rohrich RJ and Kenkel JM. The American Society for Aesthetic Plastic Surgery (ASAPS) Survey: Current trends in liposuction. *Aesthetic Surgery Journal*. 2011;31:214-224.
- Amos PJ, Bailey AM, Shang H, Katz AJ, Lawrence MB and Peirce SM. Functional binding of human adipose-derived stromal cells: Effects of extraction method and hypoxia pretreatment. *Annals of Plastic Surgery*. 2008;60;4:437-444.
- Baschert MT, Beckert BW, Puckett CL and Concannon MJ. Analysis of lipocyte viability after liposuction. *Plastic and Reconstructive Surgery*. 2002;109:761-765.
- Bi Y, Stuelten CH, Kilts T, Wadhwa S, Iozzo RV, Robey PG, *et al.* Extracellular matrix proteoglycans control the fate of bone marrow stromal cells. *The Journal of Biological Chemistry*. 2005;280;34:30481-30489.
- Bjorntorp P. Abdominal obesity and the development of non-insulin dependent diabetes mellitus. *Diabetes/Metabolism Reviews*. 2000;24;suppl 4:S41-S44.
- Blaak E. Gender differences in fat metabolism. *Current opinion in clinical nutrition and metabolic care*. 2001;4:499-502.
- Both SK, van der Muijsenberg AJ, van Bitterswijk CA, de Boer J and de Bruijn JD. A rapid and efficient method for expansion of human mesenchymal stem cells. *Tissue Engineering*. 2007;13;1:3-9.
- Bunnell BA, Flatt M, Gagliardi C, Patel B and Ripoll C. Adipose-derived stem cells: Isolation, expansion and differentiation. *Methods*. 2008;45:115-120.
- Chiou M, Xu Y and Longaker MT. Mitogenic and chondrogenic effects of fibroblast growth factor-2 in adipose-derived mesenchymal stem cells. *Biochemical and Biophysical Research Communication*. 2006;343:644-652.
- Chu NF, Spiegelman D, Hotamisligil GS, Rifai N, Stampfer M and Rimm EB. Plasma insulin, leptin and soluble TNF receptor levels in relation to obesity-related atherogenic and thrombogenic cardiovascular disease risk factors among men. *Atherosclerosis*. 2001;157:495-503.
- Coleman SR. Hand rejuvenation with structural fat grafting. *Plastic and reconstructive surgery*. 2002;110;7:1731-1744.
- Coleman SR. Structural fat grafts: the ideal filler. *Clinics in Plastic Surgery*. 2001;28;1:111-119.
- Condé-Green A, de Amorim NFG and Pitanguy I. Influence of decantation, washing and centrifugation on adipocyte and mesenchymal stem cell content of aspirated adipose tissue: A comparative study. *Journal of Plastic, Reconstructive and Aesthetic Surgery*. 2010;63:1375-1381.
- Dickens S, van den Berge S, Verdonck K, Hendrickx B, Luttun A and Vranckx J. Characterisation of mesenchymal progenitor cells from processed lipoaspirates. *Plastic and Reconstructive Surgery*. 2009;124:679.
- Dominici M, Le Blanc K, Mueller I, Slaper-Cortenbach I, Marini FC, Krause DS, *et al.* Minimal criteria for defining multipotent mesenchymal stromal cells. The International Society for Cellular Therapy position statement. *Cytotherapy* 2006;8;4:315-317.
- Edens NK, Fried SK, Kral JG, Hirsch J and Leibel RL. *In Vitro* lipid synthesis in human adipose tissue from three abdominal sites. *The American Journal of Physiology*. 1993;265:E374-E379.

- Erdim M, Tezel E, Numanoglu A and Sav A. The effects of the size of liposuction cannula on adipocyte survival and the optimum temperature for fat graft storage: an experimental study. *Journal of Plastic, Reconstructive & Aesthetic Surgery*. 2009;62:1210-1214.
- Ersek RA and Salisbury AV. Circumferential liposuction of knees, calves and ankles. *Aesthetic Plastic Surgery*. 1995;19;4:321-333.
- Fischer A and Fischer G. Revised technique for cellulitis fat reduction in riding breeches deformity. *Bulletin of the International Academy of Cosmetic Surgery*. 1977;2:40-43.
- Fischer G. First surgical treatment for modelling body's cellulite with three 5 mm incisions. *Bulletin of the International Academy of Cosmetic Surgery*. 1976;2:35-37.
- Fischer G. Surgical treatments of cellulitis. Third International Congress of international Academy of Cosmetic Surgery, Rome, May 31, 1975.
- Fleming KK and Hubel A. Cryopreservation of hematopoietic and non-hematopoietic stem cells. *TransfusApher Science*. 2006;34:309-315.
- Fong CY, Richards M, Manasi N, Biswas A and Bongso A. Comparative growth behavior and characterization of stem cells from human Wharton's jelly. *Reproductive BioMedicine Online*. 2007;15;6:708-718.
- Fossett E, Khan WS, Longo UG and Smitham PJ. Effect of age and gender on cell proliferation and cell surface characterization of synovial fat pad derived mesenchymal stem cells. *Journal of Orthopaedic Research*. 2012;30:1013-1018.
- Fournier PF and Otteni FM. Lipodissection in body sculpturing: the dry procedure. *Plastic and Reconstructive Surgery*. 1983;72;5:598-609.
- Fournier Pf. Who should do syringe liposculpturing? *The Journal of Dermatologic Surgery and Oncology* . 1988a;14:1055-1056.
- Fournier PF. Why the syringe and not the suction machine? *The Journal of Dermatologic Surgery and Oncology*. 1988b;14:1062-1071.
- Fraser JK, Wulur I, Alfonso Z and Hedrick MH. Fat tissue: an underappreciated source of stem cells for biotechnology. *Trends in Biotechnology*. 2006;24:150-154.
- Fried SK, Leibel RL, Edens NK and Kral JG. Lipolysis in intra-abdominal adipose tissues of obese women and men. *Obesity Research*. 1993;1:433-448.
- Friedenstein AJ, Petrakova KV, Kurolesova AI and Frolova GP. Heterotopic of bone marrow: analysis of precursor cells for Osteogenic and hematopoietic tissues. *Transplantation*. 1968;6:230-247.
- Fukuchi Y, Nakajima H, Sugiyama D, Hirose I, Kitamura T and Tsuji K. Human placenta-derived cells have mesenchymal stem/progenitor cell potential. *Stem Cells*. 2004;5:649-658.
- Fuller BJ. Cryoprotectants: the essential antifreezes to protect life in the frozen state. *Cryo Letters*. 2004;25:375-388.
- Fuller R and Devireddy RV. The effect of two different freezing methods on the immediate post-thaw membrane integrity of adipose tissue derived stem cells. *International Journal of Heat and Mass Transfer*. 2008;51:5650-5654.
- Gimble JM, Adam JK and Bunnell. Adipose-derived stem cells for regenerative medicine. *Circulation Research*. 2007;100:1249-1260.
- Goh BC, Thirumala S, Kilroy G, Devireddy RV and Gimble JM. Cryopreservation characteristics of adipose-derived stem cells: maintenance of differentiation potential viability. *International Journal of Heat and Mass Transfer*. 2007;1:322-324.
- Gronthos S, Mankani M, Brahim J, Robey PG and Shi S. Postnatal human DP stem cells (DPSCs) in vitro and in vivo. *Proceedings of the National Academy of Sciences*. 2000;97:13625.
- Hajer GR, van Haeften TW and Visseren FLJ. Adipose tissue dysfunction in obesity, diabetes and vascular diseases. *European Heart Journal*. 2008;29:2959-2971.

- Hamosh M, Clary TR, Chernick SS and Scow RO. Lipoprotein Lipase activity of adipose and mammary tissue and plasma triglyceride in pregnant and lactating rats. *Biochimica et Biophysica ACTA*. 1970;210:473-482.
- Harwood HJ. The adipocyte as an endocrine organ in the regulation of metabolic homeostasis. *Neuropharmacology*. 2012;63:57-75.
- Hauner H and Entenmann G. Regional variation of adipose differentiation in cultured stroma-vascular cells from the abdominal and femoral adipose tissue of obese women. *International Journal of Obesity*. 1991;15:121-126.
- Herold C, Pflaum M, Utz P, Wilhelmi M, Renekampff HO and Vogt PM. Viability of autologous fat grafts harvested with the Coleman technique and the tissue trans system (shippert method): a comparative study. *Handchirurgie, Microchirurgie, Plastische Chirurgie*. 2011;43;6:361-7.
- https://www.beckmancoulter.com/wsrportal/page/itemDetails?itemNumber=A91346#2/10//0/25/1/0/asc/2/A91346//C_TCH.CERTIFICATES OF ANALYSIS/0/0/TECHNICALDOCS/1/
- Illouz YG. Body contouring by lipolysis: a 5-year experience with over 3000 cases. *Plastic and Reconstructive Surgery*. 1983;72:591-597.
- Jeon ES, Song HY, Kim MR, Moon HJ, Bae YC, Jung JS, *et al*. Sphingosylphosphorylcholine induces proliferation of human adipose tissue-derived mesenchymal stem cells via activation of JNK. *Journal of Lipid Research*. 2006;47:653-664.
- Jones A, Kinsey SE, English A, Jones RA, Straszynski L and Meredith AF, *et al*. Isolation and characterisation of bone marrow multipotentialmesenchymal progenitor cells. *Arthritis and Rheumatism*. 2002;46:3349-3360.
- Jurgens WJFM, Oedayrajsingh-Varma MJ, Helder MN, ZandiehDoulabi B, Schouten TE, Kuik DJ, *et al*. Effect of tissue-harvesting site on yield of stem cells derived from adipose tissue: implications for cell-based therapies. *Cell and Tissue Research*. 2008;332:415-426.
- Kang YJ, Jeon ES, Song HY, Woo JS, Jung JS, Kim YK, *et al*. Role of c-Jun N-terminal kinase in the PDGF-induced proliferation and migration of human adipose tissue-derived mesenchymal stem cells. *Journal of Cellular Biochemistry*. 2005;95:1135-1145.
- Katz AJ, Llull R, Hedrick MH and Futrell JW. Emerging approaches to tissue engineering of fat. *Clinics in Plastic Surgery*. 1999;26;4:587-603.
- Keck M, Zeyda M, Gollinger K, Burjak S, Kamolz LP, Frey M, *et al*. Local anesthetics have a major impact on viability of preadipocytes and their differentiation into adipocytes. *Plastic and Reconstructive surgery*. 2010;126:1500-1505.
- Kelly IE, Hans TS, Walsh K and Lean ME. Effects of thiazolidinedione compound on body fat and fat distribution of patients with type-2 diabetes. *Diabetes Care*. 1999;22:288-293.
- Kern S, Eichler H, Stoeve J, Klüter H and Bieback K. Comparative analysis of mesenchymal stem cells from bone marrow, umbilical cord blood, or adipose tissue. *Stem Cells*. 2006;24:1294-1301.
- Kershaw EE and Flier JS. Adipose tissue as an endocrine organ. *The Journal of Clinical Endocrinology and metabolism*. 2004;89;6:2548-2556.
- Klein JA. The tumescent technique for liposuction surgery. *American Journal of Cosmetic Surgery*. 1987;4:263-367.
- Kocaoemer A, Kern S, Kluter H and Bieback K. Human AB serum and thrombin-activated platelet-rich plasma are suitable alternatives to fetal calf serum for the expansion of mesenchymal stem cells from adipose tissue. *Stem Cells*.2007;25:1270-1278.
- Kume S, Kato S, Yamagishi S, Inagaki Y, Ueda S, Arima N, *et al*. Advanced glycation end-products attenuate human mesenchymal stem cells and prevent cognate differentiation into adipose tissue, cartilage and bone. *Journal of bone and mineral research: the official journal of the American Society for Bone and Mineral Research*. 2005;20:1647-1658.

- Kurita M, Matsumoto D, Shigeura T, Sato K, Gonda K, Harii K, *et al.* Influences of centrifugation on cells and tissues in liposuction aspirates: Optimized centrifugation for lipotransfer and cell isolation. *Cosmetic*. 2008;121;3:1033-1041.
- Lee JH and Kemp DM. Human adipose-derived stem cells display myogenic potential and perturbed function in hypoxic conditions. *Biochemical and Biophysical Research Communications*. 2006;341:882-888.
- Lindroos B, Suuronen R and Miettinen S. The potential of adipose stem cells in regenerative medicine. *Stem Cell Review and Reports*. 2011;7;2:269-291.
- Liu G, Zhou H, Li Y, Li G, Cui L, Lui W, *et al.* Evaluation of the viability and osteogenic differentiation of cryopreserved human adipose-derived stem cells. *Cryobiology*. 2008;57:18-24.
- Lode A, Bernhardt A and Gelinsky M. Cultivation of human bone marrow stromal cells on three-dimensional scaffolds of mineralized collagen: influence of seeding density on colonization, proliferation and osteogenic differentiation. *Journal of Tissue Engineering and Regenerative Medicine*. 2008;2:400-407.
- Matsuo A, Yamazaki Y, Takase C, Aoyagi K and Uchinuma E. Osteogenic potential of cryopreserved human bone marrow-derived mesenchymal stem cells cultured with autologous serum. *Journal of Craniofacial Surgery*. 2008;19:693-700.
- Miyamoto Y, Oishi K, Yukawa H, Noguchi H, Sasaki M, Iwata H, *et al.* Cryopreservation of human adipose tissue-derived stem/progenitor cells using the silk protein sericin. *Cell Transplantation*. 2012;21:617-622.
- Mizuno H. Adipose-derived stem cells for tissue repair and regeneration: ten years of research and a literature review. *Journal of Nippon Medical School*. 2009;76;2:56-66.
- Novaes F, dos Reis N and Baroudi R. Counting method of live fat cells used in lipoinjection procedures. *Aesthetic Plastic Surgery*. 1998;22:12-15.
- Oedayrajsingh-Varma MJ, van Ham SM, Knippenberg M, Helder MN, Klein-Nulend J, Schouten TE, *et al.* Adipose tissue-derived mesenchymal stem cell yield and growth characteristics are affected by the tissue-harvesting procedure. *Cytotherapy*. 2006;8;2:166-177.
- Prunet-Marcassus B, Cousin B, Caton D, André M, Pénicaud L and Casteilla L. From heterogeneity to plasticity in adipose tissues: Site-specific differences. *Experimental Cell Research*. 2006;312:727-736.
- Ran J, Hirano T, Fukui T, Saito K, Kageyama H, Okada K, *et al.* Angiotensin II infusion decreases plasma adiponectin level via its type 1 receptor in rats: an implication for hypertension-related insulin resistance. *Metabolism*. 2006;55:478-488.
- Ray R, Novotny NM, Crisostomo PR, Lahm T, Abarbanell A and Meldrum DR. Sex steroids and stem cell function. *Molecular Medicine*. 2008;14:493-501.
- Rebuffe-Scrive M, Andersson B, Olbe L and Bjorntorp P. Metabolism of adipose tissue in intraabdominal depots of nonobese men and women. *Metabolism*. 1989;38:543-548.
- Rodbell M and Jones AB. Metabolism of isolated fat cells. III. The similar inhibitory action of phospholipase c (clostridium perfringens alpha toxin) and of insulin on lipolysis stimulated by lipolytic hormones and theophylline. *The Journal of Biological Chemistry*. 1966c;241:140-142.
- Rodbell M. Metabolism of isolated fat cells. II. The similar effects of phospholipase c (clostridium perfringens alpha toxin) and of insulin on glucose and amino acid metabolism. *The Journal of Biological Chemistry*. 1966b;241:130-139.
- Rodbell M. Metabolism of isolated fat cells. IV. Regulation of release of protein by lipolytic hormones and insulin. *The Journal of Biological Chemistry*. 1966d;241:3909-3917.
- Sarugaser R, Hanoun L, Keating A, Stanford WL, Davies JE. Human mesenchymal stem cells self-renew and differentiate according to a Deterministic Hierarchy. *PLoS ONE* 2009;4;8:e6498.

- Schipper BM, Marra KG, Zhang W, Donnenberg AD and Rubin JP. Regional anatomic and age effects on cell function of human adipose derived stem cells. *Northeastern Society of Plastic Surgeons*. 2008;60;5:538-544.
- Si Y-L, Zhao Y-L, Hao H-J, Fu X-B and Han W-D. MSCs: Biological characteristics, clinical applications and their outstanding concerns. *Ageing Research Reviews*. 2010;10;1:93-103.
- Song HY, Jeon ES, Jung JS and Kim JH. Oncostatin M induces proliferation of human adipose tissue derived mesenchymal stem cells. *The International Journal Biochemistry & Cell Biology*. 2005;37:2357-2365.
- Strem BM, Hicok KC, Zhu M, Wulur I, Alfonso Z, Schreiber RE, *et al.* Multipotential differentiation of adipose tissue-derived stem cells. *The Keio Journal of Medicine*. 2005;54;3:132-141.
- Takahashi K, Igura K, Zhang X, Mitsuru A and Takahashi TA. Effects of osteogenic induction on mesenchymal cells from fetal and maternal parts of human placenta. *Cell Transplantation*. 2004;13;4:337-341.
- Tchkonja T, Giorgadze N, Pirtskhalava T, Tchoukalova Y, Karagiannides I, Forse RA, *et al.* Fat depot origin affects adipogenesis in primary cultured and cloned human preadipocytes. *American Journal of Physiological. Regulatory, Integrative and Comparative Physiology*. 2002;282:R1286-R1296.
- The American Society for Aesthetic Plastic Surgery. 15th Annual Cosmetic Surgery National Data Bank 2011 Statistics. Available at: <http://www.surgery.org/sites/default/files/ASAPS-2011.pdf>. Accessed on 9 July 2012.
- The International Society of Aesthetic Plastic Surgeons. ISAPS International Survey on Aesthetic/Cosmetic Procedures in 2010. Available at: <http://www.isaps.org/files/html-contents/ISAPS-Procedures-study-results-2011.pdf>. Accessed on 9 July 2012.
- Thirumala A, Goebel WS and Woods EJ. Clinical grade adult stem cell banking. *Organogenesis*. 2009;5;3:143-154.
- Thirumala S, Gimble JM and Devireddy RV. Evaluation of Methylcellulose and Dimethyl Sulfoxide as the cryoprotectants in a serum-free freezing media for cryopreservation of adipose-derived adult stem cells. *Stem Cells and Development*. 2010;19;4:513-522.
- Thirumala S, Zvonic, Floyd E, Gimble JM and Devireddy RV. Effect of various freezing parameters on the immediate post-thaw membrane integrity of adipose tissue derived adult stem cells. *Biotechnology Progress*. 2005;21:1511-1524.
- Tommaso A, Lazzeri D, Pini A, Marino G, Quattrini AL, Bani D, *et al.* Wet and dry techniques for structural fat graft harvesting: Histomorphometric and cell viability assessments of lipoaspirated samples. *Plastic and Reconstructive Surgery*. 2012;130;331-339e.
- Trujillo ME, Scherer PE. Adipose tissue-derived factors: impact on health and disease. *Endocrine Reviews*. 2006;27:762-778.
- Von Heimburg D, Hemmrich K, Haydarlioglu S, Staiger H and Pallua N. Comparison of viable cell yield from excised versus aspirated adipose tissue. *Cells Tissues Organs*. 2004;178;2:87-92.
- Wilson A, Butler PE and Seifalian AM. Adipose-derived stem cells for clinical applications: a review. *Cell Proliferation*. 2001;44;1:86-98.
- Witort EJ, Pattarino J, Papucci L, Schiavone N, Donnini M and Lapucci A. Autologous lipofilling: Coenzyme Q10 can rescue adipocytes from stress-induced apoptotic death. *Plastic and Reconstructive Surgery*. 2007;119:1191-1199.
- Woodbury S, Schwarz EJ, Prockop DJ and Black IB. Adult rat and human bone marrow stromal cells differentiate into neurons. *Journal Neuroscience Research*. 2000;61:364-370.
- Woods EJ, Pollok KE, Byers MA, Perry BC, Purtteman J, Heimfeld S, *et al.* Cord Blood stem cell cryopreservation. *Transfusion Medicine Hemotherapy*. 2007;34:276-285.

- Yamamoto N, Isobe M, Negishi A, Yoshimasu H, Shimokawa H, Ohya K, *et al.* Effects of autologous serum on osteoblastic differentiation in human bone marrow cells. *Journal of Medical and Dental Sciences.* 2003;50:63-69.
- Yamauchi T, Kamon J, Waki H, Terauchi Y, Kubota N, Hara K, *et al.* The fat-derived hormone adiponectin reverses insulin resistance associated with both lipotrophy and obesity. *Nature Medicine.* 2001;7:941-946.
- Young DA, Gavrillov S, Pennington CJ, Nuttal RK, Edwards DR, Kitsis, *et al.* Expression of metal-lopoptiensases and inhibitors in the differentiation of P19CL6 cells into cardiac myocytes. *Biochemical and Biophysical Research Communications.* 2004;322:759-765.
- Zhang YG, Yang Z and Zhang H. Effect of negative pressure on human bone marrow mesenchymal stem cells *in vitro.* *Connective Tissue Research.* 2010;51:14-21.
- Zhou S, Greenberger JS, Epperly MW, Goff JP, Adler C, Leboff MS, *et al.* Age-related intrinsic changes in human bone marrow-derived mesenchymal stem cells and their differentiation to osteoblasts. *Aging Cell.* 2008;7;3:335-343.
- Zuk PA, Zhu MIN, Ashjian P, De Ugarte DA, Huang JI, Mizuno H, *et al.* Human Adipose Tissue Is a Source of Multipotent Stem Cells. *Molecular Biology of the Cell.* 2002;13;Dec:4279-4295.
- Zuk PA, Zhu MIN, Mizuno H, Huang J, Futrell JW, Katz AJ, *et al.* Multilineage Cells from Human Adipose Tissue: Implications for cell based Therapies. *Tissue Engineering.* 2001;7;2:211-228.



Immunophenotype characterisation and tri-lineage differentiation of peripheral abdominal adipose resident stromal cells

Double, double toil and trouble;

Fire burn and cauldron bubble.

Shakespeare W. *Macbeth* (1605), Act IV, Scene1, Line 10-11.

Introduction

Adipose tissue has become a rich and convenient source of stem cells for regenerative medicine therapeutic approaches. However, the characteristics of this heterogeneous population of cells still remains to be clarified. There are no sets of phenotypic or molecular markers known that can accurately identify adipose derived stem cells (ASCs). A precise characterisation method for future research and clinical application using these cells thus represents a *condition sine qua non* (Wagner *et al.*, 2005).

***In vitro* Characterisation**

The cell equivalence question above is partly due to the lack of a universally accepted set of standardized criteria. Various research groups in the field are therefore unable to

compare and contrast studies. To address this problem the International Society for Cellular Therapy (ISCT) proposed a set of standards to define human mesenchymal stem cells (MSCs) from the best available data in 2006 (Dominici *et al.*, 2006).

There are 3 main proposed criteria:

1) MSCs should adhere to plastic.

When MSCs are maintained under standard culture conditions, they should adhere to plastic (flasks). There have however been subsets of MSCs described that do not display this property but these isolation protocols require very specific culturing conditions (Dominici *et al.*, 2006).

2) MSCs should express a specific set of cell surface markers (marked with antigens) to determine the phenotype.

The population of MSCs must express $\geq 95\%$ positivity for CD105 (endoglin), CD73 (ecto-5'-nucleotidase) and CD90 (Thy-1). Additionally, these cells must lack expression for hematopoietic antigens ($\leq 2\%$ positivity) including CD45 (pan-leukocyte marker), CD34 (primitive hematopoietic progenitors), CD14 or CD11b (expressed on monocytes and macrophages), CD79 α or CD19 (B cell markers, could remain vital in stromal interactions) and class II human leukocyte antigen HLA-DR. The latter is only expressed if stimulated by the cytokine Interferon-gamma (IFN- γ) (Dominici *et al.*, 2006).

3) MSCs should display a multipotent differentiation potential.

MSCs should also have the capacity to differentiate into three lineages. The accepted mesenchymal lineages are bone (osteoblasts and osteocytes), adipose tissue (adipocytes) and cartilage (chondroblasts, chondrocytes and collagen type II) using standard in vitro tissue culture-differentiating conditions (Dominici *et al.*, 2006).

Dominici and co-workers in 2006 further commented with regard to using the cell surface markers to establish phenotype and suggested that many different antigens be incorporated in the research conducted by the investigator and that both positive and negative markers were encouraged to be tested. Also, to enhance the optimisation of flow cytometry, a multicolour analysis with double and triple staining should be used to illustrate that MSCs lack expression of hematopoietic antigens while co-expressing MSC markers (Dominici *et al.*, 2006).

The antigens discussed above are only considered to be minimal criteria and do not uniquely identify MSCs, therefore, other functional criteria should be used in conjunction. MSCs express HLA-DR when stimulated by IFN- γ and since this expression is desirable in some applications, these cells are considered *stimulated* MSCs. A pure MSC population ($\geq 95\%$ expression of CD105, CD73, CD90 and $\leq 2\%$ expression of the hematopoietic markers) should be considered minimal guidelines, since some applications may require a higher degree of purity (Dominici *et al.*, 2006).

Furthermore it was also suggested that these criteria should be employed by all investigators in a controlled study fashion and they should demonstrate that the prepared cells in their laboratory meet the stated criteria. This would be a global effort to standardize these cell preparations and allow for a comparison of scientific studies between laboratories (Dominici *et al.*, 2006).

***In vivo* Characterisation**

Stem cells are maintained in a specialized microenvironment, or niche, where exogenous physiological cues influence their homeostasis for either cell repair or replacement (Wang and Wagers, 2011). The stem cell niche is usually closely associated with the vascular and nervous systems, allowing for modulation of stem cell responses by metabolic signals and circadian rhythms (Kiel *et al.*, 2005; Wagers, 2012). These systems channel humoral factors as well as immune and inflammatory cells to the niche, while temperature, shear forces and chemical signals provided by the niche also influence stem cell behaviour (Chow *et al.*, 2011; Christopher *et al.*, 2011). The degree of cellular and acellular components may vary within niches from the same or different tissues. Stem cells integrate the signals provided by these cellular and acellular components which influences stem cell behaviour that determines the stem cell fate such as quiescence or proliferation, self-renewal or differentiation, migration or retention and cell death or survival (Wagers, 2012).

Differentiation

Although the characterization criteria stipulates differentiation into the three lineages (as above) to confirm the identity of MSCs, many reported studies have shown a much wider differentiation capacity of MSCs. According to the criteria MSCs should differentiate into mesodermal originating lineages of bone (osteoblasts and osteocytes), adipose tissue (preadipocytes and adipocytes) and cartilage (chondroblast and chondrocytes). A wider differential capacity is however reached within the mesodermal lineage with demonstrated differentiation into muscle (myoblasts), tendon (tendonocytes) (Alhadlaq *et al.*, 2004) and ligament fibroblasts.

Additionally, differentiation into the embryonic endoderm lineage has been shown by MSCs differentiating into smooth muscle, cardiomyocytes, vascular endothelial cells (Si *et al.*, 2010), pancreatic islets (Timper *et al.*, 2006) and hepatocytes (Seo *et al.*, 2005).

Ectodermal lineage differentiation has also been demonstrated with application to neuron-like cells (Zuk *et al.*, 2010; Si *et al.*, 2010). Some of these cells include neurons (Kang *et al.*, 2004), oligodendrocytes (Safford *et al.*, 2004) and functional Schwann cells (Kingham *et al.*, 2007; Xu *et al.*, 2008).

Trottier and co-workers demonstrated MSC differentiation into the epidermal lineages. Based on their findings they suggested that MSCs might be considered as pluripotent

rather than multipotent as the evidence indicates differentiation into different embryological lineages (Trottier *et al.*, 2006).

Additional criteria pertaining to MSC differentiation were suggested by Zuk and co-workers in 2002. It is known that adult derived stem cells originate from a heterogeneous cell population and therefore multilineage differentiation could simply occur due to the presence of multiple precursor populations, each just completing or suppressing their development. ASC clones from human and animals demonstrate differentiation capacity beyond the mesodermal lineage. Clonogenicity and clonal differentiation capacity from ASCs have till now not been accepted as a standard criterion by the ISCT. Furthermore, the differentiation capacity of MSCs into multiple cell types within all three germ layers is well documented and Zuk and co-workers in 2010 also suggested by that MSCs should be considered pluripotent rather than multipotent.

The importance of the source of MSCs (as highlighted in the previous chapter) can also influence the differentiation capacity and remains a controversial point of discussion within the field. Kern and co-workers (2006) for example illustrated that MSCs from umbilical cord blood (UCB) might not be able to differentiate into adipose tissue.

As more data from ongoing studies becomes available more questions arise pertaining to the source, processing and characterization of MSCs. This chapter contributes to the field of knowledge by describing the experience in applying the proposed criteria for characterization to adipose derived stromal cells isolated from peripheral adipose tissue as described in the previous chapter.

Materials and Methods

The first of the three characterisation criteria namely the ability of ASCs to adhere to plastic was demonstrated during the processes of proliferation and expansion of ASCs (described extensively in Chapter 3). After the initial seeding of the adipose derived stromal vascular fraction (AD-SVF) and 24 hours of incubation, the non-adherent cells were removed from the cultures with washing procedures using phosphate buffer solution (PBS), supplemented with 2% penicillin and streptomycin (pen/strep) and subsequent culture maintenance with stromal media replacements every second day.

Immunophenotypic characterisation

Flow cytometry was used to immunophenotypically characterise the ASCs according to the criteria set out in the Dominici *et al.*, 2006 paper (Dominici *et al.*, 2006).

Every culture was phenotypically characterised at almost every passage in order to determine possible fluctuations in the expression of cell surface markers that are required for characterization. During the process of passage the cells were enzymatically removed from the expansion surface using 0.25% trypsin and re-suspended in PBS

supplemented with 2% pen/strep (See Chapter 3 for detailed passage protocol). From these cell suspensions 100 μ l was used for cell counting procedures using flow cytometry, 20 μ l was used to perform the Trypan Blue (40%) dye exclusion assay and 100 μ l was placed into a 15 ml tube with the addition of 10 μ l of monoclonal mouse anti-human antibodies for immuno-phenotypic characterisation (Table 4.1.). Since the CD90 fluorescein isothiocyanate (FITC) indicated very bright excitations only 5 μ l instead of 10 μ l was used to stain the ASCs. An additional 100 μ l of cell suspension from one of the cultures being passaged on the day was used as control (or unstained). The unstained sample was not labelled by a respective antibody panel but was treated the same as the antibody-stained samples (labelled samples). An unstained sample was prepared daily with every flow cytometric experiment to ensure accurate day-to-day comparable results.

Table 4.1. Summary of the different antibody panels that were used in specific fluorescent channels. Monoclonal mouse anti-human antibodies were used as available within the laboratory.

Antibody Panel	Fluorochromes					
	FL1	FL2	FL3	FL4	FL5	FL6
Panel 1	CD90 FITC	CD105 PE		CD45 PC5	CD34 PC7	CD73 APC
Panel 2	CD73 FITC	CD105PE	CD34 ECD	CD90 PC5	CD45 PC7	
Panel 3	CD73 FITC	CD105 PE	CD45 ECD	CD90 PC5	CD34 PC7	

The 15 ml tubes containing the cell suspension and antibodies as well as the unstained control were incubated at room temperature in an area with minimal light exposure for 10 to 15 minutes. To remove free antibodies in the cell suspension, 1 ml of PBS supplemented with 2% foetal bovine serum (FBS) was added to the labelled samples as well as the unstained control before they were centrifuged for 5 min at 1200 rpm (equivalent of 184 *g*). The washing procedure that followed was repeated three times. The supernatant was aspirated and the pellet re-suspended in PBS containing 2% FBS following centrifugation at 1200 rpm for 5 min at room temperature. After the third washing centrifugation step the supernatants were aspirated and the pellets were re-suspended in sterile PBS. The samples were then transferred into centrifuge tubes before loading into the flow-cytometer. The data captured from every sample was recorded in a separate LMD file.

The remaining cell suspensions not used for density determination (See Chapter 3) or immunophenotyping were then either placed back in culture for expansion purposes or cryopreserved for future use.

The flow cytometer protocol was optimized, voltages were set to indicate the unstained sample events measurements within the first decade (1-parameter plots) and X-Y-quadrants as well as colour compensations were calibrated accordingly (Figure 4.1.). The minimum events per flow cytometric sample was 5 000 and the maximum was 20 000. Using a forward and side scatter plot the population of cells was gated as [A], excluding

measured events caused by cellular aggregates and debris (Figure 4.2.). The forward scatter (FS) measured events relative to the size and side scatter (SS) measured events relative to the granularity and structural complexity (Figure 4.2.).

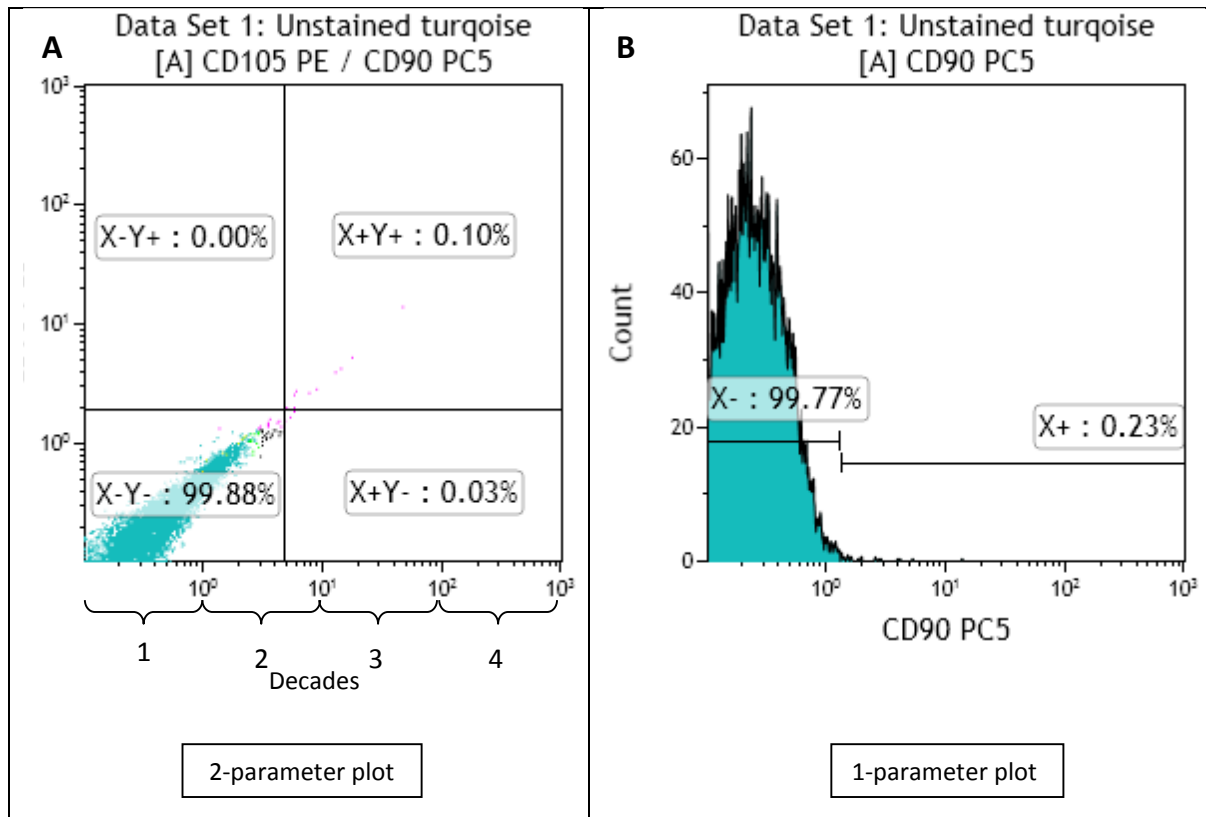


Figure 4.1. An unstained flow cytometric sample. The voltages were set to indicate a negative reading within the X-Y- quadrant of a 2-parameter plot (indicated in A) as well as in the first decade of a 1-parameter plot (indicated in B). All plots were gated on [A], which was the population of cells studied on a forward and side scatter plot.

A 2-parameter plot represents the measurements of events from 2 different fluorochromes (parameters) on the X and Y axis. A single parameter plot (histogram) represents the events of a single fluorochrome (parameter).

Analysis of flow-cytometry characterisation data

The characterisation of the cell phenotype was performed using KALUZA Flow Cytometry analysis software 1.2 (Beckman & Coulter, Miami, US). The data files were first sorted according to culture code and consecutive passage. Every sample data file was then opened in KALUZA, to export the settings of the sample data captured. The codification used for cultures was previously explained in Chapter 3 (Figure 3.14.). The settings composites extracted from the data files were used to sort the different flow cytometric protocols used on the different flow cytometers according to colour coded protocols (Appendix 4.1.).

The data from the unstained sample files were also sorted within specific colour coded groups and all the unstained files from a specific colour coded group were merged to serve as a single unstained control per colour coded group of protocols. All flow cytometric files for all passages within a colour coded group per culture, including the unstained control group were then analysed.

The gating regions on the corresponding 1-parameter plots were grouped to ensure accurate gating between the respective unstained and labelled plots. The data from the 1-parameter plots within every file was summarised and processed into tree plots (Figure 4.10). The statistics were then exported from the graft into Excel 2010 (Microsoft) for further analysis.

The tree plot considers every possible combination of expression for all the parameters. To explain this concept we can use the gated cell population of a 2-parameter plot gated on the cell population in the forward and side scatter plot (Figure 4.2).

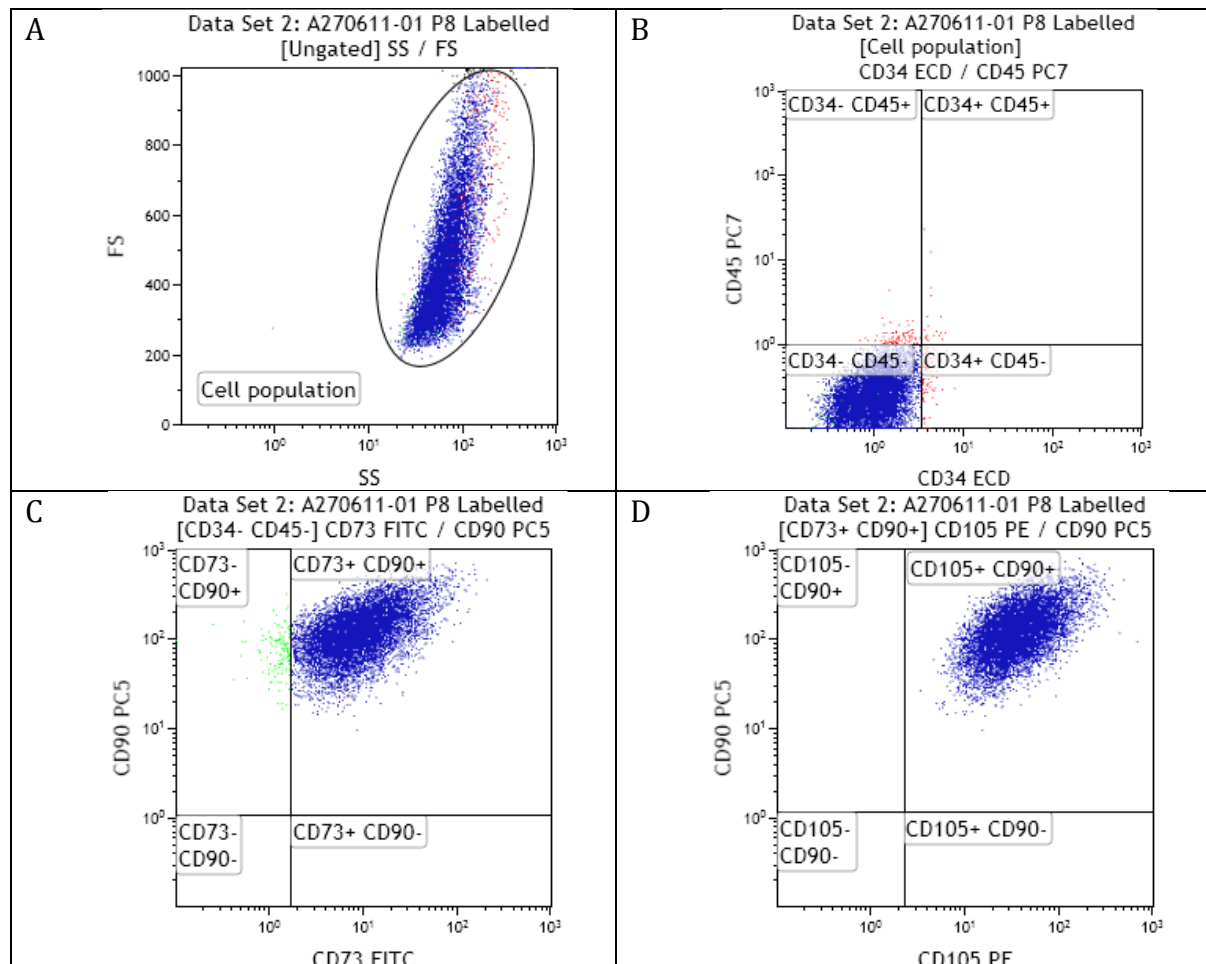


Figure 4.2. An explanation of the tree plot analysis. The forward and side scatter plot indicates the relevant cell population. Gating on this region, the 2-parameter plot in B indicates CD45- and CD34- population. Gating Figure C on the CD45- and CD34- parameter region in figure B, we are only considering the cells gated within the CD45- and CD34- parameter. Figure C demonstrates that the cell population in the CD73+ and CD90+ gating region are also CD34- and CD45- populations within the parameter from figure B. Gating figure D on the CD73+ and CD90+ only cells with CD34-, CD45-, CD73+ and CD90+ marker expression are considered. Figure D displays then a cell population with the characteristic ASCs phenotype (CD34-, CD45-, CD73+, CD90+ and CD105+).

The statistics were exported from the tree plots into Excel and all possible combinations of the antibody panels were analysed to determine the heterogeneity of an ASC population. The selected statistics displayed a specific expression panel combination as a percentage gated from the cell population in the forward and side scatter plot.

Sub-population analysis by flow cytometric analysis

All potential cell surface marker combinations were applied to each individual culture. Marker combinations were considered, when they occurred for at least two passages with a percentage gated cells expression of >0.1%. These populations were further sub-grouped according to the level of expressions: >0.1 – 1.0 % (very small); >1- 5 % (small); and >5 %. The frequencies of these combinations across all passages for individual cultures were established and the mean expression was calculated.

All the included combinations were expressed as percentages among all isolates (*e.g.* 3/8 and further compared between cultures)

Tri-lineage Differentiation

The third criteria used to characterise the ASC cultures was to demonstrate their ability to differentiate into bone, cartilage and adipose tissue lineages.

Various differentiation protocols including induction media as well as classical staining for confirmation of differentiation used for MSCs derived from different host tissues were studied, to find the most commonly used protocols per differentiated lineage (see Appendix 4.2). From this, the most common protocol for a specific lineage was selected and adapted to formulate a standard differentiation protocol.

Differentiation protocols of ASCs into adipocytes and osteocytes were adapted from Zuk and co-workers (2001 and 2002) and the differentiation protocol used for chondrocytes was adapted from Reger and colleagues (2008). A summary of the differentiation, quantification and confirmation of differentiation through classical staining is summarised in Figure 4.3.

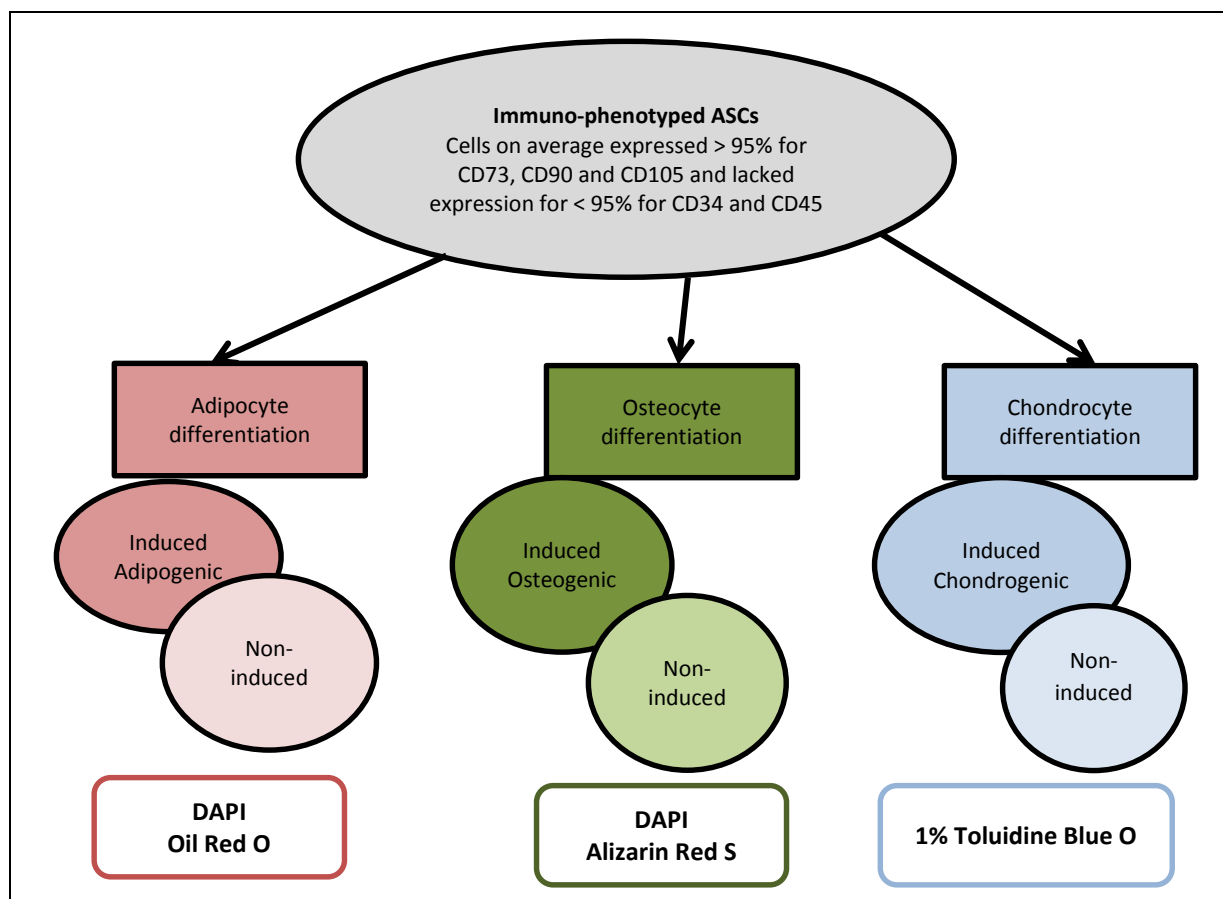


Figure 4.3. Summary of the tri-lineage differentiation characterisation of immunophenotyped ASCs. The tri-lineage cultures include induced as well as non-induced cultures for adipocyte and osteocyte differentiation, where the non-induced ASCs served as an internal control for the classical staining that was performed. Fluorescent nuclear staining using DAPI was performed for the semi-quantification of induced as well as non-induced cells within the adipocyte and osteocyte lineages. The chondrogenic induced and non-induced cultures were sectioned and stained with 1% Toluidine Blue, due to the nature of the spherical culture.

The induction media for the differentiation of ASCs into adipocytes were prepared within sterile Dulbecco Modified Eagle Medium + GlutaMax +4.5g/L D-glucose + Pyruvate (DMEM) (Gibco, Cat# 31966-021). Chemicals were added to the DMEM including 3-isobutyl-methylxanthine (Sigma, Cat# 15879-1g), indomethacin (Sigma, Cat# 18280-5g), insulin (Gibco, Cat# 12585-014) and 0.01% dexamethasone made up in PBS (Table 4.2.), the solution was stirred overnight on a magnetic stirrer at room temperature. The solution was filtered through a 0.22 µm filter (Stericup and Steritop vacuum driven filtration systems - 0.22 µm GP Millipore express plus membrane) connected to a 50 ml syringe. Only 50 ml solution was filtered through a single filter to ensure sterility. The adipocyte induction medium was supplemented with of 10% FBS (Gibco) and 1% pen/strep (Gibco, Cat# 15140-122).

Osteocyte induction media for differentiating ASCs into osteocytes included 0.01% dexamethasone in PBS, ascorbate-2-phosphate (Sigma, Cat# 49752-10g) and β-glycerophosphate (Sigma, Cat# 50020-100g) that was dissolved in DMEM using a magnetic stirrer at room temperature (Table 4.2.). The DMEM solution was filtered

through a 0.22 μm filter (Stericup and Steritop vacuum driven filtration systems 0.22 μm GP Millipore express plus membrane) connected to a 50 ml syringe. Only 50 ml at a time was filter sterilized and the osteocyte induction medium was completed with the addition of 10% FBS and 1% pen/strep.

The induction media used for differentiating ASCs into cartilage included 0.01% dexamethasone in PBS, ascorbate-2-phosphate, transforming growth factor beta-3 (TGF- β_3) (stock solution prepared in PBS), proline, pyruvate and ITS Premix solution that was dissolved in DMEM using a magnetic stirrer at room temperature. The medium was filtered through a 0.22 μm filter (Stericup and Steritop vacuum driven filtration systems - 0.22 μm GP Millipore express plus membrane) connected to a 50 ml syringe to sterilize the chondrocyte induction media (Table 4.2.). The ITS Premix consisted of: (a) 6.25 $\mu\text{g/ml}$ insulin; (b) 6.25 $\mu\text{g/ml}$ transferrin; (c) 6.25 ng/ml selenous acid; (d) 1.25 mg/ml BSA; and (e) 5.35 mg/ml linoleic acid.

The non-induced control cultures were maintained with DMEM supplemented with 10% FBS and 1% pen/strep (control media) without any induction chemicals and were treated the same as the induced cultures.

Table 4.2. The different lineage induction media and the exact concentrations of chemicals added to DMEM and volume or mass of chemicals used to produce a final 100 ml solution of the respective induction media. All induction media were stored at 4°C.

Lineage	Chemical	Molar mass (g/mol)	Required concentration	Stock solution	Volume/mass of stock used	Microscopy stains used
Adipocyte Induction Medium	3-isobutyl-methylxanthine	222.24	0.5 M	Powder	0.011 g	DAPI, Oil Red O and 0.01% Toluidine Blue O (counter stain)
	Indomethacin	357.8	200 μM	Powder	0.007156 g	
	Insulin	N/A	10 $\mu\text{g/ml}$	4mg/ml	250 μl	
	Dexamethasone	392.46	1 μM	0.01%	392.46 μl	
Osteocyte Induction Medium	Ascorbate-2-phosphate	322.05	50 μM	Powder	0.0016 g	DAPI Alizarin Red S
	β -glycerophosphate	306.11	10 mM	Powder	0.306 g	
	Dexamethasone	392.46	1 μM	0.01%	392.46 μl	
Chondrocyte Induction Medium	Ascorbate-2-phosphate	322.05	0.155 mM	Powder	0.005 g	1% Toluidine Blue
	TGF- β_3	N/A	10 ng/ml	5 $\mu\text{g}/5\text{ ml}$	1 ml	
	Proline	115.13	0.35 mM	Powder	0.004 g	
	Pyruvate	110.05	0.9086 mM	Powder	0.010 g	
	Dexamethasone	392.46	1 μM	0.01%	392.46 μl	
	ITS Premix	N/A	1%	100%	1 ml	

It was a priority to immunophenotype the cultures prior to inducing differentiation into the respective lineages to record immunophenotype purity as set out by Dominici *et al.*,

2006. The individual cultures were induced at various passages between P2 and P11 (Table 4.3).

Table 4.3. The passage number at which the cultures were induced to be differentiated.

Culture code	Passage number
A240211-01	2*
A090311-01	7
A230311-01	7
A040411-01	8*
A130411-01	9*
A130411-02 10cc	6
A200411-01	4
A050511-01	11*
A100511-01	4
A270611-01	8
A270611-02	7
A050711-01	6*
A100511-01	10*

*Induction was performed on previously cryopreserved cultures

For both adipocyte and osteocyte differentiation procedures, immunophenotyped ASCs were seeded into a 6 well plate at a density of 5 000 cells per cm² and maintained under standard culturing conditions (37°C and 5% CO₂) with stromal medium (α -MEM, containing 10% FBS and 1% pen/strep) until the wells reached about 60-70% confluence. The conditioned stromal medium was aspirated and cultures were washed with PBS containing 2% pen/strep. The adipocyte, osteocyte and non-induced cultures were cultured in a 6 well multi-dish plate: 2 wells received 2 ml adipogenic induction medium (Table 4.2.); 2 wells received 2 ml osteogenic induction medium (Table 4.2.); and 2 wells were not induced receiving 2 ml control medium (Figure 4.4.). During the total induction period of 21 days the cultures were maintained under standard conditions of 37°C, 5% CO₂ and the respective induction and control media were replaced every second day.

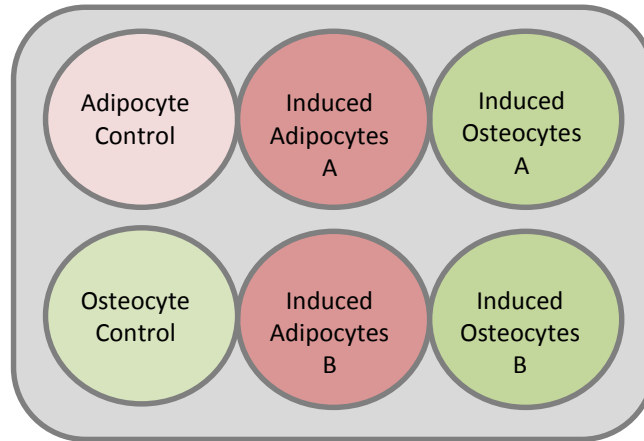


Figure 4.4. Representative 6 well plate indicating induced cultures and non-induced controls. Adipocyte and osteocyte differentiation were performed in duplicate (indicated as A and B) with two non-induced wells serving as an internal control for classical staining (one for each lineage).

A suspension culture technique was used for the differentiation of ASCs into chondrocytes. Cells were seeded in a T25 flask at a density of 5 000 cells per cm² and maintained under standard culture conditions until the culture flask reached about 60% confluence. The cells were enzymatically removed from the flask using 0.25% Trypsin. The cell suspension was transferred to a 15 ml tube after the enzymatic action of the trypsin was ceased with the addition of stromal medium (α -MEM, containing 10% FBS and 1% pen/strep). After centrifugation of 5 min at 1200 rpm and at room temperature, the substrate was aspirated carefully so that almost only the pellet of ASCs was left in the tube. The cells were re-suspended in the tube with 1 ml cartilage induction medium (Table 4.2.) and centrifuged at 400 g for 10 min at room temperature. Before placing the tubes which contain a centrifuged pellet in the incubator, the tube caps were loosened, not entirely but enough so that gas exchange could take place. The chondrogenic induced cultures were then incubated under standard conditions of 37°C, 5% CO₂ for 21 days, during which the induction medium was replaced by 0.5 ml fresh chondrocyte induction medium every second day. After 24 hours, the induced ASCs contracted into a sphere and at 48 hours the cells that did not contract into the sphere were removed with the replacement of the chondrocyte induction media (Figure 4.5.).

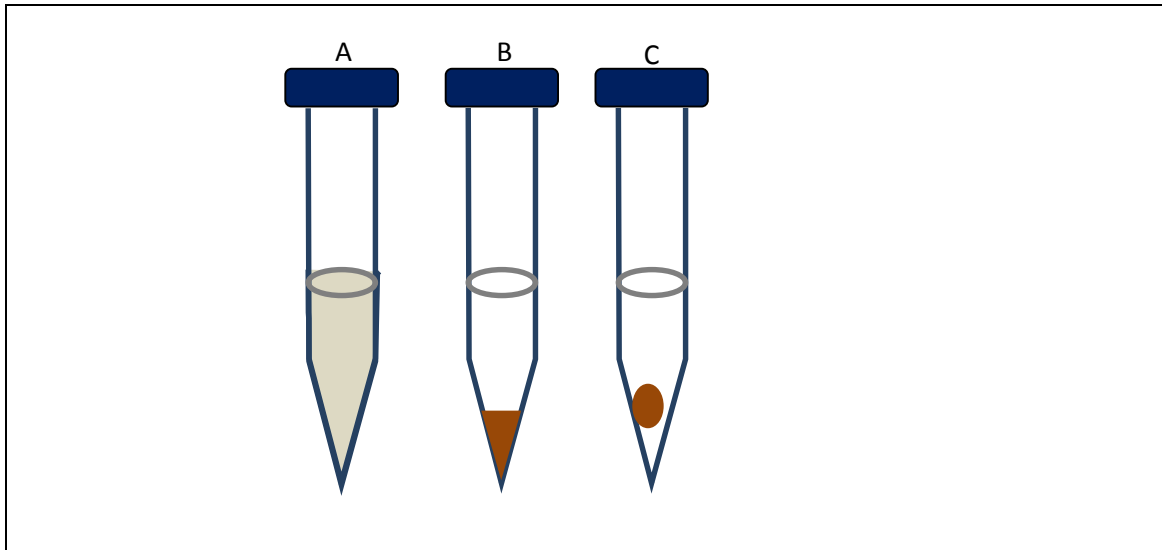


Figure 4.5. Cartilage cultures. (A) After the cells were removed enzymatically from the T25 flask, the trypsin and α -MEM were aspirated after centrifugation. The pellet was re-suspended in 1 ml cartilage induction medium. (B) The cell suspension was centrifuged to form a pellet in the 15 ml tube and incubated under standard conditions for 21 days. The induction medium was replaced every 2 days. (C) Within 24 hours of incubation the cells appear to contract into a sphere.

After 21 days of induction the 6 well plates containing the adipogenic, osteogenic induced and the non-induced control cultures as well as the chondrocyte induced suspension cultures were fixed with a 4% formaldehyde fixative solution for an hour. The respective induction media were aspirated and the cultures were washed once with sterile PBS, before the fixative solution was introduced to the cultures and left at room temperature for an hour. The fixative was then removed and sterile PBS was added to the cultures before they were sealed and stored at 4°C. The 6 well plate was sealed using parafilm and the tube was sealed with its cap, this reduced the evaporation of the PBS from the culture until the cultures was processed for microscopy for confirmation and quantification of differentiation.

Assessment of differentiation capacity

The different sealed lineage induced and respective ASC control cultures were transported to the microscopy laboratory in sterile PBS. The chondrocyte induced cultures were embedded, sectioned, stained and microscopically investigated.

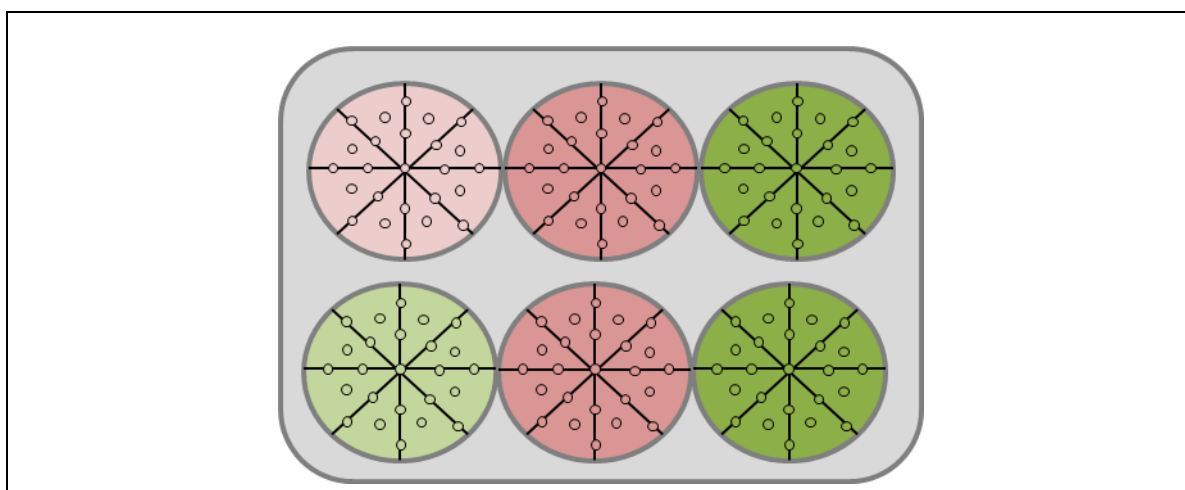
Quantification of viable cells within a culture was determined after the 21 day induction period and fixation process. The adipocyte and osteocyte induced with relative non-induced control cultures were stained with 4',6-Diamidino-2-phenylindole (DAPI), a fluorescent nucleic acid stain that preferentially stains double-stranded DNA and the binding produces an approximate 20-fold fluorescence enhancement with an emission maximum at ~460 nm wavelength.

A DAPI stock solution was first prepared in ddH₂O at a concentration of 5 µg/ml. A staining buffer was prepared for the DAPI working solution which included 1 L ddH₂O, 146 mM NaCl and 10 mM Tris Base, the solution was then adjusted to obtain a pH of 7.4, using HCl. Further additives to the buffer solution included 2mM CaCl₂, 22 mM MgCl₂ and 0.05 g bovine serum albumin (BSA). The DAPI stock solution was then diluted with the staining buffer to obtain the DAPI working solution at a concentration of 0.02 µg/ml.

The PBS was removed from the respective cultures and 1 ml working solution of DAPI was added to every well of a six well plate and left to incubate for 10 min in the dark after which microscopy analysis and photography was performed on a Zeis Axiovert 200 fluorescence microscope (München, Germany), equipped with a Zeis Axioacam MRc5 digital camera (München, Germany). Every sample was investigated under a 10x objective lens with a blue filter and the photographs were taken at a saturation of 0.8 and exposure time of 25 s.

Validation of homogeneity and estimation of the required number of visual fields per well necessary for semi-quantification.

A validation was performed to ensure that the number of photographs (vision fields) taken from a respective well would be representative of the entire service area of that well and whether the number of photographs (vision fields) could be reduced to five photographs per well. An amount of 25 vision fields were photographed on a grid format and the number of DAPI stained nuclei in a vision field were quantified using Image J software cell counter for 2 non-induced, 2 adipocyte induced and 2 osteocyte induced cultures (Figure 4.6.). Different counting strategies (number of photographs and orientation) were evaluated. The means for the respective strategies were compared for significance using one tailed analysis of variance (ANOVA) and an F value of 1 and a P value of <0.05 were regarded as statistically significant.



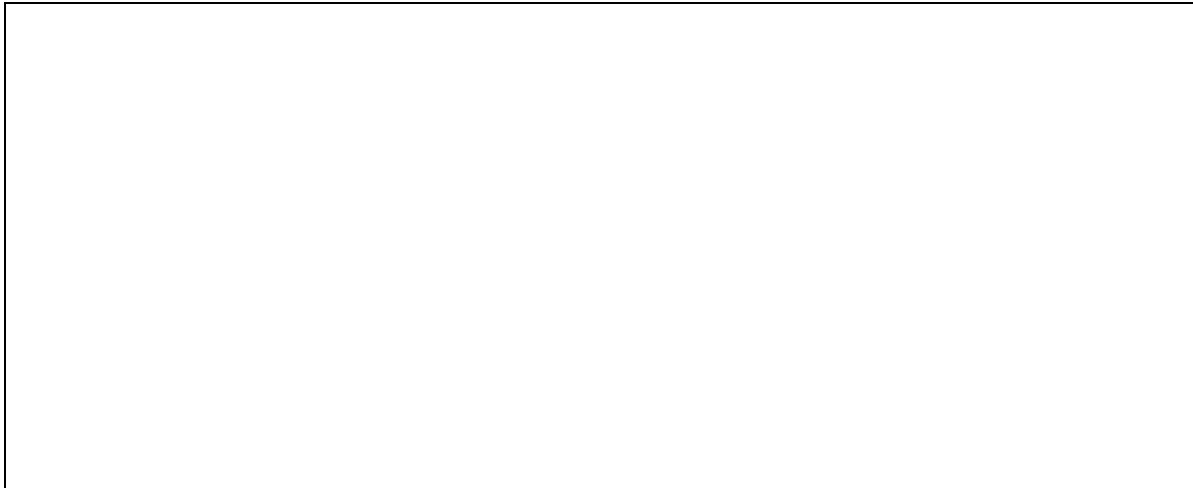


Figure 4.6. The grid formation covering a 6 well plate. Every small round dot indicates a photograph (vision field) microscopically analysed, with a total of 25 vision fields per well. The DAPI stained nuclei of the two non-induced controls, two adipocyte induced and two osteocyte induced wells were quantified using Image J software cell counter.

For every non-induced, adipogenic and osteogenic induced culture a total of 8 groups were created: (A) All 25 vision fields; (B) 5 around outside of the grid with 1 centre field; (C) 5 fields within 1 quadrant; (D) 5 random; (E) 5 random around the outside of grid; (F) 8 random; (G) 10 random; and (H) 15 random (Figure 4.7.).

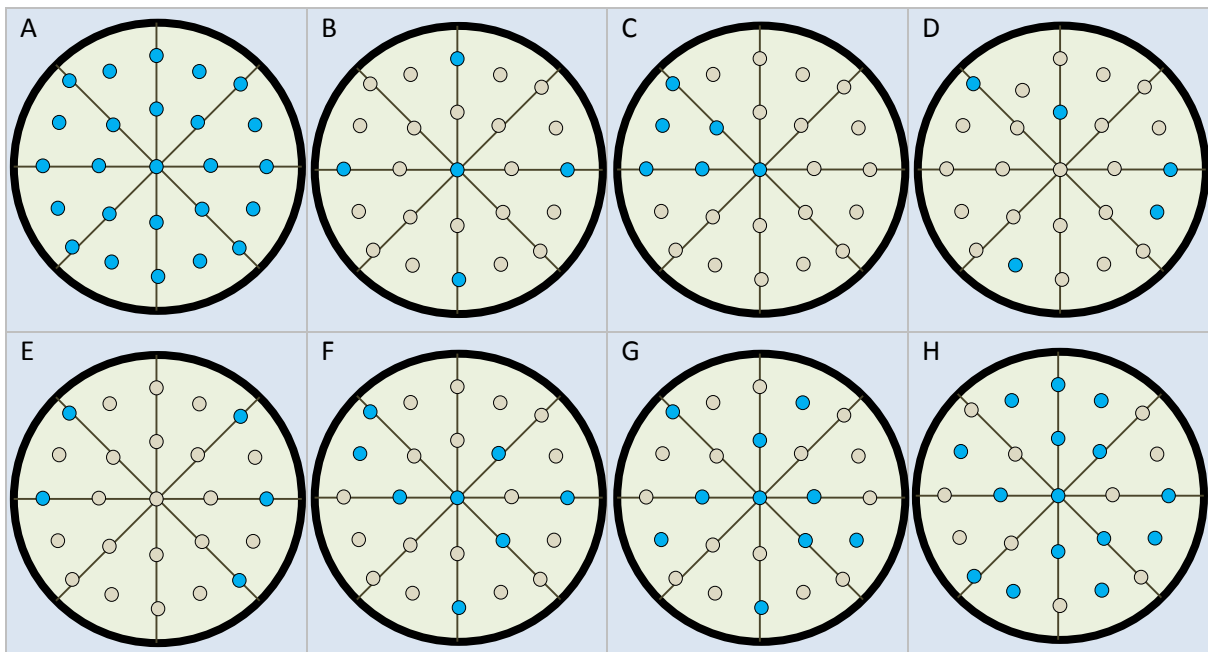


Figure 4.7. Representation of the eight different counting strategies. Every individual well was photographed and cells manually counted using Image J software cell counter, means were calculated and statistically compared: (A) All 25 vision fields; (B) 5 around outside of the grid with 1 center field; (C) 5 fields within 1 quadrant; (D) 5 random fields; (E) 5 random fields around the outside of grid; (F) 8 random fields; (G) 10 random fields; and (H) 15 random fields.

The validation showed no statistical significant difference between the means of all the different ways of quantification of the photographs. Based on these results five photographs with one in the centre and one from each quadrant (B) was selected as this method showed the smallest standard deviations of the groups that included 5 photographs (Table 4.4.) and allowed for easy standardization across all evaluated cultures. Although group G and H indicated decreased STD DEV they represent cell counts from 10 and 15 vision fields respectively. Subjectively group B was selected to decrease manual counting vision fields, but still represent an acceptable STD DEV across adipogenic-, osteogenic- and non-induced cultures.

Table 4.4. The mean cell counts of the respective counting strategies.

Groups	Control		Adipose		Bone	
	Mean	STD DEV	Mean	STD DEV	Mean	STD DEV
A	211.28	44.0	107.88	19.6	261.08	36.3
B	204.40	14.2	104.77	8.0	267.60	5.4
C	204.75	23.3	106.85	10.1	267.30	18.6
D	204.96	26.9	107.96	3.2	261.76	19.8
E	214.24	18.4	103.92	7.8	262.76	10.4
F	214.48	18.8	109.00	3.5	256.65	9.3
G	221.49	2.9	106.21	5.7	255.64	4.9
H	204.44	7.6	109.73	3.7	264.83	4.5
F value	0.22		0.12		0.34	
P value	0.98		1.00		0.93	

Adipocyte induced assessment

Oil Red O stain was used to assess the adipocyte differential capacity by detecting the lipid droplets within mature adipocytes. A 0.5% Oil Red O stock solution was prepared with the addition of 0.5 g Oil Red O powder into 100 ml isopropanol and left to stir overnight using a magnetic stirrer. After the powder dissolved, the solution was filtered through two layers of filter paper. The Oil Red O working solution was prepared just before usage in the staining procedure at a ratio of 3 stock solution: 2 ddH₂O.

The DAPI working solution was removed from the adipocyte induced and non-induced adipocyte control (adipocyte controls) cultures after fluorescence microscopic analysis was performed. The cultures were left to dry on the bench top before 1 ml Oil Red O working solution was added to the adipocyte induced- and non-adipose cultures and left to incubate for 20 min at room temperature. The Oil Red O stain was then removed from the wells and the excess stain was washed repeatedly with the aid of a 3 ml Pasteur pipette and ddH₂O. The ddH₂O in the well was firmly pipetted directly onto the culture and discarded, until little to no pink discoloration of freshly added ddH₂O was visible to the naked eye, indicating minimal excess stain.

A 0.01% Toluidine Blue counter stain (Electron Microscopy Sciences, Washington, PA) was utilized to view the cell membranes of the Oil Red O stained cells. The 0.01% Toluidine Blue stain solution with pH 11 was prepared by the addition of 0.005 g Toluidine Blue and 0.005 g NaCO₃ (Merck) to 50 ml ddH₂O, before it was subjected to the Oil Red O stained cultures for 5 min at room temperature. The excess stain was then washed off by pipetting ddH₂O directly onto the culture with a 3 ml Pasteur pipette until freshly added ddH₂O presented little to no colouration.

Only 1 ml of ddH₂O was placed in the wells moments before microscopy analysis. Five random photographs were acquired with the 10x objective lens, using white light with a saturation 0.8 and exposure time of 1.50 s.

Osteocyte induced assessment

Osteogenic differentiation was assessed using 2% Alizarin Red S classical stain which detects the calcium deposition from mature osteocytes. The 2% Alizarin Red S stain solution was prepared by the addition of 2 g Alizarin Red S powder into 100 ml of ddH₂O which was then mixed thoroughly using a magnetic stirrer until solutes were dissolved before filtered through filter paper.

The DAPI working solution was removed from the osteocyte induced and osteocyte non-induced ASC cultures and washed with 2 ml PBS, with pH 4.2, for 5 min. After the PBS was discarded, 2 ml of the 2% Alizarin Red S stain was placed in the respective cultures and left to incubate for 10 min at room temperature. The excess stain was discarded and the same washing technique was followed (see adipocyte differentiation assessment above) until the discolouration of ddH₂O was minimal.

Before microscopy analysis, 1 ml fresh ddH₂O was placed in the respective wells. Five random photographs were acquired from both osteocyte induced and osteocyte control cultures, with the 10x objective lens, using white light with a saturation of 0.8 and an exposure time of 1.50 s.

Chondrocyte induced assessment

Each chondrocyte induced sphere were transferred to a glass tube and then serially dehydrated in 30%, 50%, 70% and 90% ethanol, followed by three changes of absolute ethanol for 15 min per dehydration step. Tissue was then infiltrated with 50% LR White Resin (SPI Supplies, West Chester, PA) in absolute ethanol for one hour, followed by infiltration with 100% LR White Resin overnight. Thereafter, tissue was transferred to resin capsules and embedded in 100% LR White Resin and labelled accordingly. Samples were polymerized for 24 hours at 60°C.

About 10 to 15 serial transverse sections of between 0.5 μ m to 1.0 μ m (optimal 0.5 μ m) were cut on a Reichert-Jung Ultra E ultramicrotome (Vienna, Austria). A section was collected onto a droplet of water on a Menzelglaser glass slide and transferred to a water droplet on a glass slide with an eyelash glued to a wooden stick and then dried on a hot plate. Slides were numbered accordingly and 1 % Toluidine Blue O (Electron Microscopy Sciences, Washington, PA) in a 0.5% Na₂CO₃ (Merck) solution (pH 11) were utilized to stain the tissue sections for 30 seconds, which was followed by a gentle rinse with dH₂O and subsequent drying. A drop of dH₂O was placed on the respective glass slide and covered with a cover slip before microscope investigations. Viewing and image capturing were done as described above for the other assessments.

To view the collagen band ultra-structure, transmission electron microscopy (TEM) was performed. Ultra-thin serial sections (at an estimated thickness of 100nm each) were cut from the same LR White embedded samples using a Reichert-Jung Ultra E ultramicrotome (Vienna, Austria) with a diamond blade and collected on copper grids. After dehydration on filter paper, the tissue sections were contrasted for 10 min in 4% aqueous uranyl acetate in the dark and rinsed thrice in ddH₂O. The samples were contrasted again for 5 min in Reynold's lead citrate and rinsed again three times in ddH₂O before being analysed with a JEOL JEM-2100F transmission electron microscope (Reynolds, 1963).

Quantification of differentiation

The five photographs of each DAPI stained well of each culture (2x non-induced, 2x adipogenic induced and 2x osteogenic induced) were manually counted as described above. Every single photo was initialized with the Image J software and the markers saved for re-evaluation if necessary. Total cell counts were recorded and the means were determined (Figure 4.21.).

The five photographs of each Oil Red O stained well of the adipocyte induced cultures were manually counted according the following parameters: (1) Preadipocytes (cells displaying very large and similar morphology as adipocytes e.g. triangular shape without visual observation of Oil Red O droplets); (2) More mature preadipocytes (cells displaying single Oil red O droplets); (3) Adipocytes (cells completely filled with Oil Re O droplets or fusion of the droplets displaying a large vacuole). Total counts were recorded and means determined.

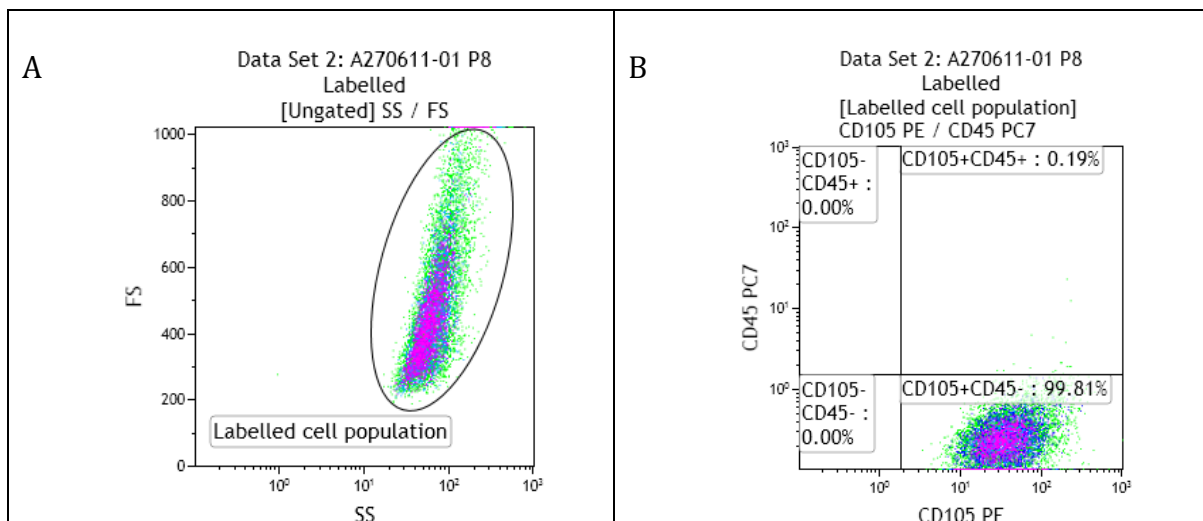
The bone differentiation visualized following staining with the Alizarin Red was qualitatively analysed and recorded.

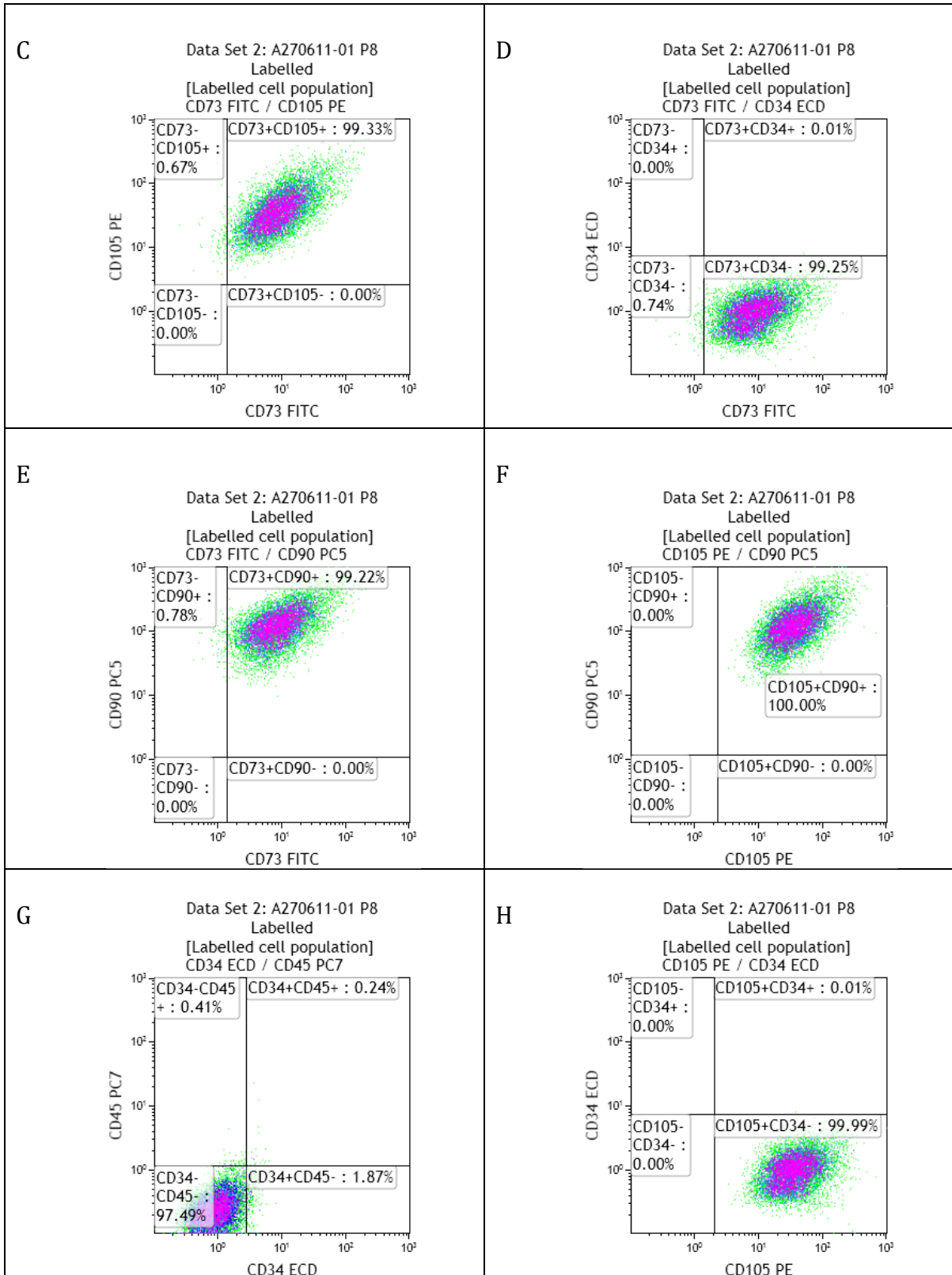
Results

Immunophenotypic characterisation

All the adipose samples collected were isolated, expanded, immunophenotypically characterised and differentiated, although only samples collected from the subcutaneous abdominal region of healthy donors, were considered for the final immunophenotypic statistical analysis. The samples excluded were A180811-01 and A040411-01 (Table 3.2), because these samples were collected from skin flaps that expanded as the patient gained weight. An additional sample, A090311-01, was also excluded from the analysis as the patient was receiving chemotherapy at the time of lipoaspirate collection. These samples were therefore not comparable as they contained excessive fibrotic scar tissue and the anatomical location of the donor sites differed.

The immunophenotypic profile of every cell within the ASC heterogeneous cell population was determined by analysing the co-expression of CD73, CD90, CD105, CD45 and CD34 on a single cell. The immunophenotypic profile analysis protocol consisted of 2-parameter plots as well as 1-parameter histograms. All the 2-parameter plots were gated on the cell population of the forward and side scatter plots (Figure 4.8.A). All possible combinations of fluorochrome parameters were analysed to calibrate the colour compensation on every parameter, as indicated by rounded cell populations on the 2-parameter plots (Figure 4.8. B-K).





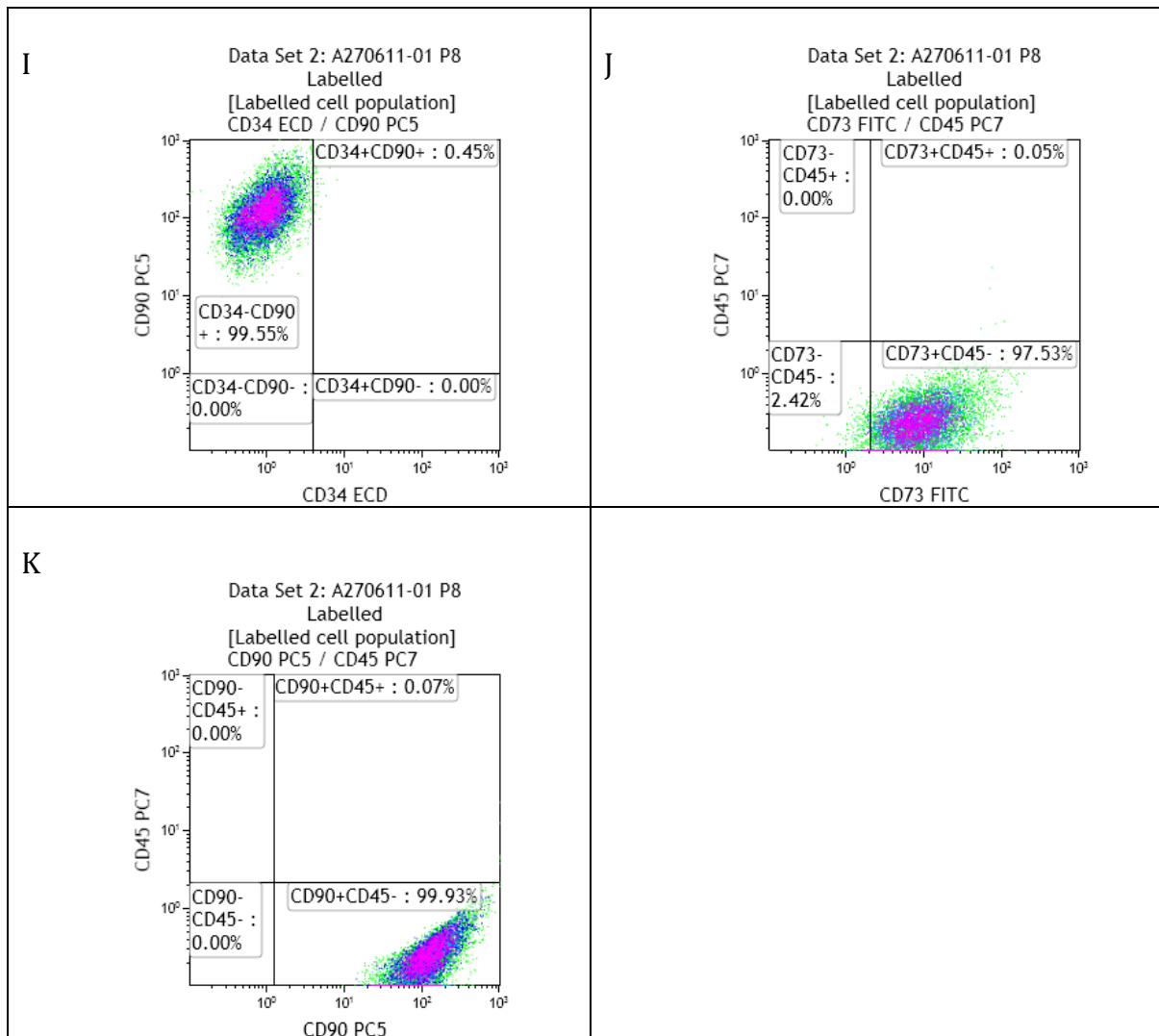
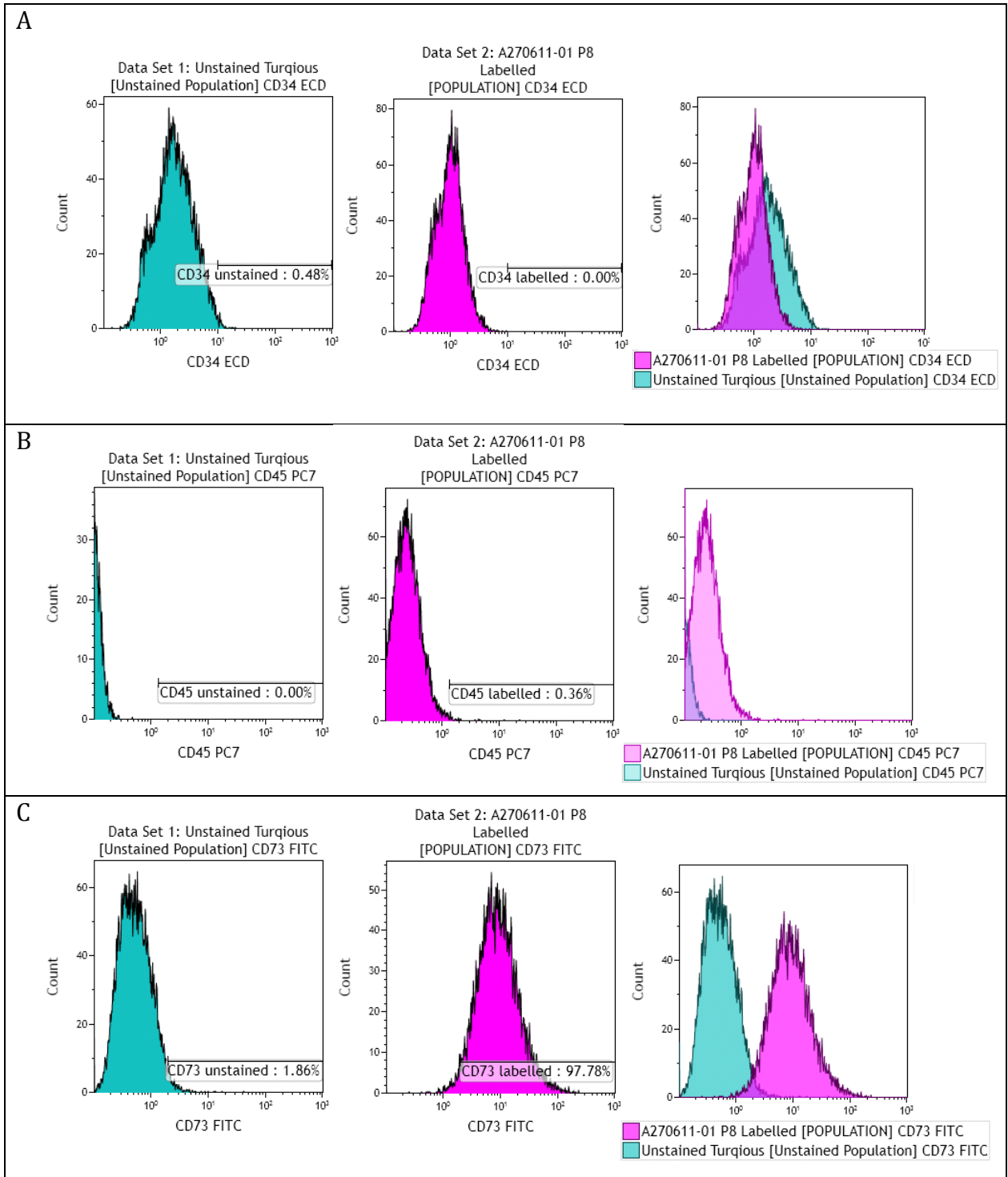


Figure 4.8. Example of all the possible 2-parameter plots, displayed in density plot formation to indicate the rounded cell populations. The 2-parameter plots were used to optimize colour compensation during the analysis process.

The voltage of the flow cytometer was calibrated to ensure that the unstained sample would be visible within the first decade of the histograms. Overlying histograms indicate the differences between the unstained and antibody labelled histograms for every surface marker measured (Figure 4.9.). A positive measurement of cell surface marker expression was demonstrated by the cell population moving right on the graph within in the second, third or fourth decade. The higher the expression of a respective surface marker, the brighter the fluorescence on a single cell and this will be displayed in a higher decade.



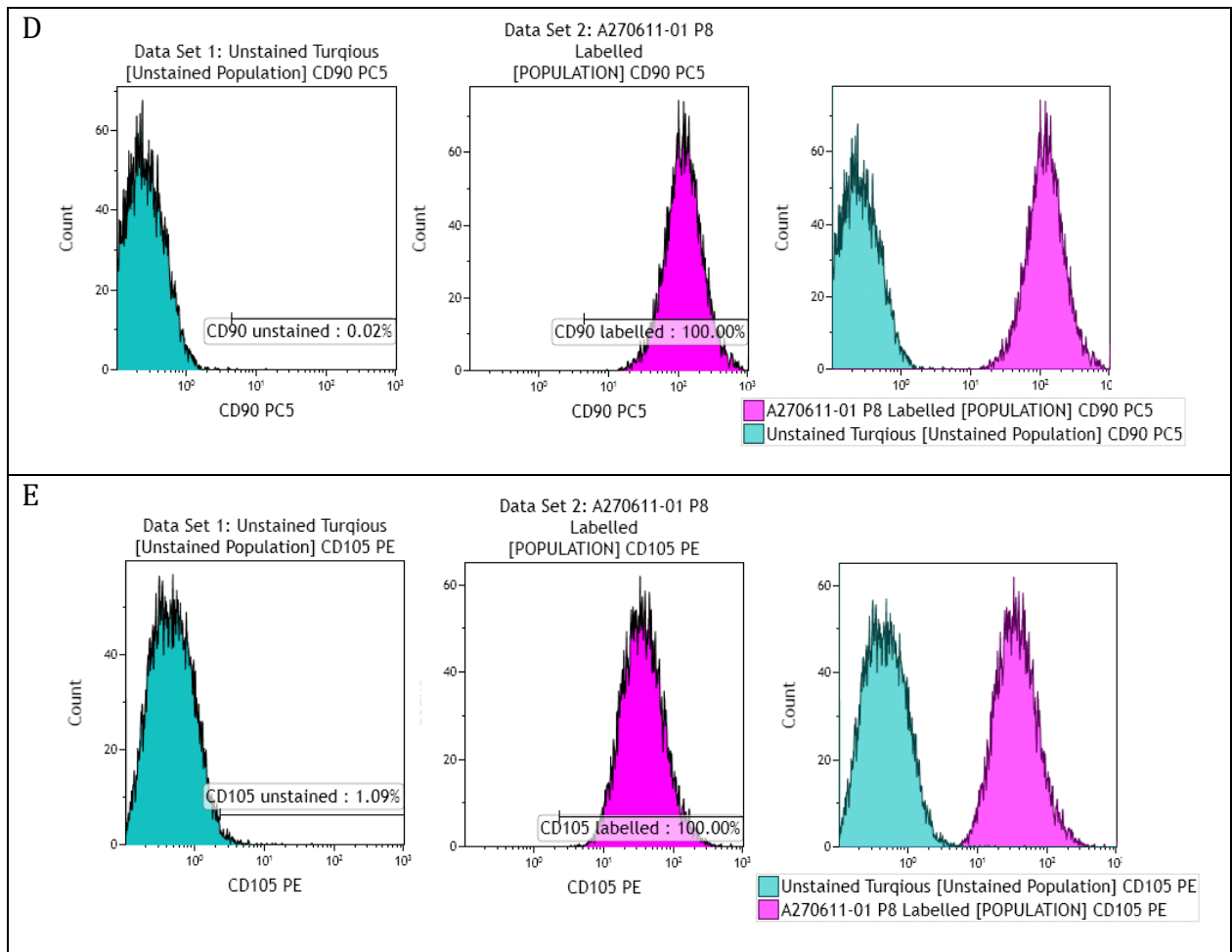


Figure 4.9. The unstained and antibody labelled 1-parameter plots as well as overlaying plots for every respective antibody expression measured. (A) CD 34; (B) CD 45; (C) CD 73; (D) CD 90; and (E) CD 105 respectively.

KALUZA generated a tree plot from the respective histograms to indicate all possible combinations of fluorochrome parameter expressions and to summarise the co-expression of a specific immunophenotypal profile on a single cell (Figure 4.10.).

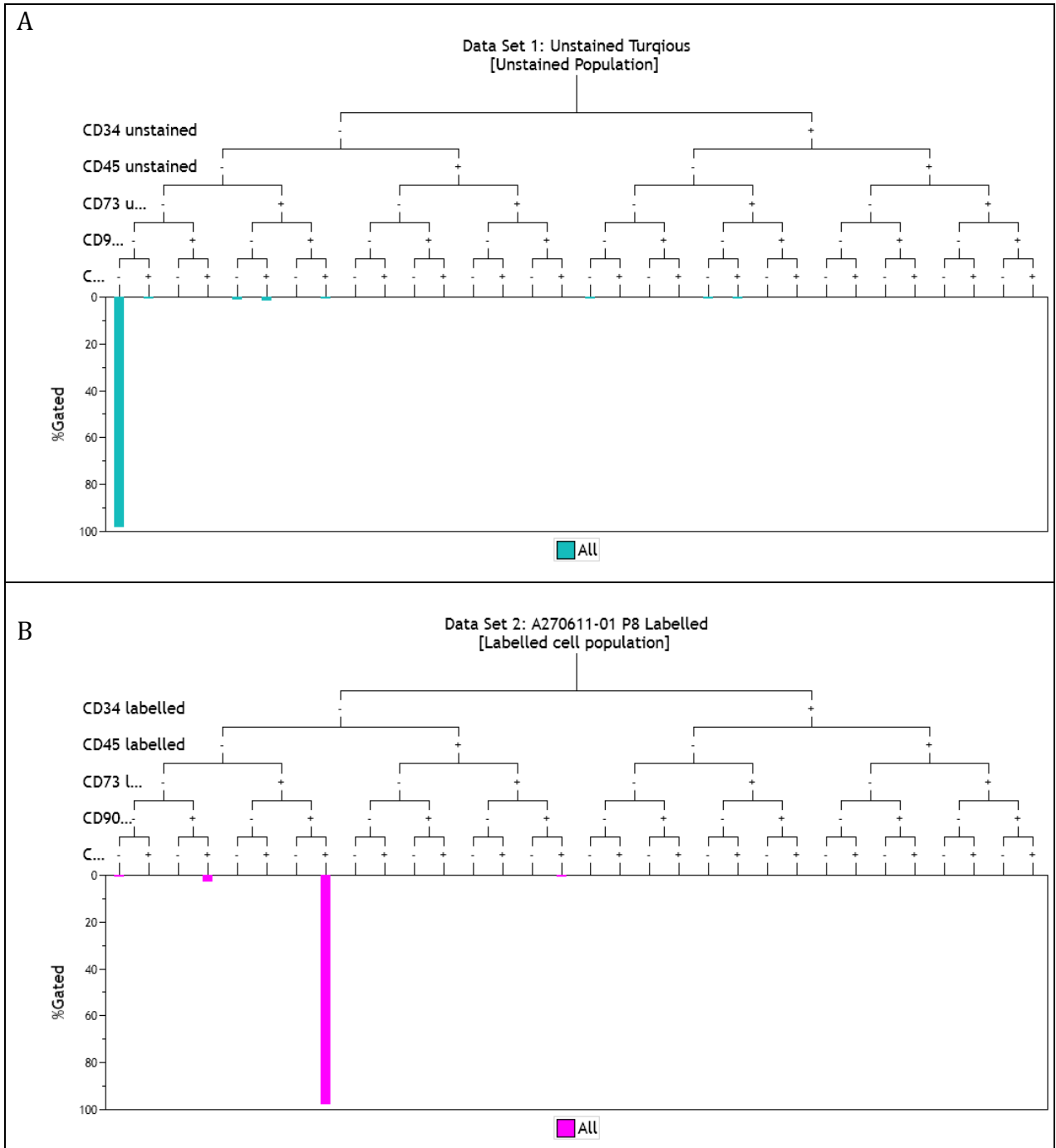


Figure 4.10. Examples of two tree plots (A) the unstained from the turquoise protocol group (see appendix 4.1) and (B) and antibody labelled sample (A270611-01 P8). The tree plot groups the cells within a specific combination phenotype expressed and displays the results as a percentage from the respective cell population gated in the forward and side scatter plot.

From the tree plots all possible combinations of positive and negative marker expression were considered in the final analysis. The statistics from the tree plot were exported into Excel and all the different combinations of positive and and negative expressions of every respective marker were expressed as a percentage from the respective cell population within the forward and side scatter plot (Figure 4.11.). Although all possible combinations were assessed, only one population was present at a high frequency (Figure

4.11., highlighted in yellow) and eight less frequent populations (sub-populations) were identified (Figure 4.11., highlighted in purple).

CD 34-CD 45-CD 73-CD 90-CD 105-	CD 34+CD 45-CD 73-CD 90-CD 105-
CD 34-CD 45-CD 73-CD 90-CD 105+	CD 34+CD 45-CD 73-CD 90-CD 105+
CD 34-CD 45-CD 73-CD 90+CD 105-	CD 34+CD 45-CD 73-CD 90+CD 105-
CD 34-CD 45-CD 73-CD 90+CD 105+	CD 34+CD 45-CD 73-CD 90+CD 105+
CD 34-CD 45-CD 73+CD 90-CD 105-	CD 34+CD 45-CD 73+CD 90-CD 105-
CD 34-CD 45-CD 73+CD 90-CD 105+	CD 34+CD 45-CD 73+CD 90-CD 105+
CD 34-CD 45-CD 73+CD 90+CD 105-	CD 34+CD 45-CD 73+CD 90+CD 105-
CD 34-CD 45-CD 73+CD 90+CD 105+	CD 34+CD 45-CD 73+CD 90+CD 105+
CD 34-CD 45+CD 73-CD 90-CD 105-	CD 34+CD 45+CD 73-CD 90-CD 105-
CD 34-CD 45+CD 73-CD 90-CD 105+	CD 34+CD 45+CD 73-CD 90-CD 105+
CD 34-CD 45+CD 73-CD 90+CD 105-	CD 34+CD 45+CD 73-CD 90+CD 105-
CD 34-CD 45+CD 73-CD 90+CD 105+	CD 34+CD 45+CD 73-CD 90+CD 105+
CD 34-CD 45+CD 73+CD 90-CD 105-	CD 34+CD 45+CD 73+CD 90-CD 105-
CD 34-CD 45+CD 73+CD 90-CD 105+	CD 34+CD 45+CD 73+CD 90-CD 105+
CD 34-CD 45+CD 73+CD 90+CD 105-	CD 34+CD 45+CD 73+CD 90+CD 105-
CD 34-CD 45+CD 73+CD 90+CD 105+	CD 34+CD 45+CD 73+CD 90+CD 105+

Figure 4.11. All possible combinations of positive and negative markers that were analyzed. The yellow highlighted combination represents the ASC phenotype used to characterize the respective population. The combinations phenotypes highlighted violet are the respective sub-populations (N=8) identified.

ASC Phenotype expression Profile

The ASC phenotype expression profile of CD34-, CD45-, CD73+, CD90+ and CD105+ was assessed for every individual culture over different passages (Figure 4.12). The recommended threshold of >95% expression of the respective combination profile was demonstrated at least once in every individual culture. Few cultures maintained this expression profile threshold and expression variability across passages within individual cultures was observed. Not all the cultures were phenotyped at every passage. No culture reached the recommended cut-off at passage 1. Expression of the ASC profile increased from passage 2 onward. The results were further sub-analyzed by moving the cut-off threshold to 90%. The total individual cultures adhering to the recommended threshold (>95%) and adjusted threshold (>90%) on every respective passage, were expressed as a percentage (Figure 4.13).

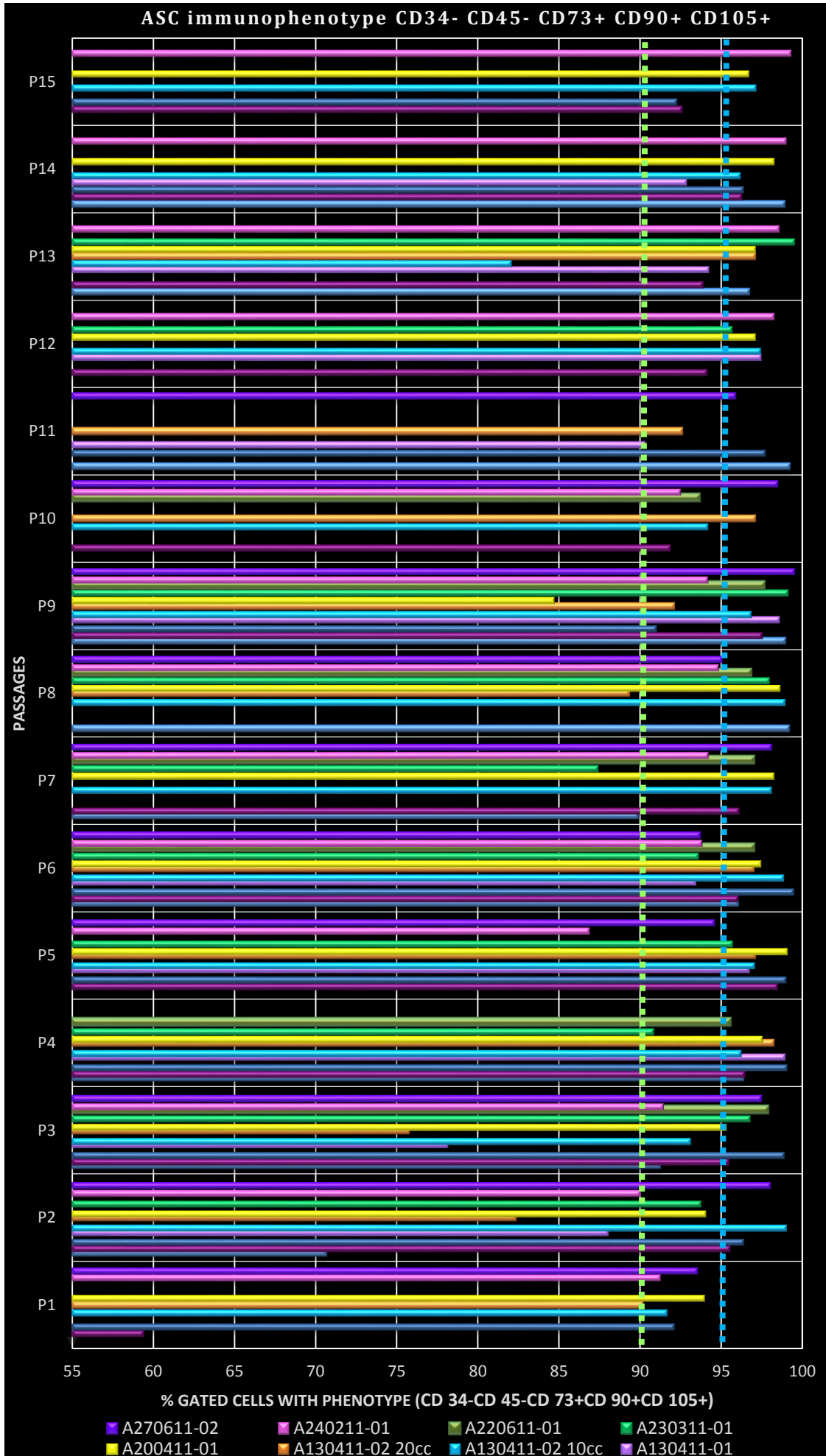


Figure 4.12. ASC phenotype of all the cultures across 15 passages. The blue dotted line indicates the threshold of the 95%, demonstrating >95% expression of CD73, CD90, CD105 and >95% lacking expression of CD34 and CD45. The Green dotted line indicates the adjusted threshold of >90%. The red gridline indicates the separation between respective passages.

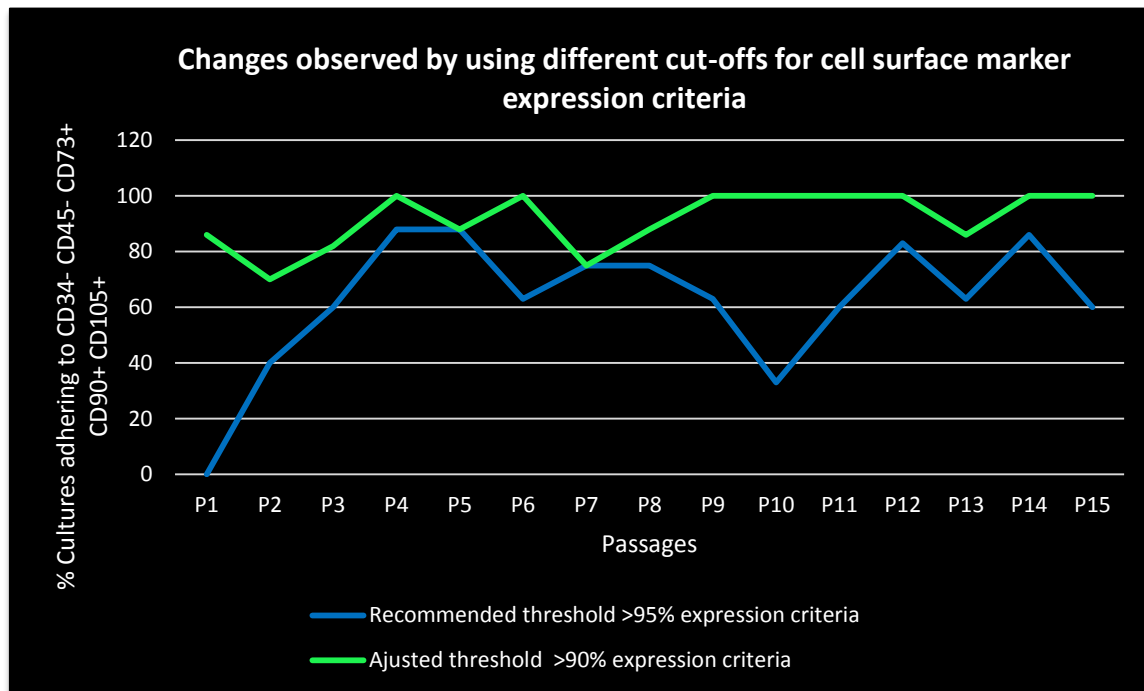


Figure 4.13. The percentage cultures adhering to the respective standard >95% expression (Blue) criteria threshold (CD34-, CD 45-, CD 73+, CD 90+ CD 105+ set out by Domenici *et al.*, 2006 and the adjusted cut off criteria threshold >90% expression (Green). (See Figure 4.12.)

The mean ASC phenotypic expression for all cultures within respective passages was assessed (Figure 4.14.). Although slight variability of the mean ASC phenotype expression occurred between passages, a linear incline of the ASC phenotype expression profile was observed with increasing passage numbers.

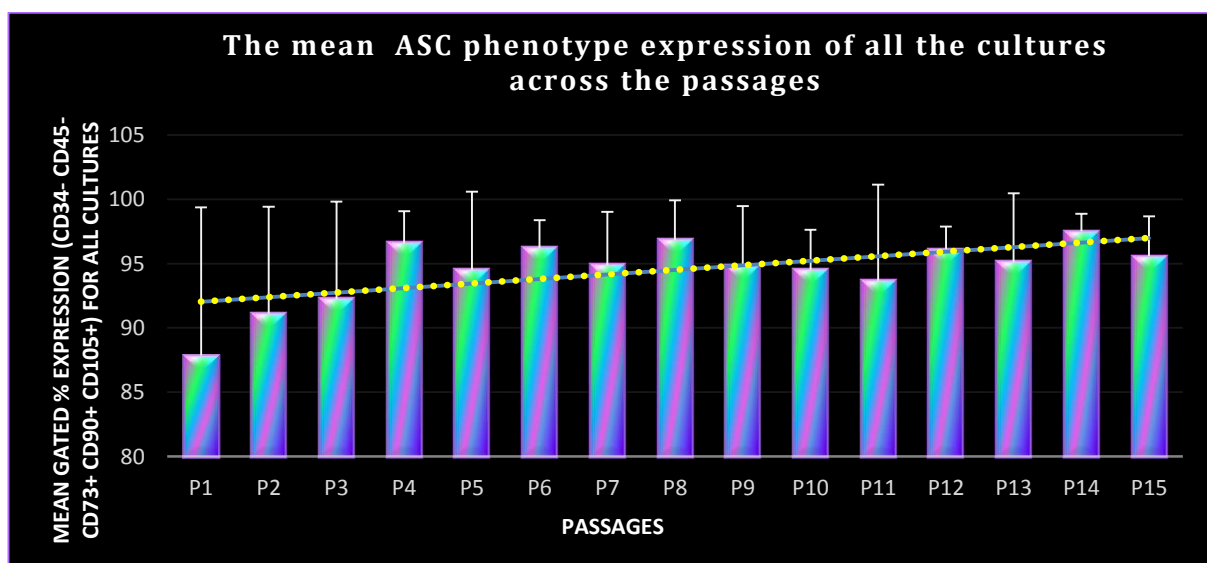


Figure 4.14. The mean ASC phenotype (CD34-, CD45 -, CD73+, CD90+ and CD105+) expression of cultures phenotyped within a respective passage. The trend line indicates a steady linear increase in the ASC phenotype expression across all passage.

Analysing the sub-populations within an individual culture demonstrates the expression variability of the sub-populations across various passages as well as inter patient expression variability. Figure 4.15. illustrates 5 sub-populations present in one culture with varying levels of expression over different passages and although all rise above 1% expression at some stage none cross the 5% threshold.

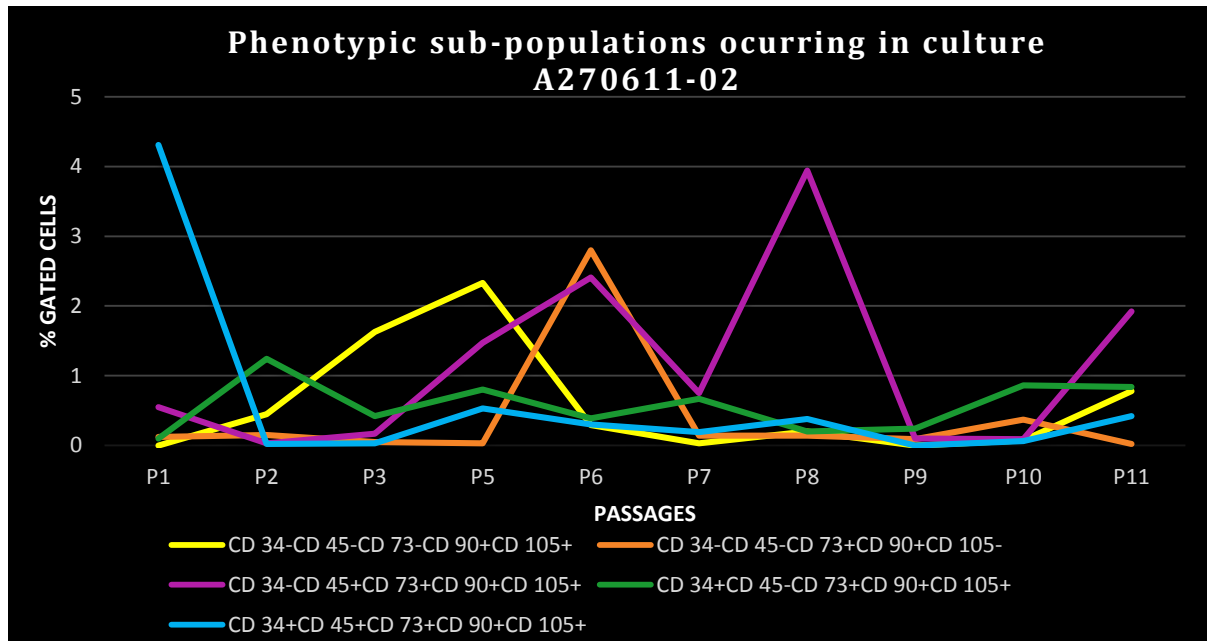


Figure 4.15. Percentage gated cells expressing respective sub-population phenotype combinations across passages in a single patient culture (A270611-02).

Different sub-populations are also found within different individual cultures, also indicating patient variability. The sub-population profile of CD34-, CD45-, CD73+, CD90- and CD105+ was not expressed according to the threshold parameters in culture A270611-02 but was expressed within culture A220611-01 (Figure 4.16).

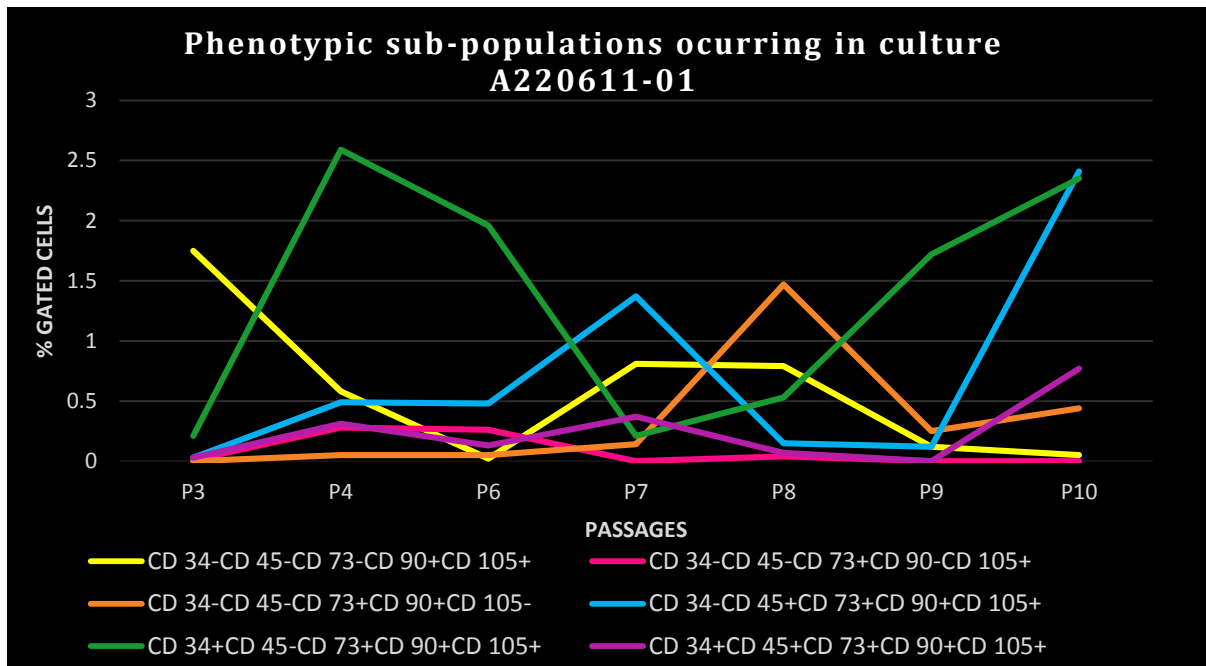


Figure 4.16. Percentage gated cells expressing respective sub-population phenotype combinations across passages in patient A220611-01.

The frequencies of sub-population expression among individual cultures are displayed in Table 4.5. The majority of sub-populations occurred at an expression level of >1.0 – 5% (45) whereas 0.1 – 1.0 (26) and >5 (21) showed lower amounts. The number of sub-populations per culture was 7.67 ± 1.78 (mean \pm SD).

Table 4. 5. The frequency of significant sub-population expressions for all passages of every culture phenotypically analyzed according to respective threshold parameters. The percentage frequency expressions across all passages for the respective culture were calculated to indicate inter patient variability.

Culture	0.1 – 1.0 %		>1.0 -5%		>5%		Total number of sub-populations
	Number of sub-populations	%	Number of sub-population	%	Number of sub-populations	%	
A270611-01	2	33.3	3	50.0	1	16.6	6
A050511-01	4	44.4	4	44.4	1	11.1	9
A050711-01	2	28.5	3	42.8	2	28.5	7
A100511-01	2	33.3	1	16.6	3	50.0	6
A130411-01	2	22.2	4	44.4	3	33.3	9
A200411-01	3	33.3	5	55.5	1	11.1	9
A230311-01	4	36.3	5	45.4	2	18.1	11
A220611-01	2	33.3	4	66.6	0	0.0	6
A240211-01	3	33.3	2	22.2	4	44.4	9
A270611-02	0	0.0	5	100.0	0	0.0	5
A130411-02 10cc	0	0.0	7	87.5	1	12.5	8
A130411-01 20cc	2	28.5	2	28.5	3	42.8	7

When considering the presence of sub-populations across all cultures in respective passages, 3 different populations were present in all the cultures at specific passages: (1)

CD 34+CD 45-CD 73+CD 90+CD 105+ (at passage 1, 2, 3, 10, 11, 12 and 14); (2) (Figure 4.17.)

In addition, the presence of four sub-populations: (1) CD34+, CD45+, CD73+, CD90+, CD105+; (2) CD34+, CD45-, CD73+, CD90+, CD105+ (3) CD34-, CD45+, CD73+, CD90+, CD105+; and (4) CD34-, CD45-, CD73-, CD90+, CD105+ were observed across all passages. Furthermore, these four sub-populations as well as an additional sub-population CD34-, CD45-, CD73+, CD90- and CD105+ were observed within all individual cultures.

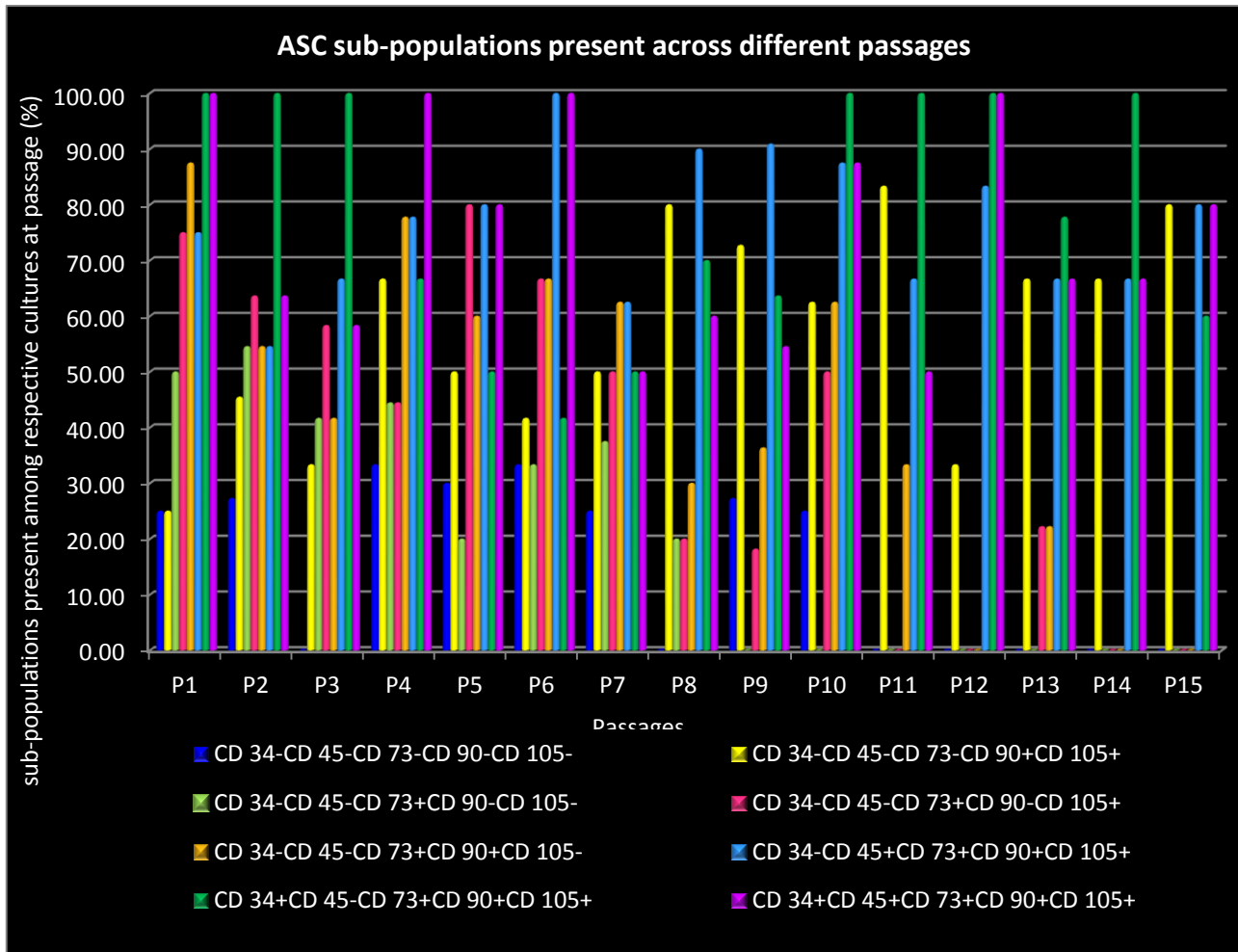


Figure 4.17. The ASCs sub-population phenotypes in the heterogeneous ASC population across 15 passages. The frequencies of significant expression across all cultures within a respective passage are demonstrated as a percentage within the passage.

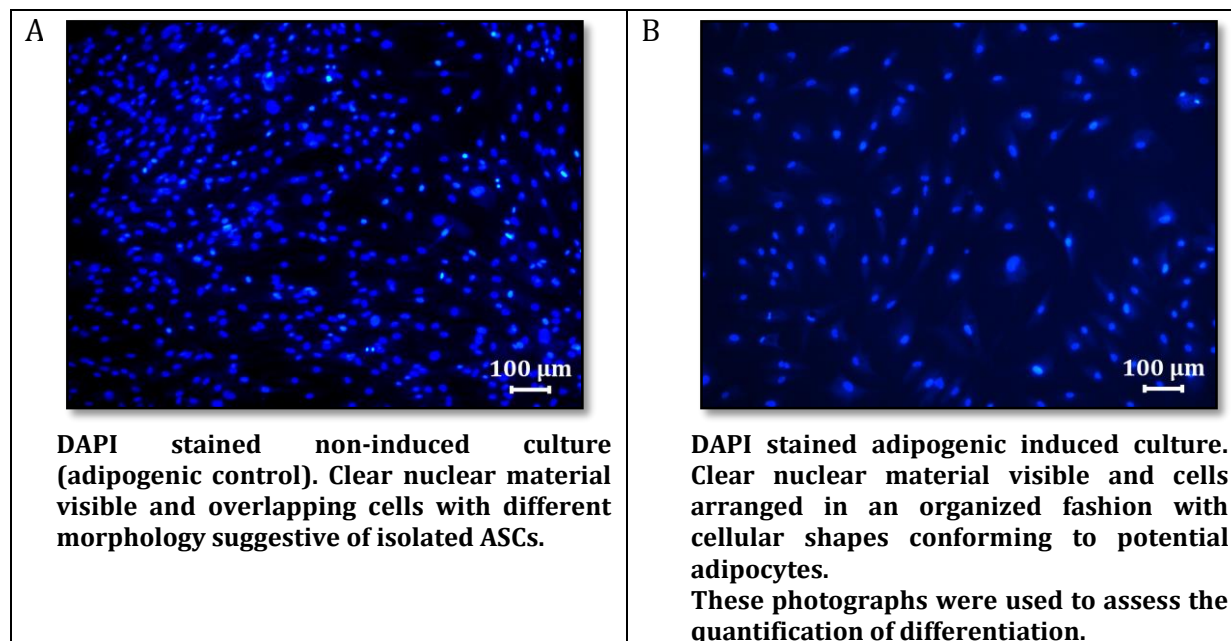
Analysis of the specific sub-populations and potential origin revealed potential explanations (Table 4.6) including decreasing debris as seen with CD34-CD45-CD73-CD90-CD105- and hematopoietic lineage CD34-CD45+CD73+CD 90+CD105+.

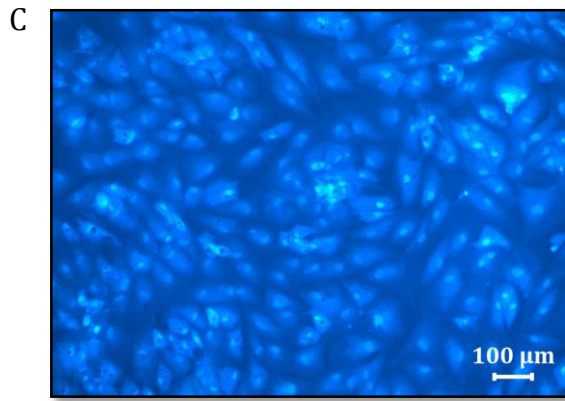
Table 4.6. Sub-population profiles found among isolated and expanded ASCs.

Sub-population profile	Proposed sub-populations or cell type contaminant
CD 34-CD 45-CD 73-CD 90-CD 105-	Sub-population or debris
CD 34-CD 45-CD 73-CD 90+CD 105+	Sub-population
CD 34-CD 45-CD 73+CD 90-CD 105-	Sub-population
CD 34-CD 45-CD 73+CD 90-CD 105+	Sub-population
CD 34-CD 45-CD 73+CD 90+CD 105-	Sub-population
CD 34-CD 45+CD 73+CD 90+CD 105+	Hematopoietic lineage (T cells, B cells or mast cells or leukocytes)
CD 34+CD 45-CD 73+CD 90+CD 105+	ASC phenotype new criteria
CD 34+CD 45+CD 73+CD 90+CD 105+	Could be HSC like cells

Tri-lineage Differentiation

The Tri-lineage induction that was performed over 21 days was successful for all cultures. Figure 4.18 illustrates the different levels of assessment for adipogenic differentiation, including the classical stains used for both induced and non-induced cultures, all respective cultures conformed to this criteria.

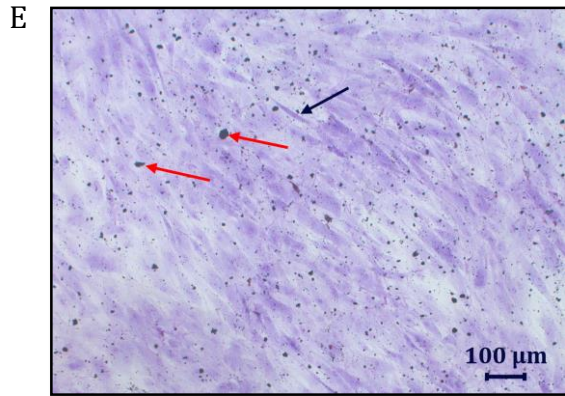




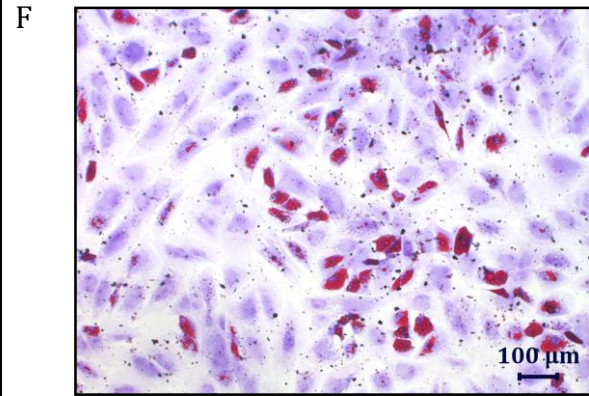
C
Observation following extended time lapse after initial DAPI stain. Induced adipocytes are visualized with both stained nuclear material and cytoplasm indicating increased visibility of the stain following time lapse.



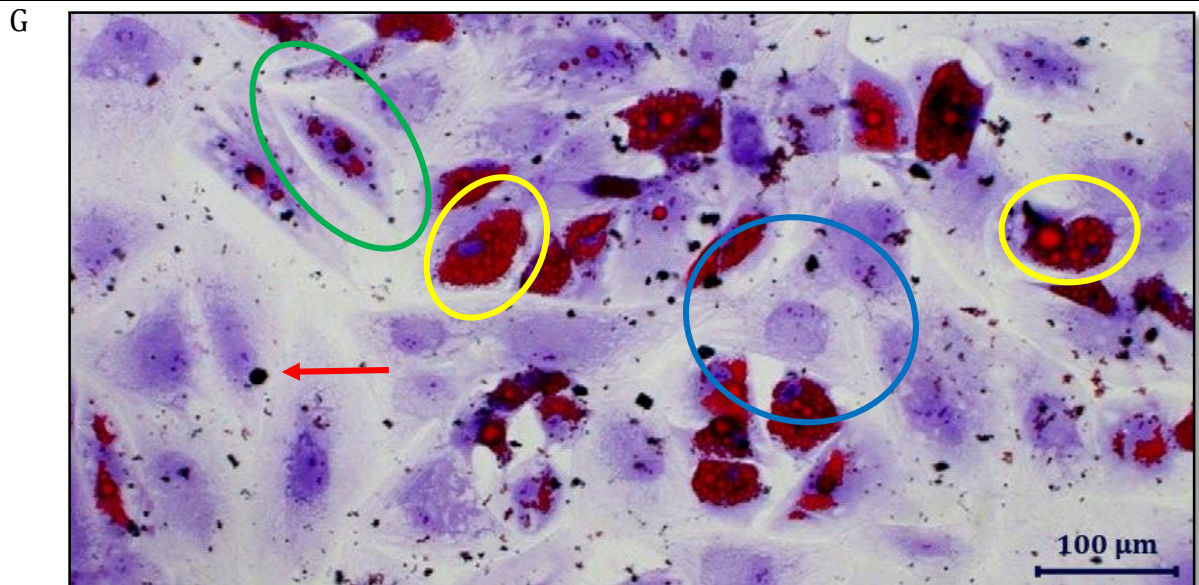
D
Oil Red O stained well without cells (blank) to serve as a negative control. The Oil Red O stained the plastic well surfaces.



E
Oil Red O stained and 1% Toluidine Blue counter stained non-induced culture. The red arrow indicates Oil Red O residue overlaying the culture. The cells are fibroblastic like, small, slender and elongated as indicated by the blue arrow and conform to ASC described morphology.



F
Oil Red O stained and 1% Toluidine Blue counter stained adipogenic induced culture. Visible Oil Red O droplets confirms differentiation into adipogenic lineage.

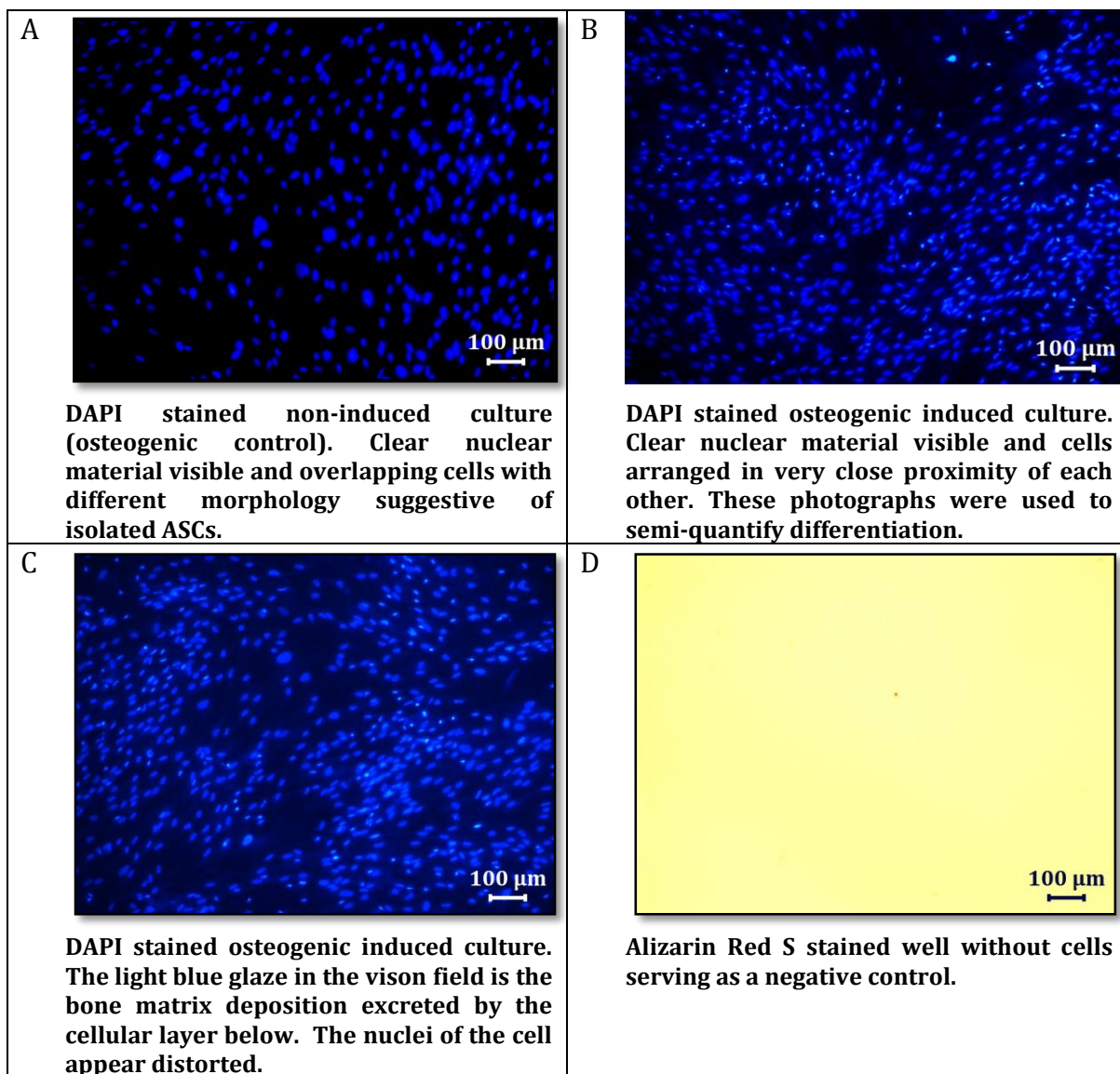


A magnification snapshot of (F). The red arrow indicates Oil Red O residue present overlaying the cell. Adipogenic quantification was performed as described before.

- Yellow circles demonstrate adipocytes (cytoplasm completely filled with lipid droplets and also fusion of the droplets with associated lipid vacuole formation)
- Green circle demonstrates a more mature preadipocyte with incomplete lipid droplet formation
- Blue circled demonstrates a preadipocyte with an enlarged triangular shaped cell that conforms to the morphology of the adipocytes but does not contain any visual Oil Red O stained lipid vacuoles.

Figure 4.18. Adipogenic lineage microscopy analysis.

All respective cultures differentiated into the osteogenic lineage. Figure 4.19. Illustrates the different assessments for both induced and non-induced cultures pertaining to osteogenic differentiation.



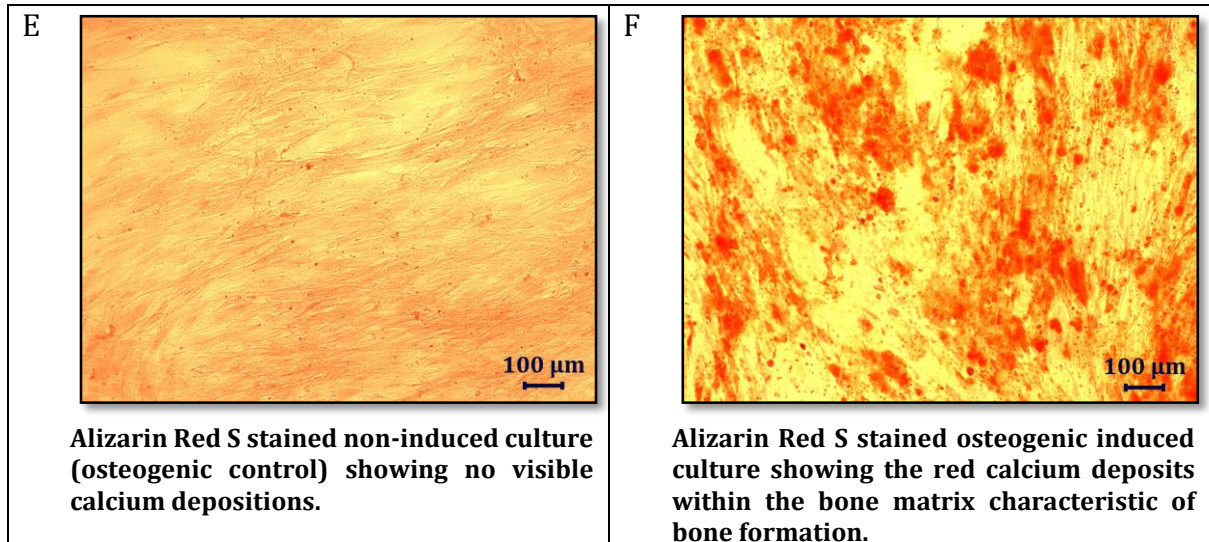
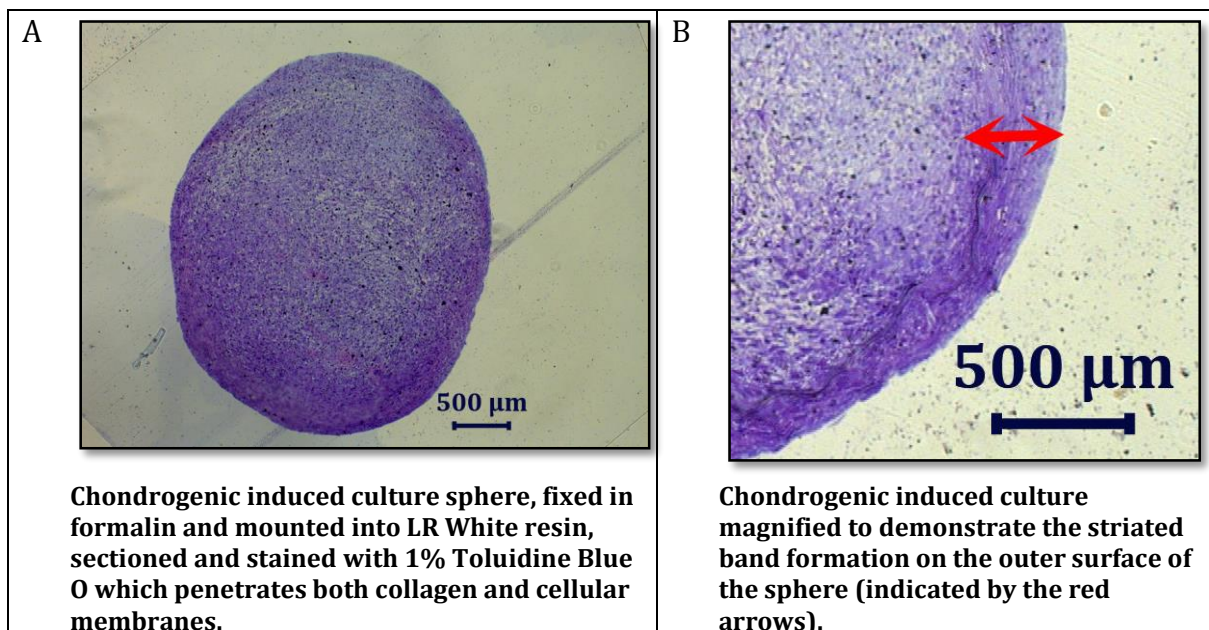
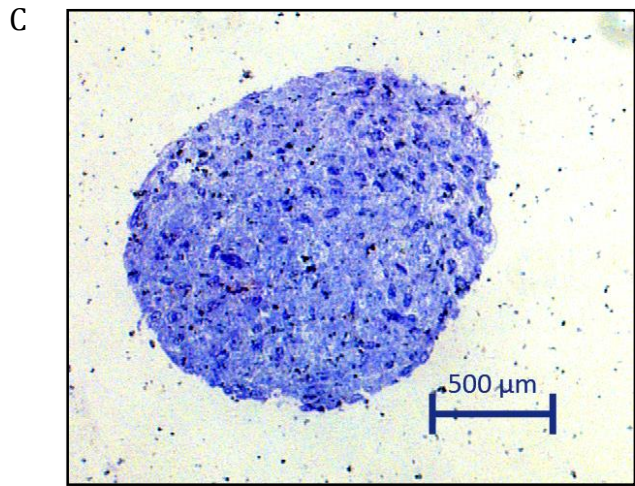


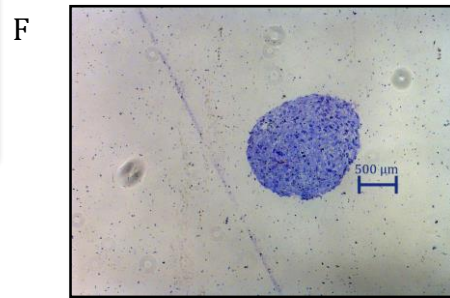
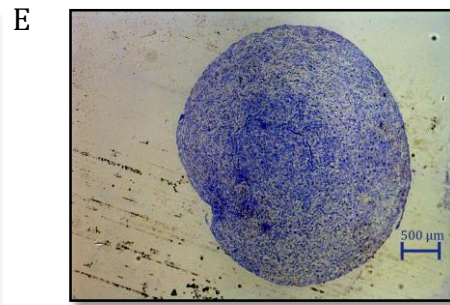
Figure 4.19. Osteogenic microscopy analysis.

All cultures demonstrated differentiation into the chondrogenic lineage. Figure 4.20. illustrates the different assessments pertaining to cartilage formation. The non-induced cultures demonstrated a decrease in spherical diameter and little collagen deposition in comparison to the induced cultures.

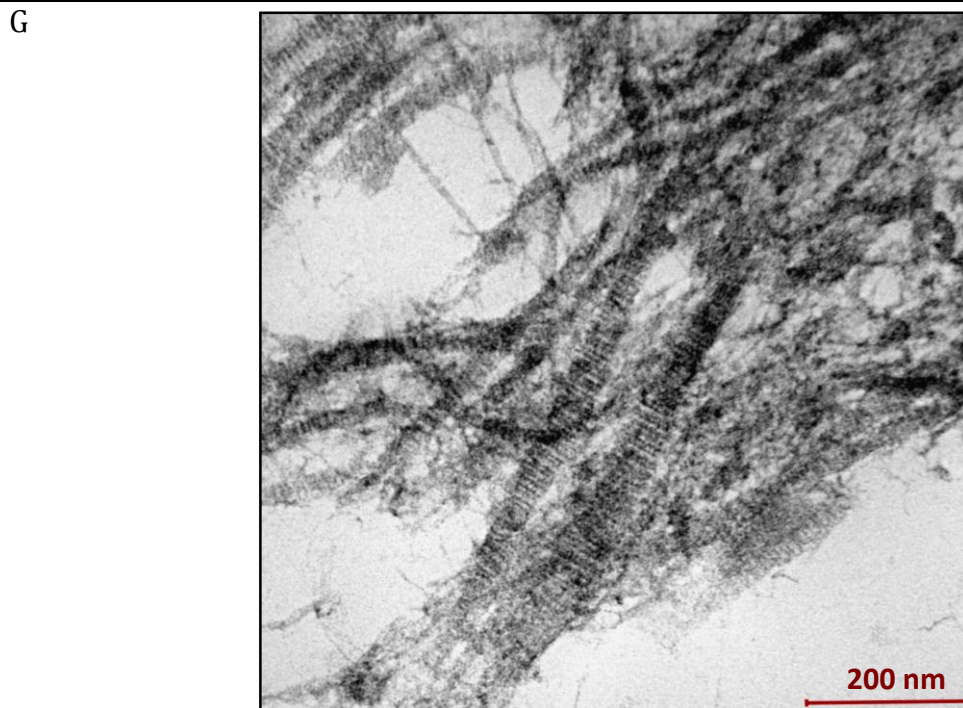




Non-induced chondrogenic culture, stained with 1% Toluidine Blue O. Pellet is significantly reduced in size when compared to induced cultures. Residual background staining visible.



Comparing the pellet size of the chondrogenic induced (E) with the non-induced (F) cultures within individual culture A200511-01 P5



A TEM photograph of sectioned chondrocyte induced culture sphere, illustrating the collagen bands within the sphere.

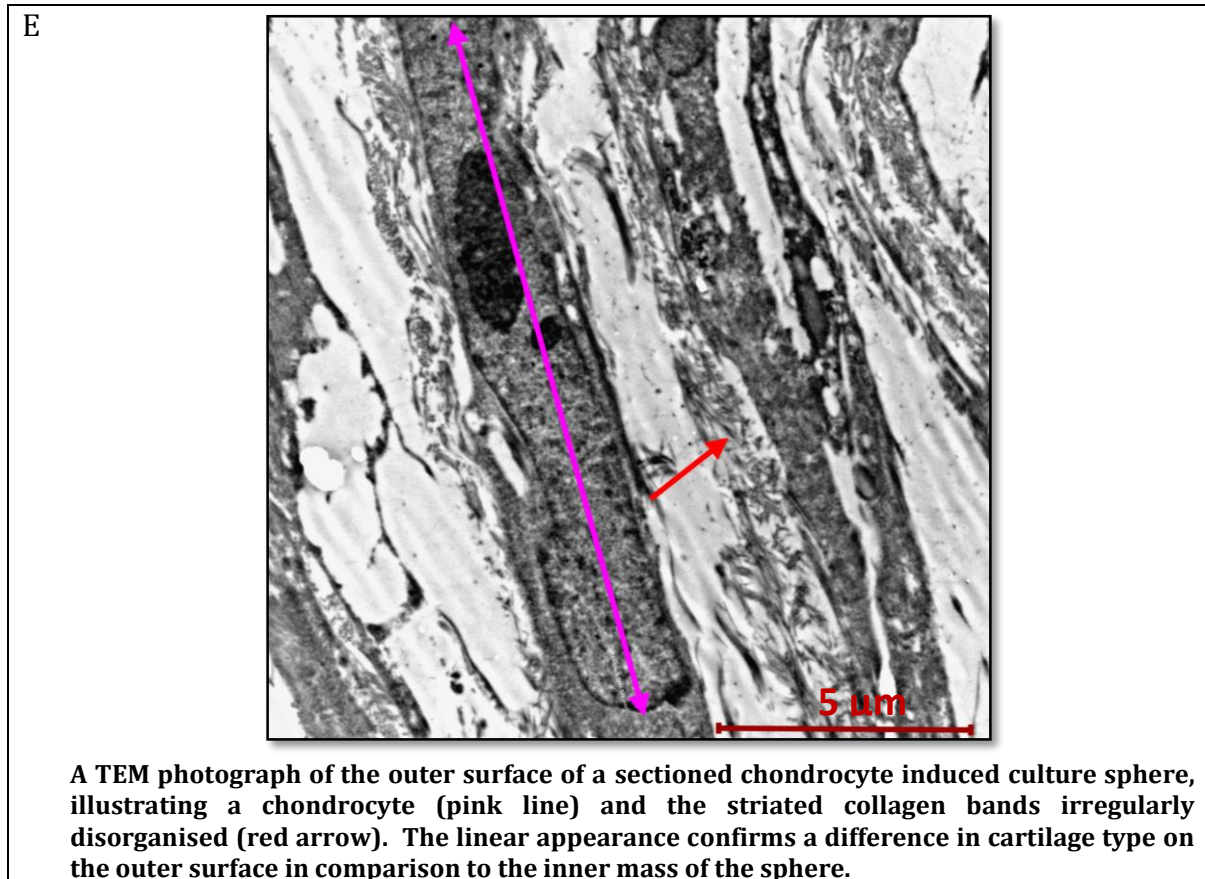


Figure 4.20. Chondrogenic microscopy analysis.

Quantification of differentiation

Results of the quantification showed great variability among the assessed cultures to differentiate into both adipogenic and osteogenic lineages. A general trend was observed indicating consistent decreased mean cell counts for induced adipogenic cultures and increased induced osteogenic cultures compared to the controls. The mean cell counts for both adipogenic and osteogenic differentiation was 150.4 (STD DEV 86.3) and 630.9 (STD DEV 335.0) respectively (Figure 4.21.). Another trend indicated slight decreased bone differentiation in the cryopreserved cultures (CP) compared to the non-cryopreserved cultures (NC). The mean cell counts for adipogenic differentiation for CP and NC was 154.8 (STD DEV 91.6) and 143.30 (STD DEV 87.2) ($P=0.4192$ 95% CI) and for osteogenic differentiation 513.1 (STD DEV 303.7) and 819.3 (STD DEV 321.5) ($P=0.04029$ 95% CI).

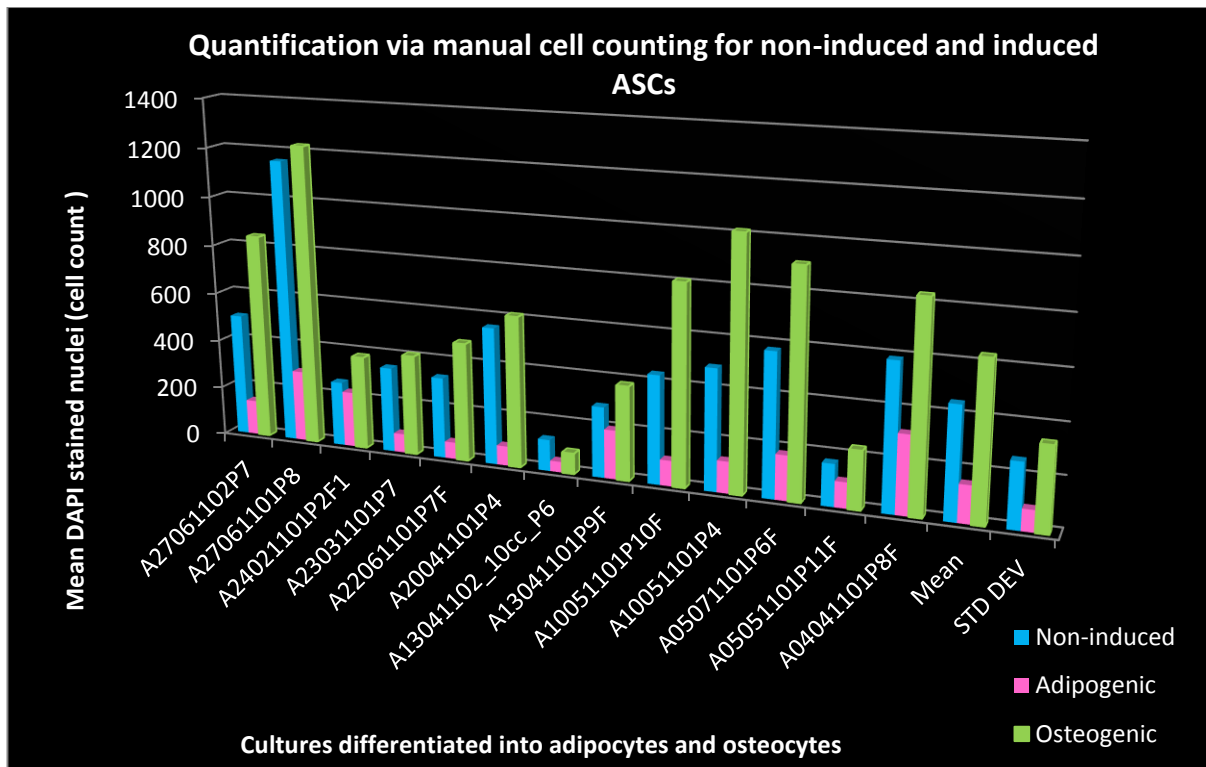


Figure 4.21. The mean cell counts of vision fields from respective DAPI stained non-induced control (blue), adipogenic (pink) and osteogenic (green) induced cultures for all cultures.

All cultures showed differentiation into the adipogenic lineage, however great variability was observed with regard to the stage of adipocyte maturation and associated uptake of the Oil Red O stain. The majority of cultures had predominant preadipocytes present with small proportions of mature adipocytes.

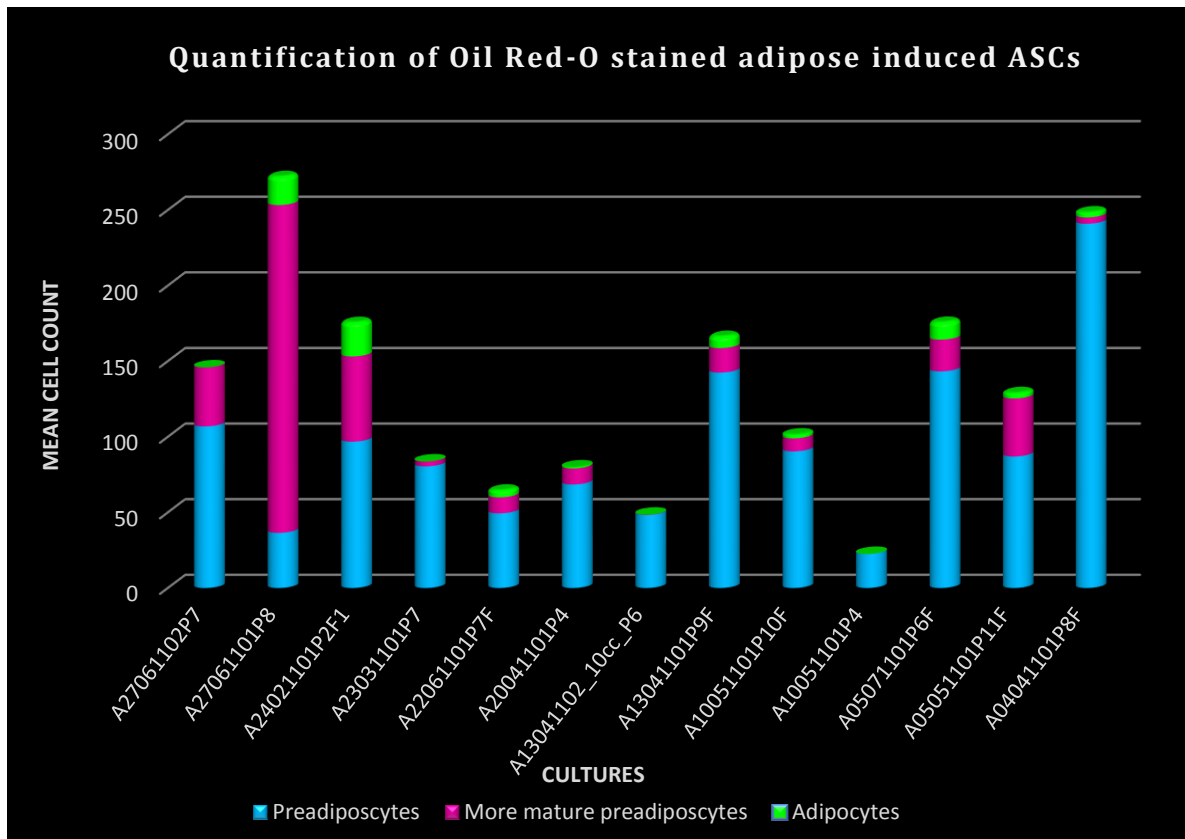


Figure 4.22. The mean cell counts from 5 vision fields of the Oil Red O stained adipogenic induced cultures. The preadipocytes (blue), more mature preadipocytes (pink) and adipocytes (green). The adipogenic induced cells were quantified according to set out parameters (See Figure 4.18.).

Quantification of osteogenic differentiation through Alizerin Red S staining is not possible and was only qualitatively assessed due to the staining of the calcium depositions within the mineral matrix. Quantification of chondrogenic differentiation was also only qualitatively assessed as the induced chondrocytes contracted into a sphere containing both chondrocytes and collagen which hampers further microscopic analysis.

Discussion

To our knowledge, this is the first study in South Africa to evaluate and characterize sub-populations of ASCs harvested from clinical collected adipose tissue and highlights various challenges when following the current recommended criteria as well as potential limitations for application in clinical practice.

Immunophenotypic characterization

Evaluating every culture for all possible combinations of positive and negative marker expression at every available passage proved to be useful in establishing both the inter-culture and inter-passage variability. Also using this methodology lead to the discovery of eight potential sub-populations.

The ASC phenotype was present at least once among all the evaluated cultures, however expression was not consistent or even increasing. This inter-passage variability could not be explained but may be affected by the patient profile (e.g. age and gender), growth conditions or simply the nature or the predominating population of cells. The low adherence to the 95% cut-off expression at passage one and the increase in adherence from passage two onwards could be explained by the initial presence of “blood contaminants” and the progressive “purification” of the ASC population due to loss of cellular contaminants including macrophages, white blood cells during passage. The ability of select cultures to maintain a high level (>95%) adherence across all passages could also not be explained and may be affected by similar factors as those described above.

The great variability raises many questions *e.g.* at what time point/passage should the population be regarded as “pure” and how often should characterization expression be performed for clinical application? Cellular contamination (endothelial cells or macrophages) could also become a more prominent population at any time point and could be the reason for a lower adherence for some of the sub-populations at sporadic passages.

The mean adherence to the defined criteria across all cultures showed an increasing trend with increasing passage number. Extensive expansion and passaging preselects for the most dominant and robust cell population which could explain attenuation of sub-populations with increasing passages. An interesting observation was made when moving the cut-off for expression to 90%, adherence to the standardized criteria dramatically increased (>80 -100%) across all passages. This also raises questions on how the standard of 95% was decided on as well as whether relaxing the cut-off slightly could provide better adherence and unnecessary misclassification? Further research would be necessary to establish new cut-offs.

Since 2006, research and new data in the field mandates a revision or an amendment of the recommended guideline criteria. Recently, the International Federation for Adipose Therapeutics and Science (IFATS) and the ISCT released new criteria for characterizing uncultured adipose tissue-derived stromal vascular fraction (SVF) as well as cultured ASCs (Bourin *et al.*, 2013).

The study described herein was based on the characterization criteria set out by Dominici *et al.* in 2006, according to which the CD 34 marker should not display expression of >5%. Recently this marker has raised some concerns. Lin and colleagues (2012) strongly questioned the positive or negative fraction of CD 34. They found that tissue resident BM-MSCs express CD34 and expression decreases due to extensive culturing. Oedayrajsingh Varma and co-workers (2007) demonstrated that AD-SVF express CD34 and with expansion the expression decreases dramatically. In addition, the revised criteria of the immunophenotypic profile confirmed that CD34 is a positive unstable marker, because it can lack or express invariably and can be present at variable levels

(Bourin *et al.*, 2013; Lin *et al.*, 2012; Oedayrajsingh Varma *et al.*, 2007; Yoshimura *et al.*, 2006).

The function of CD90 is ill defined, although it was proposed to play a role in adhesion of monocytes and leukocytes to endothelial cells and fibroblasts, stromal adherence and cell to cell interactions. The present study demonstrated a strong and uniform positive expression for CD73, CD90 and CD105 across early and late passages. Pittenger and colleagues found that only one third of the CD73 and CD105 positive clones are multipotent, suggesting that these two markers are not directly linked with differential capacity (Boxall and Jones, 2012; Pittenger *et al.*, 1999).

Sub-population analysis

The sub-population analysis helped to answer a few questions. Firstly, sub-populations were identified in all 12 cultures, however these differed with regard to expression level and frequency. Most sub-population was expressed between 1 – 5 % of cells within the gated cell population. This questions again the criteria to define sub-populations and the potential impact of this finding. Experts agrees that expression of >0.1% could be regarded as a sub-population, although there are no set guidelines. Much higher levels of up to 5% and even higher were observed within this study. We believe that populations at a level of 5% could have a significant effect on the behaviour of the culture (including the dominating population).

Secondly, we identified three sub-populations that were present in all the cultures at specific passages; this finding needs further investigation. Thirdly, the presence of debris seemed to decrease with ongoing passaging. Fourth, the potential presence of the hematopoietic lineage (CD45+) was present across all passages but not all cultures. This could again be explained by patient factors, source of respective adipose tissue and culturing conditions.

Lastly, we also detected sub-populations that conform to the new proposed criteria (Bourin *et al.*, 2013). According to these new criteria we suggest that the sub-population found (displayed as: purple in Figure 4.15.; blue in Figure 4.16; and green in Figure 4.17.) adheres to the ASC immunophenotypic profile. Contrary to findings in the literature, the sub-population profile CD34+, CD45-, CD73+, CD90+ and CD105+, increases in lower passages < 4 and increases again in higher passages >8 (Figure 4.18). This phenomenon could be due to the cells being expanded under different culture conditions. Since confluency is subjective, cultures were expanded for irregular time periods between passages.

Assessing the sub-population profile CD34+, CD45+, CD73+, CD90+ and CD105+ across passages within individual cultures, very low passages demonstrated high expression, which decreases significantly between passages 2 and 4, suggesting that this sub-population could be haematopoietic in nature (Figure 4.15; Table 4.6.).

Differentiation

All cultures demonstrated the capacity to differentiate into adipogenic, osteogenic and chondrogenic lineages, therefore complying with the third requirement of characterization.

A validation was performed to determine the least number of photographs necessary to assess the population of cells present in a single well. The validation showed no difference between the selected groups and that semi quantification using 5 photographs was adequate. Despite the dramatic decrease in the number of photographs to be analysed, this method is cumbersome and not suitable for routine analysis.

A significant decrease in mean cell counts (DAPI stained nuclei) was observed within the adipogenic induced cultures in comparison with the respective non-induced controls. Since ASCs are a heterogeneous cell population containing different sub-populations, it could be hypothesized that the adipogenic induction medium only selects for a particular sub-population, within the ASC population, to remain adherent to plastic and differentiate. Further studies will be required to determine whether sub-populations differentiate into specified lineages.

Patient-specific factors and culture conditions were also identified that could influence the differentiation capacity of individual cultures. Very low cell counts were observed across the non-induced controls as well as the adipogenic and osteogenic induced cultures in patient culture A130411-02 10cc P6. This observation could be because the patient was 82 years of age and proliferative and differential capacities of the ASCs decreases with increasing age of the patient (Schipper *et al.*, 2008). A slight decrease in cell count was observed in the cryopreserved A100511-01 P10 F1 culture compared to the same culture that was not cryopreserved A100511-01 P4.

Semi-quantitative analysis of adipogenic differentiation was also performed by evaluating Oil Red O photographs. An interesting observation was made that not all adipogenic differentiation occurs at the same rate within the same and also between different cultures when considering the progression from preadipocytes to mature adipocytes. The majority of cultures showed a predominance of preadipocytes. Semi-quantification of Oil Red O stained cultures, considering only adipocytes that are fully occupied with lipid droplets or vacuoles, would have resulted in incorrect quantification results. In addition, qualitative assessment would have been affected in cultures with preadipocytes predominance as no visible Oil Red O would have been detected. We observed Oil Red O residue as well as non-specific staining and irregular uptake by various cells in the same culture due to different stages of adipogenic maturation. This method is not reliable for quantification and researchers should be careful to classify differentiation only by the presence of Oil Red O droplets.

The Alizarin Red S stain could only be used for qualitative analysis as it stains the calcium deposits within the mineral matrix secreted by the cellular layer below. Again we

observed variability among cultures which could be due to differences in differentiation or stain uptake.

Chondrogenic quantification was not possible, as the spherical culture had to be embedded and sectioned and cell counts would be inaccurate. Different methods should be explored to measure chondrogenic differentiation.

Differences between cryopreserved and non-cryopreserved ASC are an important factor to consider within the clinical setting and although this study was not designed to determine the difference, it can be suggested that cryopreservation plays a role (in decreasing) ASC differentiation capacity especially osteogenic differentiation ($P < 0.05$).

Limitations

The study was not without limitations. The first to note is that assessments were performed from healthy tissue only. Although this is necessary to establish baseline characteristics, this may not be the case in clinical practice as often patients who are not healthy will be the donors for their respective stem cell therapies. The study however did not have a sufficient number of samples from “unhealthy” patients to evaluate and compare and this therefore needs to be addressed in future research. In general, manual counting of cells is semi-quantitative and not accurate enough to quantify all aspects of ASC differentiation. Other techniques should rather be explored, for example flow cytometry or real time PCR.

Conclusion

The primary aim of this study was satisfied, characterizing ASCs according to the criteria described by Dominici *et al.*, 2006. In addition, sub-populations were identified and semi-quantification of adipogenesis were determined. This study provides a basic platform within our laboratory on which future research can be built.

References

- Alhadlaq A and Mao JJ. Mesenchymal stem cells: Isolation and Therapeutics. *Stem cells and Development*. 2004;13:436-448.
- Baptista LS, Do Amaral RJ, Carias RB, Aniceto M, Claudio-Da-Silva, C and Borojevic R. An alternative method for the isolation of mesenchymal stromal cells derived from lipoaspirate samples. *Cytotherapy*. 2009; 11:706-715.
- Bertolo A, Thiede T, Aebli N, Baur M, Ferguson SJ and Stoyanov JV. Human mesenchymal stem cell co-culture modulates the immunological properties of human intervertebral disc tissue fragments *in vitro*. *Eur Spine J*. Published online: 23 December 2010. DOI 10.1007/s00586-010-1662-9.
- Bieback K, Kern S, Klüter H and Eichler H. Critical parameters for the isolation of mesenchymal stem cells from umbilical cord blood. *Stem Cells* 2004;22:625-634.
- Bonab MM, Alimoghaddam K, Talebian F Ghaffari SH, Ghavamzadeh A, Nikbin B. Aging of mesenchymal stem cell *in vitro*. *BMC Cell Biology*. 2006;7:14:
- Bourin P, Bunnell BA, Casteilla L, Dominici M, Katz AJ, March KL, *et al*. Stromal cells from th adipose tissue-derived stromal vascular fraction and culture expanded adipose tissue-derived stromal/stem cell: a joint statement of the International Federation for Adipose Therapeutics and Science (IFATS) and the Internationsl Society for Cellular Therapy (ISCT). *Cytotherapy*. 2013;15:641-648.
- Boxall SA and Jones E. Markers for characterisation of bone marrow multipotential stromal cells. *Stem Cells International*. 2012;doi:10.1155/2012/975871.
- Bunnell BA, Flaatt M, Gagliardi C, Patel B and Ripoll C. Adipose-derived stem cells: Isolation, expansion and differentiation. *Methods*. 2008;45:115-120.
- Chow A, Lucas D, Hidalgo A, Mendez-Ferrer S, Hashimoto D, Scheiermann C, *et al*. Bone marrow CD169+ macrophages promote the retention of hematopoietic stem and progenitor cells in the mesenchymal stem cell niche. *The Journal of Experimental Medicine*. 2011;208:261-271.
- Christopher MJ, Rao M, Lui F, Woloszynek JR and Link DC. Expression of the G-CSF receptor in monocytic cells is sufficient to mediate hematopoietic progenitor mobilization by G-CSF in mice. *The Journal of Experimental Medicine*. 2011;208:251-260.
- Curran JM, Chen R and Hunt JA. The guidance of human mesenchymal stem cell differentiation *in vitro* by controlled modifications to the cell substrate. *Biomaterials*. 2006;27:4783-4793.
- D'ippolito G, Diabira S, Howard GA, Menei P, Roos BA and Schiller PC. Marrow-isolated adult multilineage inducible (MIAMI) cells, a unique population of postnatal young and old human cells with extensive expansion and differentiation potential. *Journal of Cell Science*. 2004;117:2971-2981.
- Dominici M, Le Blanc K, Mueller I, Slaper-Cortenbach I, Marini FC, Krause DS, *et al*. Minimal criteria for defining multipotentmesenchymal stromal cells. The International Society for Cellular Therapy position statement. *Cytotherapy* 2006;8;4:315-317.
- Farrell E, Wielopolski P, Pavljasevic P, Van Tiel S, Jahr H, Verhaar J, *et al*. Effects of iron oxide incorporation for long term cell tracking on MSC differentiation *in vitro* and *in vivo*. *Biochemical and Biophysical Research Communications*. 2008;369:1076-1081.
- Francis M P, Sachs PC, Elmore LW and Holt S. E. Isolating adipose-derived mesenchymal stem cells from lipoaspirate blood and saline fraction. *Organogenesis*. 2010;6:11-14.
- Igura K, Zhang X, Takahashi K, Mitsuru A, Yamaguchi S and Takahashi TA. Isolation and characterization of mesenchymal progenitor cells from chorionic villi of human placenta. *Cytotherapy*. 2004;6:543-553.
- Kang SK, Putman LA, Ylostalo J, Popescu IR, Dufour J, Belousov A, *et al*. Neurogenesis of rhesus adipose stromal cells. *Journal of Cell Science*. 2004;117:4289-4299.
- Kasten P, Beyen I, Egermann M, Suda AJ, Moghaddam AA, Zimmermann G, *et al*. Instant stem cell therapy: characterization and concentration of human mesenchymal stem cells *in vitro*. *European Cells and Materials*. 2008;16:47-55.

- Kedong S, Xiubo F, Tianqing L, Macedo HM, LiLi J, Meiyun F, *et al.* Simultaneous expansion and harvest of hematopoietic stem cells and mesenchymal stem cells derived from umbilical cord blood. *Journal of Materials Science: Materials in Medicine*. 2010;21:3183-3193.
- Kern S, Eichler H, Stoeve J, Klüter and Bieback K. Comparative analysis of mesenchymal stem cells from bone marrow, umbilical cord blood and adipose tissue. *Stem Cells*. 2006;24:1294-1301.
- Kiel MJ, Yilmaz OH, Iwashita T, Yilmaz OH, Terhost C and Morrison SJ. SLAM family receptors distinguish hematopoietic stem and progenitor cells and reveal endothelial niches for stem cells. *Cell*. 2005;121:1109-1121.
- Kingham PJ, Kalbermatten DF, Mahay D, Armstrong SJ, Wiberg M and Terenghi G. Adipose-derived stem cells differentiate into a Schwann cell phenotype and promote neurite outgrowth *in vitro*. *Experimental Neurology*. 2007;207:267-274.
- Le Blanc K, Tammik C, Rosendahl K, Zetterberg E and Ringdèn O. HLA expression and immunologic properties of differentiated and undifferentiated mesenchymal stem cells. *Experimental Hematology*. 2003;31:890-896.
- Lee RH, Kim B, Choi I, Kim H, Choi HS, Suh KT, *et al.* Characterization and expression analysis of mesenchymal stem cells from human bone marrow and adipose tissue. *Cellular Physiology Biochemistry*. 2004;14:311-324.
- Li W-J, Tuli R, Huang X, Laquerriere P and Tuan RS. Multilineage differentiation of human mesenchymal stem cells in a three-dimensional nanofibrous scaffold. *Biomaterials*. 2005;26:5158-5166.
- Lin CS, Ning H, Lin G and Lue TF. Is CD34 truly a negative marker for mesenchymal stromal cells? *Cytotherapy*. 2012;14:1159-1163.
- Liu TM, Martina M, Hutmacher DW, Hui JHP, Lee EH and Lim B. Identification of Common Pathways Mediating Differentiation of Bone Marrow- and Adipose Tissue-Derived Human Mesenchymal Stem Cells into Three Mesenchymal Lineages. *Stem Cells*. 2007;25:750-760.
- Lu LL, Liu YJ, Yang SG, Zhao QJ, Wang X, Gong W, *et al.* Isolation and characterization of human umbilical cord mesenchymal stem cells with hematopoiesis-supportive function and other potentials. *Haematologica*. 2006;91:1017-1026.
- Lund P, Pilgaard L, Duroux M, Fink T and Zachar V. Effect of growth media and serum replacements on the proliferation and differentiation of adipose-derived stem cells. *Cytotherapy*. 2009;11(2):189-197.
- Meuleman N, Tondreau T, Delforge A, Dejeneffe M, Massy M, Libertalis M, *et al.* Human marrow mesenchymal stem cell culture: serum-free medium allows better expansion than classical α -MEM medium. *European Journal of Haematology*. 2006;76:309-316.
- Mitchell JB, McIntosh K, Zvonic S, Garrett S, Floyd ZE, Kloster A, *et al.* Immunophenotype of human adipose-derived cells: Temporal changes in stromal-associated and stem cell-associated markers. *Stem Cells*. 2006;24:376-385.
- Oedayrajsingh Varma MJ, Breuls GM, Schouten TE, Jurgens WJFM, Bontkes HJ, Schuurhuis GJ, *et al.* Phenotypical and functional characterization of freshly isolated adipose tissue-derived stem cells. *Stem Cells and Development*. 2007;16:91-104.
- Pittenger MF, Mackay AM, Beck SC, Jaiswal RK, Douglas R, Mosca JD, *et al.* Multilineage potential of adult human mesenchymal stem cells. *Science*. 1999;284:5411:143-147.
- Pittinger MF, U.S. Patent 5 827 740 (1998).
- Rada T, Reis RL and Gomes ME. Distinct stem cells sub-populations isolated from human adipose tissue exhibit different chondrogenic and osteogenic differentiation potential. *Stem Cell Reviews and Reports*. 2011;7:64-76.
- Reger RL, Tucker AH and Wolfe MR. Differentiation and characterization of human MSCs. IN Prockop, D. J., Phinney, D. G. & Bunnell, B. A. (Eds.) *Mesenchymal Stem Cells: Methods and Protocols*. Totowa, NJ, Humana Press. 2008

- Reynold ES. The use of lead citrate at high pH as an electron opaque stain in electron microscopy. *Journal of Cell Biology*. 1963;38:87-93.
- Sasaki M, Abe R, Fujita Y ando S, Inokuma D and Shimizu H. Mesenchymal stem cells are recruited into wounded skin and contribute to wound repair by transdifferentiation into multiple skin cell type. *The Journal of Immunology*. 2008;180:2581-2587.
- Schipper BM, Marra KG, Zhang W, Donnenberg AD and Rubin JP. Regional Anatomic and age effects on cell function of human adipose derived stem cells. *Northeastern Society of Plastic Surgeons*. 2008;60;5:538-544.
- Seo MJ, Suh SY, Bae YC and Jung JS. Differentiation of human adipose stromal cells into hepatic lineage *in vitro* and *in vivo*. *Biochemical and Biophysical Research Communications*. 2005;328:258-264.
- Shetty P, Cooper K and Viswanathan C. Comparison of proliferative and multilineage potentials of cord matrix, cord blood and bone marrow mesenchymal stem cells. *Asian Journal of Transfusion Science*. 2010;4:14-24.
- Si Y-L, Zhao Y-L, Hao H-J, Fu X-B and Han W-D. MSCs: Biological characteristics, clinical applications and their outstanding concerns. *Ageing Research Reviews*. 2010;10;1:93-103.
- Sotiropoulou PA, Perez SA, Salagianni M, Baxevanis CN and Papamichail M. Characterization of the optimal culture conditions for clinical scale production of human mesenchymal stem cells. *Stem Cells*. 2006;24:462-471. <http://stemcell.ibme.utoronto.ca/protocols>
- Timper K, Seboek D, Eberhart M, Linscheid P, Christ-Crain M, Keller U, *et al*. Human adipose tissue-derived mesenchymal stem cells differentiate into insulin, somatostatin, and glucagon expressing cells. *Biochemical and Biophysical Research Communications*. 2006;341:1135-1140.
- Trottier V, Marceau-Fortier G, Germain L, Vincent C and Fradette J. IFATS collection: using human adipose-derived stem/stromal cells for the production of new skin substitutes. *Stem Cells*. 2008;26:2713-2723.
- Vieira NM, Zucconi E, Bueno CR Jr., Secco M, Suzuki MF, Bartolini P, *et al*. Human multipotent mesenchymal stromal cells from distinct sources show different *in vivo* potential to differentiate into muscle cells when injected in dystrophic mice. *Stem Cell Reviews and Reports*. 2010;6:560-566.
- Wagers AJ. The stem cell niche in regenerative medicine. *Cell Stem Cell*. 2012;10:362-369.
- Wagner W, Wein F, Seckinger A, Frankhauser M, Wirkner U, Krause U, *et al*. Comparative characteristics of mesenchymal stem cells from human bone marrow, adipose tissue and umbilical cord blood. *Experimental Hematology*. 2005;33:1402-1416.
- Wang LD and Wagers AJ. Dynamic niches in the origination and differentiation of hematopoietic stem cells. *Nature Reviews. Molecular Cell Biology*. 2011;12:643-655.
- Waterman RS, Tomchuck SL, Henkle SL, Betancourt AM. A new mesenchymal stem cell paradigm: Polarization into a pro-inflammatory MSC1 or an immunosuppressive MSC2 phenotype. *Plos One*. 2010;5(4):e10088
- Xu Y, Liu L, Li Y, Zhou C, Xiong F, Liu Z, *et al*. Myelin forming ability of Schwann cell-like cells induced from rat adipose-derived stem-cells *in vitro*. *Brain Research* 2008;1239:49-55.
- Yoshimura K, Shigeura T, Matsumoto D, Sato T, Takaki Y, Aiba-Kojima E, *et al*. Characterization of freshly isolated and cultured cells derived from the fatty and fluid portions of liposuction aspirates. *Journal of Cellular Physiology*. 2006;208:64-76.
- Zuk P (2013). The ASC: Critical Participants in Paracrine-Mediated Tissue Health and Function, Regenerative Medicine and Tissue Engineering, Prof. Jose A. Andrades (Ed.), ISBN: 978-953-51-1108-5, InTech, DOI: 10.5772/55545. Available from: <http://www.intechopen.com/books/regenerative-medicine-and-tissue-engineering/the-asc-critical-participants-in-paracrine-mediated-tissue-health-and-function>
- Zuk PA, Zhu M, Ashjian P, De Ugarte DA, Huang JI, Mizuno H, *et al*. Human adipose tissue is a source of multipotent stem cells. *Molecular Biology of the Cell*. 2002;13:4279-4295.
- Zuk PA, Zhu M, Mizuno H, Huang JI, Futrell JW, Katz AJ, *et al*. Multilineage cells from human adipose tissue: implications for cell-based therapies. *Tissue Engineering*. 2001;7:211-228.

- **Zuk PA. The adipose-derived stem cell: Looking back and looking ahead. *Molecular Biology of the Cell*. 2010;21:1783-1787.**



Immunophenotypic characterisation and differentiation capacity of human adipose derived mesenchymal stromal cells transduced with lentiviral vectors expressing GFP

*Before the wound do grow uncurable;
For, being green, there is great hope of help.*

Shakespeare W, *Henry IV, Part II*(1597), Act VI, Scene 2, line 1571-1572.

Introduction

Gene therapy is based on the insertion of functional genes in the form of nucleic acids to modify the genetic material in living cells to achieve therapeutic effects or to enable delivery of therapeutic agents (Sikorski and Peters, 1997).

Conventional retroviral vectors derived from oncoretroviruses such as Moloney murine leukemia virus, displayed limitations in transduction. Poor efficacy of gene transfer was observed within target cells due to the inability of these vectors to integrate into the

genome of non-dividing cells (Amado and Chen, 1999). Although the vectors could enter these non-dividing target cells, integration was inhibited by the failure to breakdown the nuclear membrane.

Lentiviral vectors are a highly attractive gene delivery system with the unique ability to enable integration of genetic cargo into the chromosome of a target cell. This allows for the delivery of most cDNAs while minimizing the risk of the vector-transduced cells being attacked by virus-specific cytotoxic T lymphocytes. This is accomplished by not transferring sequences encoding for proteins derived from the packaging virus (Salmon and Trono, 2006).

HIV-1 based lentiviral vectors

Lentiviruses, such as the human immunodeficiency virus (HIV), are a subgroup of retroviruses that can infect both dividing as well as non-dividing cells. Infectious lentiviruses have complex genomes which include structural (*env* and *gag*) and enzymatic genes (*pol*), regulatory genes (*tat* and *rev*) and accessory genes (*vpr*, *vif*, *vpu* and *nef*). The assembly of an RNA genome that carries *cis*-acting sequences necessary for packaging, reverse transcription and nuclear translocation and integration as well as structural and enzymatic proteins leads to the budding of the virion from producer cell membrane.

A pre-integration complex composed of the enzyme integrase and a matrix protein, which is encoded by the *vpr* and the *gag* gene respectively, can traverse intact nuclear membranes of non-dividing target cells. After the contents of the lentiviral vector are released into the cytoplasm of the target cell, the localization sequence on the matrix protein is recognised by the nuclear import machinery, which docks the respective pre-integration complex at a nuclear membrane pore allowing the pre-integration complex to navigate and pass through the nuclear pore into the nucleus (Amado and Chen, 1999; Bukrinsky *et al.*, 1993).

Lentiviral vectors need a host cell to transcribe their viral RNA into DNA. The host cell would therefore have to be at least in the G_{1b} stage of the cell cycle during which RNA synthesis takes place. If the host cell is truly in a quiescent (G₀) state, lentiviruses can be harboured within the host cell for a period of time, due to a blockage at the reverse transcription step producing partially reverse transcribed lentiviral DNA. This latency can be reversed with stimulation of the host cell to enter into the mitotic cell cycle (Korin and Zack, 1998; Zack *et al.*, 1990).

A three plasmid expression system of HIV-1 based lentiviral vectors

It is mandatory to avoid the formation of replication competent recombinants (RCRs) when producing lentiviral vector stock. The HIV-1 virus in its pathogenic state contains nine genes, encoding for various virulence factors. Without altering the gene-transfer ability, six genes can be deleted to form a HIV-derived vector system that also prevents

the parental virus from reconstituting (Salmon and Trono, 2006). Biosafety measures of vector production demand the distribution of the sequences, encoding for various components, over at least three independent plasmid units. To produce a replication-competent viral entity, the three plasmid units would have to undergo multiple recombinant events within every unit. Distribution of the cis-acting elements over independent units maximizes the number of recombinant events required, thereby ensuring the production of replication-defective viruses.

The transfer vector plasmid

The transfer vector plasmid contains the therapeutic and/or reporter gene cis-acting genetic sequences (*e.g.* GFP) as well as restriction sequences for the insertion of the therapeutic genes into the host cell DNA (Naldini *et al.*, 1996).

The packaging plasmid

The packaging system of the first generation HIV-1 derived vectors that were developed contained all the core proteins, enzymes, transcriptional and accessory factors, except the *env* gene. The second generation contained a reduced HIV-packaging system and were mainly comprised of *gag*, *pol*, *tat* and *rev* genes encoding for structural, enzymatic, transcriptional and post-transcriptional functions respectively (Zufferey *et al.*, 1998). The third generation uses a chimeric 5' long terminal repeat to ensure transcription in the absence of the *tat* HIV transactivator. Removing the *tat* gene from the packaging plasmid eliminates the essential virulence factor which could contribute to possible RCRs. This 5' chimera was constructed by replacing the U3 (promotor) region of the 5' long terminal repeat with a U3 sequence isolated from either a cytomegalovirus or a Rous sarcoma virus (Amado and Chen, 1999; Dull *et al.*, 1998; Salmon and Trono, 2006). To render the vector self-inactivating the viral promotor in the U3 region 3' long terminal repeat was removed to render it replication defective.

The envelope plasmid

The envelope protein is responsible for mediating viral particle entry into the target cell. The HIV-1gp120 protein recognises the CD4 target cell receptor in combination with either CCR5 or CXCR4 co-receptors. Since the phospholipid receptor for the G glycoprotein of the vesicular stomatitis virus (VSV-G) is ubiquitously expressed on most mammalian cell surfaces, the HIV-1 receptor-binding protein could be substituted. This virion pseudotyping that alters the tropism of the lentiviral particles is also highly stable, allowing for vector particle concentration by ultracentrifugation (Dull *et al.*, 1998; Naldini *et al.*, 1996; Salmon and Trono, 2006).

Vector particles are produced by co-transfecting the producer cells (293T cells) with the three different plasmid constructs. The proteins expressed from the envelope, packaging and transfer plasmids within the producer cells assemble the vector particles (Dull *et al.*, 1998). The vector particles stably transduce target cells and localize to the host cell

nucleus where vector RNA is reverse transcribed into DNA which randomly integrates into the host cell genome. The transcribed mRNA locates to the cytoplasm where it is translated into protein. Expression of the reporter protein GFP indicates that the target cell was successfully transduced.

The longterm goal of clinical translation of cell-based therapy require both preclinical safety and efficacy to be demonstrated in animal models. This motivated the optimization of a practical *in vivo* tracking system for MSCs. The aim of this comparative study was to investigate the effects of GFP⁺ lentiviral vectors on phenotypic cell surface marker expression and differentiation capacity in transduced adipose derived stromal cells (ASCs).

Material and Methods

The production of GFP positive (GFP⁺) lentivirus vectors and the transduction of MSCs were adapted from the procedures described by Salmon and Trono in 2006.

Plasmids were co-transfected into human embryonic kidney 293T cell line (293T cells) to produce lentiviruses that are capable of transducing the GFP gene. The plasmids included psPAX2 with the function of enveloping, pMD2G for the purpose of packaging and pLVTH as the GFP gene transfer vector plasmid.

Co-transfection of plasmids in 293T cells for the production of GFP lentiviruses

The lentiviral vector stock was prepared at least one week prior to co-transfection of the 293T cells. The three plasmids pLVTH, psPAX2 and pMD2g, used in the production of lentiviral vectors, were obtained from Prof. Marco Weinberg (University of the Witwatersrand). The lentiviral vector stock was obtained through heat shock transformation of DH5 α bacteria and subsequent extraction from the cells using the Zippy plasmid Maxiprep Kit (Zymo research; D4028). The extracted plasmids were concentrated to 1 μ g/ μ l and stored in Eppendorf tubes at -20°C.

At least three cell culture dishes (100 mm diameter) were seeded with HEK 293T cells at 1-3 million cells per dish with 10 ml Dulbecco's Modified Eagle Medium (DMEM) supplemented with 10% fetal bovine serum (FBS) and 1% penicillin and streptomycin (pen/strep). The cells were left to incubate for 12hrs at 37°C and 5% CO₂.

The Eppendorf tubes containing pLVTH, pMD2G and psPAX2 plasmids were thawed on ice in a laminar flow hood and tapped individually to mix and homogenize the plasmids. The required amount of filter sterilized (0.22 μ m nitrocellulose filter, Millipore) double distilled H₂O (ddH₂O) containing 2.5mM Hepes and plasmids were added together. The respective substances were added in chronological order, from the highest amount to the

lowest amount as described below in Table 5.1. This process was repeated six times to produce 6 tubes containing the respective plasmids and Hepes solution.

Table 5.1. Adding substances together in a specific chronological order in 1 ml Eppendorfs.

Substances added	Amount of substance added (µl)	Chronological order of addition
ddH ₂ O and Hepes (2.5mM)	229 µl	1 st
Transfer plasmid: pLVTH	10 µl	2 nd
Packaging plasmid: psPAX2	8 µl	3 rd
Envelope plasmid: pMD2G	4 µl	4 th
Total Eppendorf volume	250 µl	

Thawed 0.5M CaCl₂ solution was filter sterilized (0.22µm nitrocellulose filter, Millipore) and vortexed lightly before 250 µl was added to the Eppendorf tube, containing the plasmids, ddH₂O and Hepes solution. The tube was again vortexed lightly to ensure all substances were well mixed and homogenous.

A 1000 µl pipette was used to transfer the total volume (500 µl) from the Eppendorf tube into a 15 ml tube, containing 500 µl Hepes-buffered saline 2x (HeBS2x). The 15 ml tubes, containing 500 µl Hepes-buffered saline 2x (HeBS2x) were vortexed lightly while the Eppendorf contents were added drop wise. The 15 ml tubes were incubated in the flow hood at room temperature for 30 min before the total contents of one 15 ml tube were transferred drop wise to a 293T cell culture (seeded 12 hrs in advance, as described above), already containing 10 ml DMEM (10%FBS and 1% pen/strep). The culture was mixed gently forward and backwards, as well as side to side on a horizontal plane to ensure equal distribution of the respective 1 ml contents across the whole culture. This process was repeated in six separate dishes.

After the culture was incubated for 12hrs at 37°C and 5 % CO₂, the conditioned medium was aspirated and the cultures were washed once with phosphate saline buffer (PBS) supplemented with 1% pen/strep, to remove non-adherent cells or cell debris. 15 ml of fresh DMEM (10%FBS and 1% pen/strep) was added and the cultures were incubated for 24 hrs at 37°C and 5 % CO₂.

The next day the 15 ml conditioned medium or supernatant, containing the lentiviral stock was harvested from the cultures. The first harvest pool was placed into 50 ml tubes and stored at 4°C. Before the cultures were incubated again for 24 hrs at 37°C and 5 % CO₂, 15ml fresh DMEM (10% FBS and 1% pen/strep) was very gently introduced. The next day the second supernatant pool was harvested and pooled with the first.

The pooled supernatant was then centrifuged for 10 min at 2500 rpm, to produce a pellet consisting of cells and debris. The supernatant was then decanted into a 50 ml syringe and filtered (0.45 µm, Milipore) and the pellet discarded. The filtered supernatant was

alliquotted into Beckman Konical Tubes (10 ml) and then subjected to ultra-centrifugation for 120 min at 26 000 rpm (49 460 *g*) and 16°C.

The supernatant was then gently aspirated so as not to disturb the delicate pellet and 80 µl HANKS Ca₂+Mg₂⁺ (HBS) per tube was used to quickly resuspend the pellet before it dried out. The vector stock/HBS solution was vortexed gently every 30 min while incubated within the flow hood at room temperature for 2 hrs. The vector stock from all the tubes was pooled to produce a homogenous vector stock solution and stored at -80 °C until used. Freezing and thawing cycles of the lentiviral stock was avoided, as the lentiviral titer would potentially decrease.

Optimization of ASC transduction by the GFP lentivirus vector

A GFP lentiviral titration study was performed to optimize GFP⁺ lentiviral stock concentration that was used to transduce > 80% of the cells within the ASC population.

After an ASC culture demonstrated >95% adherence to the recommended immunophenotypical threshold (See Chapter 3), two 6 well plates were seeded at a density of 5 x 10³ cells per cm² and incubated for 12 hrs at 37°C and 5 % CO₂.

The total vector stock needed for the respective experiment was thawed under the laminar flowhood at room temperature to avoid effects of excessive thawing and freezing. The 6 well plates were retrieved from the incubator and the vector stock solution was tapped to mix and homogenize. Varying amounts of vector stock were added to the wells containing adherent ASCs and 2 ml DMEM, supplemented with 1% pen/strep and 10% FBS (Table 5.2.). One of the two non-transduced wells (control) received 150 µl sterile phosphate buffered saline (PBS).

Table 5. 2. Volume of vector stock added to a 9.6 cm² ASC culture. The ASCs were seeded at 5x10³ cells/cm² 12 hrs prior to transduction.

Amount vector stock (µl) per well	Mean % gated ASCs expressing GFP
0 µl but received 150 µl PBS	0.90
0 µl	0.61
5 µl	2.71
25 µl	8.41
50 µl	5.25
100 µl	11.32
150 µl	56.93
200 µl	56.20
250 µl	74.85
300 µl	75.73

To ensure homogeneity of vector stock exposure across a well, the 6 well plates were not mixed in a circular motion, but side-to-side and forward-and-backwards on a horizontal

plane. The 6 well plates were maintained at 37°C and 5 % CO₂ and the DMEM (1% pen/strep and 10% FBS) was replaced every 48 hrs, until sub-confluence (between 80-90% confluence) was reached.

The respective cultures were passaged as described in Chapter 3. In short, the conditioned medium was aspirated and cultures washed with PBS (2% pen/strep). The cultures were trypsinized with 2 ml 0.25% Trypsin/EDTA (Gibco, Cat# 25200072) for 20 min. The enzymatic activity was halted with 2 ml DMEM (1% pen/strep and 10% FBS) and the cell suspension was centrifuged at 1200 rpm, for 5 min and at a temperature of 21°C. After aspirating the supernatant, the pellet was re-suspended in 1ml PBS (2% pen/strep). A 100 µl from every culture was used at every passage to analyse GFP expression and to determine the cell count using flow cytometry. The remaining cell suspension was used to reseed the culture at a density of 5x10³ cell per cm². The number of cells expressing GFP was measured for all the titration cultures over 10 passages.

The individual ASC cultures used in this study were first characterised according to the recommended criteria set out in Dominici *et al.*, 2006 and adherence to the criteria was demonstrated in Chapter 4.

The three individual ASC cultures were each seeded separately into 2 wells of a 6 well plate (surface area per well 9.6 cm²) containing 2ml DMEM (1% pen/strep and 10% FBS) at a seeding density of 5x10³ cells per cm² and incubated for 12 hrs at 37°C and 5 % CO₂. The remainder of the lentiviral stock solution was thawed and tapped to mix and homogenize the solution. The titration experiment demonstrated an efficient and stable GFP expression within cultures transduced with a volume of 300 µl viral stock solution. Using this volume the lentiviral stock solution was introduced into one of the two wells seeded per individual ASC culture (Figure 5.1.). The other well received 300 µl of PBS, which acted as a control group to the transduced culture (Figure 5.1.). These cultures were maintained at 37°C and 5 % CO₂ and DMEM (1% pen/strep and 10% FBS) was replaced every 48 hrs.

The non-transduced and the transduced cells for every respective individual ASC culture were treated exactly the same for all purposes, maintained at similar conditions and passaged at the same time. To identify transduced and non-transduced cultures, a 'GFP' or 'C' was added to the individual culture code, for example GFPA100511-01 and CA100511-01 (Figure 5.2.). Furthermore, The 'P' followed by a number and the 'T' followed by a number, represents the passage number of the individual culture and the passage number after transduction with lentiviral vectors, respectively.

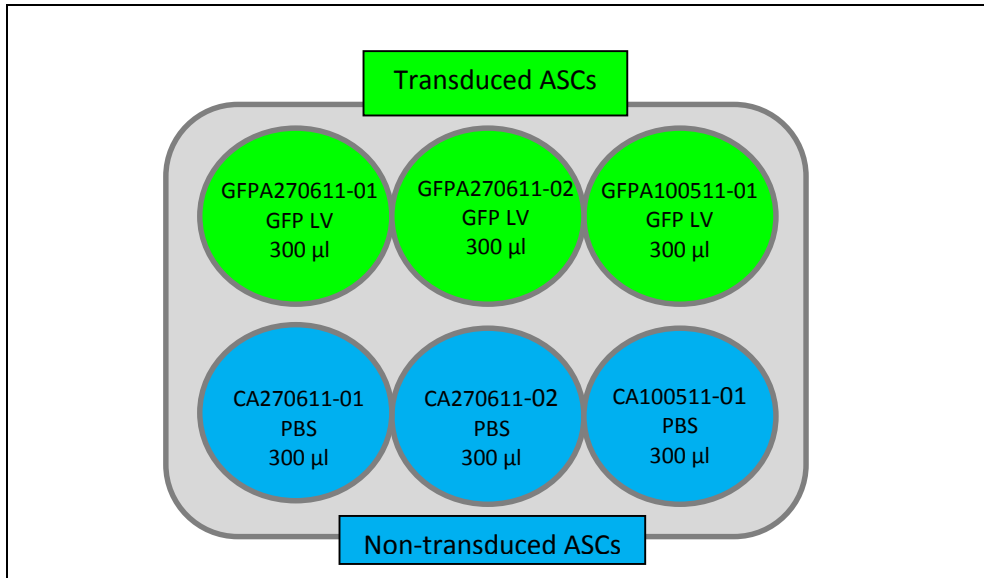


Figure 5.1. Representative 6 well plate indicating transduced (green) and non-transduced (blue) cultures within the three individual ASC cultures (A270611-01; A270611-02; A100511-01). The transduced cultures received 300 µl lentiviral stock solution (LV) and the non-transduced cultures received 300 µl PBS acting as the control group. The transduced cultures code was GFPA270611-01 and the non-transduced culture code was CA270611-01.

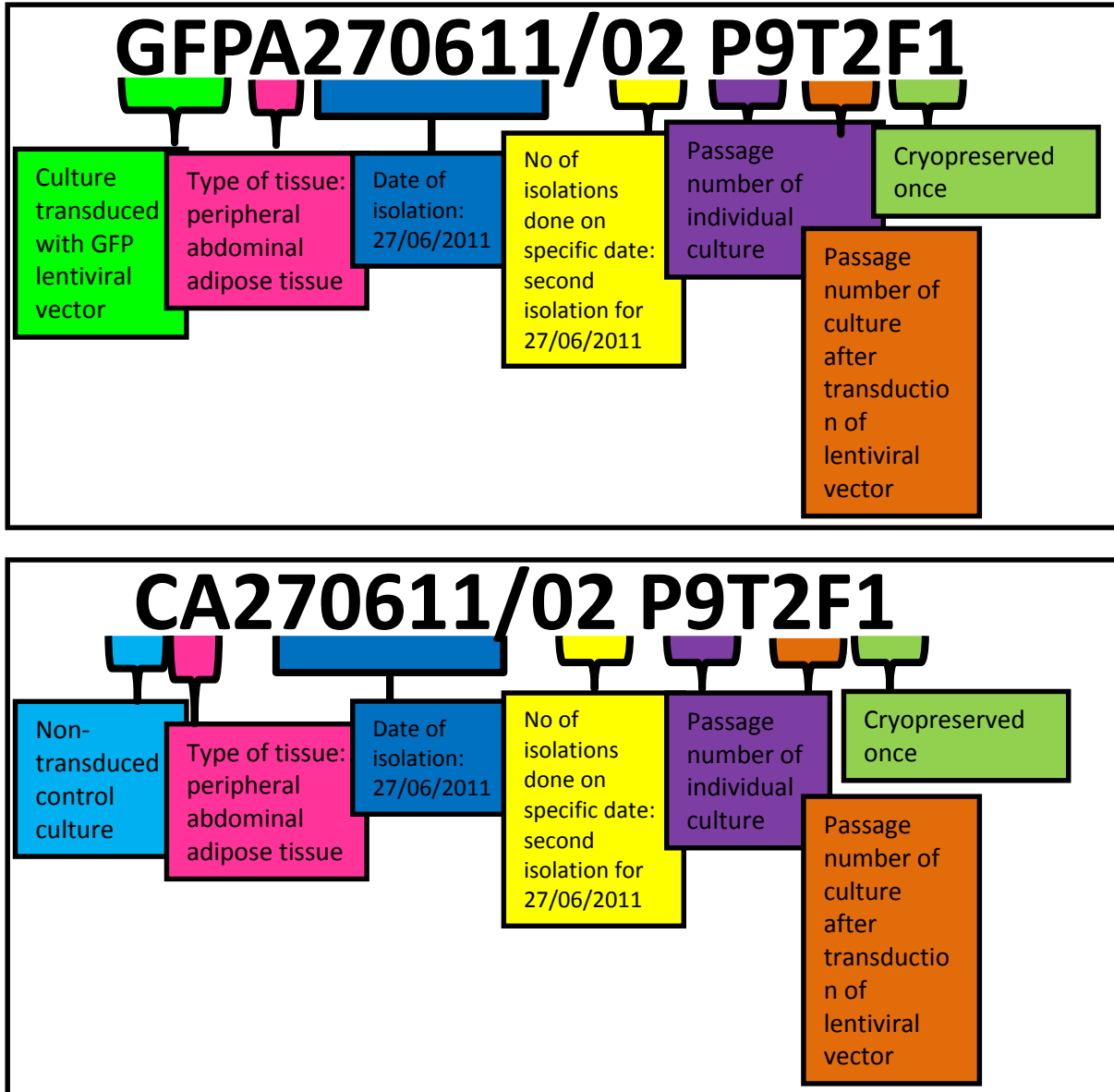


Figure 5.2. Codifications used within study. Transduced cultures received a prefix of 'GFP' and the corresponding control cultures a 'C'.

During the passaging process, cell counts were performed to determine the densities of the respective cell suspensions for the purpose of reseeding the cultures for expansion, as described in Chapter 3 (Figure 3.32 and Figure 3.33).

Immunophenotype characterization of transduced ASCs

The immunophenotype was compared between non-transduced and transduced ASCs, using flow cytometry.

The transduced and non-transduced cells from an individual ASC culture were trypsinized from the expansion surface and resuspended in PBS respectively. A 100 µl from both cell suspensions was used to stain with an antibody panel (Table 5.3.). Another

100 µl from the non-transduced cell suspension was used as the unstained, GFP negative control. The cell suspensions were incubated in the dark at room temperature for 10 min before washing the suspensions three times, with PBS supplemented with 10% FBS and 1% pen/strep, to prevent non-specific binding of antibodies.

The immunophenotype measured with antibody panel 1 was problematic, as CD73 FITC and GFP expression were both measured within the same fluorescence detection channel (FL 1). These results were slightly inaccurate and the immunophenotypic characterization experiments were repeated using antibody panel 2 (Table 5.3.).

Table 5.3. The two different antibody panels as well as the fluorescence channels used for detection on the flow cytometer used throughout the study.

Antibody Panel 1		Antibody Panel 2	
Antibody with fluorochrome	Detector channel	Antibody with fluorochrome	Detector channel
GFP	FL 1	GFP	FL1
CD 34 ECD	FL 3	CD 34 PC 7	FL 5
CD 45 PC 7	FL 5	CD 45 KO	FL 10
CD 73 Fit C	FL 1	CD 73 BV	FL 9
CD90 PC 5	FL 4	CD90 PC 5	FL 4
CD 105 PE	FL 2	CD 105 PE	FL 2

Since the cell count measurement was performed on unstained ASCs, the GFP positive population was clearly visible within the FL 1 channel. The GFP positive ASC population could be determined as a percentage of the gated cell population in the forward and side scatter plot.

The transduced and non-transduced cultures were placed in cryopreservation for 6 months. The cultures were thawed on ice and seeded again at a density of 5×10^3 cells/cm². The cultures were expanded and immunophenotyped using antibody panel 2.

Tri lineage differentiation

All three transduced and non-transduced cultures were differentiated into the adipogenic, osteogenic as well as the chondrogenic lineages as previously described (See Chapter 4).

Quantification and assessment of differentiation

The adipogenic induced and non-induced cultures were fixed on day 7, 14 and 21 of induction. During the assessment of transduced adipogenic and osteogenic cultures, DAPI staining was performed as described in Chapter 4. Photographs of the same vision fields were taken as described in Chapter 4 except for additional GFP with the green filter. These photographs were then superimposed on one another using Photoshop Light room

software (photoshop.com). Differentiation assessments were further performed as described in Chapter 4.

Statistical analysis

Analysis of variance (ANOVA) was used to assess the difference in the differentiation capacity between three cultures both transduced vs. non-transduced from three different transfections over three different time points. An F-value of >1 together with a P-value of <0.05 was considered statistically significant.

Firstly, the mean cell counts for all the controls, adipogenic and osteogenic induced cultures in both transduced vs. non-transduced groups were compared independently for significance.

Secondly, the control groups between the non-transduced and transduced cultures were compared at every week to ensure that the two groups were well balanced prior to induction for differentiation. This was followed by assessing differences between adipogenic and osteogenic differentiation across all three time points (week 1 – 3). The means of all the cultures over all three weeks were compared.

Lastly, the mean cell counts for every transduction were compared (3 cultures) and also the transductions over the end point (21 days) using the unpaired students' T test.

Results

A titration study was performed to determine the amount of vector stock solution needed to transduce the maximum number of cells within the heterogeneous ASC cell population (Figure 5.3.). A slight increasing trend was observed across all post-transduced passages using 150, 200, 250 and 300 μl (Figure 5.3). Although both 250 μl and 300 μl transduced similar percentages of cells within the gated ASCs population, the 300 μl volume established a more stable increase in expression across passages. The 250 μl demonstrated a 22% decrease in cells expressing GFP between post-transduction passage one and two and a 17% increase between 7 and 10. Little variation (72-81%) in the amount of cells expressing GFP was observed within the 300 μl volume, suggesting to be a better option for further experiments.

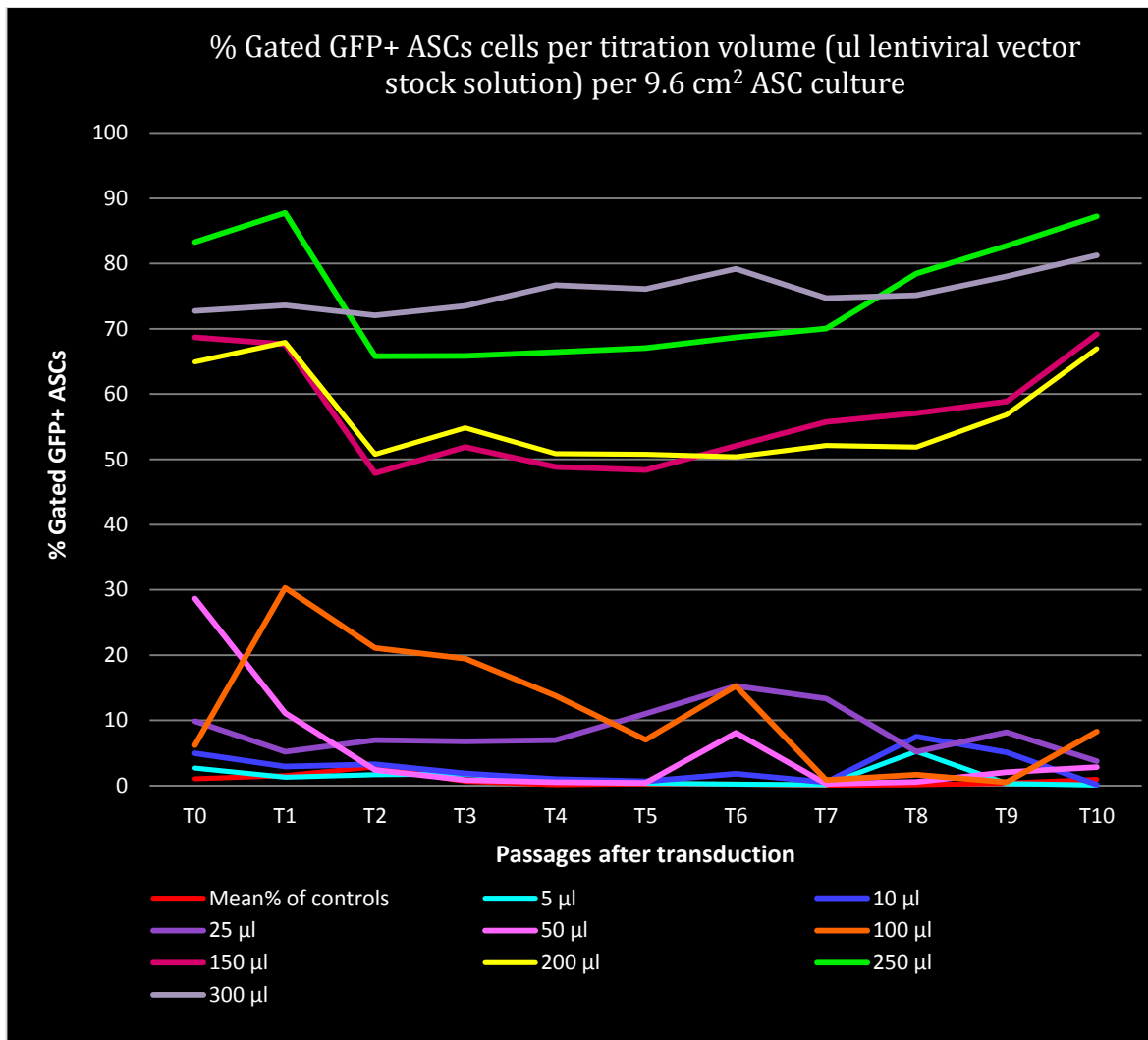


Figure 5.3. Percentage of ASCs transduced with different lentiviral vector titrations, indicated by GFP positive expression, measured over ten passages using flow cytometry. A transition phase is visible between passages 1 and 5 with a slight decrease in percentage GFP positive cells. After passage 5, the percentage positive cells steadily increased.

Transduction on 3 biological replicates were performed with 300 µl lentiviral stock solution. The GFP expression within the transduced cultures was monitored across all post-transduction passages (Figure 5.4.). The percentage of cells expressing GFP within the population gated on the side and forward scatter plot within the transduced cultures was monitored across all post-transduction passages for the three biological replicates. A stable percentage of GFP expressing cells, between 72- 96 %, within the transduced cultures were observed over 12 post-transduction passages.

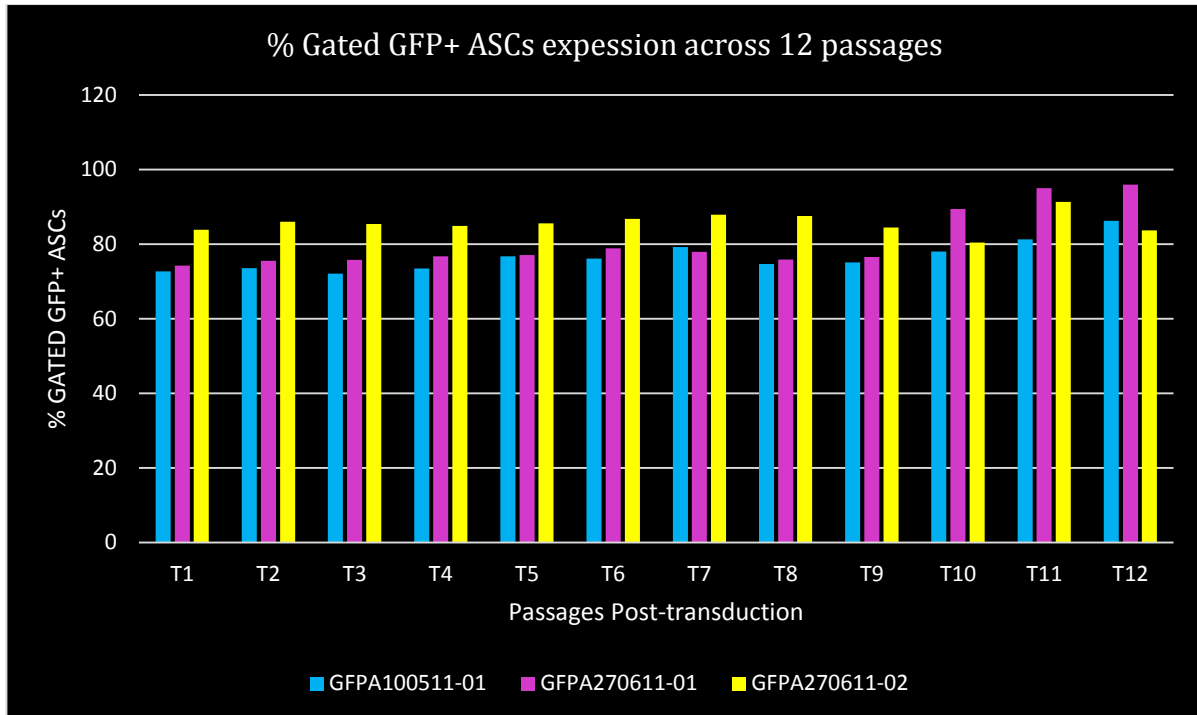


Figure 5.4. Percentage cells expressing GFP within transduced cultures (GFPA100511-01; GFPA270611-01; GFPA270611-02) across 12 passages represented by ‘T’ (passage after transduction was performed).

Immunophenotypic characterisation

The immunophenotypic characterization of the transduced and non-transduced cultures was determined and compared using antibody panel 1. The CD73 FITC antibody as well as GFP expression within transduced cultures were measured within the FL1 detector channel CD73 FITC. Evaluating the overlaying plots shows that both GFP positive and negative cells express CD73 (Figure 5.5.). The GFP positive cells not expressing CD73 are obscured within the transduced FL1 plots. In addition, GFP positive and GFP negative cell populations within the transduced cultures could not be separated for expression analysis. Although the CD73 marker was seen to be a very stable positive marker, the transduced with respective non-transduced controls were thawed and re-characterized immunophenotypically using antibody panel 2.

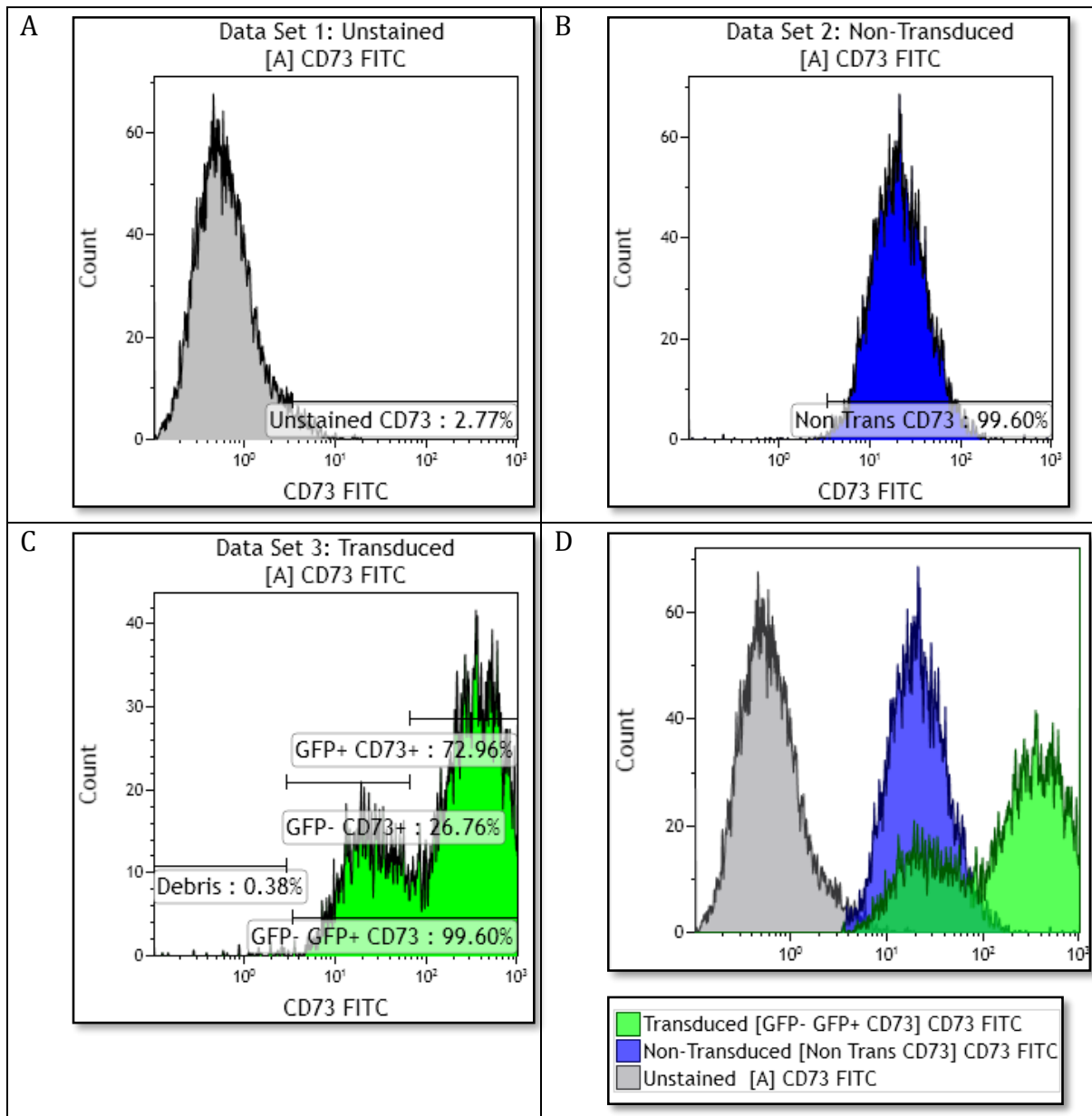


Figure 5.5. Three individual cell population expression histograms (A) unstained non-transduced control sample, indicated a true negative expression for both CD73 and GFP; (B) a CD73 FITC stained, non-transduced sample indicating a positive CD73 expression; (C) a CD73 stained transduced sample indicating two different cell populations, GFP+ and CD73+, as well as GFP- and CD73+. In the overlaying plot (D) all histograms (A-C) were superimposed to show that the left sided population of the transduced cultures (green) shows positive CD73 expression in the same region as the CD73+ cell population of the non-transduced culture (blue). It could therefore be concluded that the right sided population of the transduced cultures are the GFP+ and CD73+ population respectively.

The immunophenotypic characterization on single cell analysis was performed only with **CD34, CD45, CD90 and CD105**. Although this is not the complete criteria as set out in Dominici *et al.*, 2006, these transduced cultures displayed a similar phenotype in comparison to the non-transduced cultures (Figure 5.6).

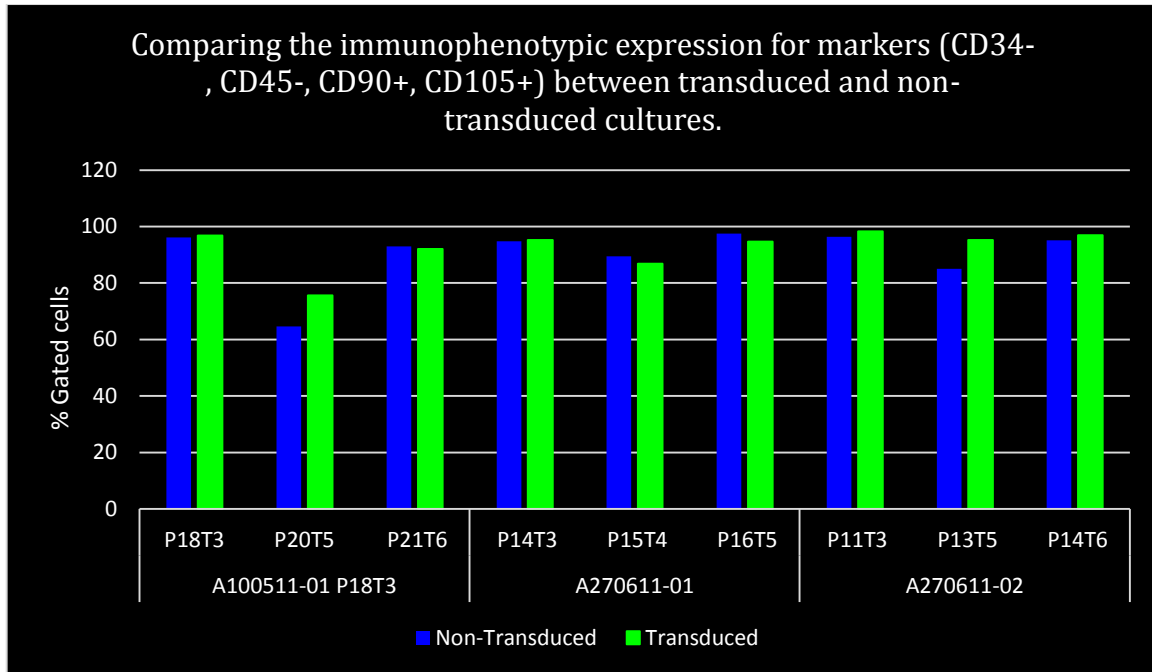
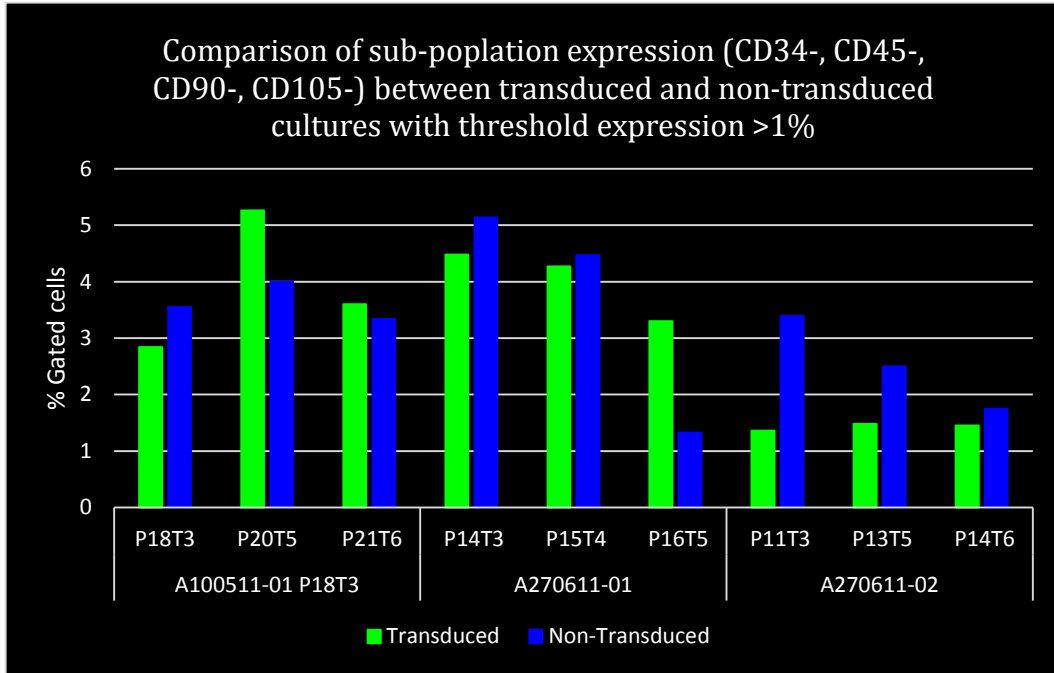


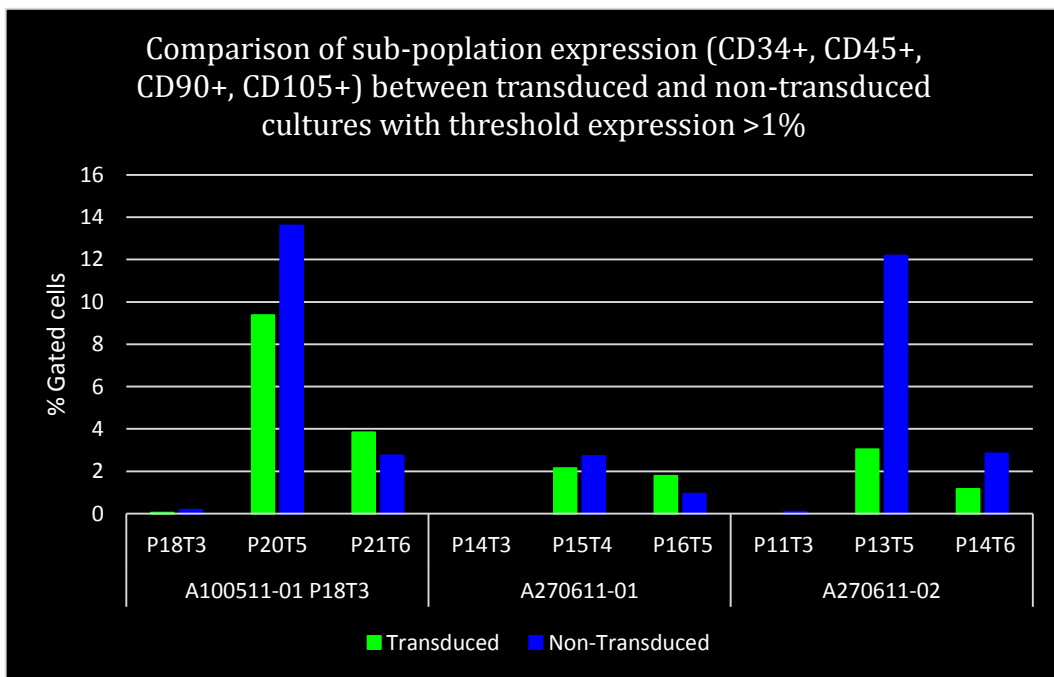
Figure 5.6. Comparing the phenotype (CD34-, CD45-, CD90+ and CD105+) of GFP positive and negative cells within transduced (green) and non-transduced (blue) cultures. Three different cultures and three different post-transduction passages.

The sub-populations within the transduced and non-transduced cultures were determined according to expression and lack of expression of CD34, CD45, CD90 and CD105 cell surface markers. The threshold for the sub-population expression was >1% gated cells within the respective cell population. This expression had to be observed > once across respective passages of all three cultures. Three different sub-populations were found (1) CD34-, CD45-, CD90- and CD105-; (2) CD34+, CD45+, CD90+ and CD105+; and (3) CD34+, CD45-, CD90+ and CD105+ (Figure 5.7.).

A



B



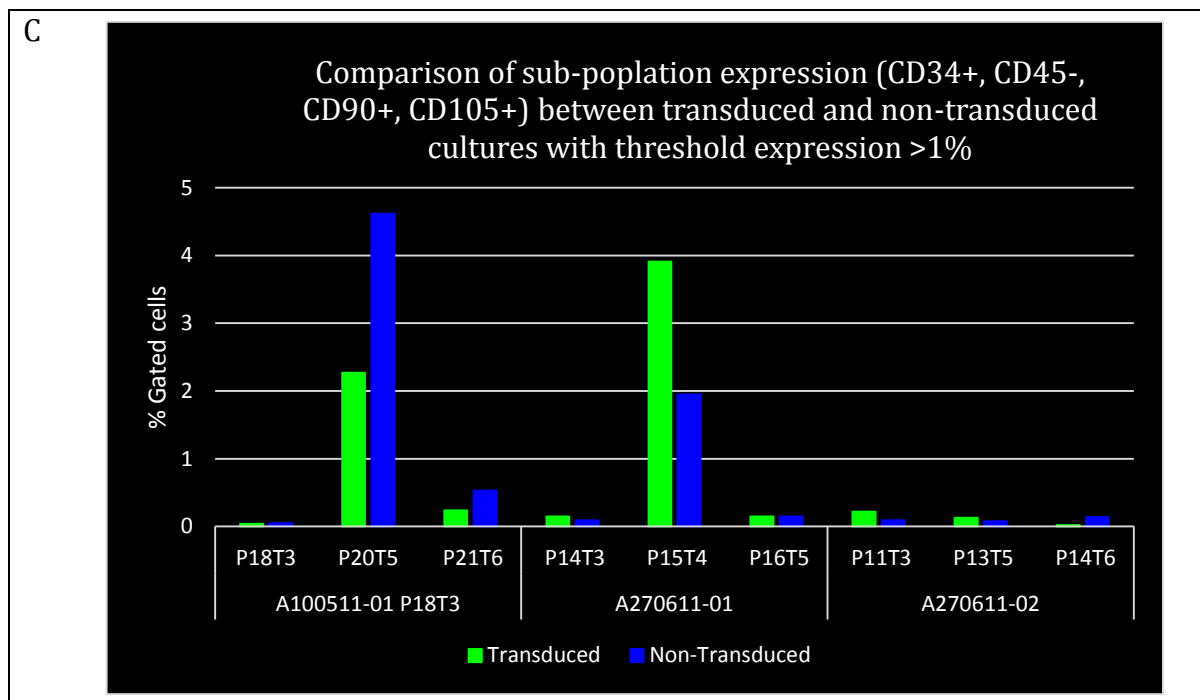


Figure 5.7. Three different sub-populations were identified using antibody panel 1. A combinational antibody threshold was >1% expression displayed in >1 culture. Comparing the percentage gated cells expressing the respective sub-populations were (A) CD34-, CD45-, CD90- and CD105-; (B) CD34+, CD45+, CD90+ and CD105+; and (C) CD34+, CD45-, CD90+ and CD105+, within the transduced and non-transduced.

To characterize ASCs according to the recommended criteria the antibody profile CD34-, CD45-, CD73+, CD90+ and CD105+ needed to be assessed. The transduced and respective non-transduced control cultures were thawed and immunophenotyped using antibody panel 2.

The percentage of GFP positive cells within the transduced cultures was analysed to determine if cryopreservation might have an influence on the percentage of GFP expressing cells. The percentage of GFP positive cells was determined within transduced cultures across passages after cryopreservation (Figure 5.8.).

A general loss of cell viability was observed with both transduced and non-transduced cultures during the cryopreservation and thawing procedures (see Chapter 3). Cell viability was spread evenly between the GFP positive and negative cells within the transduced cultures. A general increasing trend of percentage GFP positive gated cells was observed across all three transduced cultures (Figure 5.8.).

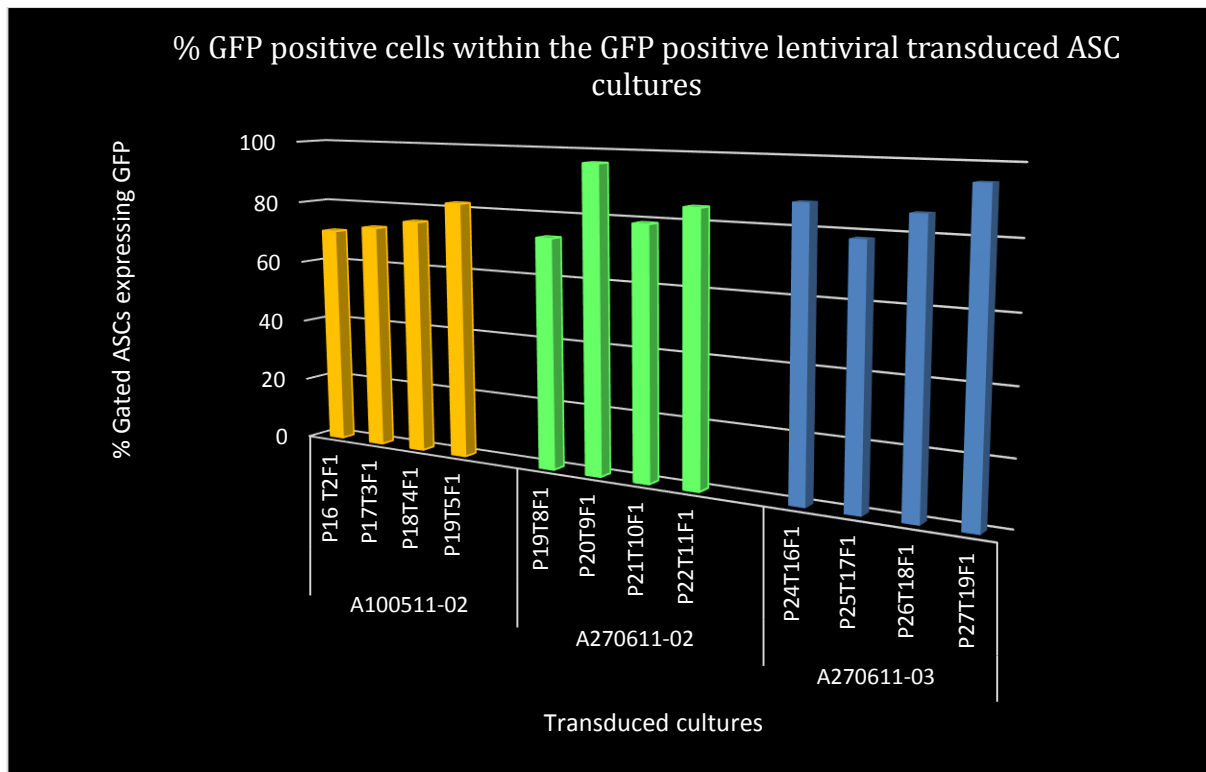


Figure 5.8. The percentage of GFP expressing cells within the gated cell population on the forward and side scatter plot of the transduced cultures after freezing and thawing.

The ASC immunophenotype was assessed to determine if the transduced cultures adhered to the respective criteria in comparison to the non-transduced cultures. The GFP positive and GFP negative cell populations within the transduced cultures were analysed separately to determine if a difference could be observed between the cell populations (Figure 5.9.).

With the CD34 marker reported to be an unstable positive marker (see Chapter 4), both the recommended immunophenotype profile, **CD34-**, **CD45-**, **CD73+**, **CD90+** and **CD105+** as well as the adapted phenotype profile **CD34+**, **CD45-**, **CD73+**, **CD90+** and **CD105+** were assessed (Bourin *et al.*, 2013; Dominici *et al.*, 2006; Lin *et al.*, 2012; Oedayrajsingh Varma *et al.*, 2007; Yoshimura *et al.*, 2006). The GFP positive cell population within the transduced cultures displayed a decrease in ASC immunophenotype expression, in comparison to the GFP negative cell population within the transduced cultures and the non-transduced cultures.

Very importantly this decrease in ASC immunophenotype expression was not due to a decrease in the CD73 marker expression. In fact, the CD73 marker expression was stably expressed between 97-99% for all respective cell populations.

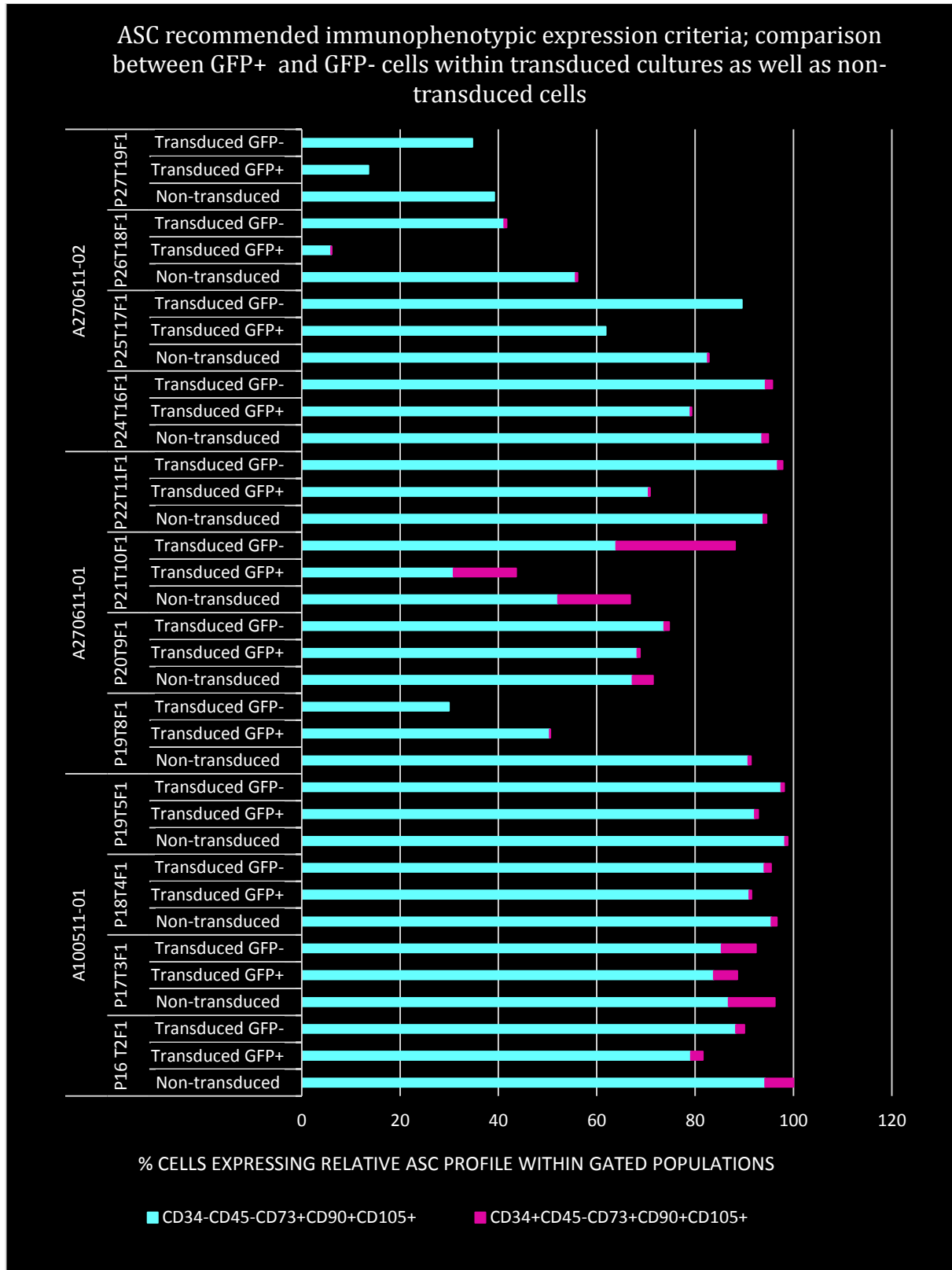


Figure 5.9. The ASC recommended criteria (turquoise: CD34-, CD45-, CD73+, CD90+ and CD105+) as well as new adopted criteria (pink: CD34+, CD45-, CD73+, CD90+ and CD105+) within the non-transduced cultures, the GFP+ and GFP- cell populations within the transduced cultures. The cells expressing relative ASC profiles were displayed as a percentage of respective gated cell populations.

The mean percentage of cells expressing the ASC recommended immunophenotypic profile (CD34-, CD45-, CD73+, CD90+ and CD105+) within the respective gated cell populations was assessed in the three individual cultures (Figure 5.10).

It was observed that the ASC immunophenotype reduced in the transduced cultures compared to the non-transduced cultures. The GFP cell population showed a decrease in ASC immunophenotype profile expression compared to the GFP negative cell population within the transduced cultures. In addition, none of the transduced or the non-transduced cultures adhered to the ASC immunophenotype recommended criteria of >95% expression of CD73, CD90 and CD105 and <5% CD34 and CD45.

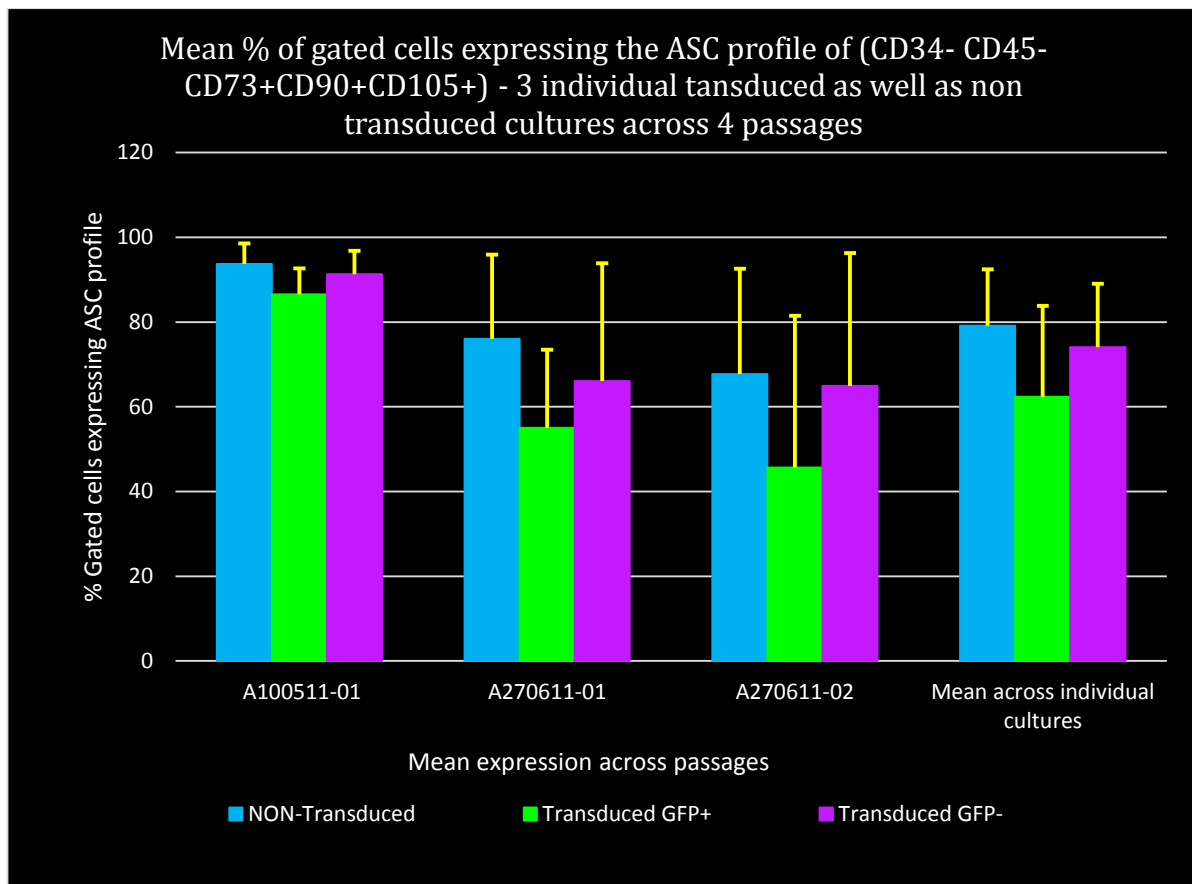


Figure 5.10. The mean percentage of cells expressing the ASC recommended immunophenotypic profile (CD34-, CD45-, CD73+, CD90+ and CD105+) across 4 passages within the respective gated cell populations in three individual cultures. Non-transduced (blue), GFP+ (green) and GFP- (purple) cell populations within the transduced culture.

Sub-population analysis from cryopreserved cultures

We next wished to look closer at what sub-populations are present within this heterogeneous population of cells within the individual cultures. We compared the non-transduced control cultures with the GFP positive and GFP negative cell populations within the transduced cultures. The GFP positive cell population (transduced GFP+)

represent 70-90% and the GFP negative cell population (transduced GFP-) represents 30-10% of the cells within the transduced cultures. The transduced GFP negative cell population represents the ASC cell population that was not transduced within the transduced cultures.

The complete immunophenotype of the non-transduced, GFP positive and negative cell populations within transduced cultures were analysed. The threshold for expression in a specific sub-population was >1% of cells expressing more than once across 4 passages. The individual culture, A100511-01, displayed very high expression for the recommended immunophenotype (blue: Figure 5.11.) as well as the adapted criteria (pink: Figure 5.11.)

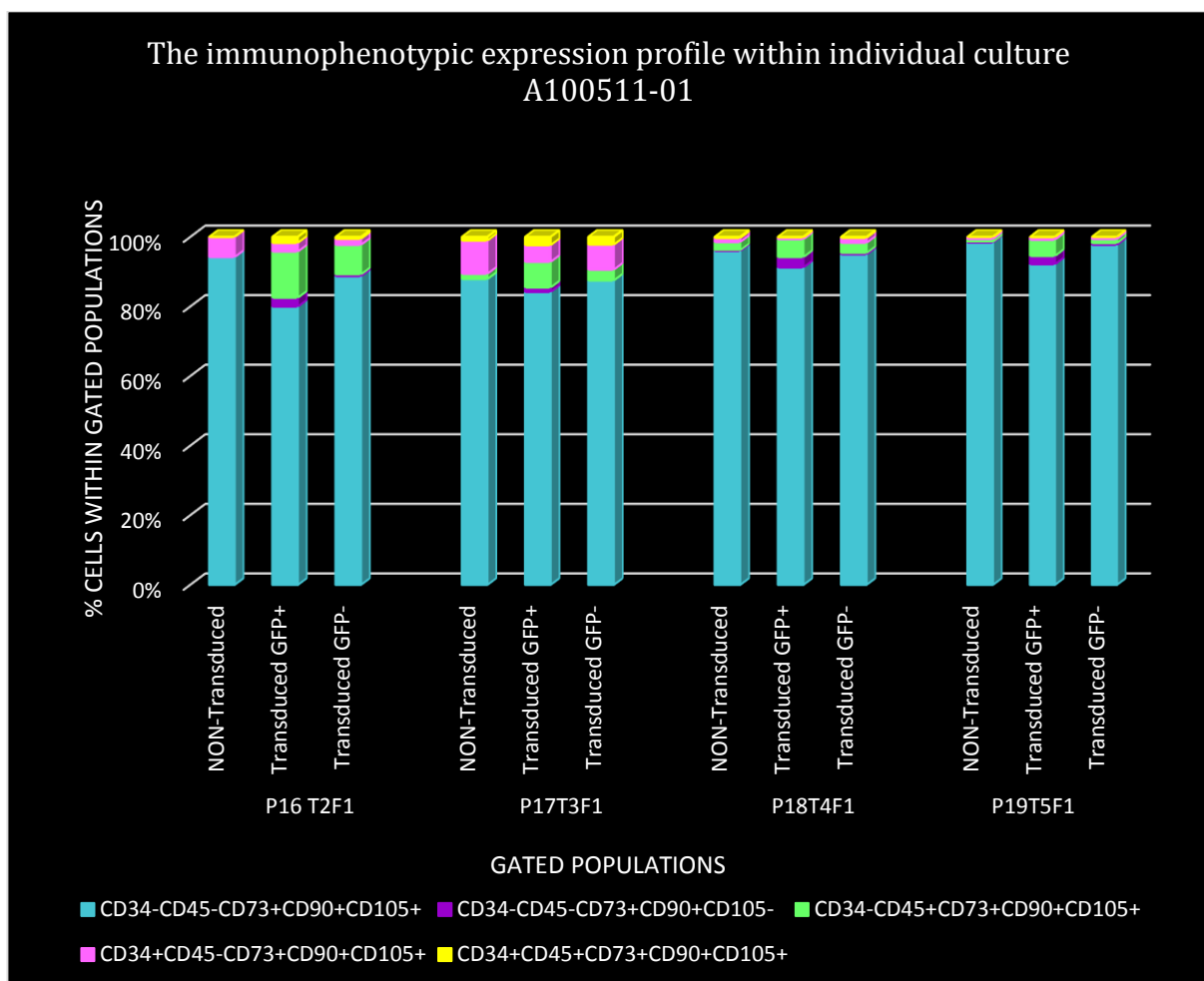


Figure 5.11. The immunophenotypic expression profile of the individual culture A100511-01. Only significant populations were considered with threshold expression of >1%, present more than once across four passages. The comparison was drawn between the non-transduced, GFP positive and GFP negative cell populations within transduced cultures.

The immunophenotype of the non-transduced, GFP positive and GFP negative cell populations within transduced cultures for the individual culture A270611-01 is shown in figure 5.12. This individual cultures showed variability in ASC recommended criteria expression after cryopreservation and thawing procedures, but showed a gradual

increase with increasing passages. Two sub-populations showed increased expression due to the CD105 lacking expression (purple: Figure 5.12.) and CD45 expression (mint green: Figure 5.12.).

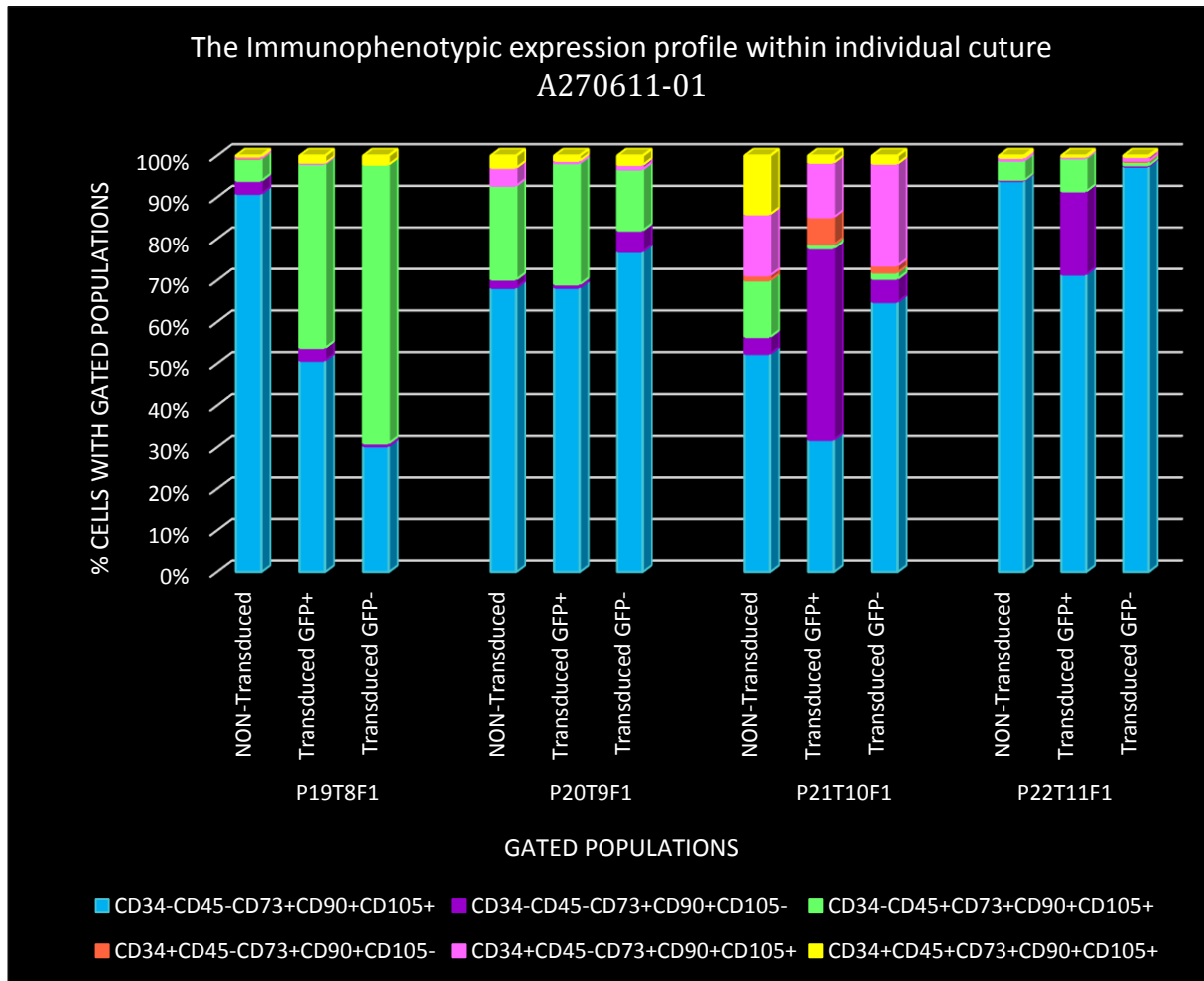


Figure 5.12. The immunophenotypic expression profile of the individual culture A270611-01. Only significant populations were considered with threshold expression >1% being present more than once across four passages. The comparison was drawn between the non-transduced, GFP positive and GFP negative cell populations within transduced cultures.

Comparing the immunophenotype between the non-transduced, GFP positive and GFP negative cell populations within transduced cultures, of the individual culture A270611-02, demonstrates irregular expression with rapid changes (Figure 5.13). The recommended ASC immunophenotype expression decreased with consecutive passages after the cryopreservation and thawing process. The expression profile **CD34-, CD45+, CD73+, CD90+ and CD105+**, increased with passaging (mint green: Figure 5.13.).

Lacking CD105 cell surface expression, the subpopulation **CD34-, CD45-, CD73+, CD90+ and CD105-**, was observed to increase with progressive passages. This subpopulation was observed to be larger within GFP positive cells than GFP negative cells within transduced cultures and hardly evident in the non-transduced cultures (Figure 5.12. and Figure 5.13.). The subpopulation **CD34+, CD45-, CD73+, CD90+ and CD105-**, was only

observed within the individual culture A270611-01. This expression was only seen at one passage across all three gated cell populations (Figure 5.12.).

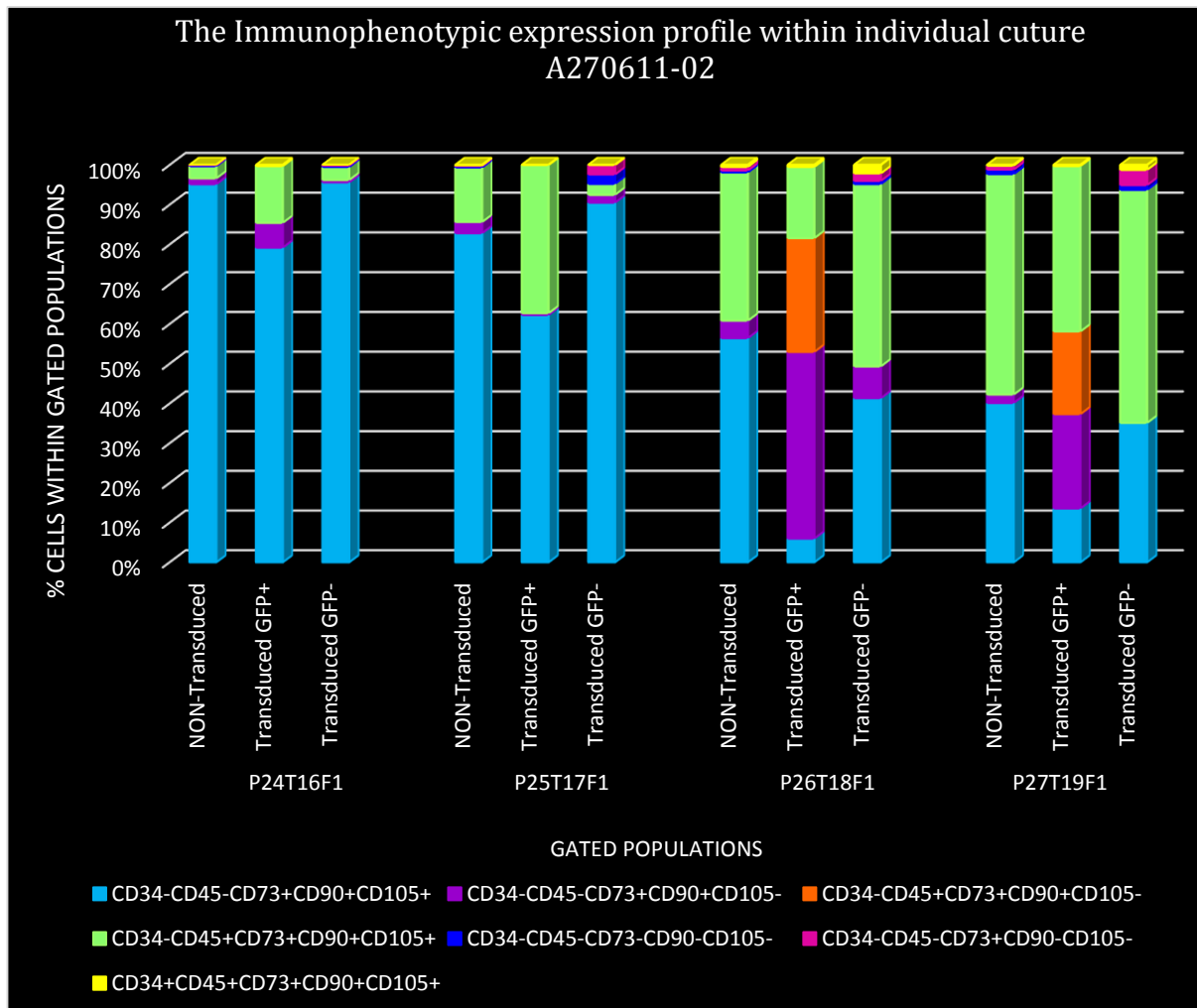


Figure 5.13. The immunophenotypic expression profile of the individual cultures A270611-02. Only significant populations were considered with threshold expression >1%, present more than once across four passages. The comparison was drawn between the non-transduced, GFP positive and GFP negative cells populations within transduced cultures.

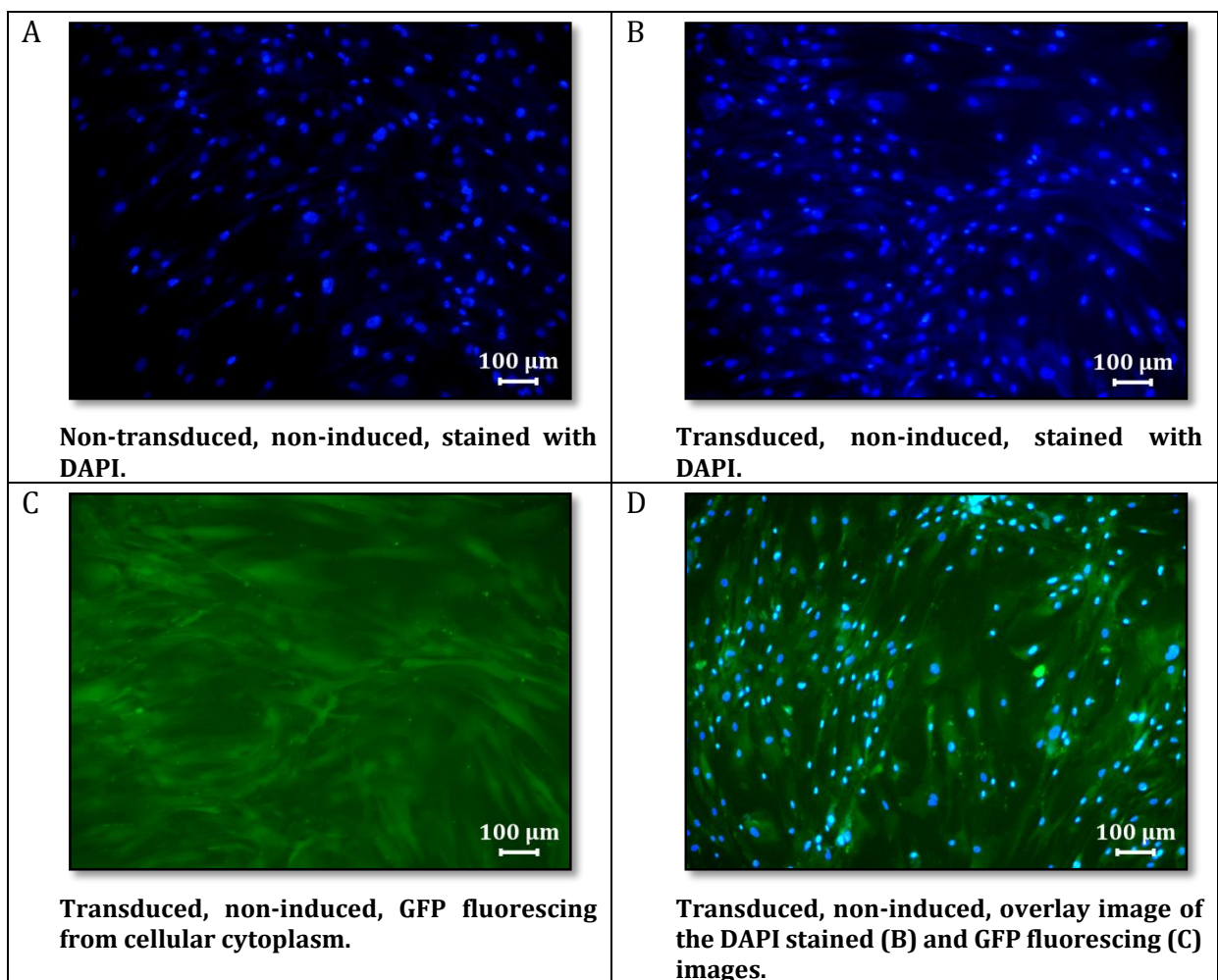
With an increase in CD45 expression and a decrease in CD105 expression, a subpopulation expression profile CD34-, CD45+, CD73+, CD90+ and CD105- was also suspected. This subpopulation was only observed within the GFP positive cell population within the individual culture A270611-02 (Figure 5.13.).

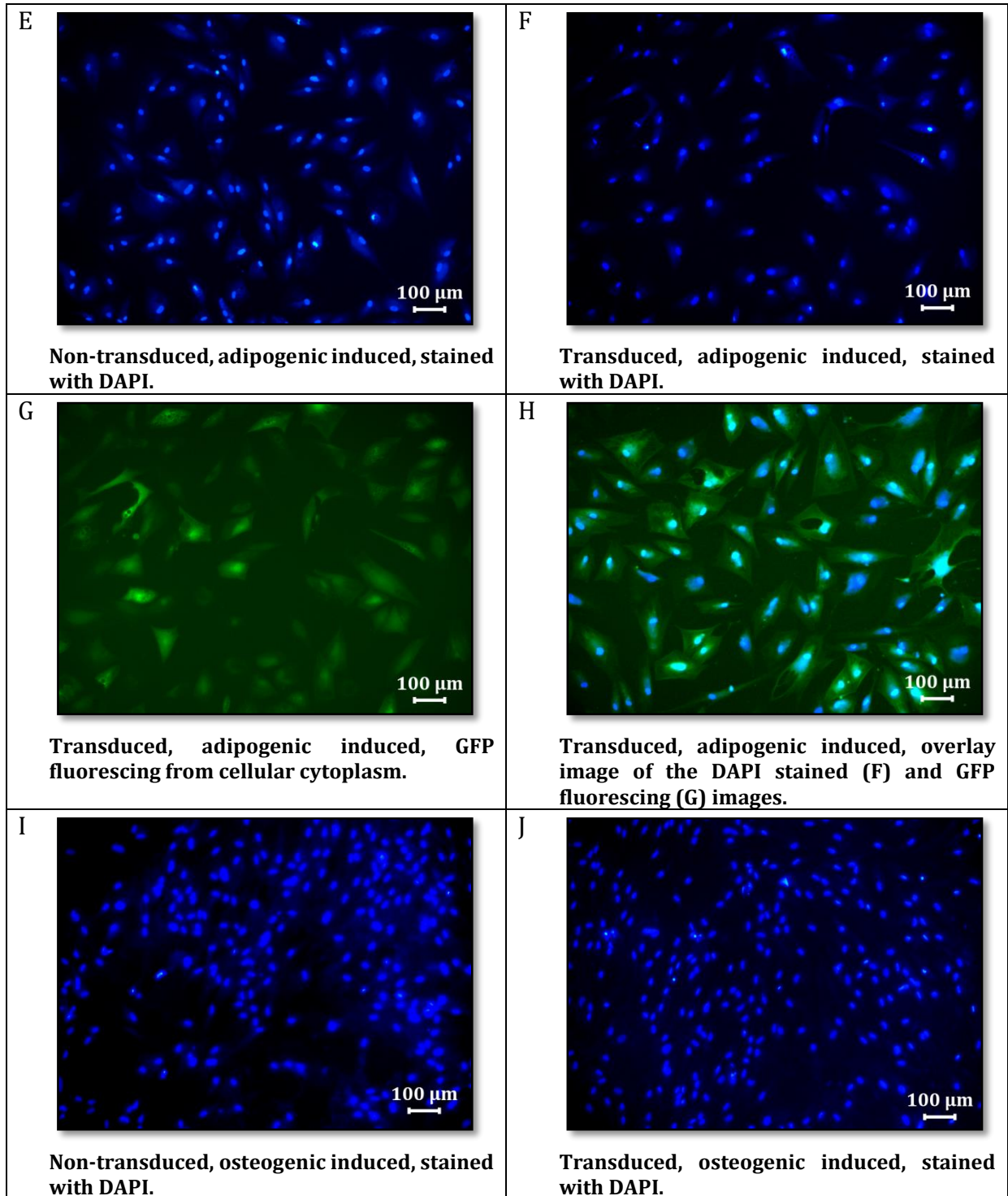
Tri-lineage Differentiation

Non-transduced as well as transduced cells of the three individual cultures were induced to differentiate into the adipogenic, osteogenic and chondrogenic lineages. The lineages were confirmed using either Oil Red O, Alizerin Red S and Toluidine Blue O for (classical stains) adipogenic, osteogenic and chondrogenic lineages respectively.

Comparing the microscopic images of the DAPI stained non-transduced (Figure 5.14. A, E and I) and transduced (Figure 5.14. B, F and J) cultures induced for 21 days, no differences were observed. The non-induced (Figure 5.14. A, B, C and D), adipogenic induced (Figure 5.14. E, F, G and H) and the osteogenic induced (Figure 5.13. I, J, K and L) cultures are presented below.

From the DAPI stained visual images it was clear that the cells were “over populated”, especially within the transduced, non-induced controls and the osteogenic induced cultures. The GFP images for these respective cultures showed overlaying bright expression making it difficult to locate individual cells. Individual GFP positive cells could be observed in the transduced, adipogenic induced cultures.





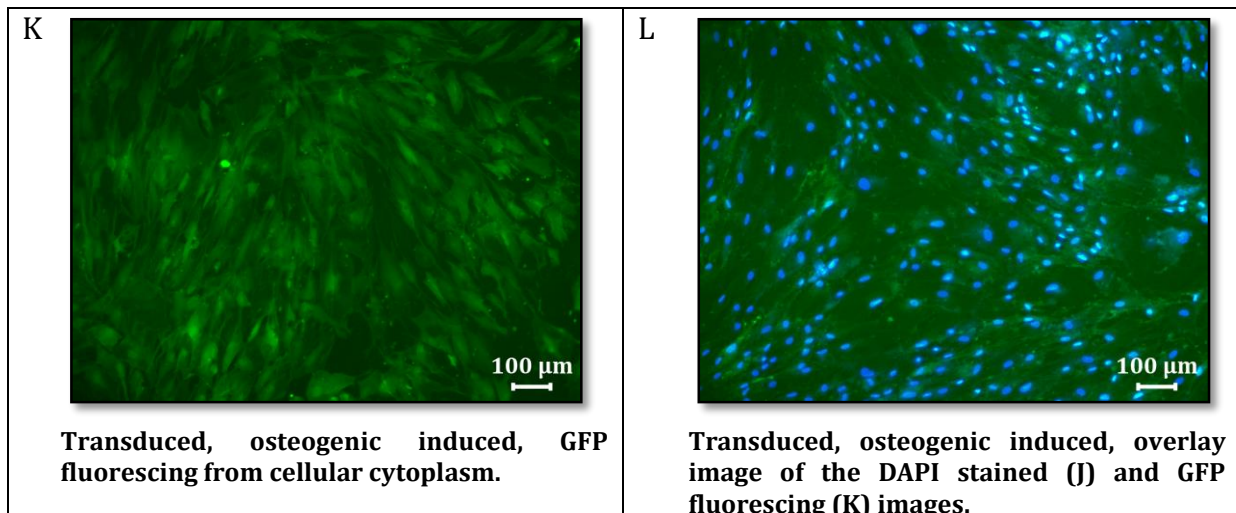
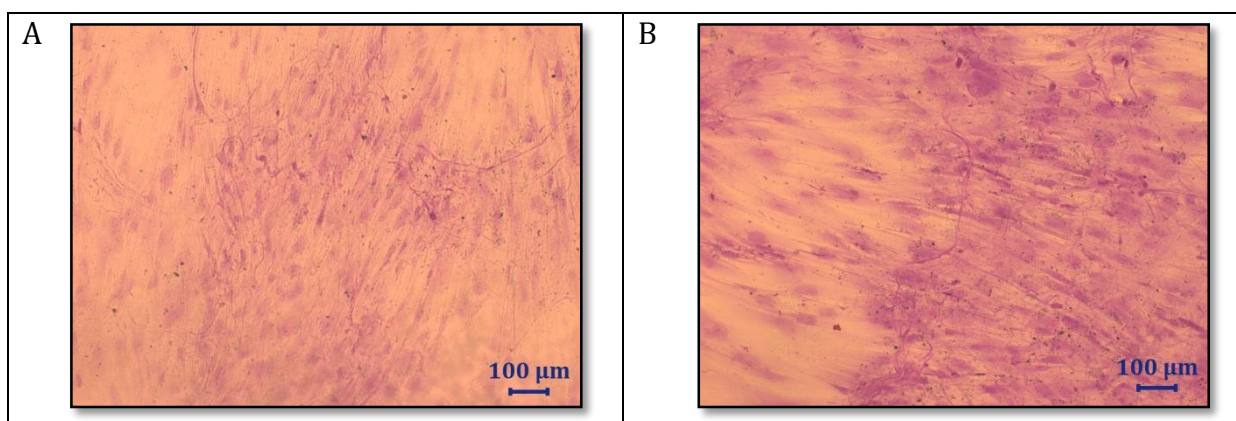


Figure 5.14. Microscopy analyses of the DAPI stained non-, adipogenic- and osteogenic induced, non-transduced (A, E and I) and the transduced (B, F and J) cultures. The transduced cultures demonstrated GFP fluorescence expression within the non-induced (B, C and D), adipogenic induced (F, G and H) and osteogenic induced (J, K and L). These images are only representative of induction timepoint week 3 (day 21).

Adipogenic and osteogenic differentiation was confirmed in both non- and transduced cultures with classical stains Oil Red O (Figure 5.15. A, B, C and D) and Alizerin Red S (Figure 5.15. E, F, G and H) respectively. No visual differences were observed in microscopic images for both the non- and the transduced cultures, comparing the non-induced (Figure 5.15. A and B) to the adipogenic induced (Figure 5.15. C and D) cultures. The non-induced and adipogenic induced cultures were counter stained with 1% Toluidine Blue to visualize cellular membranes within the cultures. Not all the cells within the adipogenic induced cultures displayed Oil Red O stained oil droplets similar to findings described in Chapter 4.

No visual difference between non- and transduced cultures were observed in the non-induced, Alizerin Red S stained cultures (Figure 5.15. E and F), but the transduced, osteogenic induced cultures (Figure 5.15. G and H) demonstrated a slight increase in calcium deposition within the mineral matrix.



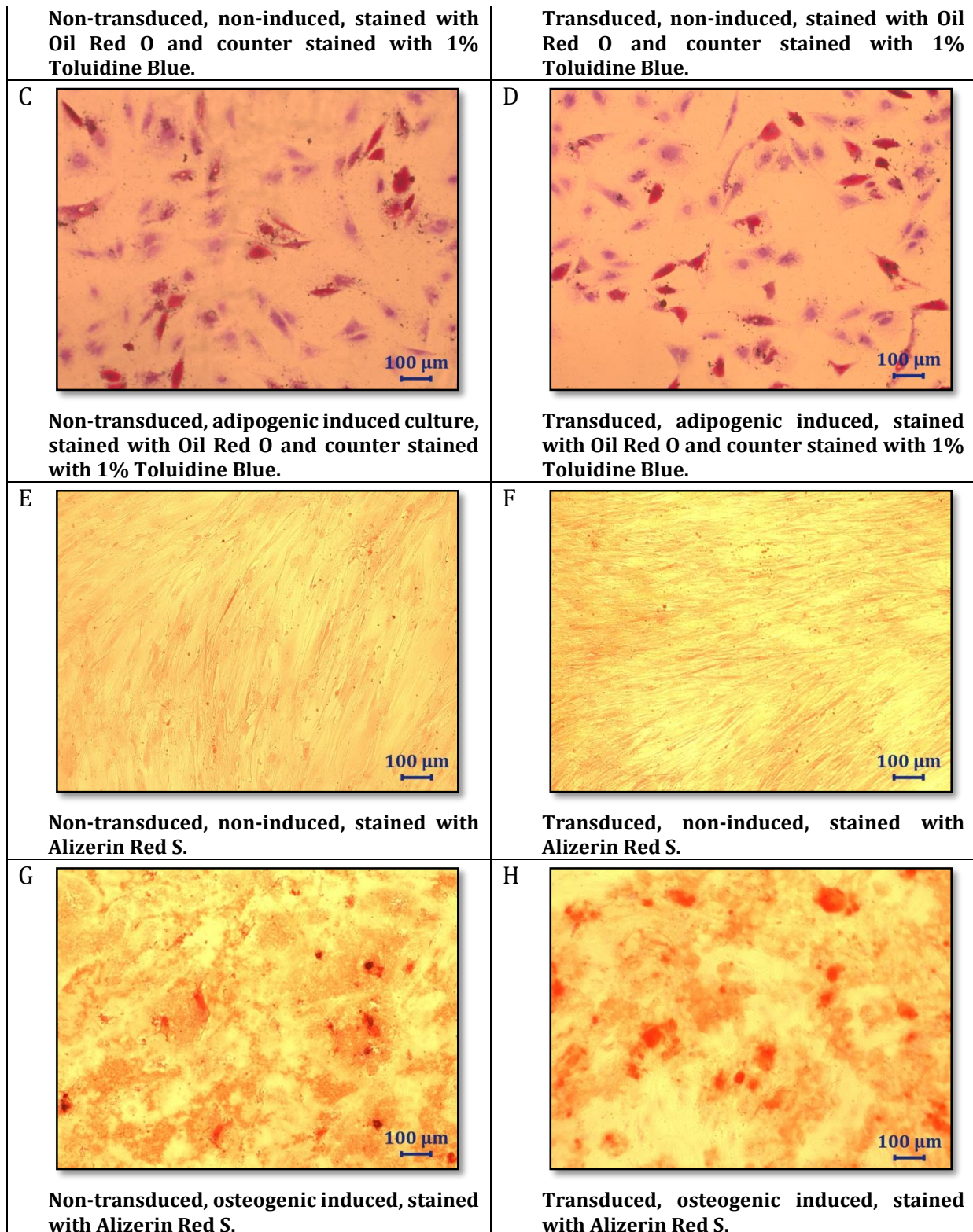


Figure 5.15. Microscopic analysis of the adipogenic and osteogenic induced cultures accompanied by their respective non-induced controls. Oil Red O stained oil droplets confirms adipogenic differentiation in the non-transduced (B) and transduced (C) cultures and Alizerin Red S stained calcium within the mineral deposition confirms osteogenic differentiation within the non-transduced (G) and transduced (H) cultures. These images are only representative of induction timepoint week 3 (day 21).

Chondrogenic differentiation was confirmed with Toluidine Blue O stain in both non-transduced and transduced cultures (Figure 5.16.).

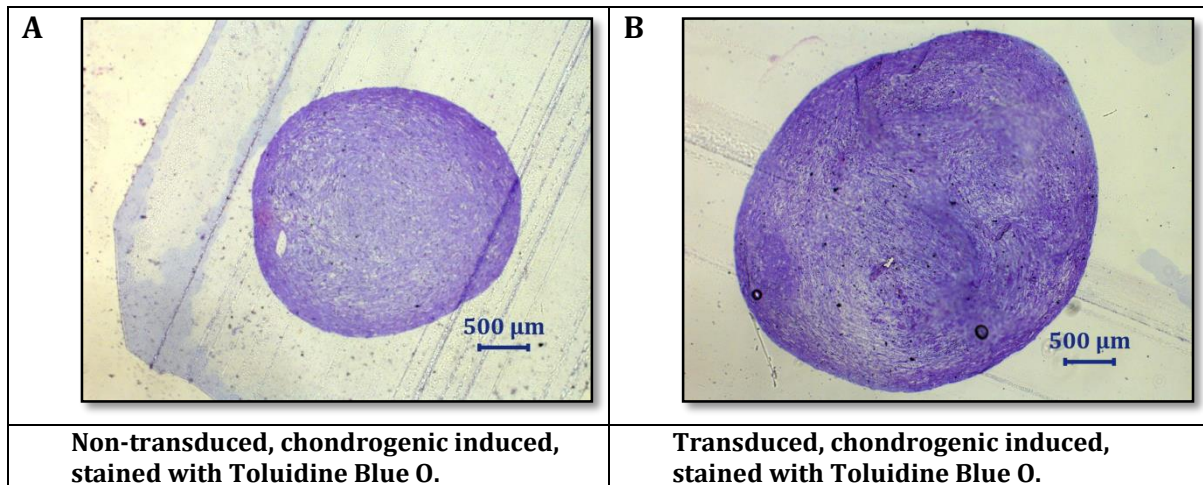


Figure 5.16. Microscopic analysis of chondrogenic induced pellet cultures stained with toluidine Blue O.

Quantification of differentiation

The mean DAPI cell counts within the non-induced, adipogenic induced and osteogenic induced cultures were determined within both the non-transduced and transduced cultures (Figure 5.17. and Figure 5.18.). Adipogenic and osteogenic differentiation for transduced and non-transduced cultures were assessed over a three week period, on day 7, 14 and 21 (Figure 5.17.)

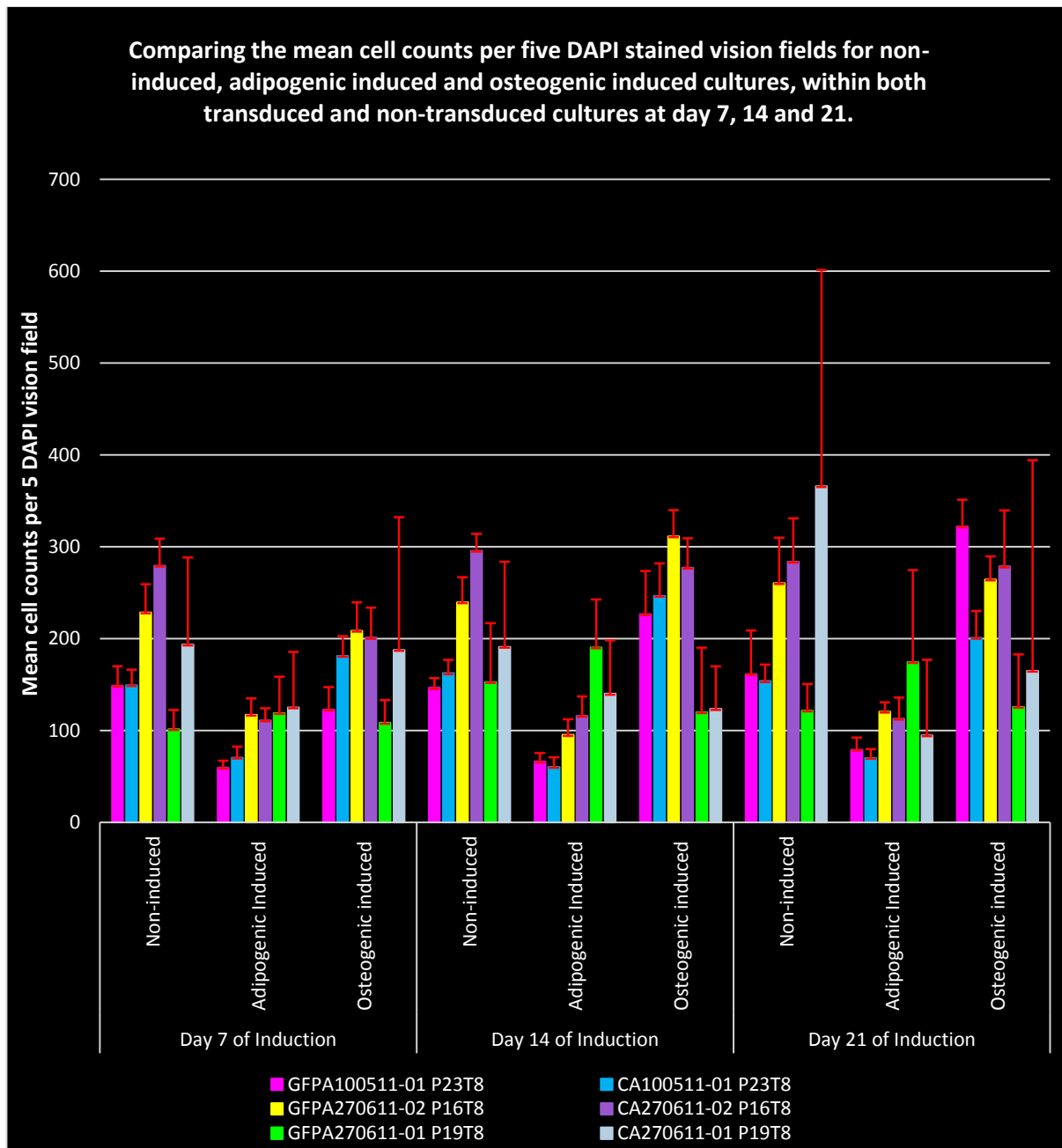


Figure 5.17. The mean number of DAPI stained cells in five images across the induction period of day 7, 14 and 21. Comparing the differences of the non-induced, adipogenic induced and osteogenic induced cultures within both the non-transduced and transduced cultures.

Results show great variability among the three biological samples. The trend of lower adipogenic differentiation compared to controls and higher osteogenic compared to adipogenic differentiation is present across all cultures except one control which showed decreased osteogenic differentiation. No major differences among the three timepoints were observed except for a slight increase in osteogenic differentiation during week 3 for selected cultures (GFP100511-01 P23T8).

The mean DAPI stained cell counts of the non-induced, adipogenic induced and osteogenic induced cultures, for both non-transduced and transduced cultures were

compared between three different post-transfection passages T2, T8 and T14 (Figure 5.18.).

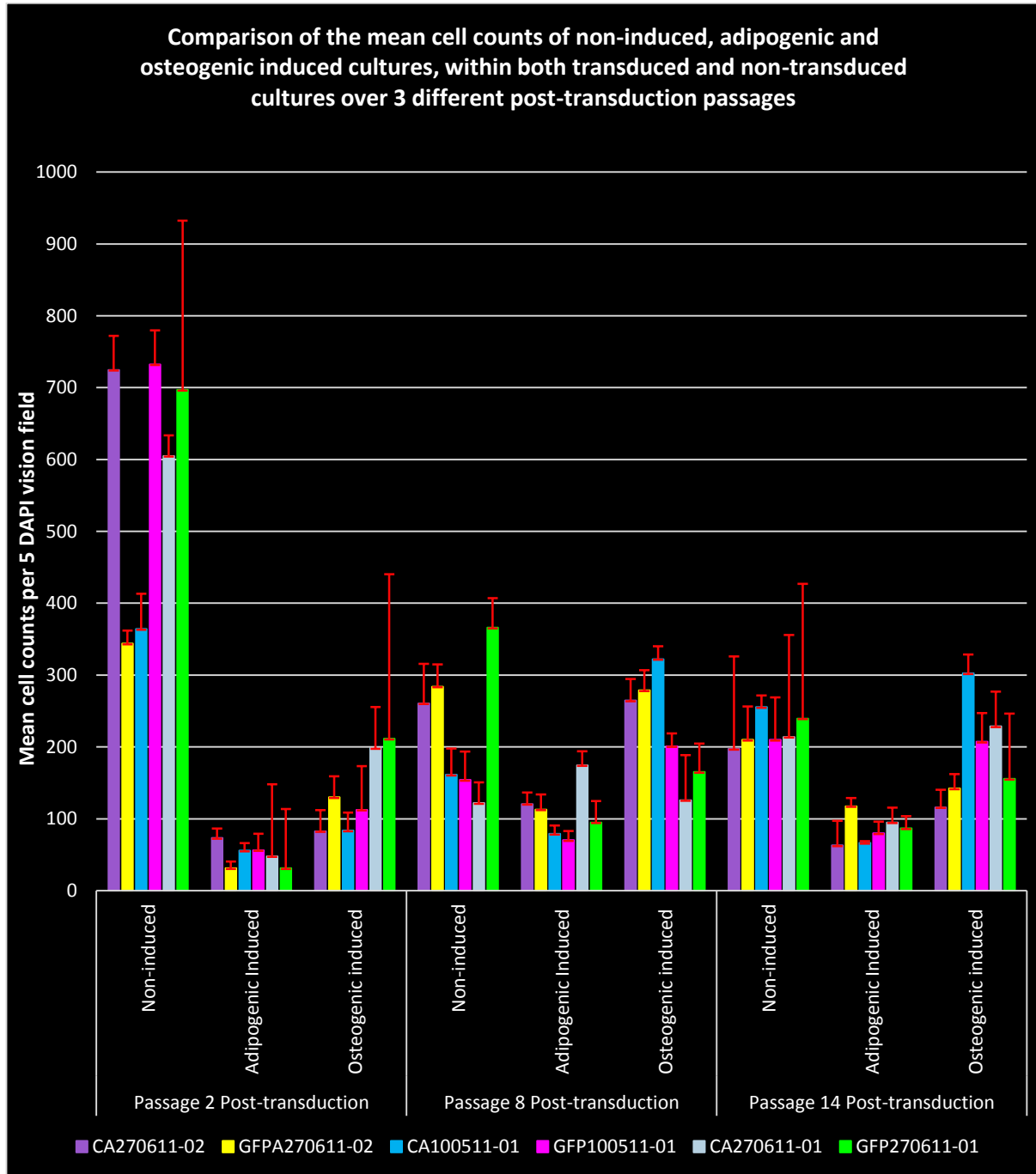


Figure 5.18. Comparing the mean cell counts for the five DAPI stained vision fields between the non-induced, adipogenic and osteogenic induced cultures, within both transduced and non-transduced cultures over 3 different post-transduction passages.

Comparing the transfections showed similar results as was observed over the three timepoints with a consistently lower adipogenic induced mean cell count.

Statistical analysis of quantification

No difference was observed when evaluating the DAPI stained cell counts from five independent images of the non-transduced cultures across all three weeks, *i.e.* control ($F = 0.89$, $P = 0.43$), adipogenic ($F = 0.74$, $P = 0.50$) and osteogenic ($F = 0.73$, $P = 0.50$). When evaluating the DAPI stained images of the transduced cultures we observed difference in the mean cell counts of the controls over week 1, however not significant ($F = 1.87$, $P = 0.19$). We did not observed any difference in the mean cell counts of the DAPI stained images of the transduced cultures in the adipogenic induced ($F = 1.14$, $P = 0.34$) or osteogenic induced ($F = 0.92$, $P = 0.42$).

Comparison of the mean cell counts of the controls between the two groups at week 1 (day 7 of induction) showed no significance ($F = 0.0014$, $P = 0.99$), whereas week two and three showed higher F values of 1.18 and 1.94 respectively but still not significant ($P = 0.66$ and 0.53).

The results of the statistical analysis for difference in differentiation between non-transduced and transduced cultures at three different time points are displayed in Table 5.4.

Table 5.4. Comparing the non-induced, adipogenic and osteogenic induced cultures over 3 weeks between the transduced and non-transduced cultures.

Lineage	Week 1		Week 2		Week 3	
	F value	P value	F value	P value	F value	P value
Non-induced	0.01	0.99	1.18	0.66	1.94	0.53
Adipogenic	0.13	0.95	0.06	0.98	0.22	0.92
Osteogenic	0.04	0.98	0.20	0.93	0.24	0.91

No difference was observed when comparing the means over all three weeks between non-transduced and transduced cultures with the controls ($F = 0.10$, $P = 0.96$), adipogenic ($F = 0.06$, $P = 0.98$) and osteogenic ($F = 0.09$, $P = 0.97$). Comparisons of transduced transfections at week 3 showed a significant difference in adipogenic differentiation between transfection two and eight with a P -value of <0.05 (Table 5.5.).

Table 5.5. Comparing the P values for non-induced, adipogenic induced and osteogenic induced between respective post-transduction passages.

Post transduction passages (T)	P value		
	Control	Adipogenic	Osteogenic
T2 vs T8	0.134	0.0492 (more in T8)	0.221
T2 vs T14	0.095	0.0916	0.738
T14 vs T8	0.811	0.303	0.367

Discussion

This study showed successful transfection of ASCs with a lentiviral vector for potential use of GFP as tracking system in future animal studies. The study is the first to analyse sub-populations of ASCs within GFP transduced cultures. In addition to the main findings we observed sustained expression of GFP during differentiation.

The titration study showed a stable expression of GFP when using 300 μ l. It must be noted that the process of preparing GFP positive lentiviral stock is very time consuming and expensive and a smaller volume could be considered; however according to our findings less than 50 μ l would not result in sufficient GFP expression. Due to the cost we also used a small surface area (9.6 cm^2) to seed (5×10^3 cells/ cm^2) for the transduction process and this could have implications with regard to expansion and differentiation as discussed in Chapters 3 and 4.

Although the GFP expression was more than 70% at all timepoints, the expression varied among the three biological samples, one being consistently more than 80% and the other showing increased expression from passage eight onwards. This might be an important finding that the expression does not decrease during progressive passaging but rather increased and this makes this marker suitable for future expansion experiments.

A limitation occurred when evaluating the initial immunophenotype which was the inability to distinguish between the expression of CD73 and GFP. By overlaying the histograms we could confirm that all the transduced cultures expressed CD73 and thus conformed to the proposed criteria.

Comparing the initial immunophenotype between transduced and non-transduced cultures showed good correlation and more importantly an increase in adherence to the proposed ASC criteria in the GFP cultures. However, the lack of inability to accurately determine the presence of CD73 necessitated repeat testing from freeze-thawed cultures. As discussed in Chapter 3, the effect of freeze and thaw on ASCs resulted in decreased cell viability. Interestingly, the percentage GFP expression remained stable after this process and was comparable with initial expression. However, within the cryopreserved cultures, none of the transduced or the non-transduced cultures adhered to the ASC immunophenotype recommended criteria (Dominici *et al.*, 2006) of >95% expression of CD73, CD90 and CD105 and <5% CD34 and CD45 (Figure 5.9.). The GFP within cytoplasm could be cytotoxic to transduced cells because a decrease in ASC immunophenotypic expression is seen in the GFP positive cell population within the transduced cultures compared to the non-transduced cultures. More of a decrease was observed within the transduced GFP positive population in comparison to the transduced GFP negative population. This finding should be taken into account for future experiments especially when combining transfections and cryopreservation procedures.

Three sub-populations were identified of which one population [CD34-, CD45-, CD90-, CD105-] was consistently present across all three cultures and all evaluated passages and in some instances reached almost 5%, which was previously discussed as being potentially significant (Chapter 4). The implications of the sub-populations needs further assessment. Further subpopulation analysis among the thawed cultures and further stratification among GFP positive and negative expression within the transduced cultures showed great variability.

We observed sub-populations after the freezing and thawing process that were different from that observed in the initial isolation. This was mainly due to the increase in expression of CD45 which could be due to sub-populations from emerging at high passages, the cryo-preservation effect or simply that cultures spontaneously differentiated due to environmental conditions. Similarly we observed a decrease in expression of CD105 and this could be due to similar reasons. We also observed a majority GFP positive population (70-90%) within the transduced cultures indicating successful transfection and also sustained fluorescence after freezing and thawing.

All the transduced and non-transduced cultures differentiated successfully into all three lineages. The DAPI stain was incredibly useful and enabled adipogenic and osteogenic quantification. Visualization of the GFP could not be used for quantification in the controls as well as the osteogenic induced cultures due to the large overlaying cell populations observed. Overlaying the DAPI stain and GFP images served as a quality control for the quantification. With this technique we could observe that all the adipocytes within the adipogenic induced culture did express GFP. Interestingly, the adipogenic induced cells did not expand to confluency compared to the osteogenic induced cells and this seems to be a consistent finding. Possible reasons include initial cell death during induction due to cytotoxicity of the induction medium or the nature of the adipocytes to be “contact inhibited” and require a specific surface area to expand. The reason for this phenomenon remains unclear but is consistent with the findings in Chapter 4. Also, from the overlaying images one can observe the matrix formation of the osteogenic induced cultures which interestingly were also GFP positive. As discussed in Chapter 4, quantification of differentiated chondrocytes was not possible.

An important finding is that we did not observe a visual decrease in GFP expression during the differentiation process. This is important when considering using this marker to investigate homing and site-specific differentiation capabilities of MSCs and also further pre-clinical applications in animal models.

Although a larger amount of calcium deposition was observed among the images within the transduced cultures, this could not be quantified and does not necessarily indicate increased differentiation. On the contrary, the size of the pellet that formed during chondrogenic induction of the transduced cultures was consistently larger compared to

the non-transduced cultures and since the controls showed no difference, this is an interesting observation that might need further investigation.

Overall we did not observe any statistically significant differences with regard to differentiation when comparing the mean cell counts across three timepoints over three transfections. The variability among the biological samples is clear and a larger sample size is necessary to evaluate these characteristics. The implication of finding no difference between the transduced and non-transduced cells is very encouraging and supports our future research efforts using this marker as a potential tracking system as it is unlikely to influence the study outcome.

Conclusion

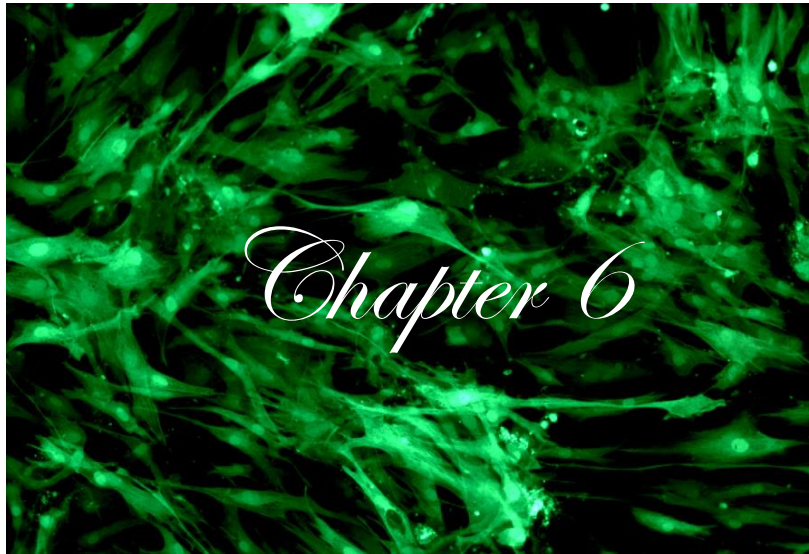
The GFP lentiviral vectors we produced demonstrated more than 80% transduction efficacy of ASCs. No significant changes in cell surface marker expression were observed during the comparison of transduced and non-transduced cultures. It can therefore be concluded that the MSC phenotype was maintained *in vitro*. Transduced cells like non-transduced cells demonstrated similar morphology and tri-lineage differentiation.

The percentage GFP positive cells seem to decrease slightly during passages 1 and 5, suggesting a transition phase, followed by a steady increase. The level of GFP expression in individual cells did not decrease with time, demonstrating persistent intra-cellular GFP protein production. With these optimized GFP positive lentiviral vector transduction procedures and experimental results demonstrated that the standardized criteria of defining human MSCs were not compromised, future research could be directed into various study platforms. Transduced MSCs could act as a gene delivery system or serve as a tracking system to study the homing and migration, regeneration and restoration of tissues and organs *in vitro* and *in vivo*.

This optimized GFP transduction technique offers a feasible tracking system for studying the characteristics of MSCs or gene delivery systems in future pre-clinical studies.

References

- Amado RG and Chen ISY. Lentiviral vectors- the promise of gene therapy within reach? *Science*. 1999;285;5428:674-676.
- Bourin P, Bunnell BA, Casteilla L, Dominici M, Katz AJ, March KL, *et al*. Stromal cells from th adipose tissue-derived stromal vascular fraction and culture expanded adipose tissue-derived stromal/stem cell: a joint statement of the International Federation for Adipose Therapeutics and Science (IFATS) and the Internationsl Society for Cellular Therapy (ISCT). *Cytotherapy*. 2013;15:641-648.
- Bukrinsky MI, Haggerty S, Dempsey MP, Sharova N, Adzhubei A, Spitz, *et al*. A nuclear localization signal within HIV-1 matrix protein that governs infection of non-dividing cells. *Nature*. 1993;365:666-669.
- Dominici M, Le Blanc K, Mueller I, Slaper-Cortenbach I, Marini FC, Krause DS, *et al*. Minimal criteria for defining multipotentmesenchymal stromal cells. The International Society for Cellular Therapy position statement. *Cytotherapy* 2006;8;4:315-317.
- Dull T, Zufferey R, Kelly M, Mandel RJ, Nguyen M, Trono D, *et al*. A third-generation lentivirus vector with a conditional packaging system. *Journal of Virology*. 1998;72;11:8463-8471.
- Korin YD and Zack JA. Progression to the G1b phase of the cell cycle is required for completion of human immunodeficiency virus type 1 reverse transcription in T cells. *Journal of Virology*. 1998;72;4:3161-3168.
- Lin CS, Ning H, Lin G and Lue TF. Is CD34 truly a negative marker for mesenchymal stromal cells? *Cytotherapy*. 2012;14:1159-1163.
- Naldini L, Bieamer U, Gallay P, Ory D, Mulligan R, Gage IM, *et al*. *In vivo* gene delivery and stable transduction of nondividing cells by a lentiviral vector. *Science*. 1996;272:263-267.
- Oedayrajsingh Varma MJ, Breuls GM, Schouten TE, Jurgens WJFM, Bontkes HJ, Schuurhuis GJ, *et al*. Phenotypical and functional characterization of freshly isolated adipose tissue-derived stem cells. *Stem Cells and Development*. 2007;16:91-104.
- Salmon P and Trono D. Production and titration of lentiviral vectors. *Current Protocols in Neuroscience*. 2006;Suppl 37;Unit 4.21.1-4.21.24.
- Sikorski R and Peters R. Treating with HIV. *Science*. 1998;282;5393:1438.
- Yoshimura K, Shigeura T, Matsumoto D, Sato T, Takaki Y, Aiba-Kojima E, *et al*. Characterization of freshly isolated and cultured cells derived from the fatty and fluid portions of liposuction aspirates. *Journal of Cellular Physiology*. 2006;208:64-76.
- Zack JA, Salvatore JA, Weitsman SR, Go AS, Haislip A and Chen ISY. HIV-1 entry into quiescent primary limphocytes: Molecular analysis reveals labile, latent viral structure. *Cell*. 1990;61:213-222.
- Zufferey R, Dull T, Mandel RJ, Bukovsky A, Quiroz D, Naldini L, *et al*. Self-inactivating vector for safe and efficient *in vivo* gene delivery. *Journal of Virology*. 1998;72;12:9873-9880.



Conclusion to dissertation.

There is nothing either good or bad,

But thinking makes it so

Shakespeare W, *Hamlet* (1600), Act II, Scene 2, line 1350-1351.

In conclusion, our aims and objectives to investigate various aspects of basic cell biology with regard to mesenchymal stem cells (MSCs) in order to optimize future experiments that could contribute to translational research, were achieved.

The following research questions were addressed:

1. Can stromal cells be isolated from human adipose tissue and meet the characterisation criteria of adherence to plastic, expression of a specific set of cell surface markers and tri-lineage differentiation into bone, adipose tissue and cartilage?
2. For the purpose of labelling ASCs, what percentage of ASCs will be transduced by the GFP lentivirus vector *i.e.* will show GFP expression?
3. Will the ASCs still adhere to plastic, proliferate, express MSC markers and differentiate into osteoblasts, adipocytes and chondrocytes when they are transduced by the GFP lentiviral vectors?

Adipose derived stromal vascular fraction was successfully isolated from healthy donor lipoaspirate. The cells were successfully expanded and immunophenotyped with an overall mean expression of 94% with regard to the required cell surface markers [CD34-, CD45-, CD73+, CD90+ and CD105+]. The heterogeneous population of cells demonstrated tri-lineage differentiation into adipogenic, osteogenic and chondrogenic lineages. The objective of characterizing MSCs using the proposed criteria was achieved.

Apart from demonstrating that > 80% of cells within the transduced ASC cultures expressed GFP, little difference was observed with regard to the ability of the transduced cultures to adhere to plastic, express ASC cell surface markers and undergo tri-lineage differentiation. This finding supports future research attempts to optimize and to explore *in vivo* tracking in animal models.

This study has laid a broad foundation for future studies by establishing and optimized lipoaspirate harvesting techniques, standard operating procedures for ASC isolation, expansion and induction into adipogenic, osteogenic and chondrogenic lineages. Furthermore, standard protocols for lentivirus production and ASC transduction were optimized. In addition, the heterogeneity of ASCs was demonstrated and tri-lineage differentiation was confirmed, using flow cytometry and microscopy techniques respectively.

The limitations of this study were that the immunophenotype expression profile criteria have recently been revised and quantification of differentiation into the respective lineages was not optimal using the respective microscopy techniques. It is therefore imperative to establish a revised immunophenotyping panel using the current criteria and also to exploring different differentiation quantification techniques. With regard to the latter, our laboratory is already quantifying adipogenesis using flow cytometric analysis of Nile Red dye uptake. Osteogenesis could be quantified using flow cytometry and osteoblast as well as osteocyte specific cell surface markers. Gene expression analysis could be performed on all three lineages using microarrays, RNA sequencing and quantitative PCR.

Further studies *in vivo* will need to establish the safety and efficacy as well as the differentiation capacity of isolated adipose derived stromal vascular fraction as well as ASCs. It will also be important to establish the optimal site/route of administration.

Future studies can build on this foundation to understand for *e.g.* ASC homing or mechanisms of tissue repair or replacement that are not yet well understood. This optimized GFP transduction technique offers a feasible tracking system for studying the characteristics of therapeutically administered ASCs or for gene delivery systems in future preclinical studies. The combination of gene-therapy and stem cell biology opens a new avenue to explore novel treatment options for incurable diseases.

In conclusion, this study supports our research group's efforts to establish a laboratory and the necessary protocols to establish a clinical facility for cell-based therapy.

Appendix 2.1. Clinical trials search using Adipose derived stem cells

ID	Country	Trail status	Condition	Source	Dose (number of cells)	Route of administration	No. of subjects	First received date	Phase
NCT01440699	Republic of Korea	Recruiting	Crohn	Allogeneic cultured	1x10 ⁷ cells/ml	Local	6	19/09/2011	1
NCT01314092	Republic of Korea	Recruiting	Complex Perianal Fistula	Autologous cultured	1x10 ⁷ cells/ml 2x10 ⁷ cells/ml	Local	40	08/03/2011	2
NCT00715546	Brazil	Active, not recruiting	Lipodystrophy	Autologous lipoaspirate	ASC enriched Lipoinjection	Local	5	11/07/2008	1
NCT01502514	Mexico	Recruiting	Ischemic congestive heart failure	Autologous	-	Intramyocardial injection and IV	10	27/12/2011	1 and 2
NCT02034669	Vietnam	Recruiting	Acute spinal cord injury	Autologous cultured	-	Local (intradural and intrathecal) and IV	48	06/01/2014	1 and 2
NCT01502501	Mexico	Recruiting	Non-Ischemic congestive heart failure	Autologous	-	Intramyocardial injection and IV	10	27/12/2011	1 and 2
NCT00992485	Republic of Korea	Completed	Crohn's Fistula	Autologous cultured	Drug: ADIPOPLUS	Local	9	29/09/2009	1
NCT02131077	Republic of Korea	Recruiting	Lateral Epicondylitis	Allogeneic	-	-	27	29/04/2014	1 and 2
NCT01011686	Republic of Korea	Terminated	Fecal Incontinence	Autologous cultured	-	Local (anal sphincter)	-	10/11/2009	1
NCT00703612	Philippines	Active, not recruiting	Type 2 Diabetes Mellitus	Autologous Activated AD-SVF	-	IV	34	19/06/2008	1 and 2
NCT01559051	United states	Recruiting	Chronic Obstructive Pulmonary Disease	Autologous AD-SVF	AD-SVF isolated from 120cc lipoaspirate	IV	200	19/03/2012	1 and 2
NCT02116933	United states	Recruiting	Fat grafting breast Augmentation	AD-SVF	Autologous fat graft enriched with AD-SVF	Local	20	18/03/2014	2
NCT01623453	Republic of Korea	Active, not recruiting	Perianal Fistula	Autologous Cultured	1x10 ⁷ cell/ml 2x10 ⁷ cell/ml	Local	40	08/06/2012	Follow up study After 2

ID	Country	Trail status	Condition	Source	Dose (number of cells)	Route of administration	No. of subjects	First received date	Phase
NCT02090140	United States	Recruiting	Degenerative lesion of articular cartilage defects	Autologous AD-SVF	-	Local	40	11/03/2014	-
NCT01011244	Republic of Korea	Completed	Crohn's fistula	Autologous cultured	Drug: ADIPOPLUS 1x10 ⁷ cells/cm ²	Local	40	10/11/2009	2
NCT02092870	United States	Recruiting	Chronic wounds	Autologous AD-SVF	Injection volume: 250 µl	Local	25	18/03/2014	2
NCT01771913	Brazil	Recruiting	Breast reconstruction	Autologous AD-SVF	AD-SVF enriched fat graft	Local	24	14/01/2013	2
NCT00703599	Philippines	Recruiting	Type 1 Diabetes	Autologous Activated AD-SVF	AD-SVF from 100-120 ml lipoaspirate	IV	30	19/07/2008	1 and 2
NCT01828723	United States	Recruiting	Facial grafting/lipoatrophy	Autologous AD-SVF	AD-SVF enriched lipoinjection	-	6	02/04/2013	1
NCT01378390	Austria, Netherlands and Spain	Terminated	Crohn's and complex perianal fistula	Autologous Cultured	20 million cells	intralesional	56	21/06/211	3
NCT01372969	Spain	Completed	Crohn's and Anal Fistula	Allogeneic cultured	20 and 40 million cells	-	24	30/08/2010	1 and 2
NCT01218945	Switzerland	Completed	Development of bone grafts	Allogeneic cultured	-	-	33	29/09/2010	-
NCT01584713	Spain	Recruiting	Enterocutaneous fistula	AD-SVF	-	Local: Intralesional injection	10	26/02/2012	1 and 2
NCT01853501	China	Enroll by invitation	Premature ovarian failure	Autologous cultured	Density of 5-10x10 ⁶	Local: intraovarian injection	4	07/05/2013	4
NCT01808378	Spain	Recruiting	Keratopathy	Autologous cultured	-	Local	8	04/09/2012	2
NCT01449032	Denmark	Recruiting	Chronic Myocardial Ischemia	-	-		60	06/10/2011	2
NCT02035085	United States	Not yet recruiting	Breast reconstruction, Breast Cancer	Autologous AD-SVF	CS-1000 labelled AD-SVF	Local (19F Hot Spot MRI <i>in vivo</i> tracking)	6	19/12/2013	1

ID	Country	Trail status	Condition	Source	Dose (number of cells)	Route of administration	No. of subjects	First received date	Phase
NCT00442806	Netherlands and Spain	Completed	ST-Elevation myocardial infarction	Autologous AD-SVF	-	-	14	28/02/2007	1
NCT01502488	Mexico	Not yet recruiting	Autism	Autologous AD-SVF	-	IV	10	27/12/2011	1 and 2
NCT01501461	Mexico	Recruiting	Frailty Syndrome	Autologous AD-SVF	-	IV	10	03/10/2011	1 and 2
NCT01541579	Austria, Belgium, France, Germany, Israel, Italy, Netherlands, Spain	Recruiting	Crohn's disease	Allogeneic	120 million cells	Local: Intralesional injection	278	21/02/2012	3
NCT01548092	Spain	Recruiting	Recto-vaginal Fistula	Autologous AD-SVF	-	Local: Intralesional injection	10	26/02/2012	2
NCT02087397	United States	Recruiting	Erectile dysfunction	Autologous AD-SVF	AD-SVF and PRPs	Local: Corpus Cavernosum	500	12/03/2014	1
NCT01586715	Spain	Recruiting	Acute Complex Perianal Fistulae	Autologous AD-SVF	-	Local: Intralesional injection	10	23/04/2012	2
NCT0099115	Spain	Completed	Recto-vaginal Fistula associated Crohn's	Allogeneic cultured	20 and 40 million cells	Local: Intralesional injection	10	20/10/2009	1 and 2
NCT01585857	France, Germany	Active, not recruiting	Osteoarthritis	Autologous Cultured	2x10 ⁶ cells/5ml injection 10x10 ⁶ cells/5ml injection 50x10 ⁶ cells/5ml injection	Local: intra-articular	18	19/03/2012	1
NCT01677520	United States	Recruiting	Breast Cancer	Autologous cultured	-	Local fat grafts	240	28/08/2012	-

ID	Country	Trail status	Condition	Source	Dose (number of cells)	Route of administration	No. of subjects	First received date	Phase
NCT01453751	United States	Recruiting	Diabetes Mellitus Type II	Autologous AD-SVF	AD-SVF and PRPs	IV	500	03/10/2011	1 and 2
NCT01314079	Republic of Korea	Active, not recruiting	Crohn's fistula	Autologous cultured	-	Local: Intralesional injection	40	08/03/2011	Observation After 2
NCT01453777	Mexico	Recruiting	Brain Lesion (General)	Autologous AD-SVF	-	Internal carotid artery with catheter and IV	10	03/10/2011	1 and 2
NCT01743222	Spain	Completed	Localized drug reaction to administration of drug	Allogeneic cultured	5 million cells in 1 ml of Hypo Termosol 10 million cells in 0.5 ml Hypo Termosol	Intra lymph node injection	10	24/08/2012	1
NCT01799694	Spain	Completed	Urinary incontinence in prostate cancer	Autologous	-	Local: Intramuscular	10	04/09/2012	2
NCT00475410	Germany, Spain, United Kingdom	Completed	Complex perianal fistulas not associated to Crohn's	Autologous cultured	20 million cells 40million cells	Local : with fibrin scaffolds	214	17/05/2007	3
NCT02024269	United States	Recruiting	Dry Macular Degeneration	Autologous AD-SVF	-	Local: intravitreal	100	17/12/2013	-
NCT02041000	United States	Recruiting	COPD	Autologous	-	IV	100	17/01/2014	-
NCT00426868	Netherlands, Spain, Denmark	Completed	Non revascularizable Ichemic Myocardium	Autologous AD-SVF	Dose Escalation	Local: Left Ventricle	27	23/01/2007	1
NCT02099500	United States	Recruiting	Critical limb ischemia	Autologous AD-SVF	AD-SVF with PRPs	Local: Intramuscular	200	19/04/2014	1 and 2
NCT01453803	Mexico	Recruiting	Parkinson's Disease	Autologous AD-SVF	-	Catheter injection vertebral artery and IV	10	03/10/2011	1 and 2
NCT01020825 From NCT00475410	Spain	Completed	Complex Perianal Fistula	Autologous cultured	20 million cells and 40 million cells	Local : with fibrin scaffolds	148	25/11/2009	Observation after 3

ID	Country	Trail status	Condition	Source	Dose (number of cells)	Route of administration	No. of subjects	First received date	Phase
NCT00616135	Belgium, Italy, Spain, United Kingdom	Completed	Breast reconstruction after mastectomy or quadrantectomy	Autologous AD-SVF	AD-SVF enhanced autologous fat graft	Local	71	05/02/2008	4 Post market study
NCT01803347	Spain	Recruiting	Anal fistula	Autologous cultured	ASCs and fibrin glue	Local: Intralesional	80	01/03/2013	3
NCT01947348	United States	Recruiting	Osteoarthritis	Autologous AD-SVF	AD-SVF and PRPs	Intra-articular and IV	30	15/03/2013	-
NCT01739504	United States	Recruiting	Osteoarthritis	Autologous AD-SVF	AD-SVF and PRPs	Local: Intra-articular	500	28/09/2012	1 and 2
NCT00115466	Spain	Active, not recruiting	Anal fistula	Autologous cultured	ASCs and fibrin glue	Local: Intralesional	50	22/06/2005	2
NCT02097862	United States	Recruiting	Degenerative disc disease	Autologous AD-SVF	AD-SVF suspended in PRPs	Local: Intra-diskally injection	100	25/03/2014	-
NCT01453816	Mexico	Recruiting	Renal failure	Autologous AD-SVF	AD-SFV administered within 1 hour of harvesting	Local: Intra renal arterial catheterization and IV	10	3/10/2011	1 and 2
NCT01914887	Spain	Recruiting	Ulcerative Cilitis Crohn's fistula	Allogeneic cultured	5 million cells/ml Total of 60 million cells per colonoscope	Local: colonic submucosa	8	18/07/2013	1 and 2
NCT01649700	Taiwan	Recruiting	Sequelae caused by severe brain injury	Autologous	5 infusions per month of 5-7x10 ⁷ cells	Infusions	2	09/04/2012	1 and 2
NCT01257776	Spain	Recruiting	Limb Ischemia in Diabetes	Autologous	0.5 million cells/kg 1 million cells/kg 2 million cells/kg	Intra-arterial	36	09/12/2010	1 and 2
NCT01856140	Republic of Korea	Recruiting	Tendon injury (lateral Epicondylitis)	Allogeneic cultured	Lesion size dependent 1 million cells/ml ALLO-ASC 10 million cells/ml of ALLO-ASC	Local: Ultrasound guided injection	12	26/04/2013	0
NCT01274975	Astrostem®	Completed	Spinal cord injury	Autologous	4x10 ⁸ cells (Astrostem®)	IV	8	06/01/2011	1

ID	Country	Trail status	Condition	Source	Dose (number of cells)	Route of administration	No. of subjects	First received date	Phase
NCT01211028	France	Recruiting	Perivascular and cardiovascular disease: Limb Ischemia	Autologous cultured	ACELLDream	Local: Intramuscular	15	31/03/2010	1 and 2
NCT01902082	China	Recruiting	Acute respiratory distress syndrome	Allogeneic cultured	1x10 ⁶ cells/kg body weight	IV	20	14/07/2013	1
NCT02135380	India	Not yet recruiting	Idiopathic Pulmonary Fibrosis	Autologous Ad-SVF and cultured	3 doses weekly of 2 million cell/kg body weight	IV	60	08/05/2014	1 and 2
NCT01663376	Republic of Korea	Completed	Critical limb ischemia	Autologous cultured	1x10 ⁸ to 3x10 ⁸ cells	Local: Intramuscular	20	08/08/2012	1 and 2
NCT01649687	Taiwan	Recruiting	Cerebellar Ataxia	Allogeneic cultured	5-7x10 ⁷ cells	IV	8	10/04/2012	1 and 2
NCT01804153	Spain	Recruiting	Urinary Incontinence	Autologous cultured	-	Local: Intralesional	10	04/09/2012	1 and 2
NCT01663116	Spain	Completed	Rheumatoid Arthritis Aggravated	Allogeneic cultured	1 million cells/kg day 1, 8 and 15 2 million cells/kg day 1, 8 and 15 4 million cells/kg day 1, 8 and 15	IV	53	05/08/2011	1 and 2
NCT01157650	Spain	Active, not recruiting	Crohn's disease	Autologous	-	-	15	05/07/2010	1 and 2
NCT01953523	United States	Recruiting	Neurodegenerative disease, Osteoarthritis, Erecte dysfunction, autoimmune, cardiomyopathies, emphysema	Autologous AD-SVF	IV, Intra-articular and local: soft tissue injection	-	3000	02/09/2013	-
NCT01453829	Mexico	Not yet recruiting	Stroke	Autologous AD-SVF	-	Inter Carotid Artery	10	03/10/2011	1 and 2

ID	Country	Trail status	Condition	Source	Dose (number of cells)	Route of administration	No. of subjects	First received date	Phase
NCT02107118	United States	Not yet recruiting	Cardiac disease and Erectile dysfunction	Autologous cultured	Frozen for 1 year then used	-	45	03/04/2014	1
NCT02052427	United States	Recruiting	Myocardial Ischemia	Autologous Cellulion system AD-SVF	0.8x10 ⁶ cell/kg body weight (not to exceed 80x10 ⁶ cells)	15 Intramyocardial injections with MYOSTAR	45	30/01/2014	2
NCT01453764	Mexico	Not yet recruiting	Multiple Sclerosis	Autologous AD-SVF	-	IV and Intrathecally	10	03/10/2011	1 and 2
NCT01769872	Republic of Korea	Recruiting	Spinal Cord Injury	Autologous Cultured	2x10 ⁸ cells/20ml 5x10 ⁷ cells/2 ml 2x10 ⁷ cells/ml	IV Intrathecal Into spinal cord	15	15/01/2013	1 and 2
NCT01399749	Spain	Not yet recruiting	Articular cartilage lesion of the femoral condyle	Autologous cultured or differentiated chondrocytes	1 million cells per lesion	Local: implantation	30	20/07/2011	1 and 2
NCT1889888	Russian Federation	Recruit by invitation	Urethral strictures in males	Autologous AD-SVF	Cytori Therapeutics Inc, Celution800/CRS System	Local: submucosal peri-urethral endoscopic injections	12	25/06/2013	1 and 2
NCT01850342	Russian Federation	Recruit by invitation	Stress Urinary Incontinence	Autologous AD-SVF	AD-SVF enriched fat graft	Local: Periurethral with endoscopic vision	12	07/05/2013	1 and 2
NCT01643681	Republic of Korea	Recruiting	Lumber intervertebral disc degeneration	Autologous cultured	4x10 ⁷ cells/ml	Local: intervertebral disc infusion	8	15/07/2012	1 and 2
NCT01643655	Republic of Korea	Active, not yet recruiting	Avascular necrosis of the femoral head	Autologous	1x10 ⁸ cells/3ml	Local: femoral head infusion	15	16/07/2012	1 and 2
NCT01300598	Republic of Korea	Completed	Degenerative Arthritis	Autologous cultured	1x10 ⁷ cells/3ml 5x10 ⁷ cells/3ml 1x10 ⁸ cells/3ml RNL-JointStem®	Local: cartilage tissue lesion	18	17/02/2011	1 and 2
NCT01216995	Netherlands, Poland	Active, not yet recruiting	Acute myocardial infarction	Autologous AD-SVF	Cytori therapeutics	Intracoronary route	-	06/10/2010	2

ID	Country	Trail status	Condition	Source	Dose (number of cells)	Route of administration	No. of subjects	First received date	Phase
NCT01943175	Republic of Korea	Recruiting	Schizophrenia	Research on ASC differentiated into neurons	-	-	30	04/09/2013	-
NCT01840540	United States	Recruiting	Atherosclerotic Renal failure Artery stenosis, Ischemic Nephropathy, Repair renal microvasculature	Autologous cultured	-	Arterial Infusion	15	23/04/2013	1
NCT01305863	United States	Active, not yet recruitment	Lower limb Ischemia	Autologous cultured	6 mm Gore PROPATEN® graft	Local: graft implantation	60	10/02/2011	1 and 2
NCT01399107	United States	Completed	Soft tissue mass removal	Researching AD-SVF preparation	Antria cell preparation	<i>In vitro</i> study	4	15/07/2011	-
NCT01974128	United States	Not yet recruiting	ST-Elevation Myocardial Infarction	Autologous AD-SVF	-	Catheter mediated injection	10	27/10/2013	1 and 2
NCT01302015	Republic of Korea	Completed	Buerger's disease	Autologous cultured	RNL-Vascostem® 5x10 ⁶ cell/kg body weight	Local: intra muscular	15	12/02/2011	1 and 2
NCT01624779	Republic of Korea	Recruiting	Spinal cord injury	Autologous cultured	3 times monthly 9x10 ⁷ cells/ 3ml	Local: intrathecal	15	18/06/2012	1
NCT00992147	Republic of Korea	Completed	Depressed Scar	Autologous cultured	Adipocell: ASCs differentiated into pure and immature adipocytes	Local: subcutaneous injection	36	28/09/2009	2 and 3
NCT01739530	Republic of Korea	Completed	Healthy	Allogeneic differentiated adipocyte	Repaircell	Local: subcutaneous injection	5	03/12/2012	1
NCT01309061	Republic of Korea	Completed	Romberg's Disease, Progressive hemifacial atrophy	Autologous AD-SVF	1x10 ⁷ cell/500 µl microlipoinjection	Local: intramuscular injections	5	02/03/2011	2

ID	Country	Trail status	Condition	Source	Dose (number of cells)	Route of administration	No. of subjects	First received date	Phase
NCT01532076	Switzerland	Recruiting	Osteoporotic fractures	Autologous AD-SVF	AD-SVF embedded fibrin gel Cellution/CR800, Cytori	Local: Graft implantation	290	05/01/2012	2
NCT01809769	China	Completed	Osteoarthritis	Autologous AD-SVF	1x10 ⁷ cells (3ml) 2x10 ⁷ cells (3ml) 5x10 ⁷ cells (3ml)	Local: intra-articular ultrasound guided injections	18	11/03/2013	1 and 2
NCT02034786	Brazil	Not yet recruiting	Lipodystrophies, aesthetic procedures	Autologous AD-SVF	AD-SVF associated hayloronic acid	Local: Transdermal injections	25	10/01/2014	1
NCT00913289	Japan	Terminated	Liver cirrhosis	Autologous cultured	-	-	6	03/06/2009	1
NCT01062750	Japan	Recruit by invitation	Liver cirrhosis	Autologous cultured	-	Intrahepatic arterial catheterization	4	03/02/2010	-
NCT01709279	Japan	Recruit by invitation	Ischemic heart disease	Autologous cultured	-	Intracoronary catheterization	6	16/10/2012	-
NCT01824069	Spain	Recruiting	Non-revascularizable criticle Ischemia of lower limbs	Autologous cultured	1 million cell/kg body weight	Local: Intramuscular injection	10	01/04/2013	1 and 2
NCT02045888	United States	Recruiting	Muscle tear	Auologous AD-SVF	Cellution system, Cytori Therapeutics Part A: 0.2 mill cells/kg body weight and 0.4 million cells/kg body weight Part B: 0.2 million cell/kg body weight and 0.4 million cell/kg body weight	Local: Intramuscular injection	70	13/01/2014	1 and 2
NCT01885819	Panama	Recruiting	Rheumatoid Arthritis	Autologous AD-SVF			20	18/06/2013	1 and 2
NCT01525472	France	Recruiting	Morbid obesity	-	<i>In vitro</i> study		225	01/02/2012	-

ID	Country	Trail status	Condition	Source	Dose (number of cells)	Route of administration	No. of subjects	First received date	Phase
NCT02068794	United States	Recruiting	Recurrent Ovarian Cancer	Allogeneic cultured	6 treatments 28 days apart: ASCs infected with oncolytic measles virus encoding thyroidal sodium iodide symporter (MV-NIS)	Local: Intra peritoneally	54	19/02/2014	1 and 2
NCT01849159	Russian Federation	Not yet recruiting	Pulmonary Emphysema	-	6 treatments every 2 nd month of 200 million cells/400 ml sodium chloride physiological solution	IV	30	24/04/2013	1 and 2

Appendix 3.1.

All Ethics approval letters and documentation

1. Approved on 21/01/2011 by Faculty of Health Sciences Research Ethics Committee with protocol number 218/2010
Protocol title: Isolation of mesenchymal stem cells from human tissues.
 - Informed consent form used for sample collection for this study.
 - Protocol amendment approved on 25/03/2011 (Umbilical cord blood and cord)
 - Protocol amendment approved on 24/06/2011 (Addition of Green Fluorescent Protein (GFP) lentiviral production and transduction protocols to the protocol description)
 - Protocol amendment approved 30/09/2011 (To determine whether HIV is present in Samples)

2. Approved on 30/09/2011 by Faculty of Health Sciences Research Ethics Committee with protocol number 179/2011 (Student Ethics)
Protocol title: Isolation and characterisation of human adipose derived mesenchymal stem cells and production of GFP-labeled primary cells for *in vivo* tracking following transplantation

3. Health Sciences MSc Committee of the University of Pretoria approval

PATIENT INFORMATION LEAFLET AND INFORMED CONSENT FORM

(Each patient must receive, read and understand this document before the start of the study)

STUDY TITLE

The isolation, characterisation and differentiation of mesenchymal stem cells from umbilical cord blood, Wharton's jelly and adipose tissue.

Dear Patient/Participant: _____

INTRODUCTION

You are invited to participate in a research study that is being carried out by the Department of Immunology at the University of Pretoria. This information leaflet is to help you to decide if you would like to participate. Before you agree to take part in this study you should fully understand what is involved. No selection criteria will be applied. Any donor will be eligible to participate (donate tissue). If you have any questions, which are not fully explained in this leaflet, do not hesitate to ask the investigator. You should not agree to take part unless you are completely happy about all the procedures involved. Your personal health will not be compromised at all by the procedures. These procedures have already been discussed with your doctor before hand.

THE PURPOSE OF THE STUDY

Researchers at the University of Pretoria would like to investigate the healing properties of adult stem cells for possible future application, in regenerative medicine. These adult stem cells, found in **fat (adipose tissue)**, could potentially be used to cure patients with various kinds of injuries or diseases. In order to use these cells to cure humans in the future, researchers must first study their behaviour and growth, in tissue cultures or animal models. The collection of adult stem cells does not make use of any unethical procedures.

HOW IS ADIPOSE TISSUE COLLECTED

During various normal plastic surgery operations, adipose tissue (fat) will be aspirated (sucked out) and discarded. This adipose tissue according to the surgical doctor does not serve a purpose to the patient's physique anymore. This discarded fat could serve a very important purpose to researchers in the field of regenerative medicine.

No additional fat will be collected, only the fat that the doctor would normally discard. The fat will be collected in the form of lipoaspirate (from liposuction) or from fat removed during abdominoplasty surgery.

There will be no added risks or discomfort with the collection of the adipose tissue other than normally associated with the specific procedure the patient will experience during normal operative procedures.

WHAT IS EXPECTED

Consent should be given by you (the patient) to the researchers to receive your discarded fat from your doctor. The consent will also allow the researchers to grow, differentiate and study the isolated stem cells from the fat tissue.

CONFIDENTIALITY

No personal information will be collected from you, the participant. Each participant will be assigned a specific code and this code will be the only information that the researchers will have. So no one will be able to identify you. Research reports and articles in scientific journals will not include any information that may identify you.

It might however be important for the doctors or researchers involved in this study to convey medical information to medical personnel or appropriate Research Ethics Committees. In such a case, you hereby authorise your investigator to release your medical records to regulatory health authorities or an appropriate Research Ethics Committee. These records will only be utilised by them in order for them to carry out their obligations toward this study, while always acting in your best interest.

ETHICAL APPROVAL

The protocol involved for this study was submitted to the Research Ethics Committee. This study has received written approval from the Research Ethics Committee of the Faculty of Health Sciences at the University of Pretoria. The study is structured in accordance with the Declaration of Helsinki, which deals with the recommendations of guiding doctors in biomedical research involving humans.

RIGHTS OF THE PARTICIPANT

Your participation in this study is entirely voluntary and you can refuse to participate or withdraw consent at any time without stating any reason. Your withdrawal will not affect your access to medical care or the quality of medical care that you will receive. Your participation or withdrawal from the study would not affect you in any way.

FINANCIAL GAIN OR LOSS

There will be no financial gain or loss to your account, should you participate or withdraw from the study. This research could potentially lead to future profitable treatments. However, you will not have access to these profits. There will be no additional financial costs for you to participate in the study.

The participant has no legal remedy and will not share in any financial gain that may be derived from the study

INFORMATION AND CONTACT PERSON

If at any time you would like to find out more information or have any questions regarding the study, please do not hesitate to contact the researchers.

Ms. Fiona van Vollenstee: 082 859 4239

Ms. Karlien Kallmeyer: 073 507 0103

Dr. Marnie Potgieter: 083 996 0078

Prof. MS Pepper: 012 420 3845 or 012 420 5317

INFORMED CONSENT

I confirm that the person asking my consent to take part in this study has told me about the nature, process, risks, discomforts and benefits of the study. I have also received, read and understood the above written information (Information Leaflet and Informed Consent) regarding the study. I am aware that the results of the study, including personal details, will be anonymously processed into research reports. I am participating willingly. I have had time to ask questions and have no objection to participate in the study. I understand that there is no penalty should I wish to discontinue with the study and my withdrawal will not affect my access to medical care or the quality of medical care I will receive.

I have received a copy of this informed consent agreement.

Participant full names (print): _____

Participant signature: _____ Date: _____

Investigator full names (print): _____

Investigator signature: _____ Date: _____

Witness full names (print): _____

Witness signature: _____ Date: _____

Witness full names (print): _____

Witness signature: _____ Date: _____

You hereby give the researchers permission to perform routine HIV, hepatitis B and hepatitis C tests on your cord blood sample since it is important for our work that we only work with tissue that are negative for these infections. If the researchers detect HIV or hepatitis B or C in the blood sample, the codified sample details will be sent to Prof. Piet Coetzee, who will notify you. If you do not wish us to test your blood for HIV or hepatitis B or hepatitis C, or if you do not wish to know the results of these tests, we will not be able to include you in the study. In the case of an HIV positive result, you will be counselled and treated by qualified medical personnel.

Patient signature: _____

INFORMED CONSENT

I confirm that the person asking my consent to take part in this study has told me about the nature, process, risks, discomforts and benefits of the study. I have also received, read and understood the above written information (Information Leaflet and Informed Consent) regarding the study. I am aware that the results of the study, including personal details, will be anonymously processed into research reports. I am participating willingly. I have had time to ask questions and have no objection to participate in the study. I understand that there is no penalty should I wish to discontinue with the study and my withdrawal will not affect my access to medical care or the quality of medical care I will receive.

I have received a copy of this informed consent agreement.

Participant full names (print): _____

Participant signature: _____ Date: _____

Investigator full names (print): _____

Investigator signature: _____ Date: _____

Witness full names (print): _____

Witness signature: _____ Date: _____

Witness full names (print): _____

Witness signature: _____ Date: _____

You hereby give the researchers permission to perform routine HIV, hepatitis B and hepatitis C tests on your cord blood sample since it is important for our work that we only work with tissue that are negative for these infections. If the researchers detect HIV or hepatitis B or C in the blood sample, the codified sample details will be sent to Prof. Piet Coetzee, who will notify you. If you do not wish us to test your blood for HIV or hepatitis B or hepatitis C, or if you do not wish to know the results of these tests, we will not be able to include you in the study. In the case of an HIV positive result, you will be counselled and treated by qualified medical personnel.

Patient signature: _____



FACULTY OF HEALTH SCIENCES
SCHOOL OF MEDICINE

To: Prof Pepper

Student name	F van Vollenstee	Student number	21104370
Name of study leader	Prof MS Pepper		
Department	Immunology		
Title of MSc	Isolation and characterization of human adipose derived mesenchymal stem cells and production of GFP-labeled primary cells for in vivo tracking following transplantation		
Date of submission	June 2011		
Comment to student and study leader	Please apply for ethics under student name External – accepted BUT provide MSc cover page with full address details PROVISIONALLY ACCEPTED		

Prof E Pretorius

Head: MSc Committee

Appendix 4.1.

Setting composites extracted from the flow cytometry data files, whereby the different flow cytometric protocol were sorted into colour codes for purpose of flow cytometric analysis.

Type of flow cytometer	Gallios	Gallios	Cytomics FC 500	Cytomics FC 500	Gallios	Cytomics FC 500	Gallios	Cytomics FC 500	Cytomics FC 500
Detector voltage for FS (parameter 1)	455	455	600	600	455	600	455	600	600
Amplifier gain used for acquisition of parameter 1	2	2	1	1	2	1	2	1	1
Detector voltage for SS (parameter 2)	0	0	75	75	0	75	0	75	75
Amplifier gain used for acquisition of parameter 2	1	1	1	1	1	1	1	1	1
Antibody used in parameter 3	FL1: CD90 FITC	FL1:CD90 FITC	FL1: CD73 FITC	FL1: CD73 FITC	FL1: CD90 FITC	FL1: CD73 FITC	FL1: CD90 FITC	FL1: CD90 FITC	FL1: CD73 FITC
Detector voltage for parameter 3	467	387	368	368	417	368	405	368	368
Amplifier gain used for acquisition of parameter 3	1	1	1	1	1	1	1	1	1
Antibody used in parameter 4	FL2: CD105 PE	FL2: CD105 PE	FL2: CD105 PE	FL2: CD105 PE	FL2: CD105 PE	FL2: CD105 PE	FL2: CD105 PE		FL2: CD105 PE
Detector voltage for parameter 4	469	419	432	432	469	432	439		432
Antibody used in parameter 5	FL4: CD45 PC5	FL4: CD45 PC5	FL3: CD34 ECD	FL3: CD34 ECD	FL4: CD45 PC5	FL3: CD45 ECD	FL4: CD45 PC5		FL3: CD45 ECD
Detector voltage for parameter 5	549	519	250	250	499	250	519		250
Amplifier gain used for acquisition of parameter 5	1	1	1	1	1	1	1		1

Antibody used in parameter 6	FL5: CD34 PC7	FL5: CD34 PC7	FL4: CD90 PC5	FL4: CD90 PC5	FL5: CD34 PC7	FL4: CD90 PC5	FL5: CD34 PC7	FL4: CD90 PC5	FL5: CD34 PC7	FL4: CD90 PC5
Detector voltage for parameter 6	547	547	429	410	587	329	547	329	547	410
Amplifier gain used for acquisition of parameter 6	1	1	1	1	1	1	1	1	1	1
Antibody used in parameter 7	FL6: CD73 APC	FL6: CD73 APC	FL5: CD45 PC7	FL5: CD45 PC7	FL6: CD73 APC	FL5: CD34 PC7	FL6: CD73 APC	FL5: CD34 PC7	FL6: CD73 APC	FL5: CD34 PC7
Detector voltage for parameter 7	420	420	546	326	580	406	420	406	420	326
Amplifier gain used for acquisition of parameter 7	1	1	1	1	1	1	1	1	1	1
Protocol colour code	Light Blue	Turquoise	Light pink	Olive Green	Yellow	Light Purple	Red	Light Grey	Red	Orange

Appendix 4.2.

Comparison of differentiation protocols used by different study groups, including induction media used and classical stains used for conformation of differentiation.

Reference	Viera <i>et al.</i> , 2010			Bieback <i>et al.</i> , 2004			Waterman <i>et al.</i> , 2010			Bunnell <i>et al.</i> , 2008			Bonab <i>et al.</i> , 2006			Sotiropoulou <i>et al.</i> , 2006		
Lineage	Adipose	Bone	Cartilage	Adipose	Bone	Cartilage	Adipose	Bone	Cartilage	Adipose	Bone	Cartilage	Adipose	Bone	Cartilage	Adipose	Bone	Cartilage
Cell density	-	-	2.5 x 10 ⁵		3.1 x 10 ⁵ /cm ²	2.5 x 10 ⁵		3 x 10 ⁴ cells/well	2.5 x 10 ⁵									
Stain	Oil red O	Von Kossa	Toluidine Blue	Oil red O	Von Kossa	Safranin O	Oil Red O	Alizarin Red	Safranin O	0.5% Oil Red O	40 mM Alizarin Red	TB	Oil Red O	Von Kossa		Sudan Black IV	Von Kossa	
Passage	3																	
Induction time (days)	21	21	21		21	4 wks												
Medium	DMEM- α g		DMEM- α g	Induction & maintenance	CellSystems	CellSystems (induction)	DMEM- α g		DMEM- α g + ITS			DMEM- α g	DMEM- α g	DMEM- α g		DMEM- α g	DMEM- α g	
FBS	10%	10%	-	10%	10%		10%						10%	10%		2%	10%	
Antibiotics													0.5 μ M Hydrocortisone			50 μ g/ml Gentamicin		
Dexamethasone	1 μ M	0.1 μ M	100 nM	1 μ M	0.1 μ M		1 μ M	10 ⁻⁸ M	0.1 μ M	0.5 μ M	1 nM	10 ⁻⁷ M		0.1 μ M		0.5 μ M	10 ⁻⁷ M	
3-isobutyl-methylxanthine	500 μ M			0.5 mM			0.5 mM			0.5 mM						0.5 mM		
Indomethacin	60 μ M			0.2 mM			100 μ M			50 μ M			60 μ M			60 μ M		
Ascorbate-2-phosphate		50 μ M	50 μ M		0.05 mM			50 μ M	50 μ g/ml		50 μ M	50 μ g/ml		50 μ M			50 μ M	
B-glycerol-phosphate		10 mM			10 mM			10 mM			2 mM			10 μ M			10 mM	
Insulin	5 μ g/ml			10 μ g/ml			10 μ g/ml						10 μ g/ml					
TGF- β 1			10 ng/ml															
TGF- β 3						10 ng/ml			10 ng/ml			10 ng/ml						
BMP-6												500 ng/ml						
Proline												40 μ g/ml						
Pyruvate			1 mM						2 mM			100 μ g/ml						
ITS + premix			1%									50 ng/ml						

Reference	Radaet <i>et al.</i> , 2010			Lund <i>et al.</i> , 2009			Kastenet <i>et al.</i> , 2008			Meulemanet <i>et al.</i> , 2006			Kedonget <i>et al.</i> , 2010			Sasaki <i>et al.</i> , 2008		
Lineage	Adipose	Bone	Cartilage	Adipose	Bone	Cartilage	Adipose	Bone	Cartilage	Adipose	Bone	Cartilage	Adipose	Bone	Cartilage	Adipose	Bone	Cartilage
Cell density			5 x 10 ⁶	300 cells/cm ²				3.5 x 10 ⁴ /24 well	1 x 10 ⁶ cells			2 x 10 ⁵	5 x 10 ⁴ /24 well					
Stain		Alizarin Red	Safranin O	Oil Red O	Alizarin Red	Alcian Blue G8	Oil Red O	Alizarin Red	TB	Oil Red O	Von Kossa		Oil Red	Von Kossa	Comixin#3	Oil Red O	Von Kossa	Toluidine Blue
Passage								2		1								
Induction time (days)		21	21		14			14	28	14	14	14-21	14	21				
Medium		α-MEM	DMEM	DMEM/F1 ₂	DMEM/F1 ₂	DMEM-hg	DMEM-hg	DMEM-hg	DMEM-hg	α-MEM	α-MEM	DMEM	IMDM					DMEM
FBS		10%	10%	10%	10%		10%	10%				1%	10%					10%
Antibiotics		1%	1%				1% P/S	S. 100 µg/ml P. 100 IE/ml						1%P/1%S 1%/1%/AB				0.1 µM
Dexamethasone		10 ⁻⁸ M	1 mM	0.1 µM	0.1 µM		1 µM	0.1 µM	0.1 µM	1 µM	0.1 µM		0.1 µM	0.1 µM	0.1 µM	0.5 µM		0.1 µM
3-isobutyl-methylxanthine				0.45 mM			0.5 mM			60 µM			0.1 mM			0.5 mM		
Indomethacin				0.2 mM			0.2 mM						0.2 µM			0.1 mM		
Ascorbate-2-phosphate		50 µg/ml	17 mM		50 µM	150 µM		0.17 mM	0.17 mM		60 µM	50 µM	50 µM	50 µg/ml			50 µM	50 µM
B-glycerol-phosphate		10 mM			10 mM			10 mM	1.25 mg/ml BSA		10 mM		10 mM				10 mM	10 mM
Insulin				170 nM			0.01 mg/ml			5 µg/ml		0.5 µg/ml						
TGF-β1			10 ng/ml									10 ng/ml TGF-β						10 ng/ml TGF-β
TGF-β3						10 ng/ml			10 ng/ml						10 ng/ml			
BMP-6															500 ng/ml			
Proline			35 mM		0.5 µM Calcitriol	0.34 mM			0.35 mM									40 µg/ml
Pyruvate			0.1 M						1 mM									100 µg/ml
ITS + premix			✓			✓			1%									50 mg/ml

Reference	Zuk <i>et al.</i> , 2001	Bunnell <i>et al.</i> , 2008	Wagner <i>et al.</i> , 2005	Reger <i>et al.</i> , 2008	Le Blanc <i>et al.</i> , 2003	Baptista <i>et al.</i> , 2009
Lineage	Adipose	Cartilage	Adipose	Adipose	Adipose	Cartilage
	Bone	Bone	Bone	Bone	Bone	Bone
	Cartilage	Adipose	Cartilage	Cartilage	Cartilage	Adipose
Cell density		8 x 10 ⁶ cells/ml	1 to 2 x 10 ⁶ cells/cm ²	1 x 10 ⁶ cells/cm ²	2.1 x 10 ⁶ cells/cm ²	1.5 x 10 ⁶ cells
Stain	Oil Red O	Alcian blue	Oil Red O	Oil Red O	Oil Red O	Alcian Blue
	AP or von Kossa		Alizarin Red (pH 4.1)	Alizarin Red	Von Kossa	Von Kossa
			Toluidine blue	Toluidine blue	Alcian Green	Oil Red O
Passage	1					3
Induction time (days)	14	14	14	21	21	14
			14 (stained after 21)			14
			21			21
Medium	DMEM	DMEM	DMEM-HG	DMEM	DMEM-HG	DMEM
FBS	10%	1%	10%	10%	10%	10%
Antibiotics	1%	1%		1%	1%	1%
Dexamethasone	1 μM	1 μM	10 ⁻⁷ M	10 ⁻⁷ M	10 ⁻⁷ M	0.01 μM
3-isobutylmethylxanthine	0.5 mM		0.5 mM	0.5 mM	0.5 mM	0.5 μM
Indomethacin	200 μM		200 μM	50 μM	100 μM	200 μM
Ascorbate-2-phosphate		50 nM	50 μg/ml	0.2 mM	50 μg/ml	5 x 10 ⁻⁶ M
B-glycerol-phosphate			2 mM	10 mM	10 mM	10 ⁻² M
Insulin	10 μM	6.25 μg/ml	10 μM		10 μg/ml	10 μM
TGF-β1		10 ng/ml				
TGF-β3			10 ng/ml		10 ng/ml	0.01 μg/ml
BMP-6			500 ng/ml		500 ng/ml	
Proline			40 μg/ml		40 μg/ml	0.35 mM
Pyruvate			100 μg/ml		100 μg/ml	1 mM
ITS + premix			50 mg/ml		5 ml	ü

MSC Chondrogenic differentiation BulletKit supplemented with 10 ng/ml TGF-β3 (Cambrex)

Reference	Liu <i>et al.</i> , 2007			Yoshimura <i>et al.</i> , 2006			Lu <i>et al.</i> , 2006			Francis <i>et al.</i> , 2010			Li <i>et al.</i> , 2005			Shetty <i>et al.</i> , 2010		
Lineage	Adipose	Bone	Cartilage	Adipose	Bone	Cartilage	Adipose	Bone	Cartilage	Adipose	Bone	Cartilage	Adipose	Bone	Cartilage	Adipose	Bone	Cartilage
	6 cells/ cm ²		2 x 10 ⁵ cells	2000 cells/cm ²	2000 cells/cm ²	2000 cells/cm ²	3000 cells/cm ²	3000 cells/cm ²	2 x 10 ⁵ cells			2 x 10 ⁵ cells			4 x 10 ⁵ cells	5000- 10000 cells/ 8-well well	3000- 10000 cells/ 8-well well	0.25-0.5 x 10 ⁶ cells
Stain	Oil Red O	Alizarin Red S	COII	Oil Red O	2.5% Silver nitrate	Alcian Blue 8 GX	Oil Red O	Von Kossa		Oil Red O	Alizarian Red	Safranin O	Oil Red O	Alizarian Red	Alcian Blue	Oil Red O	Von Kossa	Alcian Blue
Passage	2			Higher than 5			2											
Induction time (days)	3	14	21 3 & 14	28	28	28	14	14	14	14	14	21	21	21	18*	21		14 to 28
Medium	DMEM	DMEM		DMEM	DMEM	DMEM	DMEM	DMEM-LG	DMEM-LG	DMEM-LG	DMEM-HG	DMEM-LG	DMEM	DMEM	DMEM-HG	DMEM-HG		
FBS	100%	100%		100%	100%	1%	100%	100%	100%	100%	100%	1%	100%	100%	0	100%		
Antibiotics	1%	1%	1%	1%	1%	1%				1%		1%	✓	✓	✓			
Dexamethasone	1 µM	0.1 µM	10 ⁻⁷ M	1 µM	0.1 µM		1 µmol/L	100 nmol/L		1 µM	Used 0.01µM 1,25-dihydroxyvitamin D3		1 µM	0.1 µM	1 µM	1 µM		
3-isobutyl-methylxanthine	0.5 mM			0.5 mM			0.5 mmol/L			0.5 mM			0.5 mM		0.5 mM			
Indomethacin	200 µM			200 µM			60 µmol/L			200 µM					60 µM			
Ascorbate-2-phosphate		50 µM	50 µM		50 µM	50 µM		0.2 mmol/L			50 µM	50 µM	50 µg/ml	50 µg/ml				
B-glycerol-phosphate		10 mM			10 mM			10 mmol/L			10 mM		10 mM	10 mM				
Insulin	10 µM		6.25 µg/ml	10 µM		6.25 µg/ml	5 µg/ml			10 µM		6.25 µg/ml	1 µg/ml		10 µg/ml			
TGF-β1			10 ng/ml			10 ng/ml								10 ng/ml				
TGF-β3			10 ng/ml									10 ng/ml						
BMP-6																		
Proline			40 µg/ml											40 µg/ml				
Pyruvate			100 µg/ml											100 µg/ml				
ITS + premix			50 mg/ml									✓			✓			

* After 3 days the adipogenic induction medium was changed to adipogenic maintenance (AM medium) medium for 3 days (contains 10 µg/ml insulin and 10% FBS in DMEM-HG), three cycles of induction/maintenance was carried out														
Reference	Kern <i>et al.</i> , 2006			Farrel <i>et al.</i> , 2008			Igura <i>et al.</i> , 2004			Pittinger MF, U.S. Patent 5 827 740 (1998)		Le Blanc <i>et al.</i> , 2003		
Lineage	Adipose *	Bone	Cartilage	Adipose	Bone	Cartilage	Adipose	Bone	Cartilage	Adipose	Maintain	Adipose	Bone	Cartilage
	2.1x10 ⁴	3.1x10 ³	2.5x10 ⁵				2x10 ⁴	1.5x10 ⁴	2x10 ⁵	100000/35mm		2.1x10 ⁴ cell/cm ²	3.1x10 ³ cell/cm ²	7.5x10 ⁵ cell/pell
Stain	0.18% Oil Red / nucleus Mayer's hematoxylin solution	Alkaline phosphatase / von Kossa / silver nitrate	Safranin O	Oil Red O	Von Kossa	Thionine	Oil Red O	Von Kossa	Toluidine blue			Oil Red O	Von Kossa	Aealen green
Passage	0-5	0-5	0-5		From passage 4									
Induction time (days)	3 cycles	2.5 week	4 weeks		13 days			3 weeks	3 weeks	48hrs	30 days	21 days	21 days	21 days
Medium	MSCGS or DMEM-Ig+ 10% MSCGS till 70% post confluent/	MSCGS or DMEM-Ig+ 10% MSCGS till 70-80% confluent/ osteogenic basal	Complete chondrogenic differentiation medium (Cambrex)	DMEM 10%FCS	DMEM 10%FCS	DMEM serum free	DMEM high glucose	DMEM low glucose	DMEM low glucose	Induction DMEM	Maintenance DMEM	DMEM-LG	DMEM-LG	DMEM-HG
	10%	10%				No serum	10% FBS	10% FBS	10% FBS	10%	10%	10%	10%	
FBS														
Antibiotics					50 µg/ml gentamycin/ 1.5µg/ml fungizone							1% antibiotic/anti mycotic		
Dexamethasone	1 mM	100nM		1 µM	1 µM		1 µM	0.1 µM	X amount	1 µM		1 µmol/L	0.1 µmol/L	0.1 µmol/L
3-isobutyl-methylxanthine	0.5 mM			0.5 mM			0.5 mM			0.5 mM		0.5 mmol/L		
Indomethacin	100nM			0.2 mM			0.2 mM					100 µmol/L		
Ascorbate-2-phosphate		0.2mM Ascorbate			0.1 mM	25 µg/ml		50 µM					0.05 mmol/L	0.17 mmol/L
B-glycerol-phosphate		10mM			10 mM			10 mM					10 mmol/L	
Insulin	10µg/ml			0.01 mg/ml			10 µg/ml			10 µg/ml	10 µg/ml	10 µg/ml		6.25 µg/ml
TGF-β1						TGF-β2 10ng/ml								
TGF-β3									X amount					0.01 µg/ml
BMP-6									BMP-6 amount 2.500					
Proline						40 µg/ml								
Pyruvate						100mM								1 mmol/ values
ITS + premix						1%								

Reference	Lee <i>et al.</i> , 2004			Mitchell <i>et al.</i> , 2006			Bertoloet <i>et al.</i> , DOI 10.1007/s00586-010-1662-9			D'ippolito <i>et al.</i> , 2004			Kang <i>et al.</i> , 2004			Curran <i>et al.</i> , 2006		
Lineage	Adipose	Bone	Cartilage	Adipose	Bone	Cartilage	Adipose	Bone	Cartilage	Adipose	Bone	Cartilage	Adipose	Bone	Cartilage	Adipose	Bone	Cartilage
Cell density		3 x10 ⁶ cells/ml		confluent	confluent	Not Done	5x10 ⁵ cells/cm ²	5x10 ³ cells/cm ²	5x10 ⁵ cells/cm ²	10 000 cells/cm ²	10 000 cells/cm ²	250 000 cells/ml/q		1:10 dilution but grown to 80% confluent		5x10 ⁴ cells/ml		
Stain	Oil Red O	Alizarin red	Toluidine blue	Oil Red O	Alizarin Red		Oil Red O	Von Kossa	Alcian Blue	Sudan-IV	Alizarin Red-S		Oil Red O	Alizarin Red S	Safranin O	Von Kossa		Immunostaining
Passage												80% confluence						
Induction time (days)	2 weeks	2 weeks	3 weeks	9 days	3 weeks		3 weeks	2 weeks	4 weeks	3 weeks		4 weeks	3 weeks	3-4 weeks		1-28 days		
Medium	αMEM	αMEM	αMEM	DMEM/F-12 33µM biotin, 17 µM pantothenate	DMEM/F-12			DMEM/F12		α MEM 10% horse serum; 0.5µM hydrocortisone	α MEM	DMEM-HG		α-MEM		DMEM		DMEM-HG
FBS	10%	10%	1%	3%	10%			5%		10%	10%			10%		10%		1% FCS
Antibiotics				0.25µg strep/0.25µg fungzone	0.25µg strep/1000 pen/100µg fungzone			1000U/ampicillin/1000U/ml strep; 2.5mg/ml amphotericin		1000U/ml pen;1mg/ml strep	pen/ strep			1% Pen/Strep				
Dexamethasone	1µM	0.1nM		1 µM	10 nM			1 µM	40ng/ml		DMSO 0.001%	100 nM		10 ⁻⁹ M		100 nM		100 nM
3-isobutyl-methylxanthine	100 µg/ml			0.5mM				0.5 mM		0.5 mM								
Indomethacin	60 µM							0.5 mM		60 µM								
Ascorbate-2-phosphate		AA 50 µg/ml	AA 50 µg/ml		Na 50 µg/ml			0.05 mM	50 mg/ml		100 µM	50 µg/ml		AA 50 µg/ml	AA 50 ng	100 mM		100 mM
B-glycerol-phosphate		10 µM			10 mM			10 mM			10 mM			10 mM		10 mM		10 mM
Insulin	5 µg/ml		6.25µg/ml	Bovine Insulin 1µM				170 mM						10 ng/ml				
TGF-β1			10 ng/ml						5 ng/ml									10 ng/ml
TGF-β3												10 ng/ml						
BMP-6																		
Proline									50 mg/ml			40 µg/ml						
Pyruvate												Na 100 µg/ml						1 mM
ITS + premix									1x			1x						1%

*Parting is such sweet sorrow, that
I shall say goodnight till it be morrow*

Shakespeare W, Romeo and Juliet (1594), Act II, Scene 2, line 184-185.